University of Glasgow

The endodontic biofilm: effects of chitosan as a novel antimicrobial agent

Sumaya Mabrouk Abusrewil
BDS, MSc

Submitted in fulfilment of the requirements for the Degree of Doctor of Philosophy

School of Medicine, Dentistry and Nursing
College of Medical, Veterinary and Life Sciences

University of Glasgow

November 2022

Abstract

Background and objectives: Endodontic infection or root canal infection, as it is commonly referred to, is a biofilm disease that is difficult to completely irradicate with current treatment protocols, and as such, persistent microorganisms may lead to ongoing or recurrent disease. Root canal treatment is founded on the ability to eradicate microbial infection and prevent re-infection of the highly complex root canal space. There is a growing realisation that endodontic infections are polymicrobial and may contain *Candida* spp. Despite this understanding, the development of new endodontic therapeutics and models of pathogenesis remains limited to mono-species biofilm models, which are bacterially focused. The main aims of this thesis were firstly to develop and optimise an interkingdom endodontic biofilm model comprised of microbial species frequently identified in endodontic infections and to use this model to test antibiofilm actives. Secondly, to evaluate the antibiofilm efficacy of Mineral Trioxide Aggregate and Biodentine™ calcium silicate cements, used in the management of endodontic diseases, and how modification with chitosan may impact on their antimicrobial properties. Thirdly, to investigate the effect of chitosan incorporation on some of the physico-mechanical and biological properties of Biodentine.

Materials and methods: Biofilms containing *Fusobacterium nucleatum* (ATCC 10953), *Porphyromonas gingivalis* (ATCC 33277), *Streptococcus gordonii* (ATCC 35105) and *Candida albicans* (SC5314) were established. Biofilms were optimised in different growth conditions, using quantitative polymerase chain reaction and qualitative microbiology techniques. The *in vitro* biofilm model was treated with chlorhexidine, ethylenediaminetetraacetic acid and chitosan solutions. This was reaffirmed on a biological substrate (bovine dentine), to further validate this model and the antimicrobial effectiveness of chitosan. To evaluate the antibiofilm efficacy of calcium silicate materials, the regrowth of mono-species (*C. albicans*), three multispecies (*F. nucleatum*, *P. gingivalis* and *S. gordonii*) and four multispecies (*F. nucleatum*, *P. gingivalis*, *S. gordonii* and *C. albicans*) biofilms on ProRoot MTA and Biodentine discs were explored using live-dead qPCR. These were compared to regrowth on bovine dentine discs. The effect on regrowth of biofilms was assessed following the addition of 2.5 wt% and 5 wt% of chitosan medium molecular weight powder to each calcium silicate

cement. Subsequently, the setting time, disintegration, radiopacity, compressive strength, microhardness and biocompatibility of the new composite of Biodentine modified with chitosan were assessed. Next, the regrowth of the four multispecies (*F. nucleatum*, *P. gingivalis*, *S. gordonii* and *C. albicans*) biofilms on Biodentine discs were explored following the addition of 0.5 wt% and 1 wt% of chitosan powder of either high, medium or low molecular weights. This was compared to regrowth on the unmodified formula of Biodentine. Finally, the physico-mechanical and biological properties of the new composite of Biodentine modified with chitosan low molecular weight were evaluated.

Results: Assessment of antimicrobial activity of CHX, EDTA and solubilised chitosan showed significant effectiveness of each antimicrobial agent. Chitosan was similarly effective at preventing biofilm regrowth on bovine dentine. In comparison to a dentine substrate, ProRoot MTA and Biodentine did not show an ability to inhibit biofilm regrowth. The addition of chitosan powder to MTA imparted no antimicrobial enhancement. In contrast, a dose-dependent reduction in multispecies biofilm regrowth was determined upon the addition of chitosan to Biodentine. Interestingly, the antibiofilm effect of chitosan increases with the decreased chitosan molecular weight. Importantly, interkingdom interactions were noted, whereby the inclusion of *C. albicans* to the biofilm enhanced bacterial tolerance in the presence of chitosan and conversely bacterial presence reduced *C. albicans* tolerance. However, incorporation of 2.5 wt% and 5 wt% chitosan MMw compromises most of the material properties of Biodentine. In contrast, the addition of 0.5 wt% and 1 wt% chitosan LMw showed no detrimental effects on physical and biological properties of Biodentine material, however, significant reductions were noted in mechanical properties of Biodentine when chitosan was incorporated. Nevertheless, the new composite would still be applicable where other root filling materials might be considered, when the material strength and hardness are not critical issues.

Conclusion: This thesis describes a robust and reproducible multispecies interkingdom biofilm model that can be employed to assess efficacy of novel endodontic therapeutics. This work demonstrates the potential to enhance the antimicrobial properties of Biodentine, when modified with chitosan microparticles, opening the door for exploration of antimicrobial strategies for prevention and management of endodontic infections. The findings also highlight

the importance of using appropriate biofilm model systems when exploring antimicrobial properties of materials *in vitro*, so that interspecies and interkingdom interactions that modify tolerance are not overlooked.

Table of Contents

List of Tables

List of Figures

Acknowledgement

All praise be to Allah, the All-Knowing, the All-Wise, for all the blessings which He has bestowed upon me that I would not be able to enumerate.

I would like to express my sincere gratitude to my supervisors Dr William McLean, Professor Gordon Ramage and Dr James Alun Scott for their valuable knowledge, guidance and support during my PhD study. Dr McLean, you have always been a great supervisor and like an older brother to me. I owe you a debt of gratitude for your caring and unwavering support over the last seven years. Thank you for teaching me countless lessons that will live with me forever. Professor Ramage, your support at the start of my PhD, when I had no lab experience, was instrumental. Your insights and knowledge made it easier to proceed in the right direction and complete this project. I am deeply grateful to you Gordon, now and always, for all the opportunities and learning experiences you have given to me over the past four years. Dr Scott, saying “thank you” is not enough to express how grateful I am to you. Your continuous support, patience, thoughtful comments, encouragement and understanding have been invaluable to me since the first day I was honoured to work under your supervision. Thank you for being you!

I would like to thank all members of the oral science group and University of Glasgow, past and present, who have provided support and advice throughout the way. Dr Om Alkhir Alshanta, you have been always there during hard times, your care and support will never be forgotten. Dr Christopher Delany, Dr Jason Brown, Saeed Alqahtani and Mark Butcher, thank you for all the technical help and training you have provided throughout my PhD course - this was really appreciated. Dr Tracy Young, Dr Laís Arias, Dr Bryn Short, Dr Abeer Alghamdi, Dr William Johnston, Dr Khawlah Albashaireh, Dr Emily Mckloud, Hafsa Abduljalil, Suror Shaban, Krystyna Piela, Abdullah Baz and Ahmed Bakri, thank you for always being valued friends who have made my days in the school brighter and better, thank you for always being very kind, supportive and great team members.

I am also greatly thankful to Mr Steven Milligan for his technical support and dedication. Special thanks go to Mr Charchit Kumar (School of Engineering,

University of Glasgow) for his great help with the compressive strength testing. I would also like to express my gratitude to Professor Graham Chadwick (University of Dundee) for his assistance with the microhardness testing.

I would like to extend my sincere thanks to everyone within the Libyan embassy, Cultural Attaché, for their help and financial support throughout my PhD course.

Finally, I would like to express my deepest love and appreciation to my parents, my granny, my brothers and sisters. Mama and Baba, I owe you all the success I have achieved in my life. Thank you for everything you have done for me!

Author's Declaration

I declare that the above-mentioned thesis embodies the results of my own special work, that it has been composed by myself unless otherwise acknowledged or cited, under the supervision of Professor Gordon Ramage, Dr William McLean and Dr James Alun Scott. I further declare that this thesis does not include work forming part of a thesis presented for a degree at the University of Glasgow or any other institution.

Sumaya Mabrouk Abusrewil

November 2022

List of Publications Based on Thesis

Abusrewil, S., Brown, J.L., Delaney, C., Butcher, M.C., Tiba, M., Scott, J.A., Ramage, G. and McLean, W., 2021. Chitosan enhances the anti-Biofilm activity of Biodentine against an interkingdom biofilm model. *Antibiotics*, 10(11):1317. DOI: 10.3390/antibiotics10111317. Pub 2021 Oct 29. PMID: 34827255.

Abusrewil, S., Brown, J.L., Delaney, C.D., Butcher, M.C., Kean, R., Gamal, D., Scott, J.A., McLean, W. and Ramage, G., 2020. Filling the void: an optimized polymicrobial interkingdom biofilm model for assessing novel antimicrobial agents in endodontic infection. *Microorganisms*, 8(12):1988.
DOI: 10.3390/microorganisms8121988. Pub 2020 Dec 14. PMID: 33327403.

Abusrewil, S., Alshanta, O.A., Albashaireh, K., Alqahtani, S., Nile, C.J., Scott, J.A. and McLean, W., 2020. Detection, treatment and prevention of endodontic biofilm infections: what's new in 2020?. *Critical Reviews in Microbiology*, 46(2), pp.194-212.
DOI: 10.1080/1040841X.2020.1739622. Epub 2020 Apr 1. PMID: 32233822.

A paper was submitted to the journal of Dental Materials under the title:

Abusrewil, S., Alqahtani, S., Kumar, C., Butcher, M.C., Tiba, M., Mulvihill, D., Ramage, G., McLean, W., and Scott, J.A., 2022. "The effect of chitosan incorporation on material characteristics of a calcium silicate filling material".

Abbreviations, Acronyms and Chemical Formula

AAE	American Association of Endodontists
AB	Alamar blue
AgNPs	Silver nanoparticles
AnO_2	Anaerobic environment
ANOVA	Analysis of variance
App	Application
ASA	American Society of Anesthesiologists
ATCC	American Type Culture Collection
ATP	Adenosine triphosphate
AU	Arbitrary units
BA	BioAggregate
Ba	Bacteria
BD	Biodentine
BD-L	Biodentine liquid
BD-P	Biodentine powder
BMSCs	Bone marrow stem cells
BSA	Bovine serum albumin
Ca	*C. albicans*
$Ca(OH)_2$	Calcium hydroxide
CBA	Columbia blood agar
CEM	Calcium-enriched mixture cement
CFE	Colony forming equivalent
CFU	Colony forming unit
CH_3CO	Acetyl group
CHX	Chlorhexidine digluconate
CLSI	Clinical and Laboratory Standards Institute methodologies
CLSM	Confocal laser scanning microscopy
CO_2	Carbon dioxide
CRCT	Conventional root canal treatment
CS	Chitosan
C-S-H	Calcium silicate hydrate
CSI/σ_c	Compressive strength
CSNPs	Chitosan nanoparticles
Ct	Cycle threshold
CV	Crystal violet
Da	Dalton
DDA	Degree of deacetylation
DFSCs	Dental follicle stem cells
dH_2O	Distilled water
DMEM-KO	Knock-out Dulbecco's modified Eagle's medium
DMSO	Dimethyl sulfoxide
DNA	Deoxyribonucleic acid
DPSCs	Dental pulp stem cells
DT	Dentinal tubules
ECM	Extracellular matrix
eDNA	Extracellular DNA
EDTA	Ethylenediaminetetraacetic acid
EPS	Extracellular polysaccharides
ESE	European Society of Endodontology
FAA	Fastidious anaerobic agar

FBS	Foetal bovine serum
Fn	*F. nucleatum*
g	gram
GMSCs	Gingiva-derived mesenchymal stem cells
h	Hour
HA	Hydroxyapatite
HBSS	Hank's balanced salt solution
HCl	Hydrochloric acid
HEK 293	Human embryonic kidney cells
HMDS	Hexamethyldisilizane
HMw	High molecular weight
HOMD	Human oral microbiome database
HV	Vickers microhardness
ID	Intertubular dentine
ISO	International Organisation for Standardisation
kHz	Kilohertz
kV	Kilovolt
L	Litre
LDH	Lactate dehydrogenase
LMw	Low molecular weight
M	Molar
mA	Milliampere
mg	Milligram
MH	Microhardness
MIC	Minimal inhibitory concentration
Micro-CT	Micro-computed tomography
min	Minute
mL	Millilitre
mm	Millimetre
mM	Millimolar
mmAl	Millimetres of aluminium
MMw	Medium molecular weight
MPa	Megapascals
MSCs	Mesenchymal stem cells
MTA	Mineral trioxide aggregate
MTAD	Mixture of a tetracycline isomer, an acid and a detergent
MTT	3-(4,5-dimethylthiazol-2-yl)-2,5-diphenyltetrazolium bromide
Mw	Molecular weight
n	Number
NaOCl	Sodium hypochlorite
NaOH	Sodium hydroxide
NCTC	National Collection of Type Cultures
NGS	Next generation sequencing
NH_2	Amino group
nm	Nanometre
NMs	Nanomaterials
NP	Number of publications
NPs	Nanoparticles
O_2	Oxygen
OD	Optical density
OED	Oxford English Dictionary
OESCs	Oral epithelial progenitor/stem cells
p	P-value

PBS	Phosphate buffered saline
PCR	Polymerase chain reaction
PD	Peritubular dentine
PDLSCs	Periodontal ligament stem cells
Pg	*P. gingivalis*
pH	Potential of hydrogen
PI	Propidium iodide
PMA	Propidium monoazide
P-MIC	Planktonic minimal inhibitory concentration
PMID	PubMed identifier
ppm	Parts per million
PSCs	Periosteum-derived stem cells
qPCR	Quantitative polymerisation chain reaction
REPs	Regenerative endodontic procedures
RNA	Ribonucleic acid
ROE	*Rosmarinus officinalis* leaf extract
RPM	Revolutions per minute
RPMI	Roswell Park Memorial Institute medium – 1640
SAB	Sabouraud dextrose agar
SC	Scientific Committee
SCAP	Stem cells from the apical papilla
SCH	Schaedlers broth
SCI	Science Citation Index
SCs	Stem cells
SD	Standard deviation
SDT	Sclerotic dentinal tubules
SEM	Scanning electron microscopy
Sg	*S. gordonii*
SGSCs	Salivary gland-derived stem cells
SHED	Stem cells from human exfoliated deciduous teeth
spp.	Species
TC	Total citations
TGPCs	Tooth germ progenitor cells
THB	Todd-Hewitt broth
TIV	Through Indenter Viewing
™	Trademark
TPP	Sodium tripolyphosphate
TSB	Tryptic soy broth
UK	United Kingdom
UV	Ultraviolet light
USA	United States of America
v/v	Volume per unit volume
VHN	Vickers hardness number
W	Watt
w/v	Weight per unit volume
WOS	Web of Science
wt%	Percentage by weight
XTT	2,3-bis(2-methoxy-4-nitro-5-sulfophenyl)-2H-tetrazolium-5-carboxanilide
YPD	Yeast peptone dextrose
Z	Atomic number
µL	Microlitre
µm	Micrometre
µM	Micromolar

1 General introduction

The role of microorganisms in endodontic disease has been long established following the classical animal study of Kakehashi et al. (1965). In this landmark paper, comparison of gnotobiotic animals with conventional animals allowed the key role of microorganisms in causation of apical periodontitis to be established. Apical periodontitis is a consequence of endodontic infection and can be defined as a dynamic encounter between host immune defences and microbial invaders, which eventually leads to inflammatory changes and resultant bone destruction adjacent to the root (Nair, 2004). Infection of the root canal system occurs if a dental pulp becomes necrotic following caries, trauma, periodontal disease or in cases in which the dental pulp has been removed by former root canal therapy (Siqueira et al., 2015). Tooth surface loss (Field et al., 2019) and dental anomalies (Hülsmann, 1997, Ferraz et al., 2001) may also result in pulp necrosis and the necessity for root canal therapy. Endodontic failure is a widespread problem in dentistry. The endodontic flare-up can be defined as a true complication of endodontic treatment, characterised by development of pain, swelling or both, which commences within a few hours or days after the root canal procedures, and is so severe that an unscheduled visit for emergency treatment is required (Siqueira, 2003). The presence of clinical symptoms and apical periodontitis, following root canal treatment, indicate endodontic infection and treatment failure (Bergenholtz, 2016).

Previously, classifications of endodontic diseases were based mainly upon histopathological findings rather than clinical features (AAE, 2013). However, it must be understood that diseases of pulp and periapical tissues are in a dynamic state (Soames and Southam, 2005), as different conditions such as vital tissues, acute, chronic inflammation and/or necrosis may coexist in the pulp with various degrees of progression with or without symptoms. This dynamic behavior can lead to confusion and misdiagnosis as there is little correlation between histological findings and clinical features (AAE, 2013). In 2013, the American Association of Endodontists (AAE) published the most recent diagnostic terminology and definitions, based upon clinical findings, to classify endodontic diseases. The aim was to establish a universal classification that directs clinicians to the most appropriate procedures. This diagnostic classification creates a simple, reliable and accessible system. In contrast, endodontic microbiology research, with the widespread use of molecular methods, has been

focused on the determination of microbial composition and diversity (mainly bacterial communities) associated with different clinical conditions in endodontic infections (Siqueira and Rôças, 2022). With our growing understanding of the microbiological basis of endodontic disease and our ability to create a profile of an individual's root canal microbiome, it may become appropriate to start considering a more 'personal' diagnostic criterion including microbiome data to inform treatment decisions.

1.1 Aims

This chapter aims to:

- Provide a contemporary view of endodontic microbiology and to explore some of the factors occupying the attention of endodontic researchers.
- Provide insight into novel opportunities and strategies for the future diagnostics, treatment and prevention of endodontic diseases.

Elements from this chapter have been published in:

- **Abusrewil, S.**, Alshanta, O.A., Albashaireh, K., Alqahtani, S., Nile, C.J., Scott, J.A. and McLean, W., 2020. Detection, treatment and prevention of endodontic biofilm infections: what's new in 2020?. *Critical Reviews in Microbiology*, 46(2), pp.194-212. DOI: 10.1080/1040841X.2020.1739622. Epub 2020 Apr 1. PMID: 32233822.
- **Abusrewil, S.**, Brown, J.L., Delaney, C., Butcher, M.C., Tiba, M., Scott, J.A., Ramage, G. and McLean, W., 2021. Chitosan enhances the anti-biofilm activity of Biodentine against an interkingdom biofilm model. *Antibiotics*, 10(11):1317. DOI: 10.3390/antibiotics10111317. Pub 2021 Oct 29. PMID: 34827255.

1.2 Root canal system: implications in endodontic procedures

The primary goals of endodontic treatment are to remove irritants from the root canal system, to obturate the cleaned and shaped root canals and to prevent future reinfection of the sealed root canal system (AAE, 2002). A thorough understanding of the root canal morphology and its variations is a basic requirement for successful endodontic treatment (Versiani and Keleș, 2020). Treatment of complex and anomalous teeth also requires good knowledge of the internal anatomy of the root canal system before undertaking endodontic treatment (Versiani and Ordinola-Zapata, 2015). The dental pulp has the characteristic of being exclusively the non-mineralised portion of a mineralised tooth (Figure 1.1). This dental soft tissue is surrounded by a robust shell-like complex structure that includes dentine, enamel and cementum (Goldberg, 2014). The root canal system is divided into two parts: the pulp chamber and the root canal. The pulp chamber is located within the anatomical crown whereas the root canal is present within the root structure (Versiani and Keleș, 2020).

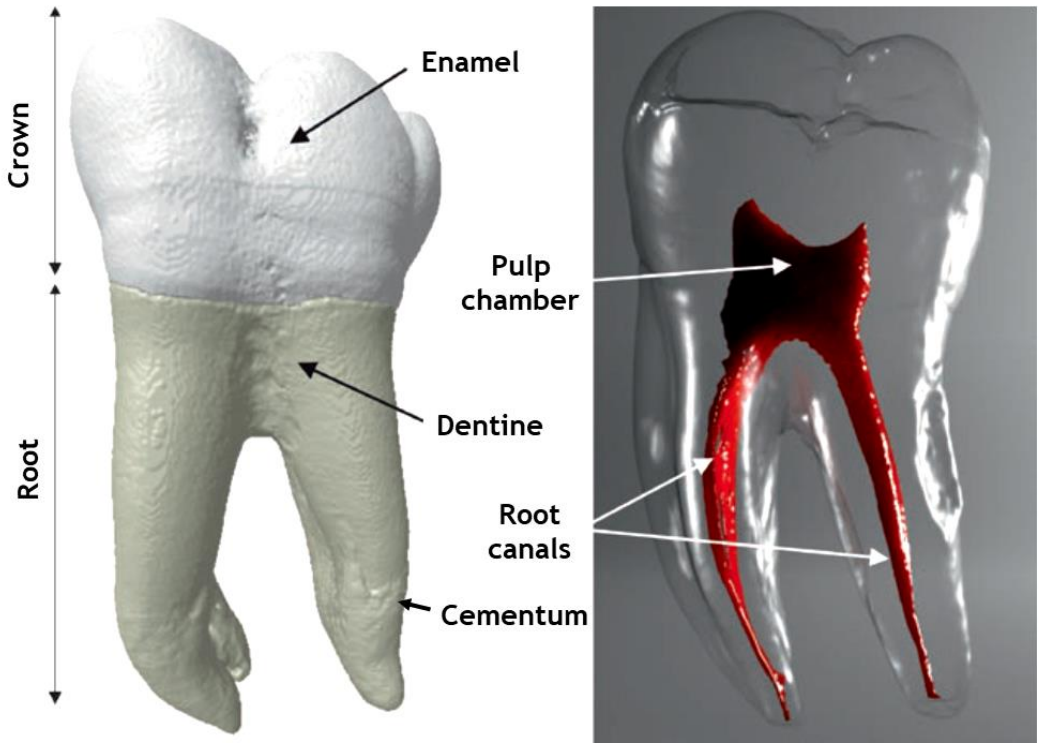

Figure 1.1. External and internal tooth components. A tooth is made up of the crown and the root, and is composed of different tissues: enamel, dentine, cementum and pulp. The pulp is a soft tissue located within a tooth in a pulp cavity that is divided into pulp chamber and root canal. Adapted from Versiani and Keleș (2020).

In the last decade, three-dimensional imaging, using micro-computed tomography (Micro-CT), has been extensively applied in experimental endodontology to reveal the anatomy of the root canal system. It can produce a detailed informative image of the root canal system before, during and after various endodontic procedures, as shown in Figure 1.2 (Versiani and Keleș, 2020).

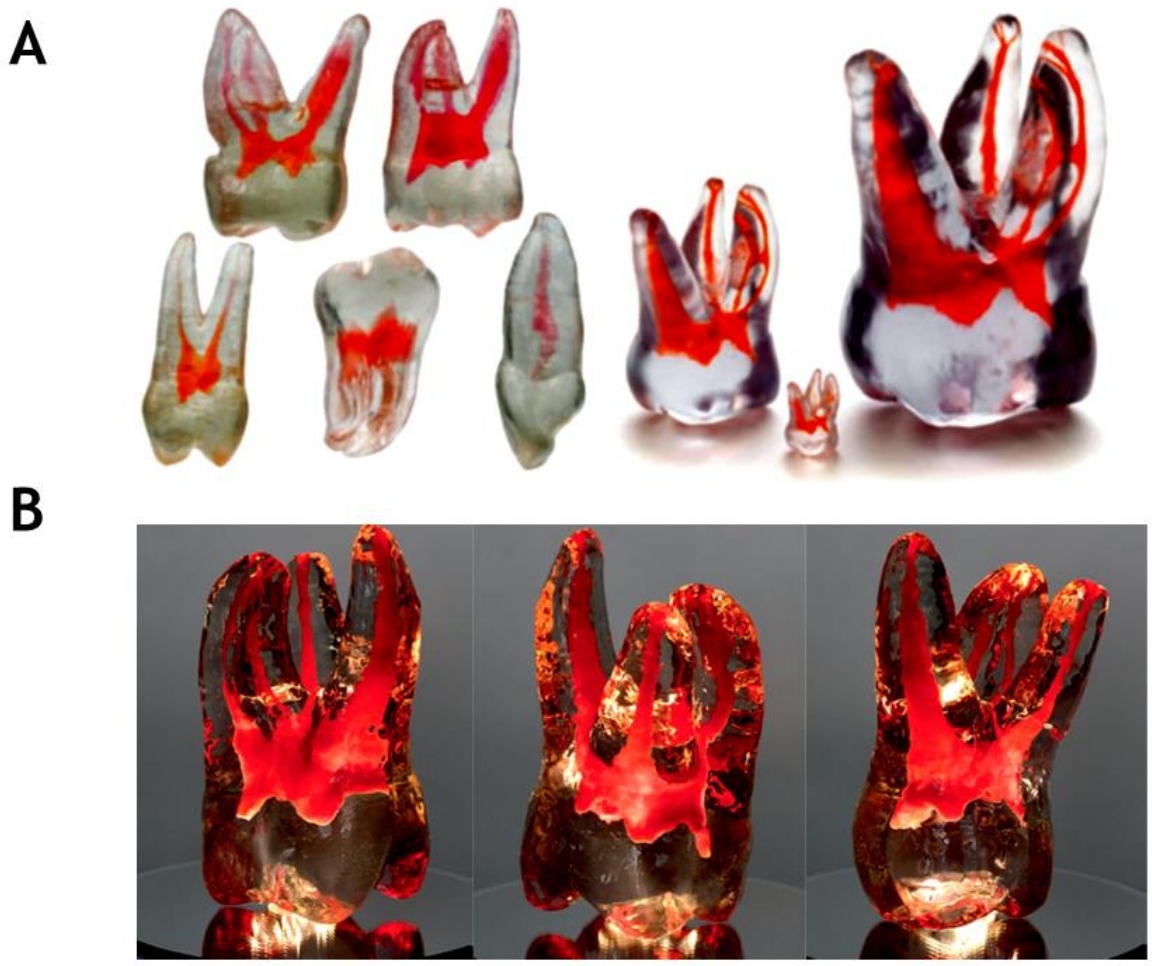

Figure 1.2. Replica of various teeth manufactured from corresponding real-tooth micro-CT scans. Training replicas were produced using 3D printing technology for teaching purposes. **(A)** True teeth. **(B)** Replicas. Taken from Versiani and Keleș (2020).

Enamel is the hardest biological tissue in the body and is the hard-protective substance that covers the tooth crown. It provides the shape and contour to the crown and covers the part of the tooth that is exposed to the oral environment. Enamel is composed of interlocking rods that are deposited in a keyhole shape by ameloblasts. Enamel is composed of approximately 96% inorganic mineral in

the form of hydroxyapatite (HA) and 4% organic material and water, by weight (Chiego, 2019). Hydroxyapatite is a crystalline calcium phosphate that is also found in dentine, cementum and bone, whereas the protein enameline is the organic component of enamel. Because enamel is formed of bending rods, tiny gaps exist between enamel rods where crystals did not form. This feature causes variability in enamel density and hardness, where some areas of enamel may be more prone to penetration by small particles, which lead to tooth destruction by dental decay. After enamel is entirely formed, no more enamel can be deposited (Chiego, 2019).

In contrast, dentine is a living sensitive tissue covered by enamel on the crown and cementum on the root, and it surrounds coronal and radicular pulp. By weight, approximately, 70% of dentine is composed of inorganic hydroxyapatite crystals and 20% is organic collagen fibers with small amounts of other proteins, and the remaining 10% of dentine is water (Chiego, 2019, Grawish et al., 2022). Dentine is classified as primary, secondary and tertiary according to the time of its development and histological characteristics. Primary dentine is the main component of the crown and the root and is the earliest secreted tissue. It consists of mantle dentine, globular dentine and circum-pulpal dentine (Goldberg, 2014, Chiego, 2019). As teeth begin to function, and roots are nearly completed, secondary dentine is produced which is deposited more slowly than primary dentine. When the pulp is affected by caries or mechanical trauma, tertiary dentine is formed focally underlying the affected area, at the site of odontoblastic activation, the function of which is to protect the pulp (Chiego, 2019). Tertiary dentine is either reactionary or reparative. Reactionary dentine is tertiary dentine matrix produced by surviving odontoblasts in response to a stimulus. Reparative dentine, in contrast, is formed by odontoblast-like cells, after the death of primary odontoblast cells, in response to much stronger stimuli (A Smith et al., 1990, Cooper et al., 2010). The resulting dentine can range from being regular tubular to irregular and atubular, depending on the formative cell differentiation status (AAE, 2020). Microscopically, dentine is composed of a circular duct dispersed in the dentine matrix called a dentinal tubule, which contains the odontoblastic process and fluid. The number of dentinal tubules ranges from 20,000 to 75,000 per square millimetre of dentine (AAE, 2020). Peritubular dentine is a highly calcified, narrow strip of dentine

that encircles the lumen of each tubule, while intertubular dentine is the calcified collagen matrix found external to the peritubular dentine (AAE, 2020). Within this unique structure, it has been found that the volume of dentinal canals (space available for bacteria to grow) was at least three times greater than the root canal volume itself that can be instrumented with current means (Burkovski and Karl, 2019).

The root canal space has been referred to as a system, as it is often complex with canals that divide and rejoin, isthmuses, fins, anastomosis, apical deltas, and accessory canals (Versiani and Ordinola-Zapata, 2015). Krasner and Rankow (2004) proposed laws for finding pulp chambers and root-canal orifices. The use of these laws can help the practitioner in locating the number and position of canal orifices on pulp-chamber floors in any individual tooth. The main root canal has its greatest diameter at the orifice level, and usually has a funnel shape and an ovoid cross section (Versiani and Ordinola-Zapata, 2015). The narrowest part of the root canal is located at the apical constriction, which opens out as the apical foramen and exits to one side of the root (Carrotte, 2004). The apical constriction is commonly considered the ideal termination for root canal treatment where the root canal obturation materials are packed against a natural stop that represents the pulp termination (M Wu et al., 2000). Importantly, it must be realised that the concept of constant topography of the apical constriction is erroneous, as four distinguishable types of apical constrictions were identified by Dummer et al. (1984), in a classical paper, as follows: “traditional” single constriction, tapering constriction, multi-constricted and parallel constriction. The location of the apical constriction can also vary among roots, and could be located up to 3 mm from the anatomical root apex (Dummer et al., 1984).

On the other hand, it is not uncommon for teeth to have band-shaped isthmuses. The canal isthmus has been defined by Weller et al. (1995) as a narrow, ribbon-shaped connection between two root canals encompassing pulp tissue. It has been found by Keleş et al. (2022) that isthmus communications were present in 13.5% of upper first molars examined. These communications may be a concern during root canal treatment, as they can be present through half of the root length (Keleş et al., 2022). Additionally, a single root canal might break up into multiple ramifications with multiple apical foramina. This morphology is called

an apical delta (Carrotte, 2004). Accessory or lateral canals are also part of anatomical complexities of the root canal system. An accessory canal is referred to as any branch that diverges from the main pulp chamber or canal and communicates with the external surface of the root (AAE, 2020). In a study by Senan et al. (2018), apical deltas and accessory canals were found in 13.2% and 52.8%, respectively, of maxillary first premolars collected for the study. Therefore, the objectives of root canal treatment may be difficult to attain in teeth with such anatomical complexities or in curved root canals (Siqueira et al., 2019), as shown (Figure 1.3).

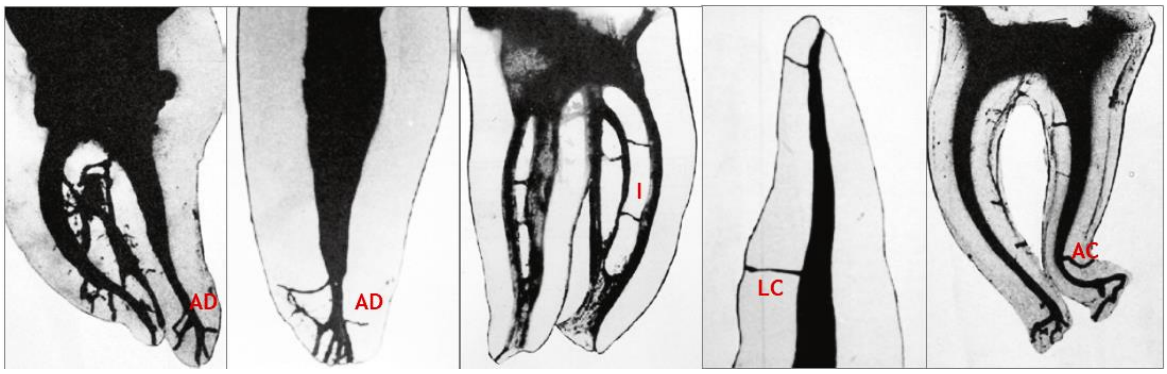

Figure 1.3. Internal complex morphology of different teeth. The root canal system showing the presence of apical delta (AD), isthmuses (I), lateral (LC) and accessory (AC) canals. Adapted from Castellucci (2019).

1.3 Endodontic infection

The ultimate biological aim of endodontic treatment is either to prevent or heal apical periodontitis. Pulpal and periapical tissue infections have long been perceived as an extension of the caries process because of the dominance of dental caries as a portal of dentine infection for decades (Ørstavik, 2019) (Figure 1.4). However, tissue infections and responses are probably an older and more general biological manifestation than dental decay. Apical periodontitis may be seen as a tissue response to infection of the pulp as a way of "taming" and "coping" with virulence expressions by infectious microorganisms (Ørstavik, 2019), or may be viewed as protective means against the spread of infection, where the process of self-induced destruction of apical periodontitis provides a space for the infiltration of specialised immune cells and creation of a barrier to prevent the spread of infection (Nair, 2004).

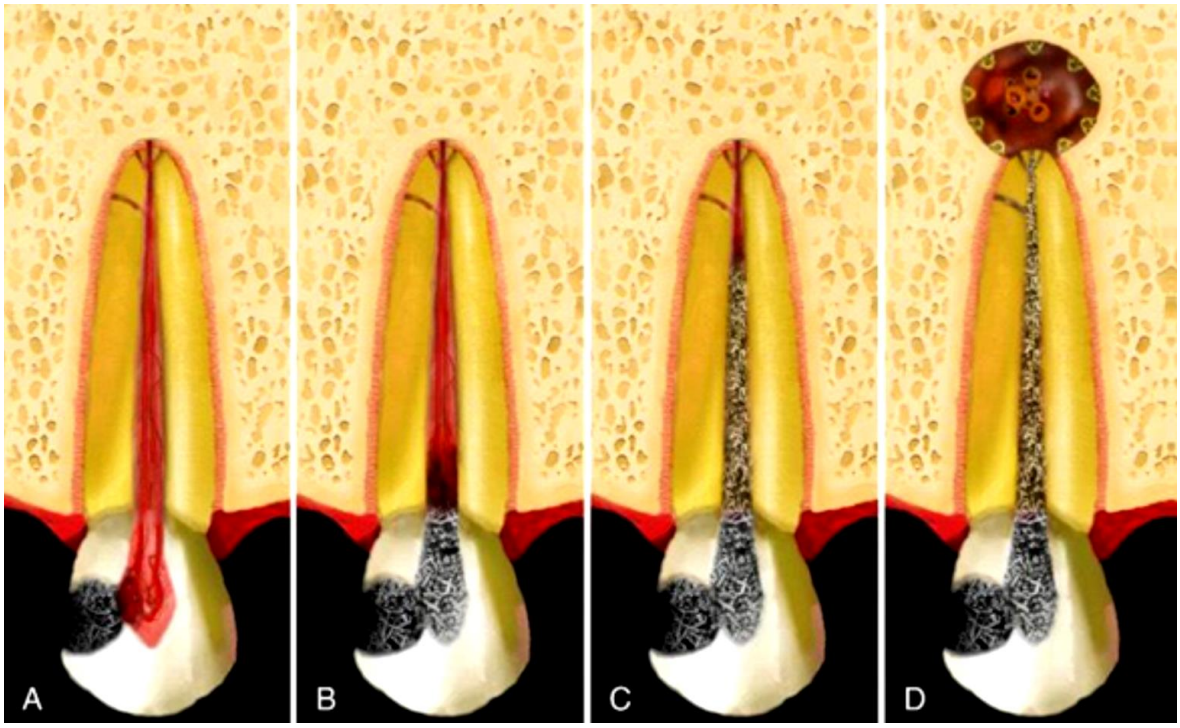

Figure 1.4. Stages of root canal infection. (A) Caries exposure and pulpal inflammation. The exposed pulp tissue is in direct contact with infectious microorganisms and responses with severe inflammation. **(B) & (C)** Colonising the pulp tissue. Infectious microorganisms move forward and colonise the pulp which is become necrotic after microbial/immune response clash. **(D)** Apical periodontitis formation. The entire root canal is necrotic and infected. Taken from Siqueira and Rôças (2016).

The substantial role of intraradicular infections, in the form of biofilms, was established in the root canal system of teeth with apical periodontitis (Ricucci et al., 2009, Ricucci and Siqueira, 2010, Ricucci et al., 2017). A biofilm is defined as a highly structured community of microorganisms encased in a protective extracellular matrix (ECM) that adheres to a biotic or abiotic surface (Hall-Stoodley et al., 2004). A very high prevalence of bacterial biofilms was reported by Ricucci and Siqueira (2010) in untreated and treated apical root canals with apical periodontitis through a histobacteriologic approach. In this study, biofilms were observed clogging the walls of apical ramifications, lateral canals and isthmuses. However, the biofilm morphologic structure varied between individuals, and no unique morphological pattern for an endodontic biofilm was identified. Planktonic cells were also seen in the specimens, and the presence of biofilms was found to be more likely in association with longstanding pathology, including large lesions and cysts (Ricucci and Siqueira, 2010). In a similar histobacteriologic study on immature teeth, bacterial aggregations of varying thickness have been observed colonising necrotic canals. In some sections, the

root canal lumen appeared to be completely filled with bacterial biofilm (Ricucci et al., 2017). Irrespective of these findings, can endodontic infections be driven by biofilms? In fact, several general diagnostic criteria for biofilm infections have been proposed in the literature to define whether a human infectious disease is caused by biofilms. These criteria were as follow: (1) the infectious bacteria are adherent to some substratum or associated with a surface, (2) direct examination of infected tissue demonstrates bacteria living in clusters or microcolonies enclosed within an extracellular matrix, (3) infection is generally confined to a specific site in the host, although dissemination may occur as a secondary incident and (4) infection is difficult or impossible to eradicate with antibiotics even though the infectious species are susceptible to eradication in the planktonic state (Parsek and Singh, 2003). Furthermore, (5) bacterial cell clusters, associated with host inflammatory cells, are located in discrete areas in the host tissue, which indicate ineffective host clearance (Hall-Stoodley and Stoodley, 2009) and finally (6) the elimination or considerable disruption of the biofilm structure and ecology leads to disease remission (Ricucci and Siqueira, 2010). Regarding criterium 4, it is well known that local or systemic antibiotics are not indicated for confined endodontic infections unless systemic involvement is evident (Segura-Egea et al., 2018). Therefore, according to Ricucci and Siqueira (2010), features observed in biofilms, from an endodontic perspective, seem to fulfil these criteria.

Primary “initial” endodontic infections are caused by microorganisms that colonise the necrotic pulp tissue and are the cause of primary apical periodontitis that can present itself as a chronic or acute disease. Secondary infections are caused by microorganisms that were introduced in the root canal following professional intervention, whereas persistent infections can be caused by microorganisms that were members of either primary or secondary infections that persist in the root canals following treatment (Siqueira and Rôças, 2009). Determining the microbial composition and diversity involved in persistent apical periodontitis and their possible relationships with various clinical features is essential for the development of new therapeutic approaches that may enhance clinical outcomes (Sánchez-Sanhueza et al., 2018). Traditionally, microbiological examination of endodontic microbiota was based upon culture techniques. A variety of bacterial species have been reported to be present in infected root

canals. The microbial flora seen in primary disease (endodontic infection that occurs in root canals that have not been previously treated) is typically polymicrobial in nature with Gram-negative and Gram-positive bacteria dominated by obligate anaerobes (Siqueira and Rôças, 2009). Historically, the most predominant species in root canal-treated teeth with persistent/secondary infections were considered Gram-positive facultative anaerobes (Siqueira and Rôças, 2009). However, Gram-negative bacteria such as *Treponema* species have been isolated from root canals with endodontic failures (Gomes et al., 2006, Nóbrega et al., 2013). More complex mixed-species were recovered from root canals with post-treatment apical periodontitis (Siqueira et al., 2016, Sánchez-Sanhueza et al., 2018), where Gram-negative bacteria were the most dominant. Recently, a significantly greater microbial diversity has been demonstrated in symptomatic infections than asymptomatic infections especially between individuals with mild and severe systemic diseases, categorised according to the American Society of Anesthesiologists (ASA) as ASA II–III (Sánchez-Sanhueza et al., 2018).

While *Enterococcus faecalis* (*E. faecalis*) is often considered important by endodontists due to its frequent association with treatment failure (Sundqvist et al., 1998, C Zhang et al., 2015, Alghamdi and Shakir, 2020), the focus has been moved from the concept of "single-pathogen" to the "community-as-pathogen". Thus, the polymicrobial aetiology of root canal infections is a more plausible scenario (Siqueira and Rôças, 2014). Using next-generation sequencing (NGS) technologies, a review outlined that the most commonly detected genera in primary and persistent endodontic infections were *Prevotella*, *Fusobacterium*, *Porphyromonas*, *Parvimonas*, and *Streptococcus* (Shin et al., 2018). In another review, the most abundant phyla, regardless of the infection type, were *Firmicutes*, *Bacteroidetes*, *Proteobacteria*, *Actinobacteria*, and *Fusobacteria* (Manoil et al., 2020).

Moreover, archaea (Brzezińska-Błaszczyk et al., 2018), viruses (Vigueras et al., 2016) and fungi (Mergoni et al., 2018) have also been implicated in endodontic disease. Yeasts are prevalent in the oral cavity, and it is unsurprising that they represent an important yet unrecognised group of microbes in this environment. A systematic review and meta-analysis demonstrated that *Candida* species occurred in a small proportion of root canal infections, with a prevalence of

8.2%, and *Candida albicans* (*C. albicans*) being the most frequently isolated species (Mergoni et al., 2018).

Many studies are bacterial biased and use 16S ribosomal ribonucleic acid (rRNA) gene analysis, which limits these studies to large-scale detection of bacterial communities. It is essential that a broader view on endodontic infections is taken. This is of clinical significance, as there is the potential for interkingdom biofilm interactions between bacteria and yeasts (Figure 1.5) in the root canal, which are likely to complicate the infection and require alternative treatment strategies (Persoon et al., 2017, Du et al., 2021).

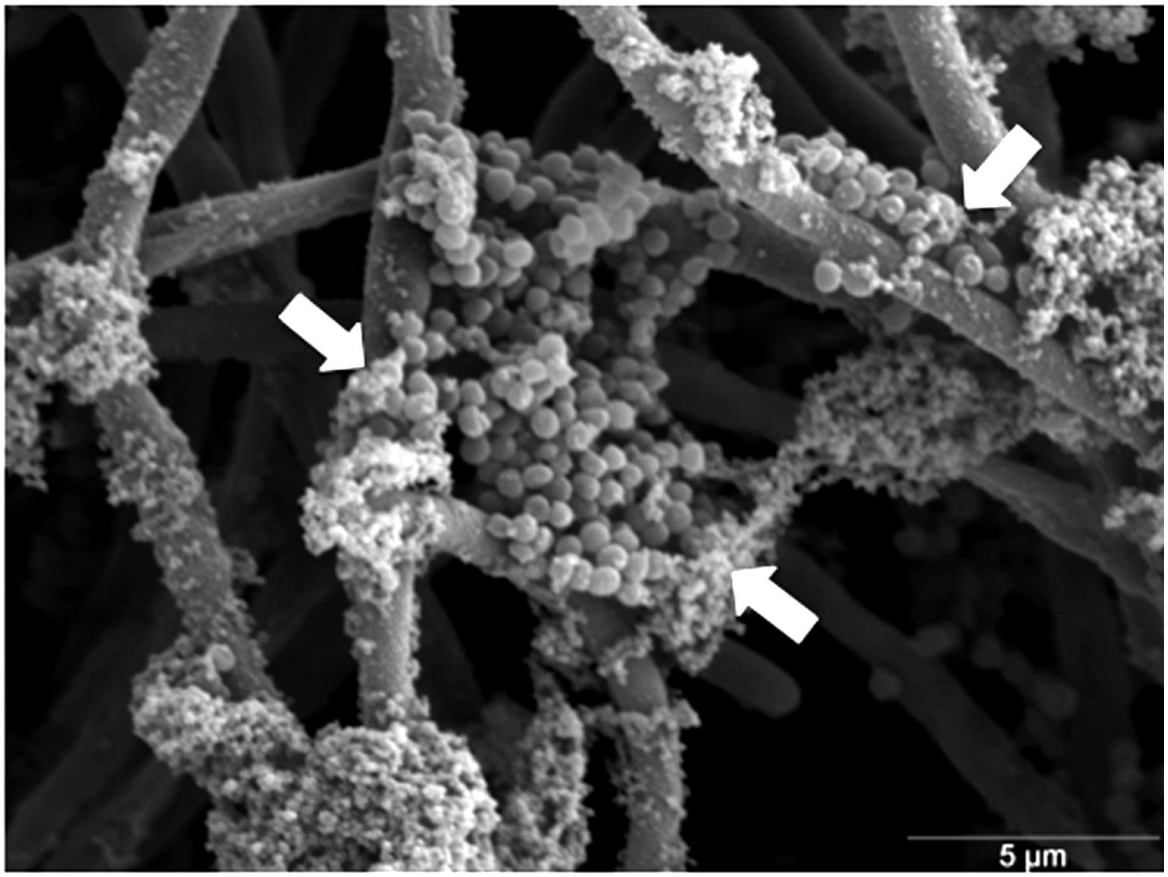

Figure 1.5. Scanning electron microscopy of *S. aureus* colonising *C. albicans* hyphae in dual-species biofilms. White arrows indicate clusters of *S. aureus* colonies adhering and embedded within the hyphae of *C. albicans*. Scale bar represents 5 µm at ×5,000 magnification (Kean et al., 2017).

Recently, there has been an evolving interest in determining the microbial composition and diversity involved in endodontic infection to include healthy teeth. Widmer et al. (2018) challenged the basic concept of natural sterility of

the dental pulp. Evidence was presented that the dental pulp spaces of pristine healthy teeth contain detectable bacterial deoxyribonucleic acid (DNA), in which *Ralstonia*, *Acinetobacter*, and *Staphylococcus* genera were predominant. The study suggested that vital pulp from intact teeth may harbour bacteria that may reach the pulp without a known external pathway (Widmer et al., 2018). Tantalising though this is, a caveat to these observations is that studies relied only on DNA detection rather than actively growing bacteria, caution is necessary in over interpretation of these findings. Nonetheless, Qian et al. (2019) aimed to uncover the composition and diversity of bacteria at the root apex in teeth with apical periodontitis, with/without root canal treatment and in healthy teeth (healthy controls). An additional healthy control was sampled from biofilm of the buccal mucosa. The results exhibited reduced richness and diversity in microbial communities from infected teeth compared to healthy controls. Possibly surprisingly, this study by Qian et al. (2019) suggested a high abundance of commensal microorganisms around the root apex of healthy teeth. The study speculates that these abundant bacteria might be essential for keeping a healthy environment prior to disruption in apical periodontitis, where both richness and diversity decrease. Irrespective, these studies all highlight the complex microbial ecology that interacts with the root canal system.

Microbiologically, polymicrobial communities of the human oral cavity have been studied extensively and represent a paradigm for biofilm-related infection. Our tacit understanding of this has evolved from initial simple, and yet biased, culture-based approaches into complex and all-encompassing next-generation sequencing of oral clinical endodontics disease. These molecular methods have greatly contributed to our understanding of the functional ecology of oral flora in health and disease (Gao et al., 2018). A vast array of different microorganisms is known to inhabit the human oral cavity. To date, it has been established by Human oral microbiome database (HOMD) that there are 774 oral bacterial species in the oral cavity (homd.org). In addition, a total number of 101 fungal species were found in healthy individuals (Ghannoum et al., 2010). Oral microbiomes play an important role in maintenance of health, with dynamic shift in these endogenous microbiomes driving oral disease (Jorth et al., 2014).

1.4 Detection: does knowledge of microbiology impact endodontic decision making?

Despite the potential shortcomings of microbial detection prior to or during treatment, the possibility of more efficient treatment to decrease persistent infections in the root canal space resulting in reduced treatment costs would certainly seem advantageous (Herzog et al., 2017). Current clinical practices aimed at detecting bacteria in the root canal space rely on subjective observations. An example of which is the appearance of clean, white dentinal shavings in the flutes of endodontic instruments used for root canal debridement (Herzog et al., 2017). Conventional microbiology techniques, such as colony-forming unit (CFU) counting, and more contemporary polymerase chain reaction (PCR) based analysis, have been employed (Berber et al., 2006, Björk and Wu, 2018). Such methods are time-consuming, making them impracticable for routine intraoperative application (Herzog et al., 2017). A number of methods have been developed to rapidly detect bacteria within the root canal during treatment. A method was developed for bacterial identification within the root canal based upon autofluorescence. This approach could identify bacteria in less than ten minutes (Giana et al., 2003). Although the bacterial identification was very efficient amongst different species, false positives and incorrect identification occurred. Sato et al. (2012) developed a method using fluorescence reagents and a membrane filter. The technique allowed determination of the number of live bacterial cells by distinguishing live and dead bacterial cells in the sample of infected root canals (Sato et al., 2012). However, the assay is somewhat time consuming. Bioluminescence-based Adenosine triphosphate (ATP) detection method as a rapid tool to detect viable bacteria during root canal treatment has also been developed by K Tan et al. (2015). The results can be obtained within approximately 5 minutes, making the assay more clinically acceptable. The ATP method only detects a bacterial signal opposed to an identification of microorganisms present within an infected root canal. False positive results may also be generated if human cells are included during sampling, thus contamination is a real risk should the sampling point penetrate the apical foramen (K Tan et al., 2015). A further system has been developed by Herzog et al. (2017), based upon an optical fluorescence-based method. This chair-side test allows clinicians to detect *ex vivo* residual vital bacteria objectively and rapidly in samples taken during root canal treatment (Figure 1.6).

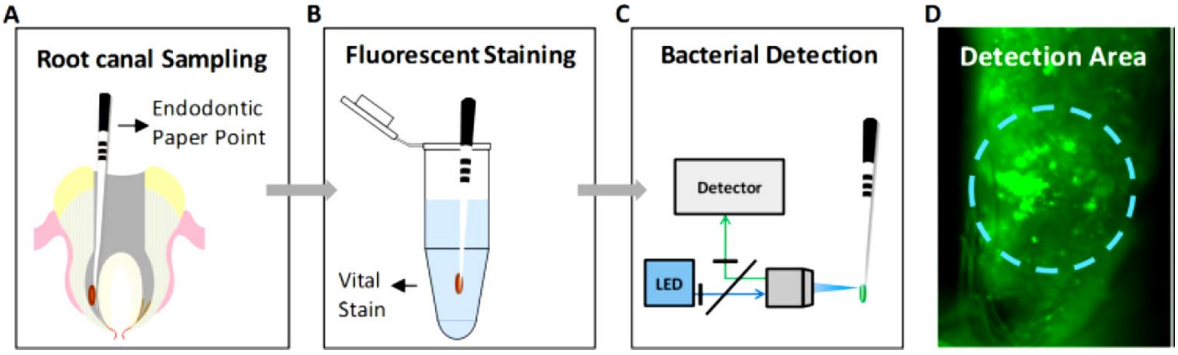

Figure 1.6. Outline of clinical bacterial detection during root canal treatment. An optical fluorescence-based method is a chair-side test allows clinicians to detect *ex vivo* residual vital bacteria in samples taken from root canals during treatment**. (A)** Sampling of the root canal space with an endodontic paper point. **(B)** Fluorescence staining of sample. **(C)** Bacterial detection of the fluorescent signal. **(D)** The indicated detection area for spectral analysis. Taken from Herzog et al. (2017).

Staining with Calcein acetoxymethyl dye in combination with spectral analysis results is a rapid method that causes minimal disruption to the clinical workflow, as measurements can be achieved in 5 min, making the technique a viable, rapid and quantitative methodology for introduction into the current workstream of dental practices (Herzog et al., 2017). If such chair-side assays were introduced into clinical practice, where would benefits be seen? As stated, it is unlikely to impact upon outcomes, however, it is with efficiencies of procedure that the true benefit will be realised. Treatment times may be reduced, or numbers of visits can be minimised. A clear endpoint for disinfection could be identified so unnecessary time spent disinfecting the already adequately disinfected canal could be minimised. Such tests could give a green light for obturation. Clearly, although outcomes may be minimally impacted, the cost benefits to dentist and patient of determining such an endpoint could be substantial. It will be necessary to package such chair-side detection systems into inexpensive and simple kits that sit within the dental operatory.

1.5 Treatment: eradication of endodontic infections

1.5.1 Chemo-mechanical disinfection procedures

The mechanical preparation of the root canal and chemical disinfection are commonly referred to as “chemo-mechanical” or “biomechanical” preparation (Hülsmann et al., 2005). The disinfecting of the root canal system and

elimination of any sources of nutrient supply, such as tissue remnants, are the key goals (Siqueira et al., 2000). Thus, chemo-mechanical procedures can be regarded as the most important phase of root canal treatment. Their main purposes are to clean, disinfect and shape the root canal. Mechanical instrumentation aims to create space in the root canal system to facilitate disinfection by irrigants and antimicrobial inter-appointment medicaments (Hülsmann et al., 2005). It generates a layer of organic and inorganic substances, such as fragments of odontoblastic processes and necrotic debris, on root canals known as “smear layer” that may also contain bacteria and their byproducts (Torabinejad et al., 2002).

Irrigants are used for their antimicrobial actions, to dissolve organic tissue in the canal, to lubricate the dentinal wall and to flush out debris (Cobankara et al., 2010). Irrigant flow is crucial during root canal treatment to create fluid dynamics that exhibits the following features: (1) ensuring distribution of the irrigant throughout the root canal system’s full extent, (2) ensuring frictional forces generated between the root canal wall and the irrigant (wall shear stress) that participate in the mechanical cleaning of the substrate, (3) maintains the irrigant solution within the root canal system and prevents its extrusion into the periapical tissues and (4) maintains a frequent replenishment of the solution to restore the desired effective concentration of the irrigant (van der Sluis et al., 2016). Various methods have been introduced to distribute irrigants more effectively to the working length, and to flush out the debris. It has been shown that passive irrigation (syringe irrigation – no agitation was applied) showed the greatest level of residual biofilm than manual agitation of irrigants (using a gutta-percha cone) or automated sonic (using an EndoActivator device) and ultrasonic methods (using a Satelec P5 ultrasonic device), where ultrasonic agitation exhibited the greatest level of biofilm removal (Mohmmed et al., 2017, Mohmmed et al., 2018). However, it was found that ultrasonic irrigation exhibits no benefits over needle irrigation (passive irrigation) in improving the healing rate of apical periodontitis (George, 2019). Nevertheless, a systematic review and meta-analysis showed that machine-assisted agitation reduces post-operative pain, during non-surgical root canal treatment, compared with syringe irrigation (Rossi-Fedele et al., 2019). Future clinical trials are required to support or refute these results.

1.5.2 Current irrigants in endodontics

Several studies have been conducted in the search for an endodontic irrigant that meets the four major desirable properties namely: antimicrobial activity, nontoxicity, water solubility and the tissue-dissolving property (Mohammadi and Abbott, 2009).

1.5.2.1 Sodium hypochlorite (NaOCl)

Sodium hypochlorite is one of the most used irrigants in root canal treatment. Although the bacterial load in infected root canals can be significantly reduced by using saline as an irrigant purely by its mechanical action, irrigation with NaOCl has a clearly superior effectiveness in bacterial reduction. This is due to that NaOCl possessing chemical antimicrobial effects in addition to its mechanical effects (Siqueira et al., 2000). These antimicrobial and tissue-dissolving abilities have been widely reported (Siqueira et al., 2000, Christensen et al., 2008, Cobankara et al., 2010). A poorer antimicrobial activity of NaOCl has been shown in the presence of smear layer (Wang et al., 2013, Morago et al., 2016). It is possible that the organic components, in contact with NaOCl, consume the free available chlorine and reduce the solution's antimicrobial activity (Siqueira et al., 2000). Another possibility is that the smear layer acts as a physical barrier, hindering the irrigant diffusion into the dentinal tubules (Wang et al., 2013). There is no universally accepted NaOCl concentration for endodontic treatment; with concentrations ranging from 0.5% to 5.25% and above (Hegde et al., 2021). Although NaOCl is generally considered safe, potentially severe complications can occur in endodontic dental practice when it contacts soft tissue (Spencer et al., 2007, Hegde et al., 2021).

1.5.2.2 Chlorhexidine (CHX)

Chlorhexidine is used widely as an endodontic irrigant and medicament (Mohammadi and Abbott, 2009). Chlorhexidine, a bis-biguanide, contains two positively charged guanide groups and three comparatively small hydrophobic portions represented by two terminal chlorophenyl groups and a central hexamethylene chain (Leach, 1977). Its efficacy is closely related to the interaction of guanide groups and negatively charged sites on the microbial cell walls, resulting in rupture of the cytoplasmic membrane (Davies et al., 1968). Its

antimicrobial properties and its clinical application as an adjunct to periodontal therapy has justified its use as a potential endodontic irrigant (Jeansonne and White, 1994). Using 2% chlorhexidine as an irrigation solution during root canal instrumentation have shown its antimicrobial activity with extended residual effects (substantivity) in the root canal system up to 48 h after instrumentation (Leonardo et al., 1999). However, unlike NaOCl, it has little or no tissue dissolution capacity (Okino et al., 2004, Naenni et al., 2004), and cannot remove the smear layer (Attur et al., 2016). The possibility of developing life-threatening hypersensitivity reactions to chlorhexidine is another concern (Donaldson and Goodchild, 2019). A few clinical studies compared the antimicrobial activities of NaOCl and CHX. For instance, a randomised clinical study reported that using either 2.5% NaOCl or 2% CHX as the main irrigant with rotary nickel-titanium instruments reduced the levels of total bacterial counts effectively, with no significant differences (Rôças et al., 2016). A systematic review and meta-analysis showed that NaOCl was more effective than CHX in reducing endotoxin levels after chemo-mechanical preparation in primary endodontic infections (Neelakantan et al., 2019). Another systematic review and meta-analysis indicated that both NaOCl and CHX were equally effective in reducing microbial infections following irrigation (Ruksakiet et al., 2020). However, both reviews show limitations in the interpretation of their findings because of the limited data extracted from the included clinical trials.

1.5.2.3 Ethylenediaminetetraacetic acid (EDTA)

Ethylenediaminetetraacetic acid is a common endodontic irrigant used to remove the smear layer by acting on inorganic material (Violich and Chandler, 2010). The sodium salts of EDTA are noncolloidal organic chelating agents that have the ability to form soluble nonionic chelates with metallic ions such as calcium in hard tissues (Nikiforuk and Sreebny, 1953). The application of NaOCl followed by 17% EDTA is a common irrigation protocol in root canal treatment (Mohammadi and Abbott, 2009, Kfir et al., 2020). This combination and sequence of irrigants remove both organic and inorganic components of the smear layer efficiently. Sodium hypochlorite removes organic material of dentine and pulp effectively, whilst EDTA removes the organic and inorganic substances in dentine and also some organic components in the pulp (Beltz et al., 2003). It has also been shown that the sequential use of these irrigants had a

significant regrowth inhibition of *Candida* strains treated with 3% NaOCl followed by 17% EDTA, when compared with NaOCl alone (Alshanta et al., 2019). Importantly, EDTA and NaOCl should be used separately as NaOCl loses its tissue-dissolving capacity when mixed with EDTA (Grawehr et al., 2003).

The use of alternative agents as a final rinse has been suggested. One such alternative is the mixture of a tetracycline isomer, an acid and a detergent (MTAD) in conjuction with NaOCl, which has been suggested bacause of its comparable efficiency for smear layer removal, compared with EDTA but without the erosive effect on tooth structure (Torabinejad et al., 2003). It has been shown that compromised dentine may have an increased potential for bacterial adherence on the exposed collagen when treated with EDTA as a final irrigant (Kishen et al., 2008). However, high-quality *in vitro* evidence provided by a systematic review suggests that conditioning dentine with EDTA positively influences the release of growth factors and improves cell migration, attachment and differentiation (dos Reis-Prado et al., 2022), which is critical for the success of regenerative endodontic procedures.

1.5.3 Natural antimicrobial compounds

The research for more biocompatible antimicrobial solutions continues. The use of herbal products as alternative antimicrobial therapeutics has gained popularity over the past few years (Almadi and Almohaimede, 2018). Propolis (bee glue) is one of the natural substances that was extensively been used by ancient Egyptians, Greeks and Romans as a medicine (Kuropatnicki et al., 2013). Propolis is a resinous substance collected by honeybees from various plant sources. As a resinous substance, propolis is used by bees to coat and seal hive parts and cell interiors of the honeycomb (Ghisalberti et al., 1978). It has been found that propolis samples, from different geographic areas, possess antibacterial, antifungal and antiviral activities despite of a variable chemical composition (Kujumgiev et al., 1999). Propolis as an endodontic irrigant has shown a comparable antimicrobial efficacy to NaOCl and CHX against *C. albicans* in the presence and absence of smear layer (Awawdeh et al., 2018b). In another study, propolis was found to be as efficient as NaOCl against *C. albicans*, *S. aureus* and *E. faecalis*. However, CHX and MTAD had the highest antimicrobial activity followed by propolis (Mattigatti et al., 2012). As an intracanal

medicament, propolis was as effective as CHX gel in reducing *E. faecalis* in dentine in extracted teeth, whereas CHX gel was found to have the highest antifungal efficacy against *C. albicans* (Carbajal Mejía, 2014). As a pulp capping material, propolis stimulated the formation of reparative dentine in rats with direct pulp capping (Sabir et al., 2005). In addition, it has been found that propolis as a storage media maintained the viability of periodontal ligament cells of avulsed teeth, better than Hank's balanced salt solution (HBSS), milk or saline (Martin and Pileggi, 2004, Ahangari et al., 2013). Most of these antimicrobial studies are *in vitro* studies which used only a single microorganism as a model for testing these novel therapeutics. However, a randomised controlled trial by Siddique et al. (2020) showed that garlic-lemon extract was as effective as NaOCl in reducing microbial load using qPCR in teeth with asymptomatic apical periodontitis following instrumentation. Amongst the large number of tested natural compounds, only a few showed antimicrobial efficacies comparable to that of NaOCl and none were superior (Table 1.1).

Table 1.1. Examples of tested natural compounds as potential alternatives to conventional endodontic antimicrobials.

Natural compound	Study	Compared to conventional antimicrobials
Propolis	(Awawdeh et al., 2018b)	Comparable
Turmeric (Curcuma longa)	(Kumar, 2013)	Comparable
Neem (Azadirachta Indica)	(Vinothkumar et al., 2013)*	Comparable
Garlic-lemon extract	(Siddique et al., 2020)**	Comparable
Tea tree oil	(Kamath et al., 2013)	Comparable
Triphala	(Prabhakar et al., 2010, Pujar et al., 2011, Divia et al., 2018)	Comparable to or inferior
Noni plant (Morinda Citrifolia)	(Podar et al., 2015, Divia et al., 2018)	Comparable to or inferior
Green Tea	(Prabhakar et al., 2010, Pujar et al., 2011, Divia et al., 2018)	Inferior
Ozonated olive oil	(Mittal et al., 2022)**	Comparable

* *In vitro* study using qPCR. ** Randomised clinical trial using qPCR.

1.5.4 Intracanal dressing: the continuing and growing debate

The combinations of mechanical instrumentation of the root canal and chemical antimicrobial agents aim to disturb and eradicate biofilm communities. The inclusion of an additional step whereby an antimicrobial agent (often a calcium hydroxide [$Ca(OH)_2$] paste) is sealed within the tooth between the disinfection and obturation (filling) visits, has been a part of many dentists' protocols. There is continued debate concerning the need or effectiveness of multiple-appointment endodontic therapy (Su et al., 2011). In fact, filling teeth with early stages of pulp infection, in one appointment, has been justified from a clinical perspective. This justification was based on the principle that all bacteria are more likely to be removed, in a single visit, when superficially located during the early stage of pulp inflammation, when most of the pulp tissue is still intact. Immediate obturation and sealing of the access opening will reduce the chances of new bacterial entry (Bergenholtz et al., 2015). Single visit was also suggested for necrotic pulps with asymptomatic apical periodontitis, with or without a patent sinus tract (Arens et al., 2009). However, the support for the ability of a calcium hydroxide inter-appointment medicament to suppress

microbial growth was shown *in vivo* by Vera et al. (2012) for teeth with primary apical periodontitis. The results showing that $Ca(OH)_2$ has maximised bacterial reduction of roots with the two-visit protocol, while residual bacteria, with the one-visit procedure, were more abundant within the root canals' ramifications, isthmuses and dentinal tubules of teeth treated without an inter-appointment medication.

This antimicrobial effect of $Ca(OH)_2$ is related to the release of calcium ions when in aqueous solution, resulting in high pH levels (Hosoya et al., 2001). The antimicrobial effects can be enhanced by incorporating different compounds into it. For instance, it was shown that a combination of intracanal medicaments of $Ca(OH)_2$ and chlorhexidine gel (Sinha et al., 2013), a mixture of chitosan nanoparticles (CSNPs) and $Ca(OH)_2$ (del Carpio-Perochena et al., 2017) and a combination of $Ca(OH)_2$ and silver nanoparticles (AgNPs) (Afkhami et al., 2015), all produced additive antimicrobial effects to the $Ca(OH)_2$ alone. Despite the studies outlined, the Cochrane database of systematic reviews (Figini et al., 2008, Manfredi et al., 2016) found no evidence to suggest that one treatment regimen (one-visit or multiple-visit) is better than other. In fact, “neither can prevent 100% of short- and long-term complications”. It is clear that there is a need for a well-designed randomised controlled trial to establish better the effect of numbers of visits/inclusion of an intracanal medicament on outcome. However, based on the available evidence, it seems that patients undergoing a single visit may experience a higher frequency of late post-operative pain and are more likely to require painkillers. It is possible that in the single visit the working time is longer, causing a more severe acute inflammatory response, manifested as pain (Figini et al., 2008, Manfredi et al., 2016).

1.5.5 Regenerative endodontics – an alternative treatment option?

Despite significant advances in endodontic materials over the past few decades, outcomes in endodontics have not improved significantly (Zanza et al., 2022). Why have we failed to achieve higher success rates? Do we need to depart from the traditional and start to explore biologically based alternatives? Dental pulp regeneration represents a major departure from traditional endodontic treatment and a potential avenue for exploration that may offer access to

improved outcomes. Pulp regeneration may be defined as the replacement of damaged tissue by cells with the same characteristics as the lost tissue, leading to complete restoration of biological function of injured tissue. Unlike regeneration, repair is the replacement of damaged tissue with a different tissue, closer to a periodontal one rather than a pulp tissue (Simon and Goldberg, 2014). Regenerative endodontics has emerged as new treatment modality for cases of immature teeth after pulp necrosis. Not only does it provide apical closure, as apexification, but also increases the dentine walls thickness and length of immature roots that otherwise are susceptible to fracture. Both the European Society of Endodontology (ESE) (Galler et al., 2016) and American Association of Endodontists (AAE, 2021) have published guidelines for immature teeth with pulp necrosis to help clinicians stay current with the advancing scientific literature in regenerative endodontics. The degree of success of regenerative endodontic procedures (REPs) is largely measured by the extent to which it is possible to achieve primary, secondary and tertiary goals. The primary goal is to eliminate symptoms and to drive bone healing. The secondary goal is to increase root wall thickness and/or increase root length. Finally, the tertiary goal is to induce a positive response to vitality testing (AAE, 2021).

Traditionally, three elements have been used to achieve pulp regeneration, namely (1) stem cells (progenitor cells), (2) scaffolds and (3) signalling molecules (e.g. growth factors) (J Yang et al., 2016). The first key element is stem cells (SCs), which can be defined as unspecialised cells with the ability to undergo self-renewal, proliferation and differentiation into more specialised functional cells (Potten and Wilson, 2009). There are two primary sources of stem cells naturally present in the human body: embryonic and adult stem cells. Many adult stem cell sources have been identified in the oral and maxillofacial region (Figure 1.7), many of which are believed to reside in mesenchymal tissues. These cells are termed collectively as mesenchymal stem cells (MSCs) (Egusa et al., 2012). The current REP guidelines advocate the practice of evoked bleeding by lacerating periapical tissues, through over instrumentation, after disinfection of the root canal system. This recruits stem cells that reside apically. The blood clot that forms inside the root canal following the resultant haemorrhage, acts as a scaffold for the regeneration of pulp tissues (AAE, 2021).

The antimicrobial properties of human MSCs have recently been investigated. It was found that MSCs exhibited high levels of direct bactericidal activities, and indirect antimicrobial effects mediated via activation of host innate immune defences, including trigger of neutrophil extracellular trap formation. In addition, soluble factors secreted by MSCs augmented the antimicrobial activity of several major classes of antibiotics (Chow et al., 2019).

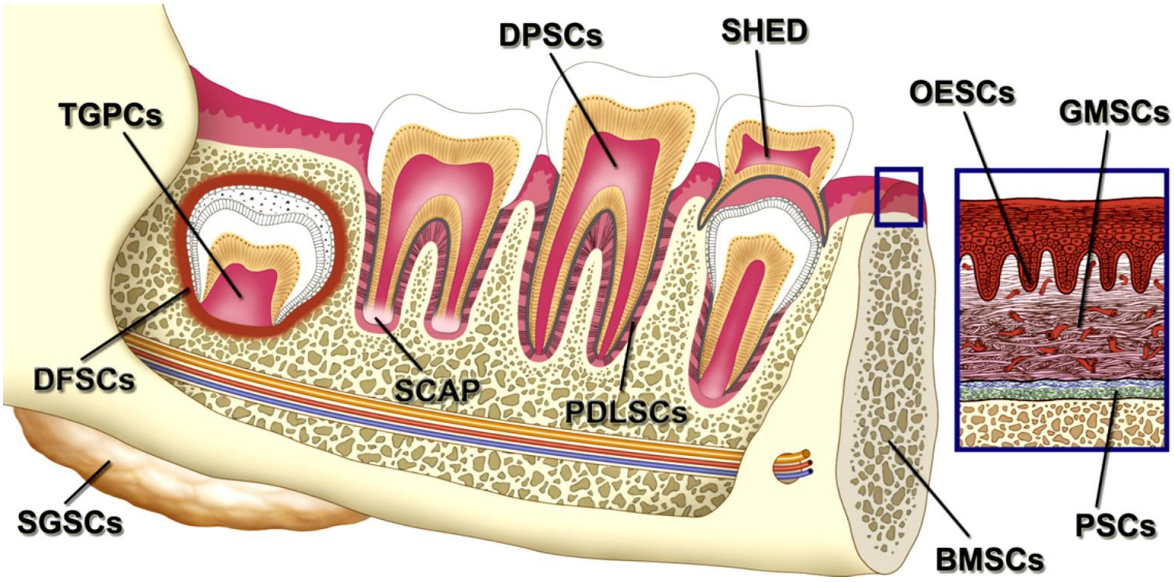

Figure 1.7. Sources of adult stem cells in the oral and maxillofacial region. Bone marrow stem cells (BMSCs), dental pulp stem cells (DPSCs), stem cells from human exfoliated deciduous teeth (SHED), periodontal ligament stem cells (PDLSCs), dental follicle stem cells (DFSCs), tooth germ progenitor cells (TGPCs), stem cells from the apical papilla (SCAP), oral epithelial progenitor/stem cells (OESCs), gingiva-derived MSCs (GMSCs), periosteum-derived stem cells (PSCs) and salivary gland-derived stem cells (SGSCs). Taken from Egusa et al. (2012).

Although REPs are currently used for immature permanent teeth, numerous case reports and one case series have been published on expanding the use of regenerative treatment to mature teeth. This potentially offers an alternative to conventional endodontic treatment, in a variety of clinical scenarios, including necrotic teeth with apical periodontitis (Paryani and Kim, 2013, Saoud et al., 2016a), replantation (Tambakad and Naidu, 2016), retreatments (Saoud et al., 2015), and root resorption (Saoud et al., 2016b). In addition, a recent randomised controlled two-armed clinical trial compared the outcomes of REPs with conventional root canal treatment (CRCT) in necrotic mature teeth with apical periodontitis. At a 1-year follow-up, favourable clinical and radiographic outcomes were found in 92.3% and 80% in both REPs and CRCT groups,

respectively, with no statistically significant differences. Half of teeth in the REPs group responded to the electric pulp test (Arslan et al., 2019). These publications demonstrate the potential for success of pulp regeneration in mature teeth and could be the beginning of the transformation of the practice of regenerative endodontics from that of the treatment of immature teeth to that of a treatment option for mature permanent teeth. The tissues regenerated in the root canals of human mature permanent teeth with necrotic pulp, treated with regenerative endodontics, have not been fully characterised. However, histological reports of animal and human immature permanent teeth with infected or uninfected pulps (Yamauchi et al., 2011, Becerra et al., 2014, Nosrat et al., 2015) show that tissue within the root canals appear to be similar to that of periodontium, consisting of fibrotic periodontal ligament, collagen fibers, blood vessels, cementum- and bone-like tissues.

A published regenerative endodontic case was documented in an immature mandibular premolar with infected necrotic pulp and a chronic apical abscess (Becerra et al., 2014). This case was successfully treated and followed for two years. The tooth was then extracted for orthodontic treatment and processed for histological examination. Despite evidence of apical closure, by cementum deposition and fibrous connective tissue growth into the canal space, there was a small portion of the repair tissue that contained inflammatory cells and bacterial cells. Thus, successful outcomes were achieved despite the presence of a low threshold of residual bacteria in the root canal. Although these tissues are not a true pulp tissue, they are vital with host response. The potential advantage of this mode of treatment is that the root canals are filled with the patient's own vital tissues, bringing with it the possibly that their immune defenses that function as a defense against microbial invasion are intact and able to manage residual microbial infection (Saoud et al., 2016b).

1.6 Prevention: how to reduce and minimise endodontic reinfections

1.6.1 Root canal obturation

Root canal obturation or filling is performed, as the second stage of endodontic treatment, following microbial control to prevent root canal reinfection or

resurgence after chemo-mechanical disinfection procedures. The aim is to maintain the (low) microbial load left after treatment below the threshold for expression of disease, and to prevent influx of periapical fluids that nourish surviving microbes in the canal space (Trope et al., 2015). Successful obturation necessitates the use of materials (usually a semi-solid core material surrounded by a sealer) and techniques capable of densely filling the root canal system entirely and providing a tight seal from the canal's apical minor constriction to the canal orifice unless a post is planned. The coronal restoration should complete this seal (AAE, 2009).

However, can residual bacteria be entombed in the root canal? In fact, the entombment of intracanal residual bacteria was suggested by L Peters et al. (1995) to be one of the main objectives of root canal obturation. Entombing remaining surviving microbes, effectively in the root canal space, by root filling should result in sealing of bacteria in dentinal tubules, apical ramification, recesses and isthmuses (M Wu et al., 2006). Thus, they cannot multiply and/or communicate with the periradicular tissues (Trope et al., 2015), and toxic bacterial elements cannot penetrate the periodontium in a sufficient quantity to cause inflammation (M Wu et al., 2006). The apical root obturation should not contain voids that could permit diffusion of such elements (M Wu et al., 2006). A material which can entirely seal the infected root canal would be ideal for clinical practice (Yoo et al., 2014). With current root canal filling techniques and materials such as gutta-percha and/or polymer-based materials, such objectives have not been achieved yet. Numerous studies have demonstrated that such materials and techniques cannot provide a complete bacterial-tight seal (Punia et al., 2011, Brosco et al., 2010, Jafarzadeh et al., 2018). Therefore, the assumption that residual bacteria can be entombed effectively in the canal system, with such materials, cannot be supported. In fact, bacterial growth was identified in specimens with adequate root canal obturation and without obturation (Burkovski and Karl, 2019). Thus, the gutta-percha core material acts only as a filler and certainly does not seal the root canal (Trope et al., 2015). But can residual bacteria be truly entombed by the root filling in the root canal? Tantalisingly, a study by Yoo et al. (2014) showed a gradual bacterial entombment within the dentinal tubules by intratubular mineralisation over time following orthograde canal obturation with mineral trioxide aggregate (MTA)

mixed with phosphate buffered saline (PBS). Therefore, Yoo et al. (2014) suggested orthograde canal obturation with an MTA–PBS paste in infected root canals, as a potential antimicrobial measure. It was shown that the use of a PBS intracanal dressing promotes carbonated apatite precipitation with a tag-like structure within MTA-dentine interface (Reyes-Carmona et al., 2010). Calcium ions released during the MTA cement hydrolysis interact with phosphate containing solutions, such as a body fluid, resulting in a crystalline deposit of calcium phosphate or hydroxyapatite on the cement surface (Camilleri, 2011, Kaup et al., 2015, Debelian and Trope, 2016). The HA crystals nucleate and grow into the root canals and fill the microscopic space between the cement and the dentinal wall (Sarkar et al., 2003). This seal is initially mechanical. With time, MTA appeared to bond chemically to dentine via "a diffusion-controlled reaction" between the apatite layer and dentine (Sarkar et al., 2005).

Could a biomimetic mineralisation strategy offer a solution to the challenges faced in obturation of the root canal system? In an *in vitro* study, a novel mono-block strategy that seals and obturates the root canal system, permanently, with a tooth-like tissue was developed (L Zhang et al., 2018). In this study, teeth were immersed, after cleaning and shaping, in a supersaturated calcium and phosphate solution containing gallic acid and fluoride. The regenerated fluoridated hydroxyapatite precipitate grew into and obturated the dentinal tubules and root canal completely with a thick, compact homogeneous and monolithic mono-block root obturation that bonds tightly to the canal dentine and seals the root canal system. The study has provided a novel method for generating an enamel-like prism structure to seal the root canal system permanently (L Zhang et al., 2018).

Is the era of gutta-percha over? Gutta-percha, as a root filling, has been and still is the core material of choice (Trope et al., 2015). Regardless of the root obturation technique used, sealers have a crucial importance of sealing and filling the gaps between the root canal wall and the gutta-percha and anatomical irregularities in order to obtain better short-term and long-term seal (Schäfer and Olthoff, 2002). Thermoplasticised gutta-percha techniques have been developed in an attempt to improve the obturation of root canal complexities and to improve density of the filling; reducing the risk of voids formation (Natera et al., 2011). With such techniques, creating a detailed

radiographic picture with the impression that a superior "3D" root filling had been placed was universally accepted as a technique for specialists or "advanced" generalists (Trope et al., 2015). However, it has been shown that melted gutta percha undergoes a large amount of shrinkage during setting (Tsukada et al., 2004). Therefore, Trope et al. (2015) suggested that such techniques, using melted gutta percha, do little to overcome the problems associated with conventional obturation techniques because of the large gap between gutta-percha and sealer following shrinkage. According to Burkovski and Karl (2019), obturation seems questionable as current obturation materials are incapable of hindering bacterial growth nor sterilising teeth, they have no antimicrobial properties and cannot seal the root canal system if a coronal restoration is missing. Tennert et al. (2017), however, demonstrated that all root canal filling techniques significantly reduced bacterial viability (*E. faecalis*) in the root canal especially with warm filling techniques, and the use of heat in warm filling techniques might enhance killing of bacteria (Tennert et al., 2017). It has been shown that ultrasonic activation of the AH plus sealer promoted a better root canal filling quality and improved the intratubular penetration of sealer, especially in the isthmus area. Additionally, the intradentinal antimicrobial activity was enhanced by ultrasonic activation in superficial dentine of the root canal (Alcalde et al., 2017). Trope et al. (2015) suggested the use of a sealer, that does not shrink and is insoluble in tissue fluids such as bioceramics, with gutta-percha impregnated and coated with nanoparticles of bioceramics, in order to eliminate the gap between them (Trope et al., 2015). So, the gutta-percha is used primarily as a "plugger" to deliver the bioceramic sealer into the anatomical irregularities of the root canal. Additionally, it will act as a pathway for post preparation and root canal retreatment.

1.6.2 Restoration of endodontically treated teeth

The long-term prognosis for endodontically treated teeth relies not only on the disinfection of the pulpal space but continued protection of that space from microbial contamination with a satisfactory permanent coronal restoration. Whether or not a full coronal coverage restoration, temporary restoration, or a post-core retained crown is indicated, it is important to consider techniques that prevent microbial ingress and root canal reinfection, while preserving remaining tooth structure (Barsness and Roach, 2016).

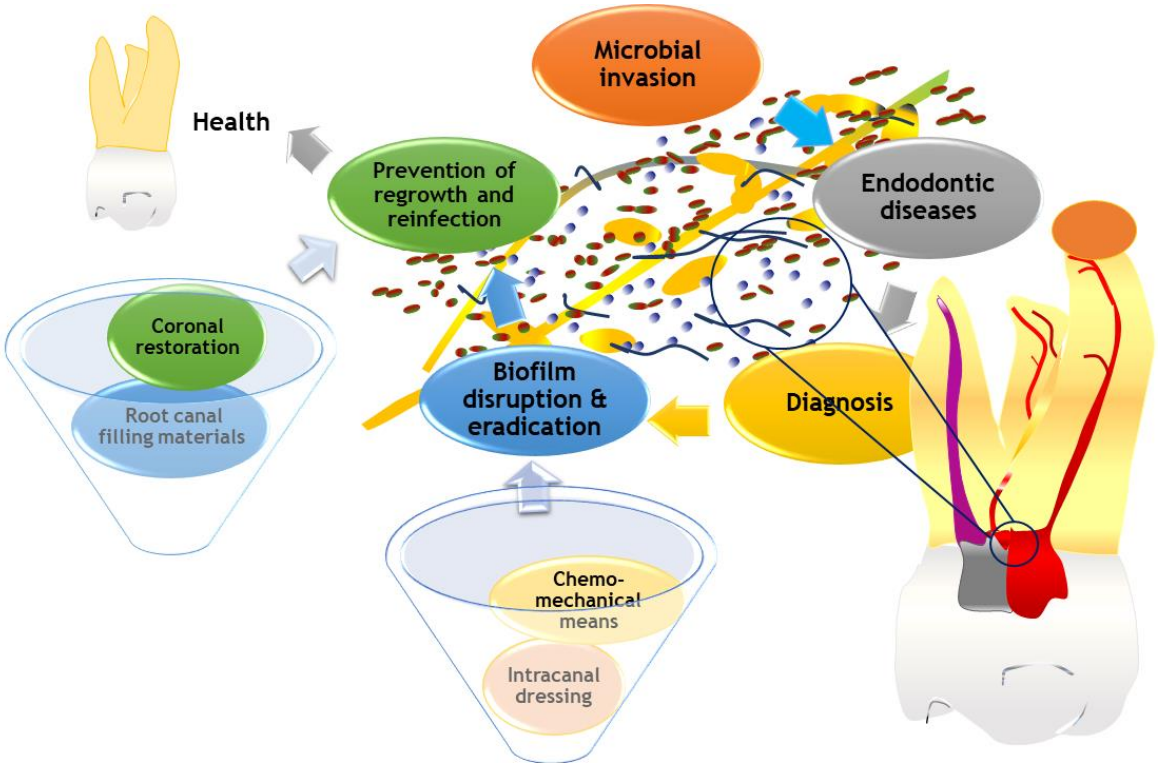

Figure 1.8. Summary of root canal treatment procedures. Following diagnosis and access cavity preparation, endodontic biofilms are disrupted with the use of mechanical instrumentation, antimicrobial irrigation and intracanal dressing in multiple visits. This is followed by root canal obturation and a tight-seal coronal restoration. Diagram was created in Microsoft PowerPoint.

Therefore, endodontic and restorative procedures should not be considered as independent phases, as it becomes apparent that both components impact the long-term prognosis for endodontically treated teeth. The successful outcomes, ultimately, rely on maintaining both coronal and apical seal of endodontically treated teeth (Barsness and Roach, 2016). Therefore, root canal treatment cannot be considered accomplished unless the dental crown is suitably restored (Atlas et al., 2019). Accordingly, the findings of a systematic review and meta-analysis suggest that the quality of the coronal restoration is equally important as the quality of root canal obturation for endodontic treatment outcomes (Gillen et al., 2011). Root canal treatment procedures are summarised in Figure 1.8.

1.6.3 Bioceramics and calcium silicate materials

The field of endodontics is constantly changing due to new technological advances. Advances in endodontic materials contribute significantly to endodontics. The term "bioceramics" was defined by Koch and Brave (2012) as "ceramic products or components employed in medical and dental applications, mainly as implants and replacements that have osteo-inductive properties". Many materials in dentistry and medicine can potentially be classified as bioceramics. Bioceramic prostheses used as implants were simply classified by Hench (1993) into: (1) bioinert, (2) porous, (3) bioactive and (4) biodegradable. Bioinert, which means non-interactive with biological systems. Aluminium oxide (alumina) and zirconia are examples of bioinert materials. Porous, which allows tissue ingrowth into pores. For examples, hydroxyapatite and HA coated porous metals. Bioactive, which is durable in tissues that can undergo interfacial interactions with surrounding tissue, such as bioactive glasses, bioactive glass ceramics and hydroxyapatite. Biodegradable which is soluble or resorbable and eventually replaced with tissues. Examples of this category are tricalcium phosphate and bioactive glasses.

There has also been a great interest, not only in developing methods of synthetically producing hydroxyapatite, but additionally in understanding how to produce HA naturally from bones, dentine, eggshells, bones of some fishes and shells of some marine molluscs (Coelho et al., 2006). Marine species, such as corals, seashells and nacres, are of special interest in the field of bioceramics for bone graft, bone cements and drug delivery applications. Most of these marine structures are composed of pure calcium carbonate with a small amount of an organic matrix (Macha et al., 2013).

According to the literature, there has been a growing interest in the production of calcium phosphate compounds from natural sources. A hydroxyapatite powder was synthesised from snail shells which are mainly composed of calcium carbonate (A Singh and Purohit, 2011). A study synthesised calcium phosphate bioceramics, which contain a mixture of hydroxyapatite and apatitic tricalcium phosphate. The antibacterial study showed that bioceramics synthesised from *Lanistes varicus* snail shell powder showed a strong inhibitory effect against *Staphylococcus aureus*, but a partial antimicrobial property against *Klebsiella*

oxytoca. The study also suggested using the *Lanistes varicus* snail shell powder as a bioactive biomaterial in dental applications (Osseni et al., 2018).

The introduction of calcium silicate-based materials, in the early 1990s, as a new group of dental cements may be considered as one of the most important advances in dental material science that have changed the face of endodontics (Raghavendra et al., 2017). The first member of the calcium silicate-based materials to be introduced was mineral trioxide aggregate (MTA), which is a mixture of Portland cement and bismuth oxide in a proportion of 4:1. The powder consists of hydrophilic fine particles that set in the presence of water. In the original patent lists, the powder of MTA principally consists of tricalcium silicate, dicalcium silicate, tricalcium aluminate and tetracalcium aluminoferrite with bismuth oxide powder added as a radiopacifying agent (Torabinejad and White, 1995). Subsequently, a variety of new formulations of purer calcium silicate-based materials, not based upon natural minerals or industrial process, have been developed based on tricalcium silicate chemistry (Camilleri, 2015). Bioceramics is the term applied to the newer modified calcium silicate-based cements used particularly in endodontics (Camilleri, 2021b). It is worth mentioning that the term “bioceramics” used for calcium silicate-based materials is a misnomer. In fact, bioceramics, as previously mentioned above, include a wide range of materials with different chemical compositions (Camilleri, 2015). Biodentine (BD), BioAggregate (BA) and calcium-enriched mixture cement (CEM) are amongst this newer group of modified calcium silicate materials. These materials are indicated for a variety of endodontic procedures, including perforation repairs, regenerative endodontic procedures, retrograde obturation, vital pulp therapy and management of immature permanent teeth, similar applications to those outlined for MTA (Camilleri, 2021a), as shown (Figure 1.9).

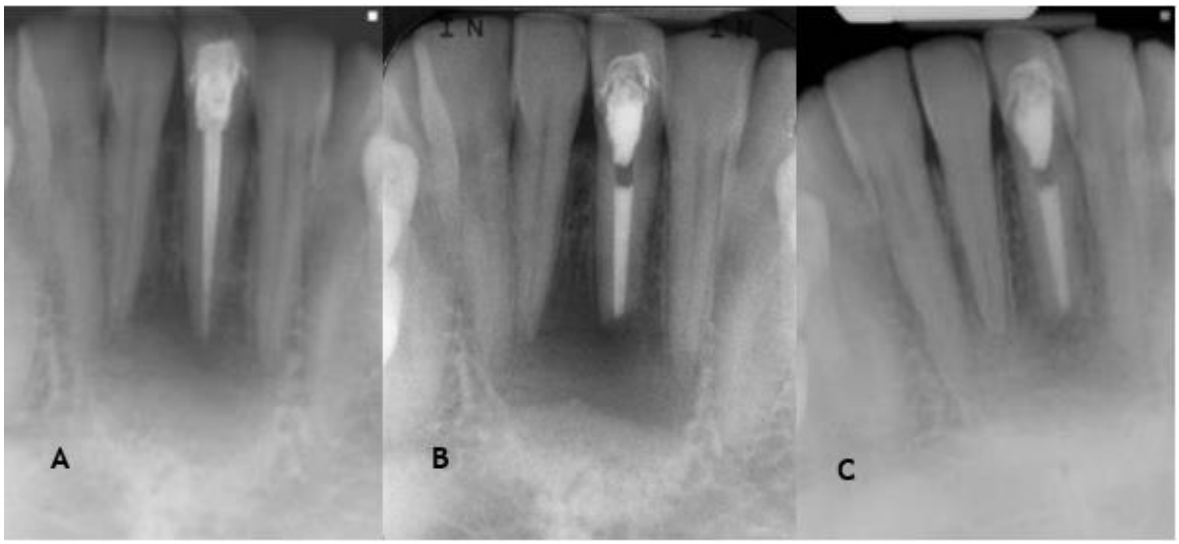

Figure 1.9. Endodontic microsurgery and MTA placement. (A) Mandibular central incisor with large apical lesion. **(B)** Post-surgery following orthograde approach, MTA placement and root resection. **(C)** On review, bone healing is evident. Courtesy of Dr William McLean.

Previous studies have shown that these materials possess antibacterial and antifungal properties against isolated bacterial and fungal species. The antibacterial efficacy of the calcium silicate-based materials has been attributed to the alkaline environment formed when calcium silicate undergoes hydrolysis in water, producing calcium silicate hydrate and calcium hydroxide. The presence of precipitated $Ca(OH)_2$ results in an alkaline pH (Camilleri, 2007, Camilleri, 2011). While this appears a useful function of the materials, there are limitations on the applicability of studies of this phenomenon. Many of these studies used material suspensions, in either media or sterile water, to test activity against only planktonic microbial cells, with the assessments based on determining minimum inhibitory concentrations or suspension turbidity (Kangarlou et al., 2009, Kangarlou et al., 2012, Hiremath et al., 2015). Such methods do not mimic the microbial interactions occurring in clinical scenarios where it has been shown that microbes exist within biofilms, displaying unique phenotypic characteristics compared to their free-floating planktonic counterparts, including a notorious resistance to antimicrobial agents (Ceri et al., 1999, Ramage et al., 2001). Moreover, as highlighted, these studies used only mono-species systems that do not fully represent the polymicrobial nature of the infected root canal (Lovato and Sedgley, 2011, Damlar et al., 2014, R Kim et al., 2015, Donyavi et al., 2017, Atom et al., 2021, Bossù et al., 2021).

Different methods have been used to assess the antimicrobial activities of calcium silicate materials. By using the disc diffusion method, the zones of bacterial growth inhibition were measured when tested materials were placed into the inoculated agar plates (R Kim et al., 2015, Donyavi et al., 2017, Atom et al., 2021). The direct contact test was another assessment method to be used in other studies, by placing the mixed test materials in microtiter well plates and adding microbial suspensions for 1 h, followed by 10-fold serial dilution of microbial suspension, for enumerating colony forming units of microbial strains inoculated onto agar plates (Lovato and Sedgley, 2011, Damlar et al., 2014). Notably, the positive control used in these studies, for establishing the antimicrobial effect, was microbial suspensions added into microtiter wells, which were uncoated with tested calcium silicate materials. The crystal violet staining assay was also used in a recent study for assessing the antibiofilm ability of MTA and Biodentine against *S. mutans* biofilm grown on the surface discs of the materials, where no control was used (Bossù et al., 2021). These single biofilm models have typically failed to address the complexity of endodontic biofilms and the potential for interkingdom interactions.

Confirming the importance of assessing the effect on biofilms, in a study by Jerez-Olate et al. (2021), ProRoot MTA and Biodentine showed higher antibiofilm activity against anaerobic multispecies biofilms containing bacterial species only, using scanning electron microscopy (SEM) and confocal laser scanning microscopy (CLSM). However, Jardine et al. (2019) designed an *ex vivo* biofilm model, with unknown microbial compositions, investigating the antimicrobial activity of NeoMTA Plus, Biodentine and MTA Angelus against multispecies microcosm biofilms grown intraorally with unknown compositions. In this study, volunteers wore retainers with small human dentine blocks for 72 h. Subsequently, the blocks were incubated aerobically for biofilms growth. The materials were then placed in contact with these infected blocks. The results of CLSM showed a high level of viable microorganisms even after 7 days of contact of tested materials with the blocks, and none of the materials were effective against multispecies biofilms. These data might suggest the need for augmenting materials with antibiofilm active agents.

It is challenging to predict the antimicrobial behaviour of calcium silicate materials in the host environment. Other biological factors may enhance or

drastically reduce their antimicrobial properties in *in vivo* conditions. In a study by Farrugia et al. (2017), ProRoot MTA showed a highly significant drop in its antimicrobial activity against *E. faecalis* when in contact with blood. Another study assessed the antimicrobial effectiveness of BioAggregate and MTA against *E. faecalis*. Suspensions of fresh powders and crushed set cements were prepared and mixed with equal amounts of a sterilised crushed human radicular dentine (obtained from an extracted wisdom tooth). The results showed that the addition of dentine powder to the suspension of both set and fresh powders of either cement, resulted in complete killing of bacteria after a short time of exposure (1–6 min). Dentine powder alone did not eliminate the viable bacteria during the 24-h experiment. This study showed a slight reduction in pH value. Therefore, it seems that the quick elimination of *E. faecalis* by both cements, in the presence of dentine powder, is caused by factors other than pH value alone. The presence of dentine powder enhances the antimicrobial activities of MTA and BioAggregate (H Zhang et al., 2009). In a recent study, the antibiofilm activity of three calcium silicate-based sealers against *E. faecalis* biofilm was assessed in either a neutral condition or an acidic condition (pH 5.2), to simulate the low pH environment in inflammation. The findings of this study highlight the impact of pH changes on the antimicrobial efficacy of these materials. Calcium silicate sealers, in acidic pH, showing a significant declining trend in their antimicrobial activity, while they appear to have an adequate antimicrobial activity in pH neutral conditions (Bosaid et al., 2022).

1.7 Nanomaterials in endodontics

The prefix “nano”, according to the Oxford English Dictionary (OED), is referred to a Greek prefix meaning “dwarf” or something very small. A nanometre (nm) is an International System of Units that represents one thousand millionth (billionth) of metre in length (10^{-9} m) (oed.com). The European Commission Recommendation defined a nanomaterial as “a natural, incidental or manufactured material containing particles, in an unbound state or as an aggregate or as an agglomerate and where, for 50 % or more of the particles in the number size distribution, one or more external dimensions is in the size range 1-100 nm” (European Commission, 2011). A nanoparticle has been defined as a particle of any shape that ranges between 1 to 100 nm in dimension (Vert et al., 2012).

Nanomaterials/nanoparticles (NMs/NPs) are classified, based upon their origin, into either naturally occurring (produced in nature), incidental or synthetic (engineered). Naturally formed NMs are present in the Earth's spheres, such as the atmosphere, the hydrosphere (oceans, lakes and rivers), the lithosphere (rocks, soils and lava) and the biosphere (the bodies of organisms, insects, plants, animals and human). In contrast, synthetic NMs are manufactured by either grinding or are synthesised by physical, chemical, biological or hybrid methods. Incidental NMs are generated incidentally as an industrial processes by product (Jeevanandam et al., 2018). Based on composition, NMs can be categorised into carbon-based NMs (containing carbon), inorganic-based NMs (including metal and metal oxide), organic-based NMs (made mostly from organic matter) and composite-based NMs (NPs are combined with other NPs or with any form of bulk materials) (Jeevanandam et al., 2018).

Researchers recognised the significance of these materials when they found that nanomaterials possess special physicochemical properties, due to their ultrasmall sizes (Khan et al., 2019). It has been suggested that this nanoscale size results in a large surface area, which could possibly promote interactions between the surface of living organisms and the nanomaterials (Navya and Daima, 2016). The use of nanoparticles in endodontics has substantially progressed and grasped significant attention over the last decade (Wong et al., 2021). The aim is mainly to overcome the endodontic microbial challenge (Shrestha and Kishen, 2016). The potential use of nanoparticles in endodontics encompasses various applications, such as endodontic irrigation and disinfection strategies, photodynamic therapy, intracanal medicaments, obturation materials and regenerative endodontics (Wong et al., 2021).

1.7.1.1 Silver

Historically, silver has been a major therapeutic agent in numerous medical conditions over at least six millennia, especially in infectious diseases, mostly empirically before the realisation that microbes were the infectious agent. It was the most important antimicrobial agent available before the clinical introduction of antibiotics (Alexander, 2009). The increase in antibiotic resistance has prompted interest in the use of this metal as an antimicrobial agent. Additionally, silver has been proposed as an alternative strategy for

reducing the attachment of microorganisms on medical devices (Monteiro et al., 2009). Advances in the field of nanotechnology have created new horizons and opportunities in nanomedicine. We are now capable of allowing the synthesis of nanoparticles that can be assembled into complex architectures. One of the most extensively used nano-systems in dentistry is silver nanoparticles (Elizabeth et al., 2019), which attract much attention because of their potent antimicrobial effectiveness (Franci et al., 2015).

In dentistry, it has been shown that the application of a silver nano-coating on dentine surface had inhibited bacterial adhesion on the dentine surface (Besinis et al., 2014). It has also been found by D Wu et al. (2014) that 0.02% AgNP gel as a root canal medicament significantly disrupted the structural integrity of *E. faecalis* biofilms, compared with 0.01% AgNP gel and calcium hydroxide groups. However, as a root canal irrigant, the concentrations of 0.1% AgNPs was not able to disrupt *E. faecalis* biofilms and the number of residual viable bacterial cells, following treatment, was comparable to that of the saline group.

Silver nanoparticles have also been incorporated into endodontic materials. Adding AgNPs up to 5 wt% could not improve the antimicrobial properties of zinc oxide eugenol sealer against *E. faecalis* (Haghgoo et al., 2017). In contrast, 17% EDTA-AgNPs solution was found to be an effective antimicrobial agent against mono-species biofilms, compared to EDTA alone, without losing its chelating ability (Martinez-Andrade et al., 2018). Adding 100 ppm and 200 ppm of AgNP suspensions (0.01% and 0.02%) into the powder of both MTA and calcium-enriched mixture cements significantly improved their antimicrobial efficacy against planktonic microorganisms (Jonaidi-Jafari et al., 2016). In another study, the incorporation of 12 ppm and 25 ppm of AgNPs (0.0012% and 0.0025%) into MTA enhanced the antibacterial properties of MTA significantly, against a bacterial suspension of *E. faecalis* and *Pseudomonas aeruginosa* (*P. aeruginosa*) (Bedier, 2017). An *in vitro* and *in vivo* study showing that AgNPs at 25 µg/mL (0.0025%) were not cytotoxic, but cytotoxicity was shown at higher concentrations. Therefore, further studies are recommended to ensure safety of clinical use (Takamiya et al., 2016).

1.7.1.2 Chitosan

Chitosan is a modified natural carbohydrate polymer produced by deacetylation of chitin (Austin et al., 1981). Chitin is widely distributed in nature, and is derived from the exoskeletons of arthropods (including crustaceans and insects), the endoskeleton of cephalopods (Hackman and Goldberg, 1981, Arrouze et al., 2017), corals (Bo et al., 2012), sponges (Shaala et al., 2019), algae (Rahman and Halfar, 2014) and from cell walls of fungi (T Wu et al., 2004). Chitin and chitosan are composed of N-acetyl-D-glucosamine (acetylated units) and D-glucosamine units (deacetylated units), linked by ß-(1,4) glycosidic bonds. Chitin consists mainly of N-acetyl-D-glucosamine units, while chitosan contains mainly D-glucosamine units (Gonçalves et al., 2021). Chitosan, the poly-(ß-1,4)-2-amino-2-deoxy-d-glucopyranose, is a collective name for a group of partially and fully deacetylated chitin (Tikhonov et al., 2006).

The extraction process of chitin mainly relies on chemical processes and usually occurs in two stages: (1) demineralisation, using hydrochloric acid (HCl), to remove calcium carbonate and (2) deproteinisation, using a sodium hydroxide (NaOH) solution, to remove protein (Gopal et al., 2019). The chitin deacetylation is considered in the literature as the main method for obtaining chitosan (Figure 1.10). However, Gopal et al. (2019) reported a phyto-extract mediated novel method using Graviola, a small tropical tree, for recovery of chitosan directly from solid marine wastes (Gopal et al., 2019).

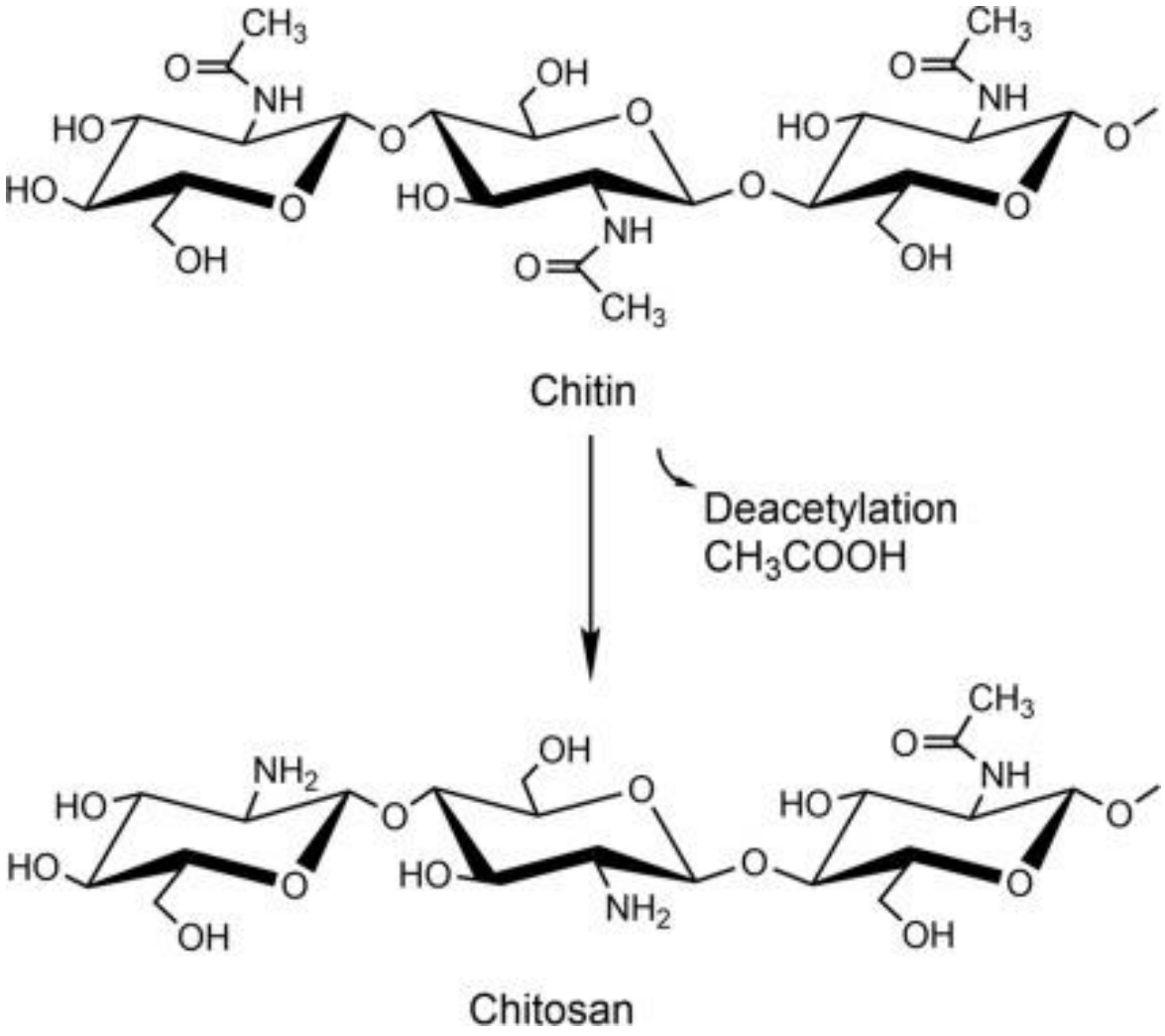

Figure 1.10. Deacetylation reaction of chitin to chitosan. Chitin is the second most abundant natural polysaccharide after cellulose. Chitin is composed of N-acetyl-D-glucosamine and D-glucosamine units. Chitosan is the most common chitin derivative obtained by partial deacetylation of chitin by removing the acetyl group (CH_3-CO). Taken from Farinha and Freitas (2020).

Chitosan has attracted considerable attention over the past decade, because of its antimicrobial properties (Matica et al., 2019), biocompatibility, biodegradability and non-toxicity (Chandy and Sharma, 1990, Xu et al., 2012). Chitosan can be distinguished by its molecular weight into high molecular weight (HMw), medium molecular weight (MMw) and low molecular weight (LMw). It was found that a longer reaction time at a higher temperature during the deacetylation process produces low molecular weight (Jia and Shen, 2002). In fact, the properties of chitosan have been related to its molecular weight. It is known that chitosan is insoluble in water and organic solvent. It is soluble in dilute aqueous acidic solution (pH < 6.5) (Kumar et al., 2004), and its

solubilisation is generally carried out using acetic acid. However, the water-solubility of chitosan was found to increase as the molecular weight decrease (Jia and Shen, 2002). There have been attempts to create particulate systems that form dispersion within solutions formed of reactive surface areas. This shift of physical state, due to size effects, is likely to create variations in its antimicrobial properties (Kong et al., 2010).

Chitosan can be easily fabricated into various forms, such as membranes (Mi et al., 2001), solutions/gels (Yadav et al., 2017, Akca et al., 2018), hydrogels (Ahmadi et al., 2015), nanofibers (Homayoni et al., 2009), films (Coma et al., 2002), beads (Jayakumar et al., 2006), nanoparticles (Chávez de Paz et al., 2011), scaffolds (L Yang et al., 2016) and sponges (Huang et al., 2015). The methodologies to synthesise nanoparticles are commonly catalogued into physical (top-down) and chemical (bottom-up) methods. The physical approach is based on reducing the size of bulk (source) materials into nano-objects using a specific technique, such as mechanical milling. This, however, may lead to contamination if a milling medium is utilised. In the bottom-up approach, the source material is dissolved in a certain medium, then nanoparticles are created by nucleating and growing particles from an atomic or molecular level in the solution (Chan and Kwok, 2011).

Chitosan nanoparticles have been synthesised using various chemical methods (Seyam et al., 2020). The ionotropic gelation method is one of the most common methods reported in the literature. This method was firstly reported by Calvo et al. (1997). Briefly, the cationic solution of chitosan is prepared by dissolving chitosan in acetic acid aqueous solution. An anionic crosslinker solution is prepared by dissolving sodium tripolyphosphate (TPP) in distilled water. Following this, ionic gelation occurs by adding the TPP solution into the chitosan solution under mechanical stirring at room temperature. Spherical nanoparticles are formed instantly by electrostatic forces, as shown (Figure 1.11).

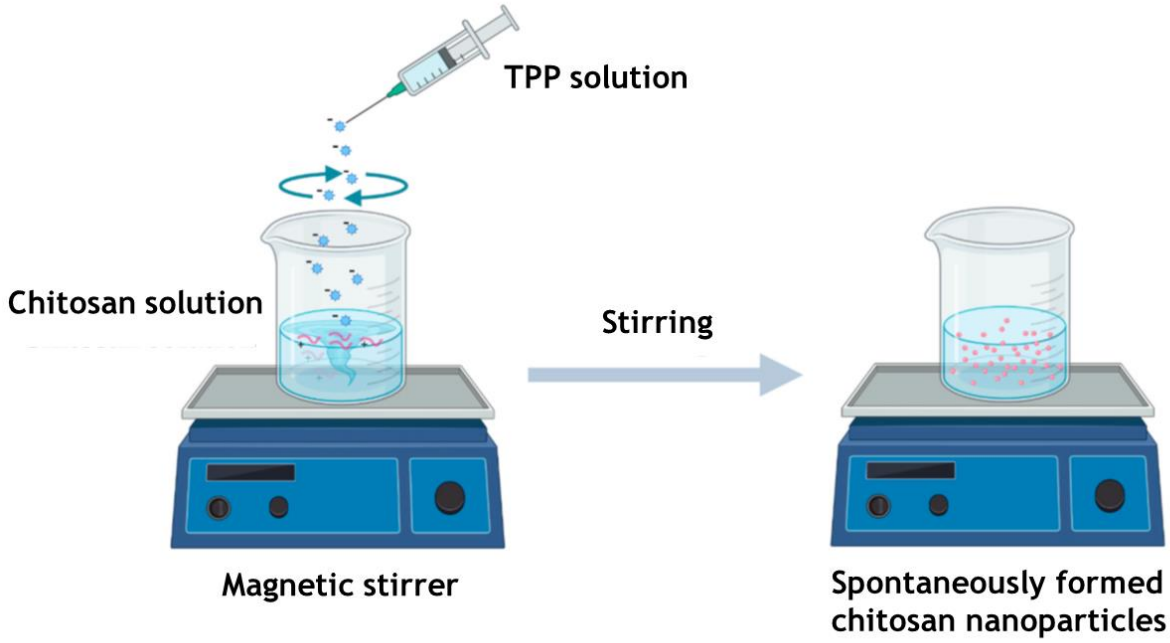

Figure 1.11. A schematic diagram of chitosan nanoparticles prepared via ionic gelation method. Taken from Seyam et al. (2020).

Chitosan is known to possess antimicrobial activity against a variety of Gram-positive and Gram-negative bacterial strains and fungi (Park et al., 2008, Shrestha et al., 2010, Goy et al., 2016, MubarakAli et al., 2018). The antimicrobial properties of chitosan solutions/nanoparticles have been shown when used as an irrigant and when incorporated into endodontic sealers (DaSilva et al., 2013, del Carpio-Perochena et al., 2015a). The exact antimicrobial mechanism of action of chitosan is still unclear, but different mechanisms have been proposed (Kong et al., 2010, Rabea et al., 2003), and it is assumed to be mainly electrostatic (Figure 1.12). It has been suggested to be attributed to the affinity of the positively charged chitosan molecules for the negatively charged microbial plasma membrane which supports the interaction with anionic components of the cell membrane and leads to cell membrane disruption, intracellular contents leakage and ultimately cell death (Park et al., 2008, Beck et al., 2019). It has also been hypothesised that chitosan exhibits a chelating activity against essential trace metals and thereby inhibit fungal growth and toxin production (Cuero et al., 1991). It has been found that the mode of chitosan action is influenced by different factors, one of which is the type of microorganisms. In a study by Palma-Guerrero et al. (2010), an increased

antifungal activity of chitosan was observed against fungi with a higher amount of polyunsaturated fatty acids in their plasma membranes. In contrast, a decreased antifungal activity was seen with a mutant fungus with a reduced amount of unsaturated fatty acids. This study confirmed that chitosan binds to the negatively charged phospholipids that alter the fluidity of the cell membrane and leads to membrane permeability (Palma-Guerrero et al., 2010). An RNA sequencing analysis has shown that chitosan may exert its antifungal effect by inhibiting genes involved in cell integrity and protein biosynthesis (Meng et al., 2020). In another study, chitosan was found to inhibit bacterial growth via downregulation of genes involving in growth and metabolism (Raafat et al., 2008).

Overall, these advances in nanotechnology have opened potential new applications in endodontics. Although many of these antimicrobial studies are *in vitro* studies with simple microbial models, the nanoparticulate system has shown the potential for enhancing the antimicrobial ability of existing materials. Therefore, work is required to explore this further using an appropriate biofilm model.

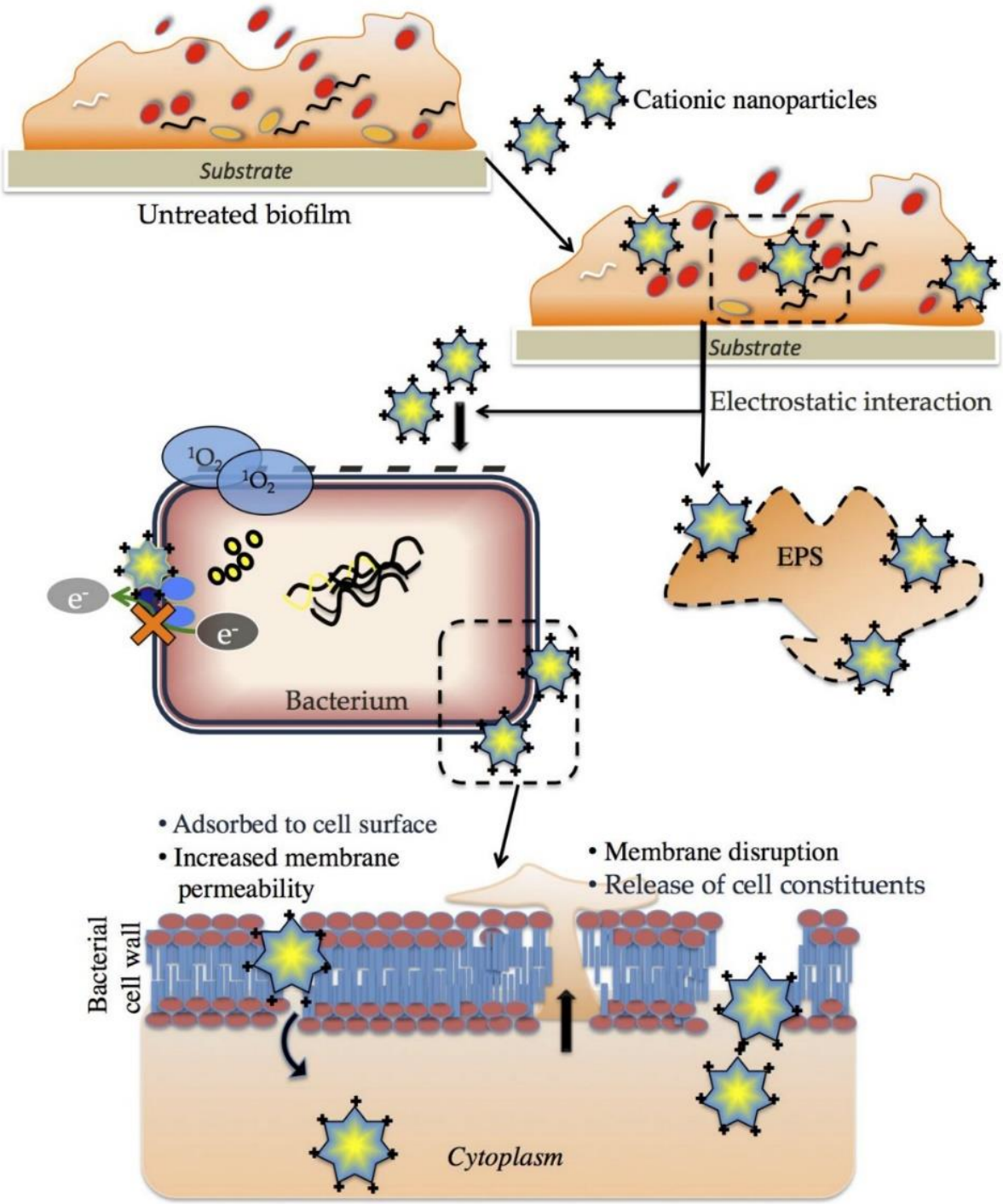

Figure 1.12. A schematic diagram showing the antibacterial mechanism of chitosan nanoparticles. Cationic (positively charged) nanoparticles interact with anionic (negatively charged) bacterial cells. Increased membrane permeability eventually lead to bacterial cell death (Shrestha and Kishen, 2016).

1.8 Hypothesis and aims

The overall hypothesis of this thesis indicates a fundamental shortcoming in endodontic research, whereby non-representative models have been used to explore treatment strategies. The development of a representative biofilm model opens-up the possibility of exploring existing and novel treatment strategies in a relevant and reproducible way that can inform our clinical practice.

The aims of this thesis are:

1. To analyse the trends in endodontic microbiology research over the last three decades, using a combination of bibliometric and ontological analyses of the literature.

2. To develop and optimise a defined multispecies interkingdom biofilm model, a representative model of endodontic infection.

3. To investigate the antibiofilm efficacy of endodontic calcium silicate-based cements (MTA and Biodentine) modified by one of the novel antimicrobial biomaterials (chitosan), and to assess the interkingdom interactions that may modify microbial tolerance to treatment.

4. To assess the material characteristics of the new mixture of the modified calcium silicate-based material (Biodentine) with chitosan, compared to the unmodified formula.

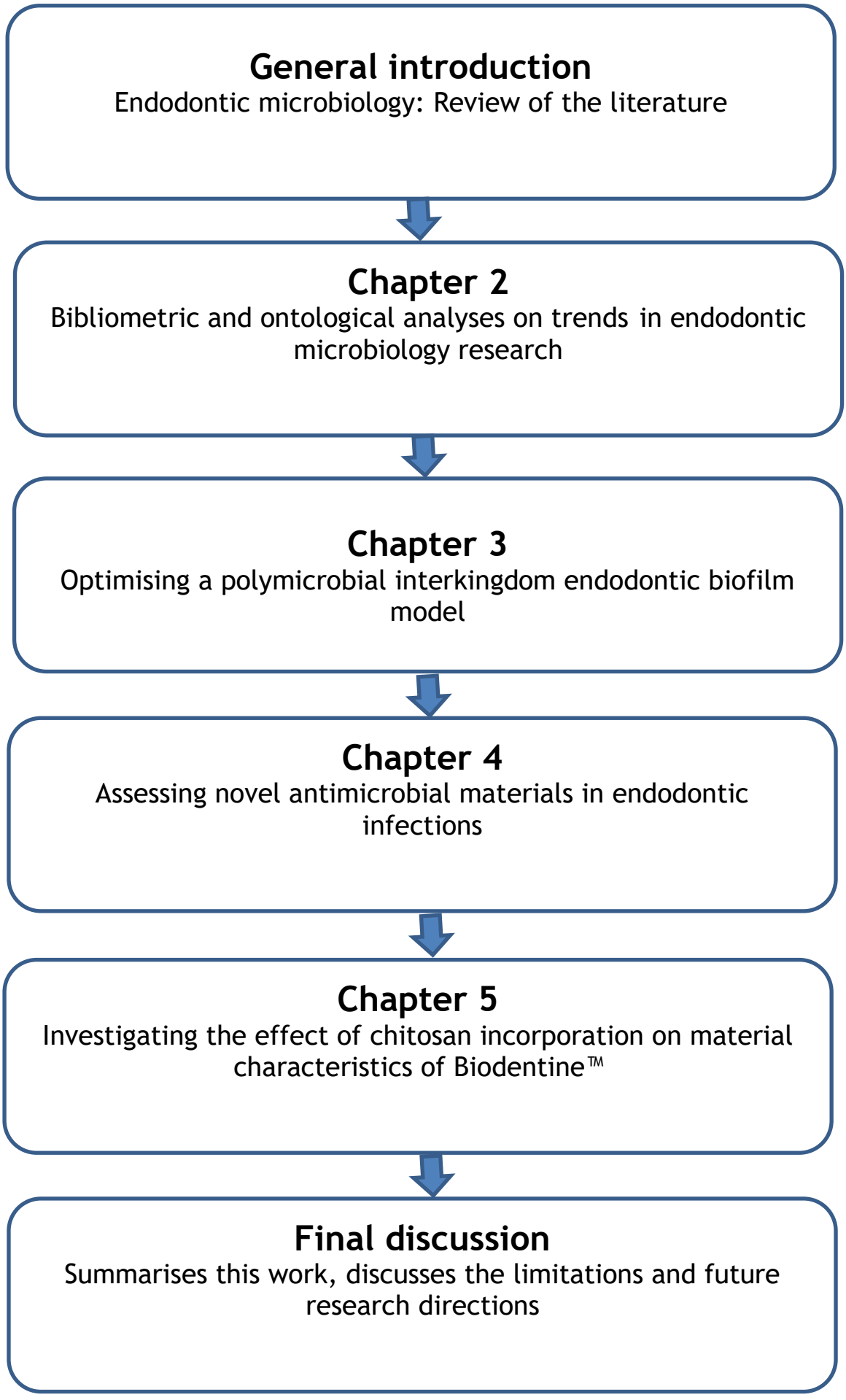
General introduction
Endodontic microbiology: Review of the literature
Chapter 2
Bibliometric and ontological analyses on trends in endodontic microbiology research
Chapter 3
Optimising a polymicrobial interkingdom endodontic biofilm model
Chapter 4
Assessing novel antimicrobial materials in endodontic infections
Chapter 5
Investigating the effect of chitosan incorporation on material characteristics of Biodentine™
Final discussion
Summarises this work, discusses the limitations and future research directions

2 Bibliometric and ontological analyses on trends in endodontic microbiology research

2.1 Introduction

Knowledge in the field of endodontic microbiology is constantly evolving and therefore so is best practice in endodontics. With the exponential growth in the volume of research productivity, keeping up to date with such a vast amount of available literature is an enormous challenge (Koci et al., 2018). Measuring and monitoring the accountability, excellence and quality of scientific research is a theme that has attracted increasing attention of governments, institutions and funded bodies (Agarwal et al., 2016). Therefore, the analysis of the growth in the rate of scientific publications is required to quantify research outcomes and their impact on the scientific community (Tarazona et al., 2017).

Amongst many statistical studies in science, bibliometrics is one of the few subfields aimed at measuring scientific research outputs (Godin, 2006). Bibliometrics is a quantitative measure used increasingly to analyse scientific production, author performance and impact of scholarly publications, within a topic of interest (Ellegaard and Wallin, 2015). Bibliometric terminologies started to emerge as the discipline began to mature (Thompson and Walker, 2015). Historically, bibliometrics was introduced in 1926 when Alfred Lotka investigated patterns of author productivity, counting names and number of articles listed for each. The initial laws of bibliometrics, later called “Lotka's law”, was produced as a result of his work (Lotka, 1926). In 1934, Samuel Bradford analysed the frequency distribution of publications across scientific journals in a specific research discipline. His work resulted in formulating a key law of bibliometrics “Bradford's law” (Bradford, 1934). In 1955, the beginning of the modern bibliometric era was launched by Eugene Garfield when he developed the concept of a scientific citation index (Garfield, 1955). By 1964, Garfield had created the Science Citation Index (SCI) and introduced it as a “new dimension in indexing” (Garfield, 1964). In 1969, the term “bibliometrics” was coined by Alan Pritchard, who defined it as “the application of statistical and mathematical methods to books and other media of communication” (Pritchard, 1969).

Bibliometric analysis is the process of extracting measurable data from scholarly publications through statistical analysis and how the knowledge within a

published research study is used (Agarwal et al., 2016). The use of bibliometric analysis is gradually extending to all disciplines (Aria and Cuccurullo, 2017) and currently is being used in various fields, including medical science (Lewison et al., 2016, Saquib et al., 2017, W Yang et al., 2020) and health care (Adunlin et al., 2015). In endodontics, bibliometrics has also been adopted to analyse the trend in endodontic research worldwide. It has been shown that microbiology was the first topic in endodontics to have secured importance. It was the most frequent subspecialty in endodontics (Fardi et al., 2011, Yilmaz et al., 2019). This indicates the worldwide increasing interest in the microbiological aspect of endodontics.

As in most fields, typical bibliometric analyses involve multistep analyses, each of which uses different software tools, which increases the risk of human errors and complicates the analysis for other researchers (Guler et al., 2016). Recently, the Bibliometrix R-package was developed by Aria and Cuccurullo (2017). This is an open-source tool used for producing a comprehensive science mapping analysis that follows the classic logical bibliometric workflow.

Ontology-based approaches have also been adopted in many domains to extract and retrieve information more easily (Blake, 2004). Ontologies illustrate controlled dictionaries of words on a specific theme that define terms in a description logic (Vogt, 2009, Koci et al., 2018). The manual approach is highly accurate and can distinguish relevant data from irrelevant data, better than any available software tool. However, it is time consuming and is unable to adapt to the increasing amount of literature. An automatic text-mining system is another approach which can be used to help in annotation and ontology with the least waste of time and effort (Winnenburg et al., 2008).

A text-mining tool “PyTag” was developed by Koci et al. (2018), which automatically text-mines ontological terms in online databases that offer metatags with rich textual information in a time-efficient manner. By text-mining published abstracts and categorising terms used into an existing broad range of domain ontologies, it is likely to complete the demanding laborious task of manual management, analysis and interpretation of a huge number of available publications, free from reviewer’s bias. Such an approach can be

useful for systematic reviews as it benefits from the ability to rapidly annotate thousands of articles (Koci et al., 2018). Capturing additional details presented in a scientific paper can be possible when a statistical analysis of metadata is performed. Such information and patterns cannot be possibly revealed with a traditional, manual methodology applied in systematic reviews (Koci et al., 2018).

2.2 Aims

This chapter aims to:

- Identify the topmost cited articles and authors in the field of endodontic microbiology, using a bibliometric analysis. This includes providing a historical perspective on endodontic microbiology research that reflects the research trends in the field.
- Analyse the frequency of microorganisms in the endodontic literature associated with endodontic infections, using an ontology-based analysis. This information can be used to develop a multispecies endodontic biofilm model suitable for assessing novel antimicrobial materials.

2.3 Materials and methods

2.3.1 Bibliometric analysis

An electronic search was performed using the Web of Science - Core Collection (WOS), Advanced Search Builder, from 1990 to June 2020. The aim was to identify original research articles, in the English language, related to the field of microbiology in endodontic infections. The search strategy included two distinct blocks of search terms, which were searched using truncation by adding an asterisk (*) to the 'root' form of a key word, to search for any other alternative endings. The two blocks of keyword were combined by the Boolean search command 'AND' to retrieve publications that incorporate the two blocks of interest. The list of keywords is described (Table 2.1).

A total of 8606 publications were retrieved, and were then exported as 18 plaintext files, which were then merged into one plaintext file. The most recent version of RStudio was downloaded (bibliometrix.org). The Bibliometrix R package (version 3.0.1, released in 2020) was installed and loaded through RStudio. The Biblioshiny app was started by inputting the code biblioshiny() in the R console. The one merged plaintext file was uploaded into the Bibliometrix shiny application. All reviews, book sections and editorials were then excluded from consideration. After filtering documents, the database search yielded 7200 original articles, from January 1990 to June 2020. Biblioshiny is a shiny app providing a web-interface for the Bibliometrix package. It allows non-coders to use Bibliometrix easily to analyse bibliometric parameters for each article, including research performance analysis and science mapping (bibliometrix.org/biblioshiny). Tables were downloaded from the Biblioshiny app as Excel sheets, for data analysis.

2.3.2 Ontological analysis

An electronic search was performed using the Web of Science - Core Collection, Advanced Search Builder. All publications related to the microbiology of endodontic infections, in the English language, were included from 1990 to June 2020. The search result of the WOS database for all possible combinations of the key search terms (Table 2.1) yielded a total number of 8596 publications, which

were then imported into EndNote X8. After the removal of reviews, editorials and book sections, a total number of 7569 original research articles were included. These journal references were then grouped in single years and exported in a BibTeX format where each entry was described by a number of article records including author, title, journal, a digital objective identifier (DOI), a unique accession number or document identifier. Following this, the BibTeX files were processed by a custom written script called "PyTag" as described previously by Koci et al. (2018). The PyTag script accepts the BibTeX files in a given folder as input and supports nine ontologies used in the EXTRACT 2.0 system (Pafilis et al., 2017).

These supported ontologies recovered mentions for the following: "biological process", "cellular component", "chemical compound", "disease", "environment", "genes and proteins", "molecular function", "organism" and "tissue". PyTag utilised these ontologies on the PubMed (PM) abstracts using the associated PubMed identifiers (PMIDs). Following the annotation process of all the abstracts and grouping terms used into the existing ontologies, the resulting frequency of the identified terms was converted to two-dimensional tables in Excel worksheets, where number of mentions for a defined term (one mention per abstract) was recorded for each year. A manual approach was then performed for selected ontologies of interest by accessing the relevant imported abstracts from this collection. Finally, graphs were created using GraphPad Prism (version 9.3.1). This whole automated annotation workflow is summarised in Figure 2.1.

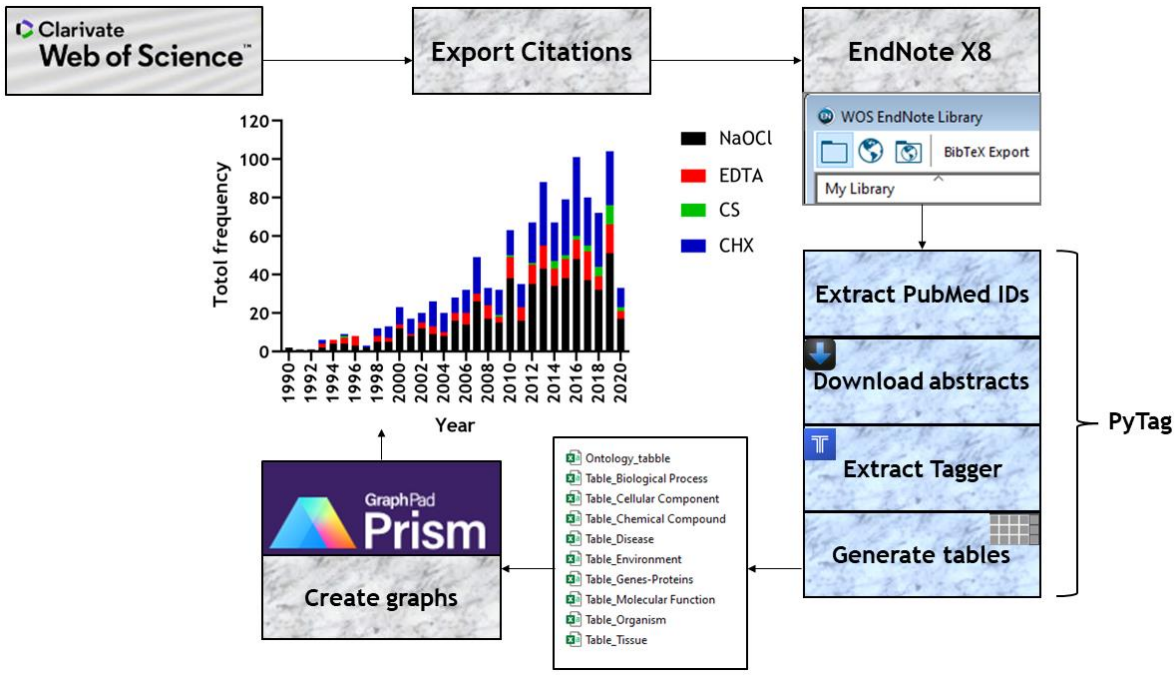

Figure 2.1. A workflow diagram for an ontology-driven annotation processed by a PyTag script. An electronic search of Web of Science - Core Collection database was performed. Abstracts recovered were imported into EndNote X8. The imported journal references were exported in a BibTeX format, where each abstract was described by a number of article records. The BibTeX files were processed by PyTag, as described by Koci et al. (2018), where all the ontological terms were listed and annotated. Frequency tables of identified terms were generated, and graphs were created using GraphPad Prism. The PyTag annotation was processed by Dr Christopher Delaney. Diagram was created in Microsoft PowerPoint and GraphPad Prism (version 9); adapted from Koci et al. (2018).

Table 2.1. Key search terms used for bibliometric and ontological analyses.

	Search terms
Block 1	(TS=(endodontic* OR endodontic treatment OR endodontic retreatment OR teeth OR root canal* OR dental pulp OR necrotic pulp OR endodontic infection* OR root canal infections OR periapical OR periapical abscess OR apical lesions OR endodontic lesions OR apical periodontitis)) *AND*
Block 2	(TS=(fungi OR yeast* OR Candida albicans OR Candida OR mycobiome OR microbiome OR microorganisms OR microbiota OR microbiology OR mycology OR microbiologic OR microbial OR polymicrobial OR bacteria OR bacterial composition OR 16S ribosomal RNA OR 16s rRNA)) *AND*

A literature search was performed in 2020, using the Web of Science - Core Collection, Advanced Search Builder, with the aim of identifying original search articles of endodontic microbiology. The search strategy included two distinct blocks of keywords relevant to: endodontic infections (Block 1) and microorganisms (Block 2). Keywords in each block were separated by the Boolean Operator 'OR'. The final query combined the two keyword blocks by the Boolean Operator 'AND', to collect publications that incorporate the two blocks of interest. A field tag selected was TS=Topic. The tag "TS" searches for the following fields: title, abstract, author keywords and Keywords Plus.

2.4 Results and discussion

2.4.1 Bibliometric analysis

2.4.1.1 Most local cited authors

Local citations measure the number of citations that an author (or a document), included in this analysed collection, received from other documents included in the analysis. Bibliometric analysis revealed that Siqueira's papers collected the highest number of local citations over the 30 years (n = 3175), followed by Rôças (n = 2418) and Gomes (n = 1723), as shown (Figure 2.2).

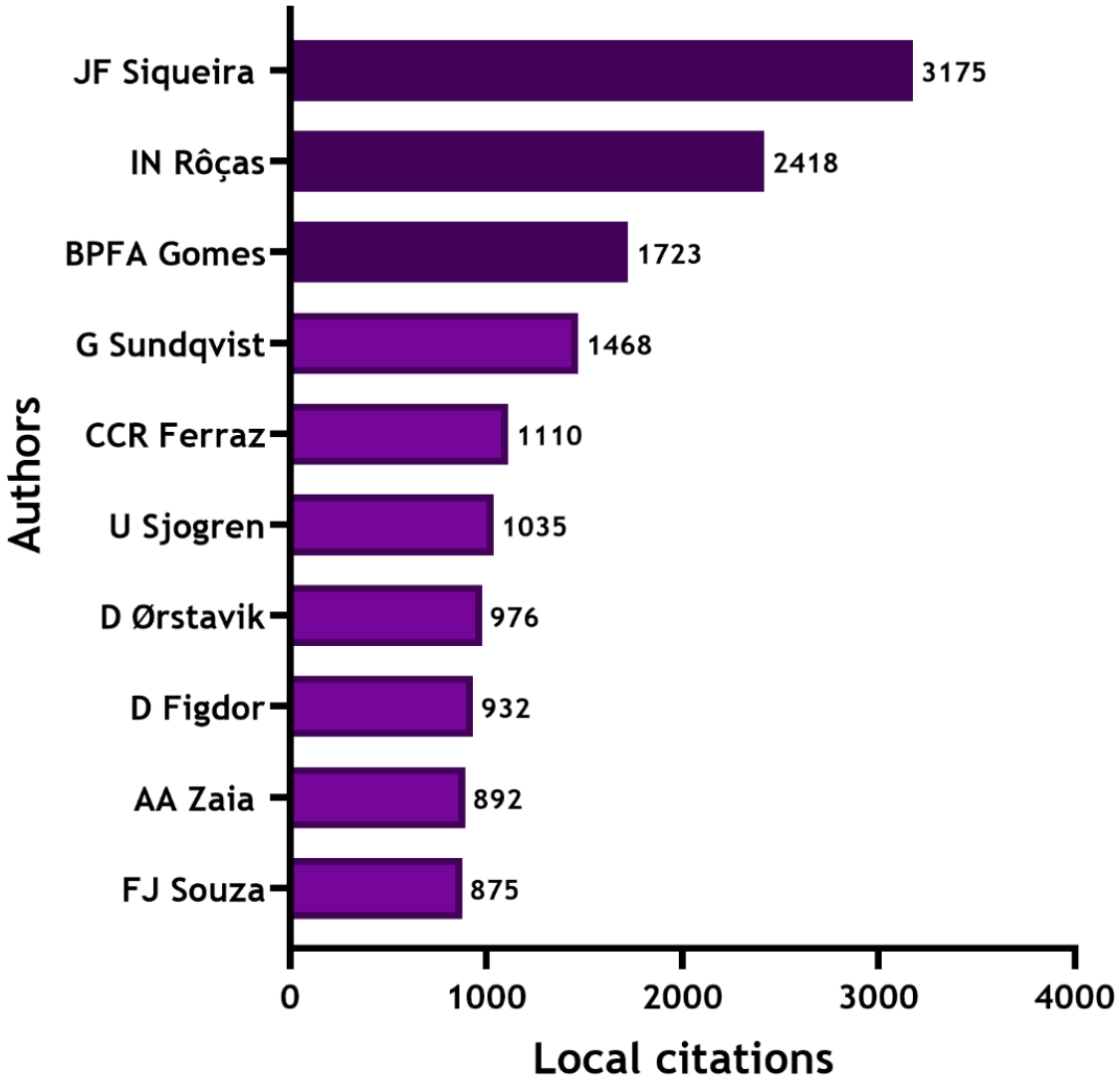

Figure 2.2. Most local cited authors. The bar chart shows the top ten authors by local citation from documents included in this collection. The GraphPad Prism (version 9.3.1) was used to present the local citation computed by the Bibliometrix R-package.

2.4.1.2 Authors' impact on research

Currently, the *h*-index can be used to assess outputs of authors. The *h*-index was introduced as a new measure of research impact by Hirsch (2005) to help in characterising researchers' scientific outputs. The *h*-index is defined as the number of papers with a citation number equal to or greater than *h* (Hirsch, 2005). Thus, the two concepts of productivity and impact are combined in a single indicator. For example, an *h*-index of three simply means that an author published at least three articles, each of which has been cited at least three times. The *h*-index started to be increasingly utilised as an indicator for evaluating the quality of journals (Masic and Begic, 2016). Despite its popularity, the *h*-index faces growing debate for evaluating the quality of researchers' work (Barnes, 2017). The index favours older researchers as the number of citations they receive may increase even if no new papers are published. Furthermore, the index can never lessen and is weakly sensitive to the number of received citations (Rousseau and Leuven, 2008). For instance, Sundqvist and Baumgartner received total citations of 3221 and 1416, respectively. However, the *h*-indices for both authors were 19 and 24, respectively, as shown in Table 2.2. Regardless, analysis from the Bibliometrix R package indicates that Siqueira, Rôças and Gomes were the top-cited authors with the highest scientific production outputs in endodontic microbiology research over the last three decades (Figure 2.2 and Table 2.2).

Narin (1976) stated that the truly creative scientists contribute to the progress of science by publishing a large number of heavily cited papers. However, some would dispute this observation, as Dumont (1989) stated: "The use of citation analysis as a tool to evaluate science is unfair, erroneous and dangerous. It leads to wrong ideas about what science is". In fact, quality versus quantity in publishing academic works has always been a sensitive topic of any citation analysis (Dumont, 1989, Agarwal et al., 2016). It has been shown by Eyre-Walker and Stoletzki (2013) that assessors tend to over-rate papers published in high-ranking journals. The study concluded that the subjective post-publication peer review, the number of citations received by articles and the journal impact factor, in which the article was published, are considered poor measures of scientific merit since they all depend upon subjective assessments.

Table 2.2. Author impact on endodontic microbiology research.

Author	*h*-index	TC	NP
JF Siqueira	48	6275	139
IN Rôças	40	4572	113
BPFA Gomes	33	3374	77
JC Baumgartner	24	1416	32
CCR Ferraz	23	2026	35
M Haapasalo	23	1936	40
AA Zaia	23	1683	36
D Ørstavik	22	2235	32
G Sundqvist	19	3221	24
M Trope	19	2050	21

TC; Total (global) citations, NP; Number of publications in the last three decades.

2.4.1.3 Analysis of the three top-cited authors' production

The scientific production of the three top-cited authors, with the highest *h*-index and highest number of publications, was analysed.

As revealed from the analysis (Figure 2.3), the first three articles published by Siqueira were in 1996, implying the start of his scientific production in the field. In 2004, the number of documents published reached ten articles, which was the highest publication number recorded per year, with total citations of 50.63. Two of these ten publications were heavily cited (Siqueira and Rôças, 2004, Rôças et al., 2004), where *E. faecalis* was strongly associated with persistent endodontic infections. His scientific production in endodontic microbiology research continued over the years with some fluctuations. In 2019, only three publications were recorded for Siqueira (Zandi et al., 2019, Gazzaneo et al., 2019, Cabreira et al., 2019), which received total citations of 2.25 by mid-2020. One of these was a randomised clinical study by Zandi et al. (2019). The study showed no significant differences in endodontic retreatment outcomes between 1% NaOCl and 2% CHX when used as root canal irrigants, where 81% and 82% of teeth with apical periodontitis healed in the NaOCl and CHX groups, respectively, at the 4-years follow-up. As the analysis showed, Rôças was the main co-author to

Siqueira in most of his publications. She started her scientific production in 2000 and continued over the time with a similar trend to Siqueira's.

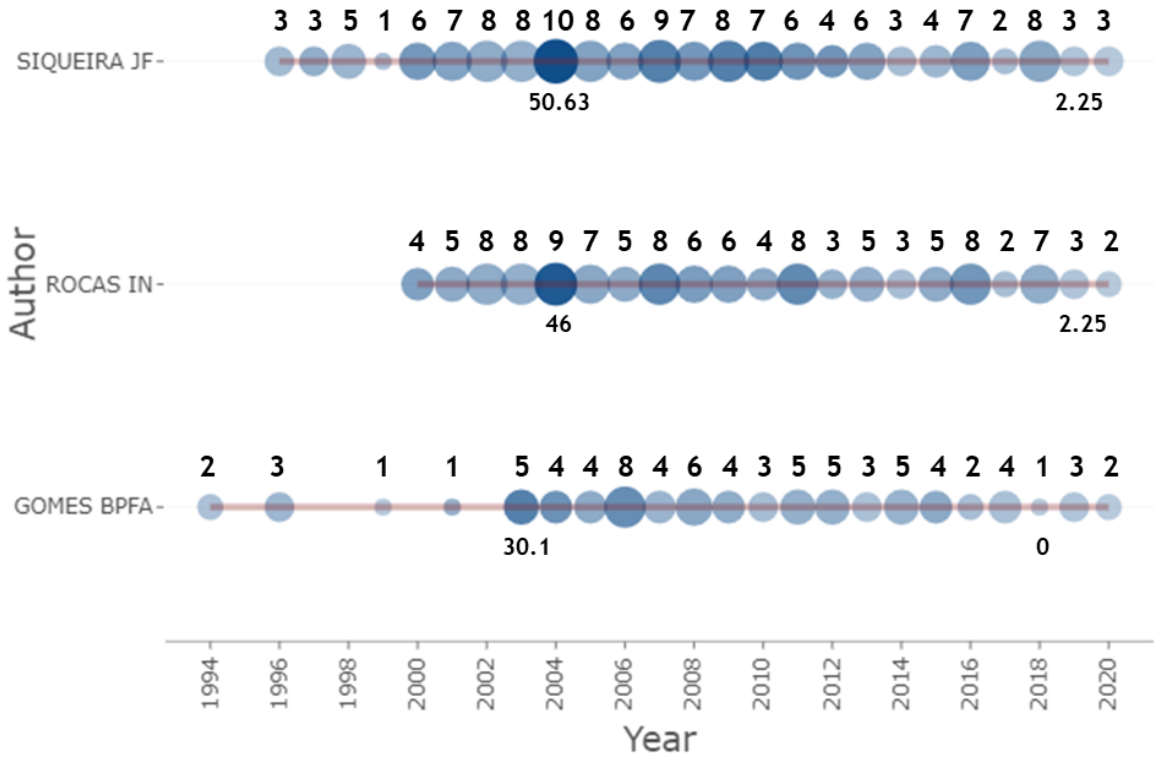

Figure 2.3. Author's annual production over time. Each author's timeline is represented by a line. Gomes had the longest timeline from 1994 to 2020. The bubble size is proportional to the number of articles. Number of articles published per year was shown above each bubble. The colour intensity is proportional to the total citations per year (darkest bubbles indicate high citations). The highest and lowest total citations per year were shown below the lightest and the darkest bubbles, respectively, for each author. The plot was downloaded from the Biblioshiny app as a PNG image.

The beginning of Gomes's scientific production was in 1994, with two publications, and this production continued over the time specified for this analysis (Figure 2.3). In the period from 1994 to 2003, 12 articles were recorded. Notably, in 2001, only one study was published by Gomes (Gomes et al., 2001), which assessed and confirmed the effectiveness of NaOCl and CHX (gel and liquid), *in vitro*, in several concentrations, in elimination of *E. faecalis* when used as endodontic irrigants. This study by Gomes et al. (2001) received high citations (total citations of ten), per year. The annual production, however, became notable in 2003, where five articles were published with the highest

total citations of 30.1 per year. In the subsequent decade, from 2004 to 2013, the number of publications rose by 3.8-fold, where 46 articles were recorded. In 2018, only one article was published (Muniz et al., 2018), which received no citation, by mid-2020. The study was the first in assessing the correlation between the periodontal bone loss and pathogenic bacteria presented in the root canal or apical lesion. Importantly, the findings suggested no direct correlations (Muniz et al., 2018).

Regardless of these results, it is particularly important to understand the appropriate uses and limitations of bibliometrics in order to employ bibliometric data to their best advantage (Agarwal et al., 2016). One of the limitations of bibliometric analysis is that recent articles receive fewer citations because of the time effect, as they have less time to amass citations (Adnan and Ullah, 2018). Therefore, it is not surprising that the recent publications of the three top-cited authors have received fewer citations than the previous ones (Figure 2.3). In a study by Fardi et al. (2011), the first top-cited article was a classical study published by Kakehashi et al. (1965) that established a cause-effect relationship between microorganisms and apical periodontitis. Another issue with citation is oriented or biased citing, consciously or unconsciously, in various ways, without any malicious intent, such as self-citation bias, or bias towards friends, colleagues or specific journals. Cultural or the English language biases are other factors. Less innocent biases can also occur by omission of competitors' publications or when information disagrees with one's own results (Dumont, 1989).

Other issues can arise in bibliometric research when searching for particular researchers. For example, one issue is the inconsistency in researchers' names in different publications. Some authors have been cited with name variations, despite all being the same person. Another issue is one of a name change, notably by female researchers who change their names after marriage or who reassume their maiden names (MacRoberts and MacRoberts, 1989). Another issue in terms of publication analysis which is not uncommonly encountered is "homonymy"; when different individuals have an identical author name (Aksnes, 2008). This problem was addressed by Soler (2007), who has a program available that uses a mathematical algorithm to break down a WOS publication list into

cluster related articles. Thus, all the articles of a cluster are likely to belong to the same author. This can separate homologues by selecting the appropriate clusters based on similar topics. It is also imperative to understand the chosen databases and their limitations. In this study, WOS constitutes the source of this bibliometric analysis. The WOS database covers all authors' addresses whilst other databases may only cover the corresponding author (Thompson and Walker, 2015).

Although the assessment of academic impact and reputation of researchers does not merely rely on their research output, bibliometric analysis provides an objective measure of their productivity and influence on the scientific community (Agarwal et al., 2016). However, evaluating scientists' achievements should be more comprehensive than just solely counting the number of their articles published in a high impact journal. The researcher's characteristics, number of patents and awards they receive, their national and international reputation and teaching responsibilities are all very important aspects in assessment of a scientist's profile (Agarwal et al., 2016). Therefore, in order to provide the most robust assessment, Agarwal et al. (2016) suggested using a combination of qualitative information, such as peer review, and quantitative bibliometric tools with multiple indicators.

2.4.1.4 Top-locally cited articles in endodontic microbiology

Citation analysis is one of the key methods in bibliometrics that construct and apply a series of indicators on research publications by deriving citation data to quantify the importance of research as indicated by the citation counts that a manuscript obtains (Moed, 2009). A fundamental aspect of scientific papers is the list of references referring to preceding publications (L Smith, 1981). A reference is an acknowledgment that one article gives to another. A citation is an acknowledgment that one article receives from another. The evaluation of such relationships between a cited and citing document is defined in bibliometrics as "citation analysis" (L Smith, 1981).

The term "citation classics" is a bibliometric concept introduced by Garfield (1977) to identify, as well as, acknowledge the top-cited articles and their impact on a particular speciality. In the study by Ordinola-Zapata et al. (2020),

only a few topics in endodontics have been highly cited, since 1980, and can be considered as classics. These topics are on the microbiological aetiology of endodontic diseases, endodontic treatment outcomes, regenerative endodontic procedures, discovery and use of nickel-titanium and the development and use of mineral trioxide aggregate.

Our study has also identified the 30 top-locally cited articles in endodontic microbiology from 1990 to 2020, the review of which will help researchers and clinicians to identify the most influential studies that impacted upon this field. The local citations were obtained to reduce the bias since a large part of global citations could be received from other disciplines.

The top 30 articles are listed in (Table 2.3) in a descending order, based on the number of local citations they received. The top-cited papers appeared in seven different journals: *International Endodontic Journal* (n = 10), *Journal of Endodontics* (n = 9), *Oral Surgery Oral Medicine Oral Pathology Oral Radiology and Endodontology* (n = 4), *Oral Microbiology and Immunology* (n = 3), *Journal of Clinical Microbiology* (n = 2), *Journal of Dental Research* (1), *Dental Traumatology* (n = 1). The most cited articles were classical studies published by Sundqvist et al. (1998), Molander et al. (1998) and Sjögren et al. (1997). The most and the least cited articles received 403 and 74 local citations, respectively.

Table 2.3. Analysis of 30 top-cited articles in endodontic microbiology.

Rank	Article title	Author & year	Journal	Local citations
1	Microbiologic analysis of teeth with failed endodontic treatment and the outcome of conservative re-treatment	(Sundqvist et al., 1998)	*Oral Surg. Oral Med. Oral Patho. Oral Radiol. and Endod.*	403
2	Microbiological status of root-filled teeth with apical periodontitis	(Molander et al., 1998)	*International Endodontic Journal*	297
3	Influence of infection at the time of root filling on the outcome of endodontic treatment of teeth with apical periodontitis	(Sjögren et al., 1997)	*International Endodontic Journal*	247
4	Microorganisms from canals of root-filled teeth with periapical lesions	(Pinheiro et al., 2003)	*International Endodontic Journal*	188
5	Intraradicular bacteria and fungi in root-filled, asymptomatic human teeth with therapy-resistant periapical lesions: a long-term light and electron microscopic follow-up study	(Nair et al., 1990)	*Journal of Endodontics*	187
6	Polymerase chain reaction–based analysis of microorganisms associated with failed endodontic treatment	(Siqueira and Rôças, 2004)	*Oral Surg. Oral Med. Oral Patho. Oral Radiol. and Endod.*	159
7	Microbial status of apical root canal system of human mandibular first molars with primary apical periodontitis after “one-visit” endodontic treatment	(Nair et al., 2005)	*Oral Surg. Oral Med. Oral Patho. Oral Radiol. and Endod.*	156
8	Association of *Enterococcus faecalis* with different forms of periradicular diseases	(Rôças et al., 2004)	*Journal of Endodontics*	151
9	*Enterococcus faecalis* – a mechanism for its role in endodontic failure	(Love, 2001)	*International Endodontic Journal*	148
10	Bacteria isolated after unsuccessful endodontic treatment in a North American population	(Hancock III et al., 2001)	*Oral Surg. Oral Med. Oral Patho. Oral Radiol. and Endod.*	143
11	Associations between microbial species in dental root canal infections	(Sundqvist, 1992)	*Oral Microbiology and Immunology*	141
12	Microbiological examination of infected dental root canals	(Gomes et al., 2004)	*Oral Microbiology and Immunology*	141
13	Reduction of intracanal bacteria using nickel-titanium rotary instrumentation and various medications	(Shuping, 2000)	*Journal of Endodontics*	131
14	Isolation of yeasts and enteric bacteria in root-filled teeth with chronic apical periodontitis	(Peciuliene et al., 2001)	*International Endodontic Journal*	130

15	The antimicrobial effect of calcium hydroxide as a short-term intracanal dressing	(Sjögren et al., 1991)	*International Endodontic Journal*	116
16	Molecular and cultural analysis of the microflora associated with endodontic infections	(Munson et al., 2002)	*Journal of Dental Research*	115
17	*In vitro* antimicrobial activity of several concentrations of sodium hypochlorite and chlorhexidine gluconate in the elimination of *Enterococcus faecalis*	(Gomes et al., 2001)	*International Endodontic Journal*	114
18	Bacteria in the apical 5 mm of infected root canals	(Baumgartner and Falkler, 1991)	*Journal of Endodontics*	104
19	Biofilms and apical periodontitis: study of prevalence and association with clinical and histopathologic findings	(Ricucci and Siqueira, 2010)	*Journal of Endodontics*	104
20	Biofilm formation in medicated root canals	(Distel et al., 2002)	*Journal of Endodontics*	98
21	PCR-based identification of bacteria associated with endodontic infections	(Fouad et al., 2002)	*Journal of Clinical Microbiology*	92
22	Fungi in therapy-resistant apical periodontitis	(Waltimo et al., 1997)	*International Endodontic Journal*	90
23	Inactivation of local root canal medicaments by dentine: an *in vitro* study	(Haapasalo et al., 2000)	*International Endodontic Journal*	90
24	Observation of bacteria and fungi in infected root canals and dentinal tubules by SEM	(Sen et al., 1995)	*Dental Traumatology*	86
25	Molecular identification of microorganisms from endodontic infections	(Rolph et al., 2001)	*Journal of Clinical Microbiology*	85
26	Microbiological findings and clinical treatment procedures in endodontic cases selected for microbiological investigation	(Siren et al., 1997)	*International Endodontic Journal*	84
27	Viable bacteria in root dentinal tubules of teeth with apical periodontitis	(L Peters et al., 2001)	*Journal of Endodontics*	83
28	The effectiveness of increased apical enlargement in reducing intracanal bacteria	(Card et al., 2002)	*Journal of Endodontics*	79
29	Molecular analysis of bacteria in asymptomatic and symptomatic endodontic infections	(Sakamoto et al., 2006)	*Oral Microbiology and Immunology*	77
30	The role of environmental changes on mono-species biofilm formation on root canal wall by *Enterococcus faecalis*	(George et al., 2005)	*Journal of Endodontics*	74

Oral Surg. Oral Med. Oral Patho. Oral Radiol. and Endod.; *Oral Surgery, Oral Medicine, Oral Pathology, Oral Radiology, and Endodontology*.

According to the results, a few areas of endodontic microbiology have been explored among the 30 top-cited publications since 1990. Most studies looked at the microbial composition present in necrotic and failed endodontically treated teeth. The topmost cited articles found were classical studies published by Sundqvist et al. (1998), followed by Molander et al. (1998). The findings of the Sundqvist et al. (1998), Molander et al. (1998), Pinheiro et al. (2003) and Hancock III et al. (2001) stand with the classical observation in which *E. faecalis* and *Enterococcus* are commonly recovered from root canals of teeth with endodontic failures. Siren et al. (1997) observed that *E. faecalis* was more frequently recovered from canals with an inadequate seal between the appointments and from cases treated with a high number of visits. It is hypothesised that it has been introduced in the root canal system at some time following the professional intervention. Such traditional culture studies harboured distinct and fewer microbial species recovered from root canals with treatment failure compared to untreated teeth with infected canals, as shown in four of these top-cited papers published by Baumgartner and Falkler (1991), Sundqvist (1992), L Peters et al. (2001) and Gomes et al. (2004).

Based on these observations, it was concluded that some microorganisms could withstand antimicrobial measures and survive the harsh conditions during root canal treatment procedures, in which restricted nutrition and minimum cooperative relationships with other bacteria can exist. Therefore, there has been a growing interest in testing the effectiveness of different antimicrobial agents against *E. faecalis* species and examining a possible mechanism in which they could survive and reinfect obturated canals. The study by Love (2001) suggested that the ability of *E. faecalis* to invade dentinal tubules and attach to collagen may explain this resistance. However, observations by George et al. (2005) showed that the depth of *E. faecalis* penetration was significantly greater in nutrient-rich conditions compared to the nutrient-deprived ones. Additionally, Distel et al. (2002) illustrated that the ability of *E. faecalis* to form biofilm in root canals could be another mechanism of resistance. In contrast, Gomes et al. (2001) demonstrated the efficacy of different concentrations of NaOCl and chlorhexidine in killing *E. faecalis*. However, Haapasalo et al. (2000) observed an inhibitory effect of dentine powder on calcium hydroxide, NaOCl and chlorhexidine when tested on *E. faecalis*.

The possible role of fungi in endodontic failures appeared for the first time in these 30-top cited articles in the study by Nair et al. (1990). The study revealed, with the use of light and electron microscopy, the presence of bacteria and yeasts in periapical lesions of root-filled teeth. Sen et al. (1995), with the use of scanning electron microscopy, observed extensive yeast penetration into dentinal tubules and root canals of teeth with necrotic pulps. Other cultural studies observed a high prevalence of yeasts in root-filled teeth with apical periodontitis (Waltimo et al., 1997, Peciuliene et al., 2001).

The beginning of a new era of microbial identification started with the use of culture-independent, molecular-based methods, as Siqueira and Rôças (2004) revealed that *E. faecalis* was the most prevalent species detected in 77% of teeth with failed endodontic treatment. However, *C. albicans* was found in 9% of the cases. Rôças et al. (2004) investigated the association of *E. faecalis* with different patterns of endodontic diseases. The results showed that *E. faecalis* was much more likely associated with failed endodontic treatment than in primary infections. In this collection, four molecular-based studies identified a more diverse microflora associated with endodontic infections than previously described by culture methods (Rolph et al., 2001, Fouad et al., 2002, Munson et al., 2002, Sakamoto et al., 2006). Sakamoto et al. (2006) also showed that a higher number of taxa were present in symptomatic samples compared to asymptomatic samples. However, these previous molecular studies are limited to detection of bacteria.

In these top-cited publications, there was also an interest in achieving root canal disinfection to a satisfactory standard. Sjögren et al. (1991) demonstrated that dressing the canal with calcium hydroxide for 7 days efficiently eliminates bacteria. The study by Sjögren et al. (1997) emphasises the importance of obtaining a bacteria-free canal before root canal obturation to achieve eventual healing outcomes, which cannot be achieved without the use of an inter-appointment antimicrobial dressing. The findings of Nair et al. (2005) also supported the use of multiple-visit treatment with infected and necrotic root canals, particularly in view of the interest towards single visit treatment growing following the introduction of rotary nickel-titanium instruments to endodontic practice. Shuping (2000) advocated that the use of NaOCl irrigation with rotary instrumentation and calcium hydroxide intracanal medication was significant in

the reduction of the intracanal bacteria during endodontic treatment. A significant reduction of microbial load was also observed in another study in these 30 top-cited articles after instrumentation with rotary instruments and NaOCl irrigation (Card et al., 2002). Finally, the study by Ricucci and Siqueira (2010) established the substantial role of endodontic infections in the form of biofilms in the root canal system of teeth with apical periodontitis.

This quick mapping of the literature showing the weight of classical publications which were cited heavily by other subsequent works. These 30 top-cited studies over the last three decades, indeed, have created landmark delineations for subsequent publications in the field.

2.4.2 Ontological analysis

2.4.2.1 Most frequently observed microbial species in endodontic microbiology

Since ontological analysis is thought to be a perfect complement to the bibliometric analysis, an ontology-based analysis was used to identify the most frequent microorganisms present in the literature of endodontic infections over the past 30 years. The most frequently mentioned 'organism-related' terms were identified from a total of 110 'organism-related' terms.

Not surprisingly, the frequency of the term '*Enterococcus faecalis*' grew rapidly over the years, particularly between 2014 and 2019, to become the most frequent over the last three decades (n = 932). Clearly, *E. faecalis* appeared to be central in the research field between 1990 and 2020. Other 'organism related' terms, within the field of endodontic microbiology, were also amongst the most frequently used in this collection, including '*Candida albicans*' (n = 200), which manifested a small increase over the years, '*Fusobacterium nucleatum*' (n = 182) and '*Porphyromonas gingivalis*' (n = 168), as shown (Figure 2.4). The frequent use of these terms suggests that these species were common in endodontic infections, although an overall rise in the annual frequency was not appreciable (Figure 2.4B).

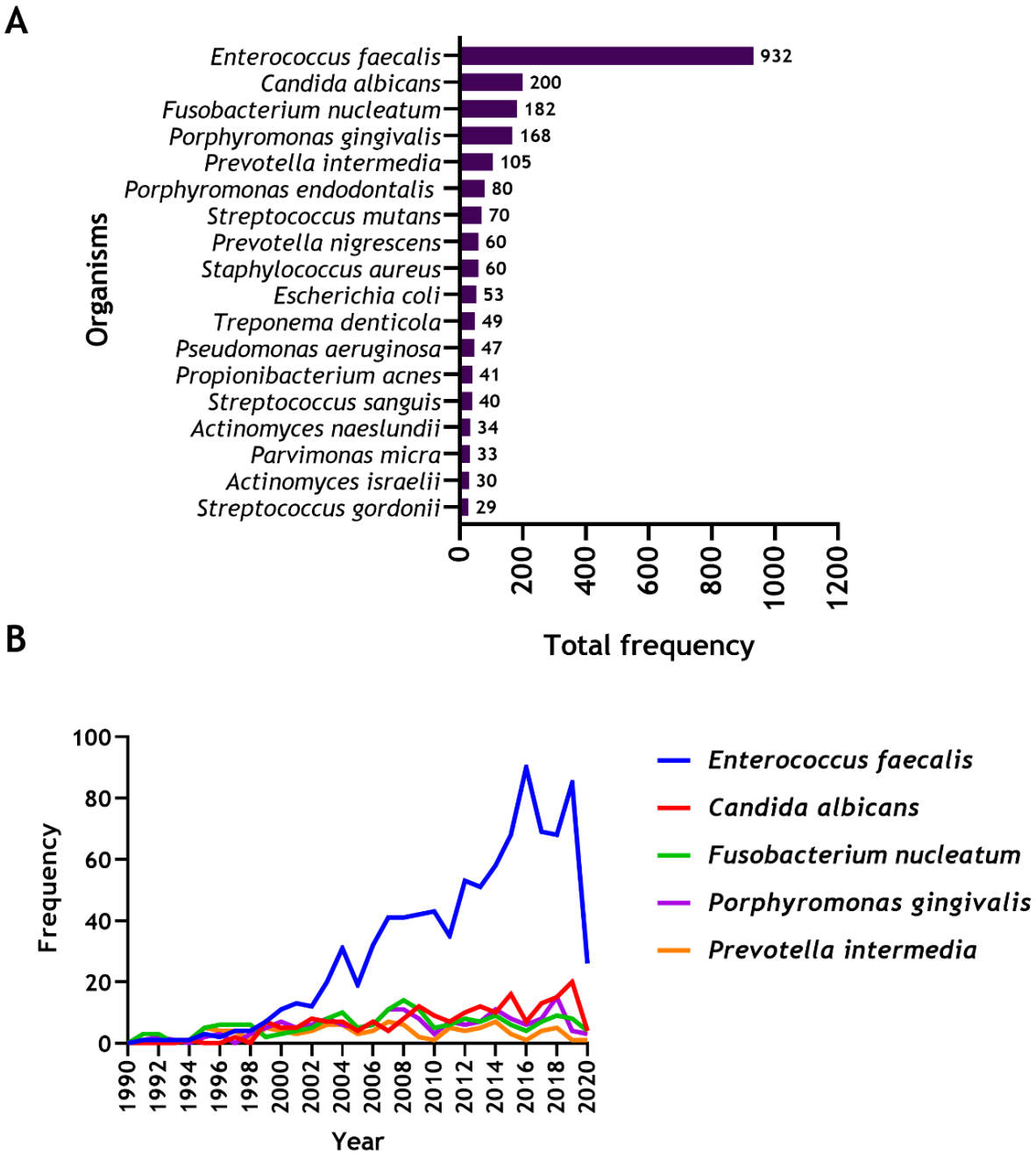

Figure 2.4. Most frequent terms and their patterns in the literature of endodontic microbiology between 1990 and mid-2020. (A) The top 18 frequent microbial species mentioned in the literature over the 30 years. **(B)** The top five frequent species mentioned in the endodontic microbiology literature per year over the last three decades. Frequency = the number of mentions per year. Total frequency = the number of mentions over the 30 years.

Scientific publications in the field of endodontic microbiology have been overwhelmed, until recently, with studies investigating *E. faecalis*. It has been reported that *E. faecalis* was used in 79% of all biofilm model systems for root canal disinfection, and more alarmingly in 92% of mono-species biofilm model studies (Swimberghe et al., 2019). However, NGS studies showed several key

genera most commonly detected in primary and persistent endodontic infections, where *Enterococcus* was not one of the key genera detected. The key genera most commonly detected, recently, in endodontic infections were *Fusobacterium*, *Porphyromonas*, *Streptococcus*, *Parvimonas*, and *Prevotella* (Shin et al., 2018). *Fusobacterium nucleatum* was associated with the most severe forms of inter-appointment endodontic flare-ups (de Paz Villanueva, 2002) and found to be the most predominant species in acute periapical abscesses in primary teeth (W Zhang et al., 2020). Isolation of *Streptococcus mutans* from root canals of primary and secondary/persistent infections has been reported (Lima et al., 2020). Other streptococci like *Streptococcus gordonii* and *Streptococcus sanguis* have also been detected in root canals with persistent infections (de Paz et al., 2005, Murad et al., 2014). *Porphyromonas gingivalis* was isolated from infected root canals of primary infections (Zargar et al., 2020). Importantly, a high frequency of *Porphyromonas gingivalis*, *E. faecalis* and *Fusobacterium nucleatum* was found in teeth with endodontic failures, with a large variety of other species (Gomes et al., 2021). This ought to be considered when developing biofilm models for studying endodontic diseases that can be used to assess conventional and novel endodontic therapeutics.

2.4.2.2 Chemical compounds in endodontics

The frequency of conventional antimicrobial irrigants were also assessed. The term ‘sodium hypochlorite’ was found to be the most frequent term used in the literature (n = 555), followed by ‘chlorhexidine’ (n = 380) and ‘EDTA’ (n = 163). The term ‘chitosan’ was identified in 32 abstracts (n = 32), where its frequency reached the peak in 2019 (n = 10). Overall, there has been a clear upward trend in the number of mentions, for all the compounds, in the last decade (Figure 2.5), where a significant amount of *in vivo*, *ex vivo*, *in vitro* and clinical studies have been published describing different approaches, instruments and materials that have been tested to define the best practice in eliminating endodontic infections.

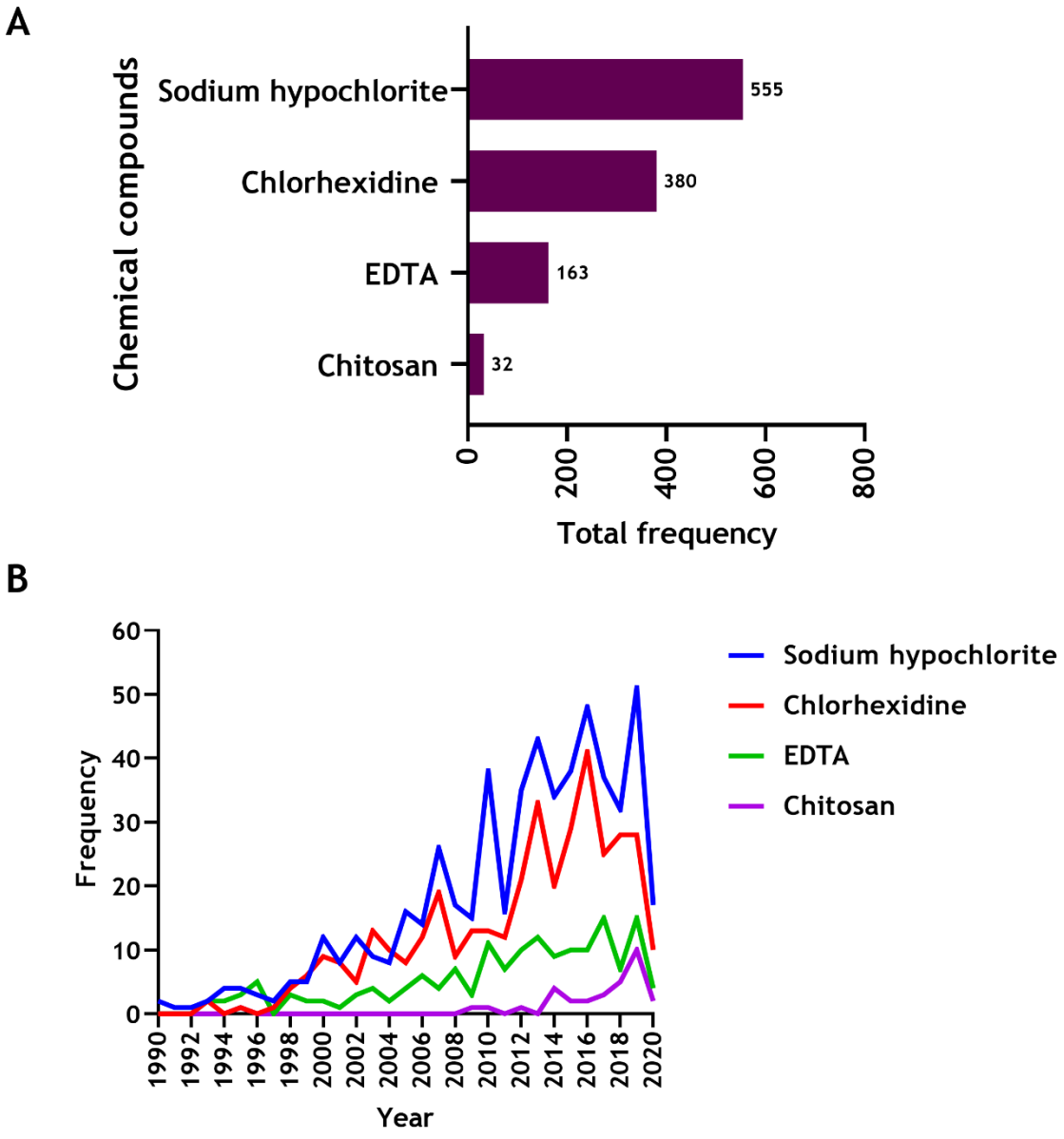

Figure 2.5. The frequency and patterns of selected chemical compounds used in endodontic treatment from 1990 to mid-2020. (A) The total frequency of 'chemical compound-related' terms (the number of mentions over the 30 years) in the endodontic microbiology literature. **(B)** Trend patterns of the selected chemical compounds used in the literature. Frequency = the number of mentions per year.

In this study, a rapid, automated ontology-driven workflow was used, which involved the annotation of the scientific literature with rich metadata, using the associated PubMed identifiers. Therefore, one of the limitations of this method is that articles without PMIDs cannot be annotated. In addition, with any software used, irrelevant data could be incorporated. Therefore, the manual

approach was then performed to confirm the results for these selected ontologies of interest.

Ultimately, whether using a bibliometric analysis or an ontological analysis, there is a blinded preponderance of activity relating to *E. faecalis*. It is crucial we have an awareness of the polymicrobial nature of endodontic infections, whether primary or secondary, as the physical and structural basis of the microbial biofilm is undoubtedly a key factor in treatment success. Therefore, harnessing nature alongside positively directing the host environment is certainly a step in the right direction.

CHAPTER FINDINGS

- The interpretation of the available publications can be subjective and reflects reviewer's bias.
- Bibliometrics and the ontology-based annotation are two advanced quantitative measures employed to analyse scientific research outputs and trends in a time-efficient manner.
- It is now possible to reduce the vast amount of information to a far more inclusive and controllable set of deductive patterns.
- It seems rational to employ interkingdom microbial consortia of microorganisms related to root canal infections to develop a biofilm model suitable for assessing novel antimicrobial materials.

3 Optimising a polymicrobial interkingdom endodontic biofilm model

3.1 Introduction

Endodontic disease is primarily driven by a microbial insult to pulpal and periapical tissues (Gutmann and Manjarrés, 2018). There has been a considerable interest in determining the microbial composition and diversity involved in endodontic infections. Understanding which species are involved in persistent apical periodontitis provides important insights into the development of new therapeutic approaches that may enhance clinical outcomes (Sánchez-Sanhueza et al., 2018). Until recently, the field of endodontic microbiology has been swamped with studies investigating *Enterococcus faecalis* (Swimberghe et al., 2019). However, with the advent of next generation sequencing, combined with more careful and accurate sampling procedures, we have developed a greater insight into the polymicrobial nature of the infected root canal (Tran et al., 2013, Nardello et al., 2020). The improvement in sequencing techniques and sampling methodologies has allowed researchers to show that the infected root canal is an ideal microenvironment for polymicrobial interactions (Nardello et al., 2020). These microbiome studies have illuminated our limited understanding by revealing a great diversity of bacteria that represent many of the common 'garden variety' oral species associated with cariogenic and periodontal diseases. To make matters more complex, mycobiome studies and other mycological investigations have revealed that *Candida* spp. play an important, yet unrecognised, role in supporting these complex communities (Delaney et al., 2018). This is of clinical significance, but the correlation of mycobiome-bacteriome interkingdom interactions with root canal infection and treatment success is still uncertain (Persoon et al., 2017).

These consortia exist within complex polymer enclosed biofilms, and demonstrate interspecies and interkingdom interactions, which may be synergistic or antagonistic in nature (Freilich et al., 2011). The underlying mechanisms of polymicrobial interactions that lead to inflammatory diseases remain largely unknown (Hajishengallis et al., 2011), yet it is likely that these interactions play a significant role in development and progression of endodontic disease. Regardless, these biofilm structures demonstrate inherent tolerance to physical and chemical intervention, thus creating significant challenges for clinical management (Neelakantan et al., 2017).

Accordingly, biofilm model systems are a requisite in supporting the development of novel chemo-mechanical therapeutic approaches to investigate and modify existing treatment protocols. A vast plethora of polymicrobial oral biofilm models have been developed that are now commonplace in most research laboratories investigating the pathogenicity of different oral diseases (Brown et al., 2019b). However, to date, a limited number of endodontic models exist that accurately recapitulate the microenvironment of the root canal. In fact, existing endodontic biofilm models have been very limited in scope and complexity. It was highlighted that 86% of existing endodontic models reported in the literature consisted of simple single-species biofilms, with 92% of these studies containing only *E. faecalis* (Swimberghe et al., 2019). These findings represent the significant issues facing innovations in the endodontic field. Nowadays, recognition of fastidious and uncultivable microbial species and the characterisation of the microflora associated with endodontic infections are possible due to the progress of molecular methods based on the detection of specific genomic sequences for each microbial species (Shahi et al., 2018). Therefore, ideally, when it comes to selecting the microbial composition for an endodontic biofilm model, then typical members of microbiota that are commonly isolated from infected root canals are included. Such engineered biofilm systems with defined laboratory strains provide an opportunity to control the model, opposed to undefined 'natural' consortia that are inherently problematic, which has important repercussions in testing and developing new endodontic irrigants. A defined engineered biofilm has been developed from a number of known species that are usually well-characterised laboratory strains, whereas an undefined natural biofilm is designed from unknown species secluded directly from the natural environment of interest, which closely mimics the microbial composition of the environment as it captures the natural diversity (C Tan et al., 2017). The defined engineered biofilm system is commonly used by different laboratories due to being highly reproducible, easily manipulated, time- and cost-effective and rather simply analysed and interpreted (C Tan et al., 2017), whereas undefined consortia are extremely diverse microbial populations that are imprecise for replicate experiments by researchers (Marsh, 1995). In addition, the analysis is complex and costly (C Tan et al., 2017).

With these issues to consider, we must be aware of the necessity for the employment of suitable robust model systems. Although this may not immediately be extrapolated to our clinical practice, it should enlighten our further exploration of endodontic microbiology. Therefore, it is clearly suitable to design appropriate multispecies biofilm models, instead of simple mono-species models, that reflect the clinical situation, at least with some degree of realism.

3.2 Aims

The following chapter aims to:

- Develop and optimise a defined multispecies interkingdom biofilm model comprised from a paradigm of oral species frequently identified in endodontic infection, in a simple and a reproducible manner.

- Provide a platform for assessing the interkingdom interactions within the optimised biofilm model, that may help in developing new effective management strategies in endodontics.

Data from this chapter have been published in:

- **Abusrewil**, S., Brown, J.L., Delaney, C.D., Butcher, M.C., Kean, R., Gamal, D., Scott, J.A., McLean, W. and Ramage, G., 2020. Filling the void: an optimized polymicrobial interkingdom biofilm model for assessing novel antimicrobial agents in endodontic infection. *Microorganisms*, 8(12): 1988. DOI: 10.3390/microorganisms8121988. Pub 2020 Dec 14. PMID: 33327403.

Work from this chapter has been presented at the 6th European Congress on Biofilms, EUROBIOFILMS, September 2019, Glasgow, Scotland, UK.

3.3 Materials and methods

All media and reagents were obtained from Sigma-Aldrich (UK) unless otherwise stated. Biofilms, in this work, are composed of defined laboratory strains of oral microorganisms, grown in microtiter well plates. All biofilm studies reported in this work was carried out in accordance with the minimum information guidelines specified for biofilm formation in microplates (Allkja et al., 2020). Both technical and biological repeats have been included to obtain validity. Technical repeats are repeated measurements performed on several samples of the same biofilm from a single starter culture grown in identical conditions, whereas biological repeats represent parallel tests on a biofilm grown according to the same experimental parameters, but from another starter culture and at another timepoint (Swimberghe et al., 2019). All microbiology experiments were performed three times with at least three technical replicates (n = 3), unless otherwise stated.

3.3.1 Biofilm model development

3.3.1.1 Microbial strains, culturing and standardisation

The strains of microorganisms used throughout this thesis were *Candida albicans* (strain SC5314 / ATCC MYA-2876), *Streptococcus gordonii* (strain Challis / DL1 / NCTC 7868 / ATCC 35105), *Porphyromonas gingivalis* (ATCC 33277) and *Fusobacterium nucleatum* (ATCC 10953), as listed in Table 3.1.

Table 3.1. Laboratory strains of microorganisms used throughout this thesis.

Name	Reference
Candida albicans strain SC5314 (ATCC MYA-2876)	(Gillum et al., 1984)
Streptococcus gordonii strain Challis (NCTC 7868)	(Colman and Williams, 1965)
Porphyromonas gingivalis (ATCC 33277)	(Coykendall et al., 1980)
Fusobacterium nucleatum (ATCC 10953)	(De Araujo et al., 1963)

All strains were stored at -80°C in Microbank™ vials (Pro-Lab Diagnostics, Birkenhead, UK) prior to propagation on agar media. The strain of *C. albicans* was regularly cultured on Sabouraud dextrose agar (SAB [Sigma-Aldrich, Dorset,

UK]) plates and incubated aerobically at 30°C for 24-48 h until colonies of about 1 mm in diameter were formed. The plates were then kept at 4°C. Yeast cultures were routinely propagated by inoculating 10 mL of yeast peptone dextrose (YPD) (1% w/v yeast extract, 2% w/v peptone, 2% w/v dextrose, 1.5% agar [Sigma-Aldrich, UK]) with a loopful of yeast colonies in a 25 mL universal tube (Sterilin® Limited, Cambridge UK) and incubated overnight in an orbital benchtop shaker (IKA KS 4000 I control, Staufen, Germany) at 200 revolutions per minute (rpm) for 16-18 h at 30°C. Following growth, the yeast cells were pelleted by centrifugation at 3,000 rpm for 5 minutes. The pellet was then washed via resuspension twice in sterile phosphate buffered saline (PBS) (10 mM phosphate buffer, 2.7 mM potassium chloride, 137 mM sodium chloride, pH 7.4 [Sigma-Aldrich, UK]). The cells were diluted 100 times by adding 10 µL of the cell suspension into 990 µL of PBS in a sterile Eppendorf tube. The cells were then counted using a Neubauer haemocytometer (cell count × dilution factor × volume of square = colony forming unit [CFU/mL]).

The strain of *S. gordonii* was cultured on Columbia blood agar (CBA [Sigma-Aldrich, UK]) supplemented with 5% horse blood. The agar plates were incubated in a 5% CO_2 incubator (Heracell, Heraeus, UK) for 24 h at 37°C and then kept at 4°C. Suspension cultures were grown overnight inside the same incubator in 10 mL of Trypticase soy broth (TSB [Sigma-Aldrich, UK]) for 16-18 h at 37°C. After incubation, cells were recovered by centrifugation and the supernatant was discarded. The pellet was resuspended in PBS prior to standardisation to 1×10^8 cells/mL. Dilutions were performed to obtain the desired bacterial cell concentration (1×10^8 cells/mL), calculated by measuring the optical density of 0.5 with a spectrophotometer at 550 nm (OD_{550}), as determined by diluting pure colonies using the Miles and Misra colony counting technique (Miles et al., 1938).

P. gingivalis and *F. nucleatum* were cultured on Fastidious anaerobic agar plates (FAA [Sigma–Aldrich, Dorset, UK]), containing 5% defibrinated horse blood, and maintained in an anaerobic incubator (85% N_2, 10% CO_2 and 5% H_2 [Don Whitley Scientific Limited, Bingley, UK]) at 37°C for 48 h. The plates were kept in the anaerobic incubator. Bacterial suspension cultures were propagated as previously mentioned by inoculating 10 mL of Schaedler broth (SCH [Oxoid, Basingstoke, UK]) with a loopful of bacterial colonies and incubated for 16-18 h

in the same incubator, before being resuspended in PBS following centrifugation. Bacterial cells were standardised using a spectrophotometer at 550 nm, with the absorbance value of 0.2, approximately equating to 1 × 10^8 cells/mL. A summary of microbial growth conditions and standardisation is listed and illustrated in (Table 3.2 and Figure 3.1).

Table 3.2. Microbial growth conditions and standardisation.

Organism	Identifier	Agar	Broth	Conditions	OD 550 $_{nm}$ (1x10^8 cells/mL)
C. albicans	ATCC MYA-2876	SAB	YPD	30˚C O_2	Count in haemocytometer
F. nucleatum	ATCC 10953	FAA	SCH	37˚C AnO_2	0.2
P. gingivalis	ATCC 33277	FAA	SCH	37˚C AnO_2	0.2
S. gordonii	ATCC 35105	CBA	TSB	37˚C 5% CO_2	0.5

SAB; Sabouraud dextrose agar, FAA; Fastidious anaerobic agar, CBA; Columbia blood agar, YPD; Yeast peptone dextrose, SCH; Schaedler, TSB; Trypticase soy broth, OD; Optical density.

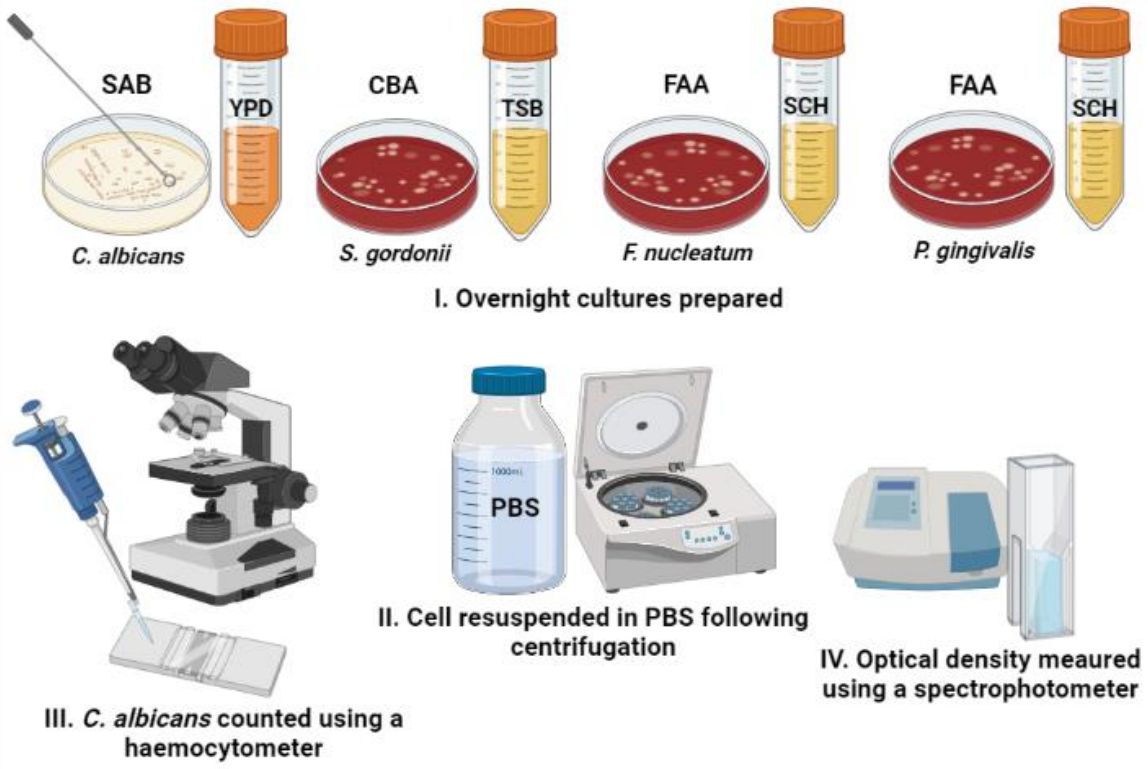

Figure 3.1. A summary of microbial growth conditions and standardisation. (I) Overnight cultures were prepared by inoculating microbial colonies into a specified medium for each microorganism for 16-18 h. **(II)** Microbial cells were harvested by centrifugation and then resuspended in PBS. **(III)** *C. albicans* were counted using a Neubauer haemocytometer (cell count × dilution factor × volume of square = CFU/mL), before being diluted to 1 × 10^6 CFU/mL in appropriate media. **(IV)** Bacterial cell concentrations of 1 × 10^8 cells/mL were obtained by measuring the optical density with a spectrophotometer at 550 nm, before being diluted to 1 × 10^7 cells/mL in appropriate media. Diagram was created in BioRender.com.

3.3.1.2 Development of single and mixed-species biofilms in microtiter well plates

The optimal media, atmospheric conditions and incubation times were determined for mono-species and mixed-species (4 species) biofilm model grown in 24-well flat-bottom plates (Costar®, Corning Incorporated, Corning, NY, USA). Standardised cultures of *C. albicans* were first diluted to 1×10^6 CFU/mL and the bacteria (*S. gordonii*, *P. gingivalis* and *F. nucleatum* at 1×10^8 cells/mL) were diluted to 1×10^7 cells/mL in the culture broth. The broth consisted of a 1:1 mixture of Roswell Park Memorial Institute-1640 (RPMI [Sigma–Aldrich, Dorset, UK]) and Trypticase soy broth (Sigma-Aldrich, UK) media (1:1 RPMI/TSB). Mono- and Mixed-species biofilms were grown in pre-sterilised polystyrene 24-well flat-bottom plates by pipetting 500 µL of the standardised dilutions into each well. The plates were incubated at three different environments for testing: aerobically (atmospheric), 5% CO_2 and anaerobically for 24 h and 48 h at 37°C.

Next, to assess the effect of serum on the biofilm formation, mono- and multispecies biofilms (4 species) were grown into a mixture of 1:1 RPMI/TSB ± 10% foetal bovine serum (FBS) for 24 h and 48 h at 5% CO_2.

Two mixtures of growth media were then assessed. Biofilms were grown for 24 h and 48 h into a 1:1 mixture of either RPMI/TSB or RPMI and Todd Hewitt broth (THB [Sigma-Aldrich, UK]) supplemented with 0.01 mg/mL hemin and 2 µg/mL menadione (1:1 RPMI/THB), both mixtures were supplemented with 10% FBS. The 24-well plates were all incubated at 37°C inside the 5% CO_2 incubator. Appropriate media controls (wells containing media only) were run in parallel for each experimental condition to assess for microbial contamination.

3.3.2 Biofilm characterisation and optimisation

3.3.2.1 Measurement of metabolic activity

Following incubation, the spent supernatant was discarded, and biofilms were washed in 500 µL of PBS to remove any non-adherent cells. The PBS was aspirated and the metabolic activity of the cells within the biofilms was estimated, by using the XTT (2,3-bis-[2-methoxy-4-nitro-5-sulfophenyl]-2H-tetrazolium-5-carboxanilide [Sigma-Aldrich, Dorset, UK or Fisher Scientific, UK

or Abcam, UK]) reduction assay along with the electron-coupling menadione, as previously described (Ramage et al., 2001). Before use, 0.25 g/L of XTT was dissolved in distilled water (dH_2O) and filter-sterilised, using a 0.22-µm-pore size filter unit and kept at -80°C until needed. A 10 mM menadione (2-Methyl-1,4-naphthoquinone, also known as vitamin K3 [Sigma-Aldrich, Dorset, UK]) stock solution was prepared in 100% acetone and kept at -20°C. Prior to use, XTT was thawed and menadione was added to XTT to a final concentration of 1 µM. A 250 µL aliquot of XTT/menadione solution was subsequently added to each pre-washed biofilm and to control wells and incubated for 2 h in the dark inside the incubator (LEEC Classic, UK) at 37°C. After incubation, a volume of 100 µL of the formazan salt-based XTT from each well was transferred into a new 96-well flat-bottom plate (Costar®, Corning Incorporated, NY, USA) for absorbance reading. The microtiter plate reader (Sunrise, TECAN, Theale, UK) was set to measure the absorbance at a wavelength of 492 nm.

3.3.2.2 Quantification of biomass

For biomass assessment, standard crystal violet (CV) was used, as described previously (Sherry et al., 2014). Briefly, a stock solution of 1% CV w/v (Sigma-Aldrich, Gillingham, UK) was made using dH_2O and diluted to 0.05% v/v prior to use. The developed adherent colonies were washed in 500 µL PBS and left to dry overnight at room temperature. Biofilms were stained with 250 µL of 0.05% CV solution for 15-20 minutes at room temperature. Following staining, biofilms were indirectly washed with slow running tap water in the sink until the unbound dye was removed. Next, 250 µL of 100% ethanol were added to each well and this was mixed thoroughly by pipetting to release the dye. A volume of 100 µL was transferred to a fresh 96-well flat-bottom microtiter plate. The CV absorbance was then measured spectrophotometrically using the microtiter plate reader (Sunrise, TECAN, Theale, UK) at a wavelength of 570 nm. All absorbance values were blank corrected based on the negative control where no biofilms were formed.

3.3.2.3 Biofilm compositional analysis using quantitative polymerase chain reaction (qPCR)

To quantify the relative composition of the biofilms, a real-time quantitative PCR was performed. Mixed-species biofilms were grown in 6-well microtiter plates (Corning Incorporated, NY, USA) into a 1:1 mixture of either RPMI/TSB or RPMI/THB, both supplemented with 10% FBS, for 24 h and 48 h, as described above in 3.3.1.2, by pipetting 3,000 µL of the standardised microbial dilutions into each well. Mono-species *C. albicans* was also grown as a control. This was to assess whether the bacteria in multispecies biofilms promote or inhibit *C. albicans* when co-cultured all together. Following incubation times, spent biofilm media were discarded by pipetting, and biofilms were detached by scraping in 1 mL of PBS (PBS was pipetted onto the biofilm, and biomass was mechanically disrupted). The biofilm, scraped in PBS, was then transferred into 1.5 mL Eppendorf tubes (Greiner Bio-one, Kremsmünster, Austria, UK) for DNA extraction. Manual scraping of biofilms is an alternative method to sonication used for DNA extraction and qPCR methods (Brown et al., 2022). Therefore, microtiter plates were used to ensure that sufficient biomass was recovered for DNA extraction that permits accurate qPCR analyses.

DNA was then extracted from samples using the QIAamp DNeasy Mini Kit (Qiagen, Manchester, UK), according to manufacturer's instructions. Briefly, biofilm suspensions were firstly centrifuged (Hettich, Germany) at 13,000 rpm, for 10 minutes. Supernatant was then discarded, and the cell pellet was resuspended in 180 µL of cell lysis ATL buffer supplemented with 20 µL of proteinase K. The mixture was then incubated in a water bath (Grant instruments, UK) at 56°C for 20 minutes. Following incubation, samples were transferred to bead beating tubes (Thistle Scientific, UK) containing sterile 0.5 mm glass beads. A bead beater (Fisher Bead Mill 24, UK) was then used for 3×30 second cycles at maximum speed. Samples were centrifuged at 7,000 rpm for 10 minutes and supernatants were transferred to a new RNase free Eppendorf tube. A volume of 200 µL of buffer AL was added to each sample and mixed by pulse-vortexing for 15 seconds before being incubated in the water bath at 70°C for 10 minutes. 200 microlitres of 100% ethanol were then added to each sample, pulse-vortexed for 15 seconds and centrifuged at 7,000 rpm for 1 minute. The full mixture for each sample was then transferred to a spin column and centrifuged for 1 minute at

8,000 rpm. Each filter was placed in a clean collection tube and the old one with filtrate was discarded. 500 microlitres of buffer AW1 were added and centrifuged at 8,000 rpm for 1 minute. The collection tube was again discarded and 500 µL of AW2 were added (twice) for a final wash step, centrifuged for 3 minutes at 13,000 rpm. After this, the spin column was centrifuged at 13,000 rpm for 1 minute to dry the filter and then placed in a clean RNase free Eppendorf tube with the lid cut off and a volume of 100 µL of AE elution buffer was added into the centre of each filter and left to saturate for 5 minutes. The spin column was centrifuged for 1 minute at 8,000 rpm, and the filtrate was then kept in the freezer at –20˚C. Following this, biofilm compositional analyses were enumerated using qPCR. In brief, 1 µL of extracted DNA was added to a mastermix containing 10 µL SYBR™ GreenER™, 7 µL UV-treated RNase-free water and 1 µL of 10 µM forward/reverse primers for each microbial species. The primers used were previously published by (Sherry et al., 2016), and are listed in Table 3.3. The total volume of 20 µL was added to MicroAmp fast-optical 96-well 0.1 mL reaction plates (Applied Biosystems, Waltham, MA, USA) and filled into the StepOnePlus™ Real-Time PCR system (Applied Biosystems, USA). For the reaction, thermal profiles used were as follows: 50˚C for 2 minutes, 95˚C for 2 minutes, followed by 40 cycles of 95˚C for 10 seconds and 60˚C for 30 seconds using the StepOnePlus software version 2.3 (ThermoFisher, Paisley, UK) for data compilation. Samples were quantified by calculating the colony forming equivalent (CFE) based upon an established standard curve of serially extracted DNA of bacterial and fungal colony forming units ranging from 1×10^3 to 10^8 CFU/mL, of which DNA was extracted as above, and each dilution was run in the qPCR. All samples were run in duplicate in the qPCR, with negative control samples containing water, primers and mastermix only were used to assess for DNA contamination.

Table 3.3. Primer sequences used for compositional analysis of multispecies biofilm models.

Organism	Primer	Forward primer 5'-3'	Reverse primer 5'-3'
S. gordonii	*Streptococcus*	GATACATAGCCGACCTGAG	CCATTGCCGAAGATTCC
F. nucleatum	*F. nucleatum*	GGATTTATTGGGCGTAAAGC	GGCATTCCTACAAATATCTACGAA
P. gingivalis	*P. gingivalis*	GGAAGAGAAGACCGTAGCACAAGGA	GAGTAGGCGAAACGTCCATCAGGTC
C. albicans	18S	CTCGTAGTTGAACCTTGGGC	GGCCTGCTTTGAACACTCTA
Bacteria	16S	TCCTACGGGAGGCAGCAGT	GGACTACCAGGGTATCTAATCCTGTT

3.3.2.4 Scanning electron microscopy imaging

For visualisation microscopically, biofilms were grown on 13 mm Thermanox™ coverslips (Fisher Scientific, Loughborough, UK) placed within 24-well plates. Biofilms grown in either RPMI/TSB + 10% FBS or RPMI/THB + 10% FBS, in a 5% CO_2 incubator at 37°C, were visualised at 90 minutes, 8 h, 24 h and 48 h. Following growth, biofilms were prepared for scanning electron microscopy, as described previously by Erlandsen et al. (2004), with a little modification. In brief, biofilms were fixed in 500 µL of a fixing buffer of 2% paraformaldehyde, 2% glutaraldehyde, 0.15 M sodium cacodylate buffer and 0.15% (w/v) alcian blue and stored overnight at 4°C. Following fixation, the fixative solution was discarded, and samples were treated with 500 µL of 0.15 M sodium cacodylate buffer rinse and stored at 4°C until processing. Sodium cacodylate buffer was removed, and subsequently stained with 500 µL of uranyl acetate stain. Samples were then wrapped in tin foil and incubated at room temperature for 1 h. Following incubation, uranyl acetate stain was discarded prior to a series of dehydration steps were carried out where 3 × 10-min washes of 30%, 50% and 70% ethanol and 4 × 5-min washes of 100% (absolute) ethanol and molecular sieve 100% (dried absolute) ethanol, followed by 3 × 5-min washes of hexamethyldisilizane (HMDS). Subsequently, all samples were placed in desiccator to allow evaporation. Samples were gold/palladium sputter coated and then mounted. Digital images were acquired using Jeol JSM-IT100 InTouch™ Scanning electron microscope and representative images were taken at magnifications of ×1,000 and ×3,500.

3.3.2.5 Fluorescence microscopic imaging

A live/dead cell imaging assay was performed to investigate whether the mixed-species biofilm model was viable and functional before treatment with any test antimicrobial agents. For this, one growth medium (1:1 RPMI/THB + 10% FBS) and one incubation time (24 h) were selected as optimised conditions for testing. Biofilms were grown on Thermanox™ coverslips, placed within a 24-well plate in a 5% CO_2 incubator at 37°C. Pre-treatment staining of the biofilms was carried out using fluorescent dyes: SYTO™ 9 (5mM stock, ThermoFisher scientific), for staining total cells, propidium iodide (PI [1 mg/mL stock, life technologies]) for staining dead cells/eDNA and calcofluor white (CFW [1 g/L

stock, Sigma-Aldrich]) for staining yeast cells. Two microlitres of SYTO™ 9 and PI, and 1 µL of CFW were combined in 1 mL of sterile water. 500 microlitres of the cocktail of all the stains were added per biofilm. The plate was incubated in the dark inside the aerobic incubator (LEEC Classic) for 15 minutes at 37°C. Following stain discarding and washing with PBS, the samples were covered with 2% paraformaldehyde and then incubated for 1 h in the classic incubator. Stained and fixed biofilms were washing with PBS, dried overnight in the dark. Samples were then transferred to a glass slide and one drop (10 µL) of a mounting medium (VECTASHIELD®) was added on top of each sample. A 0-thickness coverslip is placed over the top and pressed down gently on the coverslip. Clear nail varnish was used to hold the glass coverslip over the biofilm glass slide. Samples were viewed using EVOS FL Cell Imaging System (ThermoFisher Scientific, Waltham, MA, USA).

3.3.3 Biofilm characterisation on bovine dentine

To further mimic the interactions between host and microorganisms in endodontic infections, the multispecies biofilm model was grown on a biological substrate (dentine) placed in a 24-well plate in the optimised conditions as described in 3.3.2.5. Bovine dentine discs (Modus laboratories, Reading, UK) were used in this study. The specifications for these discs were as follows: round cross-sections, approximately 7 mm in diameter, 1 mm in thickness, polished (P2500) on one side and transverse cross-sections (the orientation of dentinal tubules is perpendicular). The dentine discs were autoclaved before use (122°C for 16 minutes). The biofilm structure grown on dentine discs was assessed using SEM as described in 3.3.2.4. This whole workflow for biofilm optimisation and characterisation is summarised in Figure 3.2.

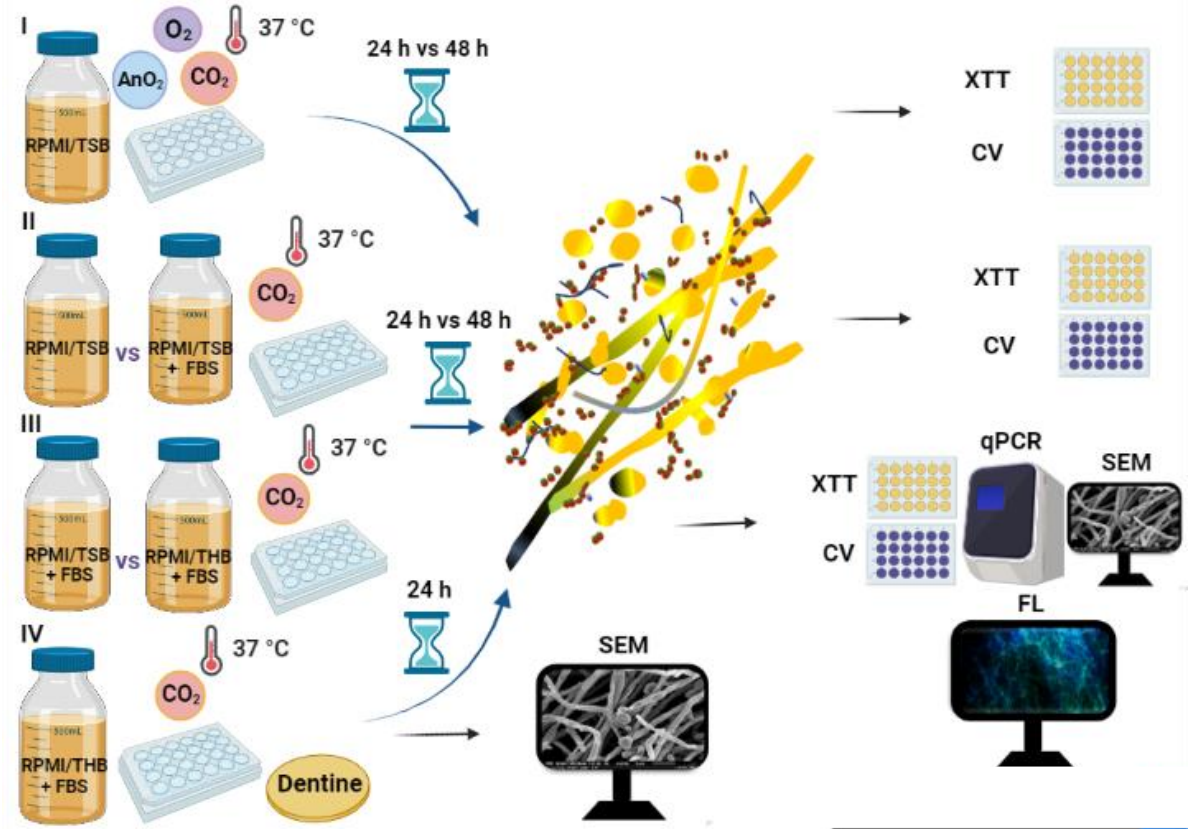

Figure 3.2. A workflow illustration for biofilm optimisation and characterisation. (I) Optimal incubation conditions were determined for biofilms grown in a 1:1 mixture of Roswell Park Memorial Institute-1640 and Trypticase soy broth (RPMI/TSB), in 24-well plates in either O_2, CO_2 or AnO_2. Metabolic activity and biomass were assessed using XTT and crystal violet (CV) assays, respectively. **(II)** The effect of foetal bovine serum (FBS), in RPMI/TSB, on microbial growth was assessed in the optimal atmospheric condition (CO_2), using XTT and CV assays. **(III)** Two growth media: 1:1 RPMI/TSB and 1:1 RPMI/Todd Hewitt broth (RPMI/THB) supplemented with 10% FBS were compared in different incubation timepoints, and the biofilms grown were assessed using XTT, CV, quantitative polymerase chain reaction (qPCR), and scanning electron microscopy (SEM) imaging techniques. The optimal incubation time and growth medium were then selected (RPMI/THB + FBS for 24 h) and biofilms grown in optimal conditions were further assessed by fluorescence microscopic (FL) imaging. **(IV)** Biofilm ultrastructure grown on a clinically relevant substrate (bovine dentine), in the optimised growth conditions, was characterised using SEM imaging. Diagram was created in Microsoft PowerPoint and BioRender.com.

3.3.4 Interkingdom interactions within the optimised biofilm model

In order to further assess the interactions between *C. albicans* and bacterial species, *C. albicans* was co-cultured with either *F. nucleatum*, *P. gingivalis* or *S. gordonii* or all together for 6 h, 8 h and 24 h in RPMI/THB + 10% FBS in 24-well plates. *C. albicans* mono-species and media controls were also run in parallel. Metabolic activity and biomass were assessed using XTT and CV assays.

To further assess the effect of the three bacterial species on *C. albicans*, a qPCR analysis was performed to quantify the relative CFE/mL of *C. albicans* when co-cultured with bacteria in dual- and mixed-species biofilms formed in 1:1 RPMI/THB ± 10% FBS. This was created in parallel with other three derived models, one of which contained *C. albicans* only, one contained *S. gordonii* only and one contained bacterial species only (*S. gordonii*, *P. gingivalis* and *F. nucleatum*). Compositional analyses were also performed to assess the importance of *C. albicans* in supporting the growth of biofilms in the presence and absence of serum. Primers used were 16S and 18S for bacteria and *C. albicans*, respectively as shown (Table 3.3).

Next, *C. albicans* was grown on Thermanox™ coverslips for 4 h in 24-well plates in 1:1 RPMI/THB. Following 4 h incubation, supernatant was discarded, and sequential addition of standardised bacteria was then employed. This was to assess the effect of each bacterial species on *C. albicans* after initial hyphal formation. Plates were then incubated inside the 5% CO_2 incubator at 37°C for additional 20 h. Following incubation and discarding spent media, coverslips were individually washed gently with 500 µL of PBS and then transferred into a bijoux tube containing 1 mL PBS and sonicated at 35 kHz in a sonic bath for 10 minutes. The sonicate was then transferred to 1.5 mL Eppendorf tubes (Greiner Bio-one, Kremsmünster, Austria, UK) for DNA extraction. Compositional analyses were then performed as described in 3.3.2.3.

3.3.5 Statistical analysis

All graphs, data distribution and statistical analysis were performed using GraphPad Prism version 9 (GraphPad, San Diego, CA, USA). Before analysis, data distributions were assessed using a D'Agostino-Pearson omnibus normality test, unless otherwise stated. Kruskal-Wallis with Dunn's tests were used to determine the P-value (p) for multiple comparisons when data weren't normally distributed. Parametric data of multiple comparisons were analysed by analysis of variance (ANOVA) with Dunnett's tests to compares every mean to the control mean. Differences were considered statistically significant if $p < 0.05$. Each error bar represents the standard deviation (SD).

3.4 Results

3.4.1 Single and mixed-species biofilms characterisation and optimisation

3.4.1.1 Metabolic activity and biomass

The optimal media, atmospheric conditions and incubation times were optimised for mono- and mixed-species biofilm models grown in 24-well flat-bottom plates. First, a mixture of 1:1 RPMI/TSB, three different atmospheric conditions (O_2, 5% CO_2 and AnO_2) and two incubation times were selected for testing at 37°C. Following incubation, biofilm viability was measured by the XTT assay and biomass was quantified by the crystal violet assay. The results indicated that *F. nucleatum* and *P. gingivalis* displayed minimal metabolic activity and biomass under any environmental condition when grown as mono-species models. Conversely, *S. gordonii* exhibited a higher metabolic activity at 24 h under all conditions with a significant reduction at 48 h (** $p < 0.01$). For biomass, *S. gordonii* formed equally dense biofilms after 24 h and 48 h in all atmospheric conditions tested (Figure 3.3 and Figure 3.4).

C. albicans mono-species and mixed-species (4 species) biofilms showed comparable metabolic activity at 24 h, with significant increases at 48 h in O_2 and CO_2 conditions. The highest significant metabolic activity for *C. albicans* mono-species and mixed-species biofilms was observed under atmospheric O_2 and CO_2 conditions, compared to the anaerobic environment, at 48 h (** $p < 0.01$ and * $p < 0.05$, respectively, for *C. albicans* only; ** $p < 0.01$ for mixed species). For biomass, the highest biomass was observed at both timepoints under atmospheric O_2 and CO_2 conditions for *C. albicans* only and mixed species. The greatest changes were significant at 24 h and 48 h for *C. albicans* only between CO_2 and AnO_2 conditions (** $p < 0.01$ and *** $p < 0.001$, respectively). For the mixed-species biofilm, significant changes were observed at 24 h in CO_2 conditions compared to AnO_2 at (* $p < 0.05$). However, these differences were not statistically different at 48 h (Figure 3.3 and Figure 3.4).

Taken together, the metabolic activity and biomass results presented here show that *C. albicans* and mixed-species biofilms grown in RPMI/TSB formed denser

biofilms at 5% CO_2 than those grown under normal atmospheric or anaerobic conditions.

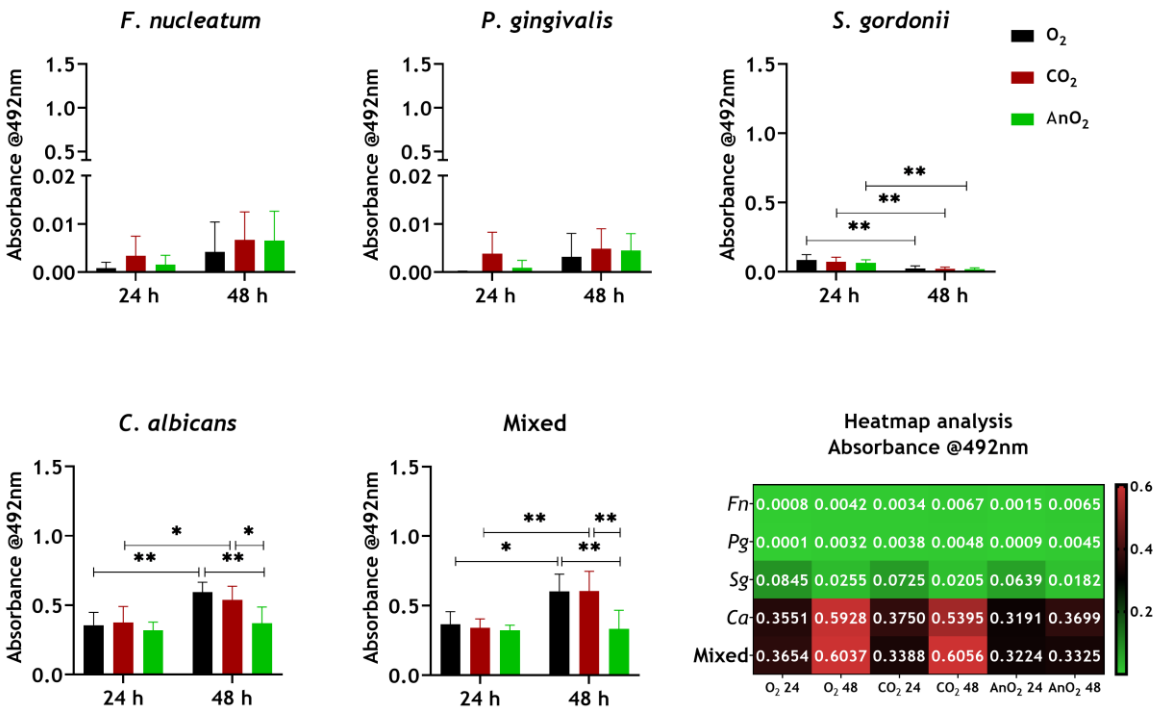

Figure 3.3. Metabolic activity measurement of mono- and multispecies biofilms grown in three different incubation conditions. Mono- and mixed-species (*F. nucleatum*, *P. gingivalis*, *S. gordonii* and *C. albicans*) biofilms were grown in 1:1 RPMI 1640/TSB in 24-well flat-bottom plates for 24 h and 48 h, at three different environments: aerobically (atmospheric [O_2]), 5% CO_2 and anaerobically (AnO_2). Viability was measured by the XTT assay. Each bar represents the mean (average) of data obtained from four technical repeats of three independent experiments. Error bars represent the standard deviation. The mean absorbance values are presented in a heatmap. Data were analysed by Kruskal-Wallis with Dunn's tests. * Indicates statistically significant differences (* $p < 0.05$, ** $p < 0.01$).

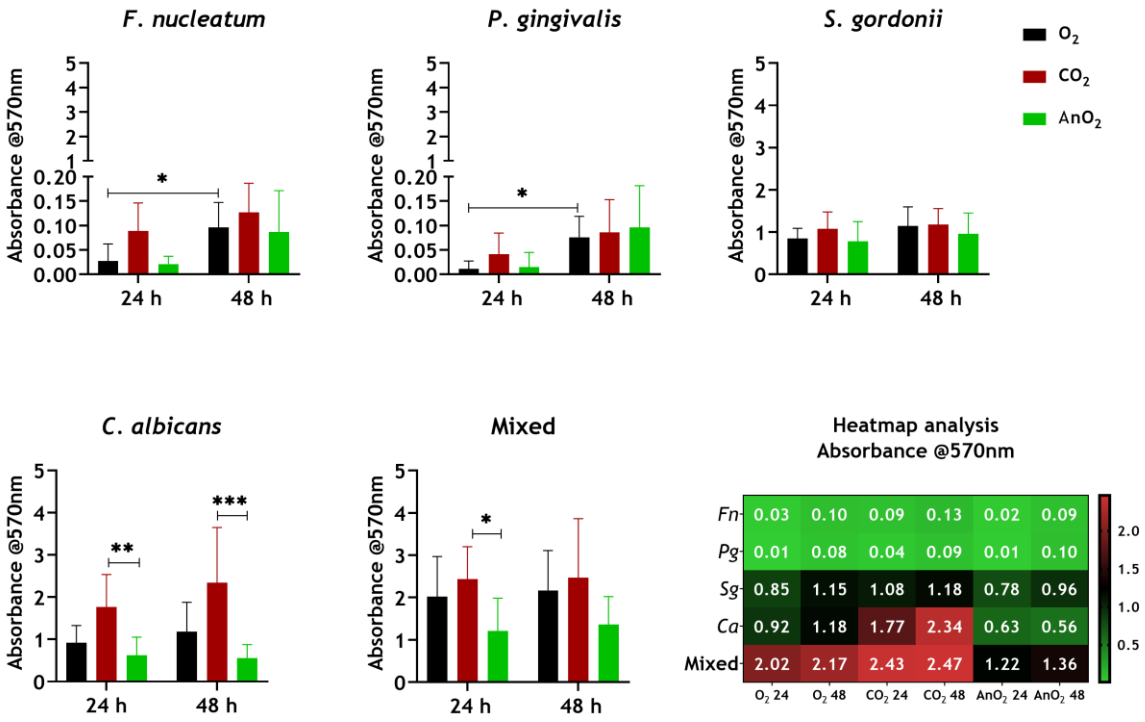

Figure 3.4. Biomass quantification of mono- and multispecies biofilms grown in three different incubation conditions. Following XTT (Figure 3.3), biomass was quantified by the crystal violet assay. Each bar represents the mean of data obtained from four technical repeats of three independent experiments. Error bars represent SD. Data were presented in a heatmap as mean values from the three independent experiments. Data were analysed by Kruskal-Wallis with Dunn's tests. * Indicates statistically significant differences (* $p < 0.05$, ** $p < 0.01$, *** $p < 0.001$).

In order to assess the importance of serum on the formation of biofilms, a mixture of 1:1 RPMI/TSB ± 10% FBS was tested at two incubation times with the optimal atmospheric condition (5% CO_2) selected for testing. These results similarly indicated that *F. nucleatum* and *P. gingivalis* developed minimal biofilm formation when grown as mono-species models, with either the presence or absence of serum. However, a significantly higher biomass was observed for *P. gingivalis* in the presence of 10% FBS at 48 h (Figure 3.5 and Figure 3.6).

For *S. gordonii*, the addition of 10% FBS to the mixture of RPMI/TSB resulted in a significant decrease of the metabolic activity when grown as mono-species biofilms at 24 h (* $p < 0.05$). For biomass, *S. gordonii* formed equally dense biofilms in ± FBS at both timepoints. In contrast, *C. albicans* mono-species and multispecies biofilms were more proliferative in the presence of serum. For *C. albicans* only, significant increases in the metabolic activity and biomass were

observed at 24 h and 48 h (** $p < 0.01$ and *** $p < 0.001$), respectively. For the multispecies biofilm, statistically significant changes in the metabolic activity and biomass occurred at 48 h between – FBS and + FBS (** $p < 0.01$ and * $p < 0.05$, respectively) as shown (Figure 3.5 and Figure 3.6).

The results demonstrate that FBS may have an inhibitory effect on *S. gordonii*, whereas *C. albicans* and mixed-species biofilms formed denser biofilms in the FBS-supplemented medium than those grown without serum.

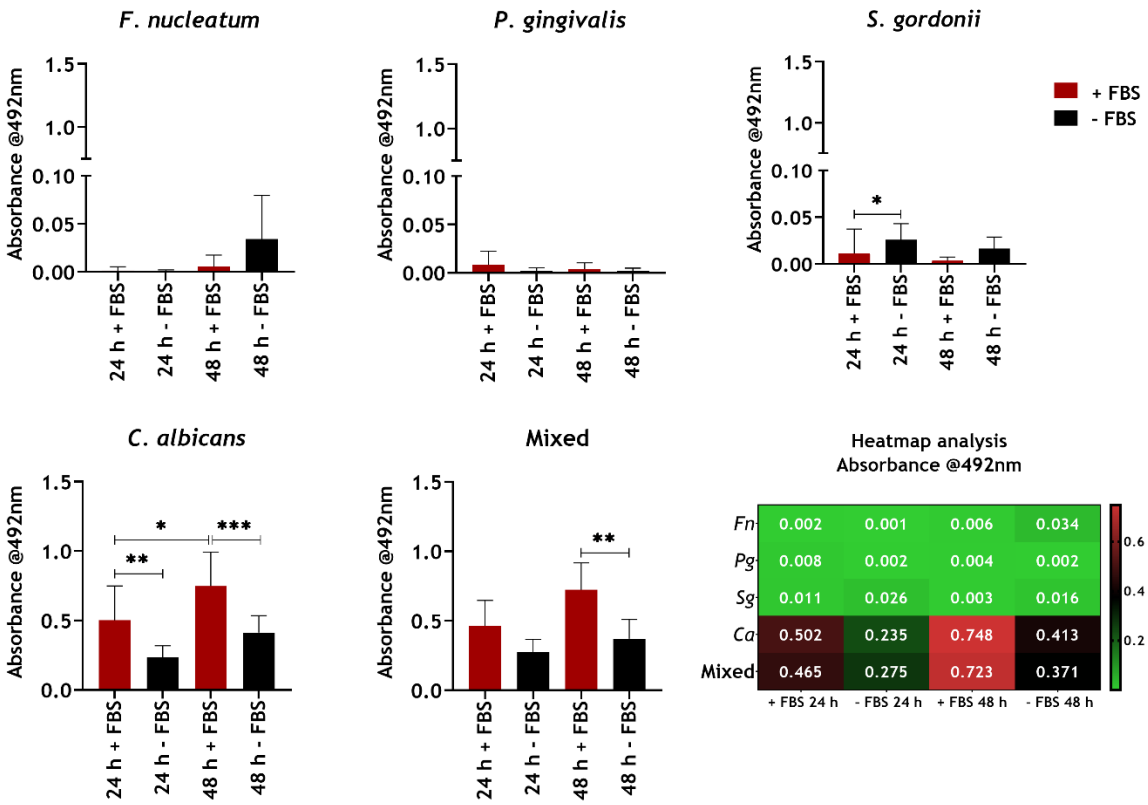

Figure 3.5. Metabolic activity measurement of mono- and multispecies biofilms in the presence and absence of foetal bovine serum. Mono- and mixed-species (*F. nucleatum*, *P. gingivalis*, *S. gordonii* and *C. albicans*) biofilms were grown in 1:1 RPMI 1640/TSB ± FBS for 24 h and 48 h in 24-well flat-bottom plates. Viability was measured by XTT. Each bar represents the mean of data obtained from four technical repeats of three independent experiments. Error bars represent the standard deviation. The mean absorbance values are presented in a heatmap. Data were analysed by Kruskal-Wallis with Dunn's tests. * Indicates statistically significant differences (* $p < 0.05$, ** $p < 0.01$, *** $p < 0.001$).

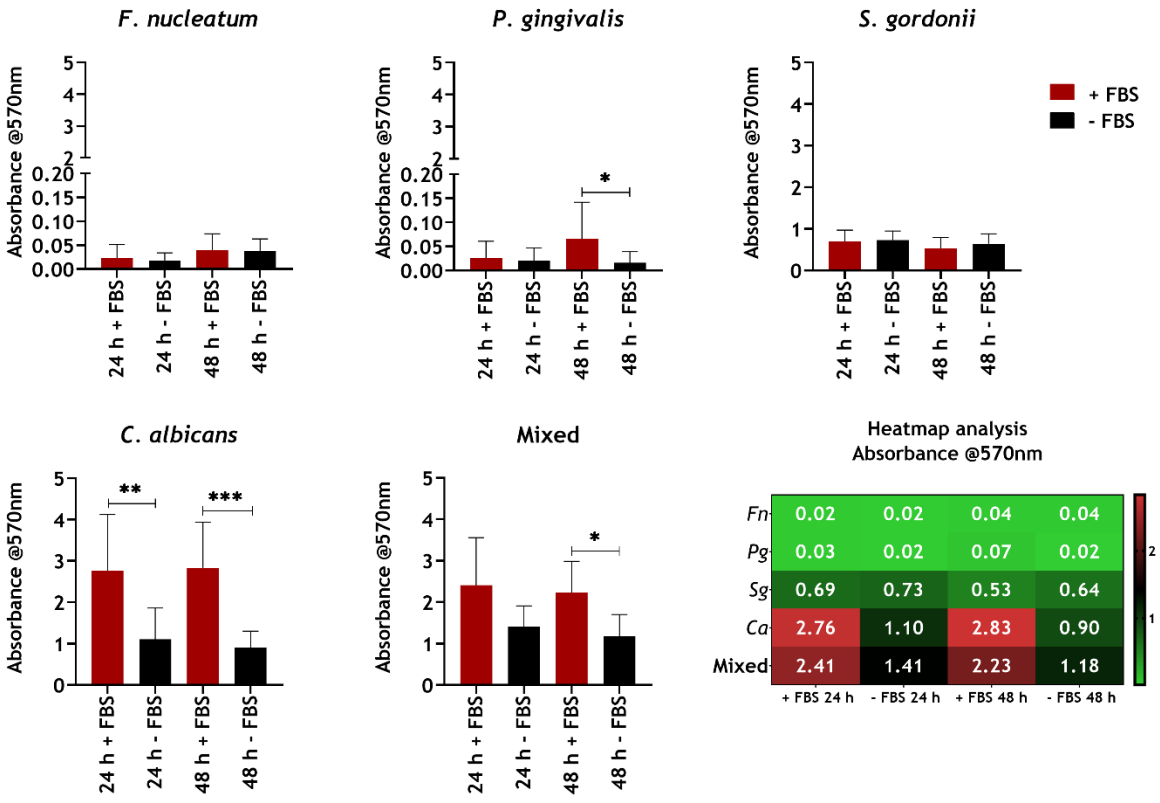

Figure 3.6. Biomass quantification of mono- and multispecies biofilms in the presence and absence of foetal bovine serum. Following XTT (Figure 3.5), biomass was quantified by the crystal violet assay. Each bar represents the mean of data obtained from four technical repeats of three independent experiments. Error bars represent the standard deviation. Data were presented in a heatmap as mean values from three independent experiments. Data were analysed by Kruskal-Wallis with Dunn's tests. * Indicates statistically significant differences (* $p < 0.05$, ** $p < 0.01$, *** $p < 0.001$).

Next, a 1:1 mixture of either RPMI/TSB + 10% FBS (TSB) or RPMI/THB + 10% FBS (THB) media were tested at 24 h and 48 h in a CO_2 incubation condition. When comparing the two media, higher metabolic activities and denser biofilms were shown for *S. gordonii* when grown in THB (Figure 3.7 and Figure 3.8), with statistically significant differences at 24 h (*** $p < 0.001$ and * $p < 0.05$, respectively). For *C. albicans* only, the metabolic activity was not significantly different between the two media tested. However, *C. albicans*, grown in TSB, exhibited a significantly higher metabolic activity at 48 h compared to 24 h (*** $p < 0.001$). For mixed-species biofilms, no statistically significant differences were found between the two media tested (Figure 3.7 and Figure 3.8).

Overall, both FBS-supplemented media support the formation of mixed-species biofilms, equally, although bacterial single species grew denser biofilms in RPMI/THB than those grown in RPMI/TSB.

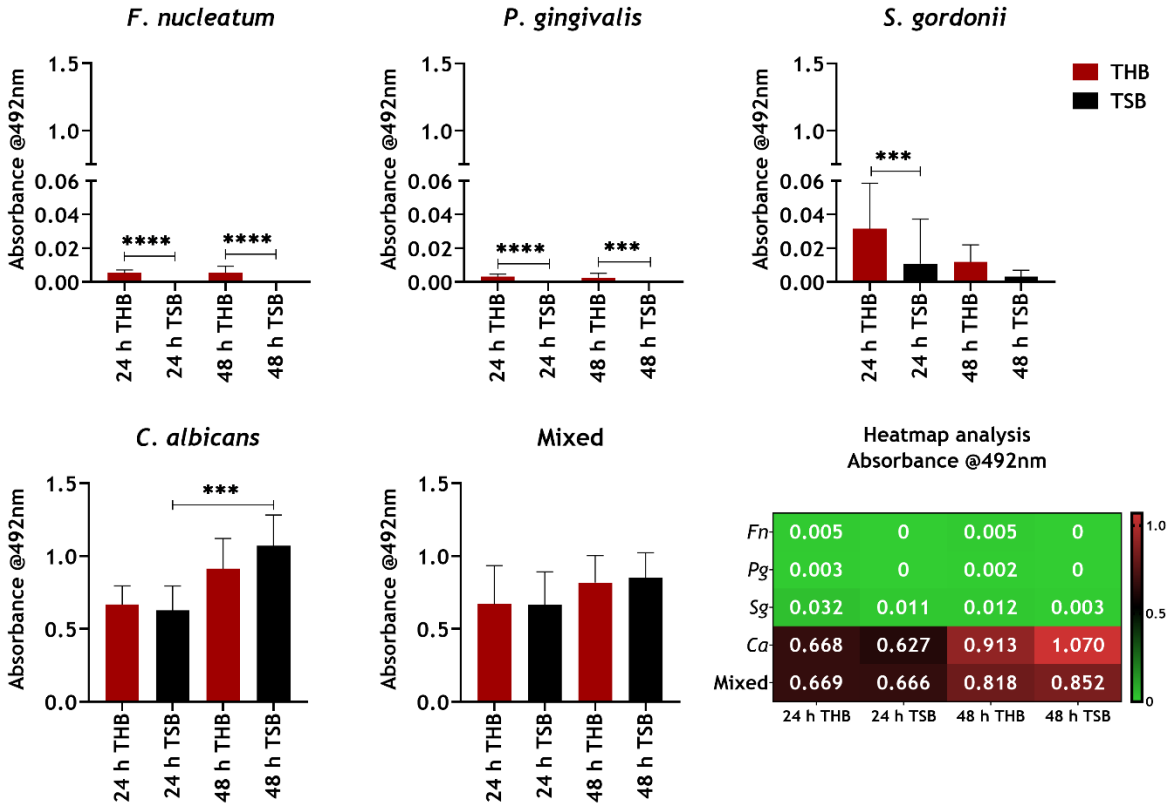

Figure 3.7. Metabolic activity measurement of mono- and multispecies biofilms grown in two different media. Mono- and mixed-species (*F. nucleatum*, *P. gingivalis*, *S. gordonii* and *C. albicans*) biofilms were grown in a 1:1 mixture of either RPMI/TSB + 10% FBS (TSB) or in RPMI/THB + 10% FBS (THB), for 24 h and 48 h, in 24-well flat-bottom plates. Viability was measured by XTT. Each bar represents the mean of data obtained from four technical repeats of three independent experiments. Error bars represent the standard deviation. The mean absorbance values are presented in a heatmap. Data were analysed by Kruskal-Wallis with Dunn's tests. * Indicates statistically significant differences (*** $p < 0.001$, **** $p < 0.0001$).

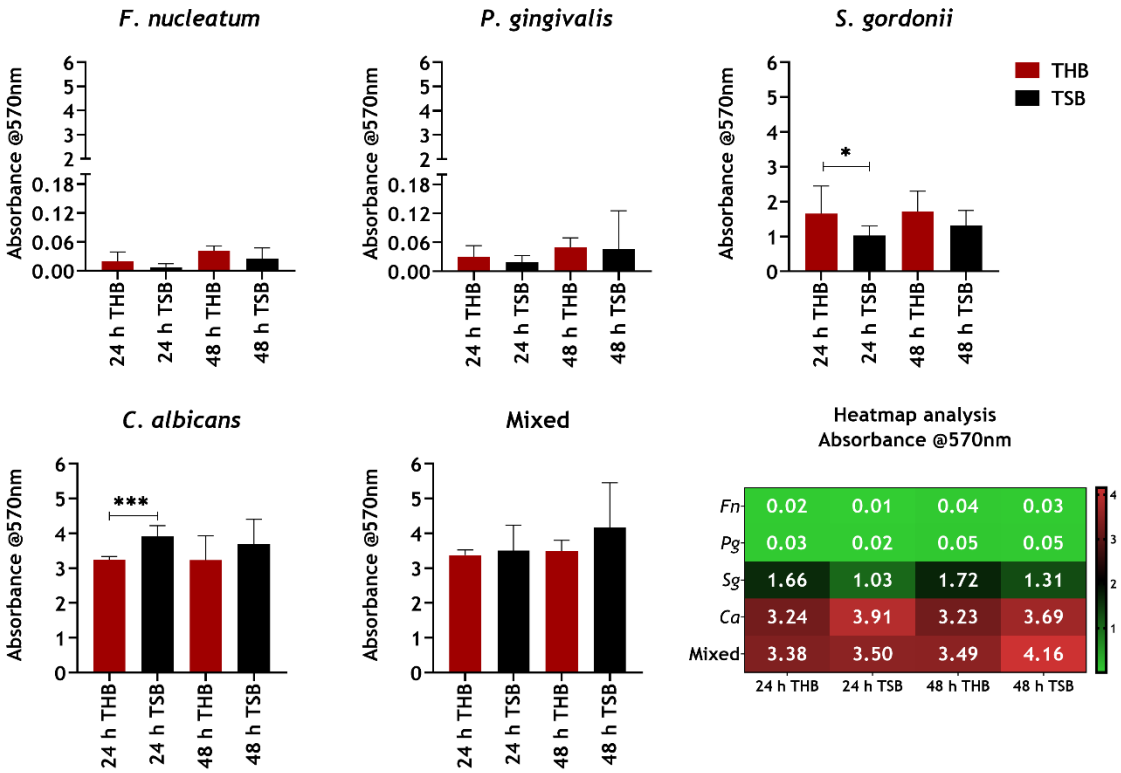

Figure 3.8. Biomass quantification of mono- and multispecies biofilms grown in two different media. Following metabolic activity measurement shown in Figure 3.7, biomass was quantified by CV. Each bar represents the mean of data obtained from four technical repeats of three independent experiments. Error bars represent the standard deviation. The mean absorbance values are presented in a heatmap. Data were analysed by Kruskal-Wallis with Dunn's tests. * Indicates statistically significant differences (* $p < 0.05$, *** $p < 0.001$).

3.4.1.2 Compositional analysis

Because of the limitation of the previous colorimetric assays, a qPCR analysis was performed for biofilms grown in the two previous FBS-supplemented media, to quantify the relative composition of the biofilms formed. *C. albicans* single species was also grown as a control to assess the effect of bacteria on *C. albicans* when they co-cultured together.

Significant reductions in the total colony number of *C. albicans* were observed in multispecies biofilms compared to *C. albicans* only at 24 h in either THB or TSB (** $p < 0.01$ and * $p < 0.05$, respectively), whilst no significant differences were observed at 48 h (Figure 3.9A). When comparing the total colony forming equivalent per mL (CFE/mL) of microorganisms in mixed-species biofilms, these were comparable between the different inoculation media tested (TSB vs THB).

Mixed-species biofilms grown in THB at 24 h and 48 h were 1.01 × 10^9 CFE/mL and 1.304 × 10^9 CFE/mL, respectively. Whereas 8.826 × 10^8 CFE/mL and 6.894 × 10^8 CFE/mL were the total for all microorganisms in the mixed-species biofilms grown in TSB at 24 h and 48 h, respectively, and no significant differences were found between the two timepoints.

All biofilms were predominantly composed of *S. gordonii* followed by *C. albicans* (> 90% and 3.9-8.6%, for both microorganisms, respectively). *F. nucleatum* and *P. gingivalis* were present in all biofilms, but as a relatively low proportion (0.2-0.6% and 0.001%, respectively) as shown (Figure 3.9B). Of note, the CFE/mL counts of *P. gingivalis* and *F. nucleatum* in mixed-species biofilms were estimated to be approximately 5 $\log_{10}$ and 2-3 $\log_{10}$ units, respectively, lower than the total CFE/mL counts of the mixed-species biofilms.

Overall, it was determined that bacteria had an inhibitory effect on the growth of *C. albicans* when co-cultured for 24 h. However, this inhibitory effect diminished after 48 h of incubation. These results also demonstrated that either THB or TSB supplemented with FBS were equally supportive of biofilm growth, which were dominated by *S. gordonii*, followed by *C. albicans*.

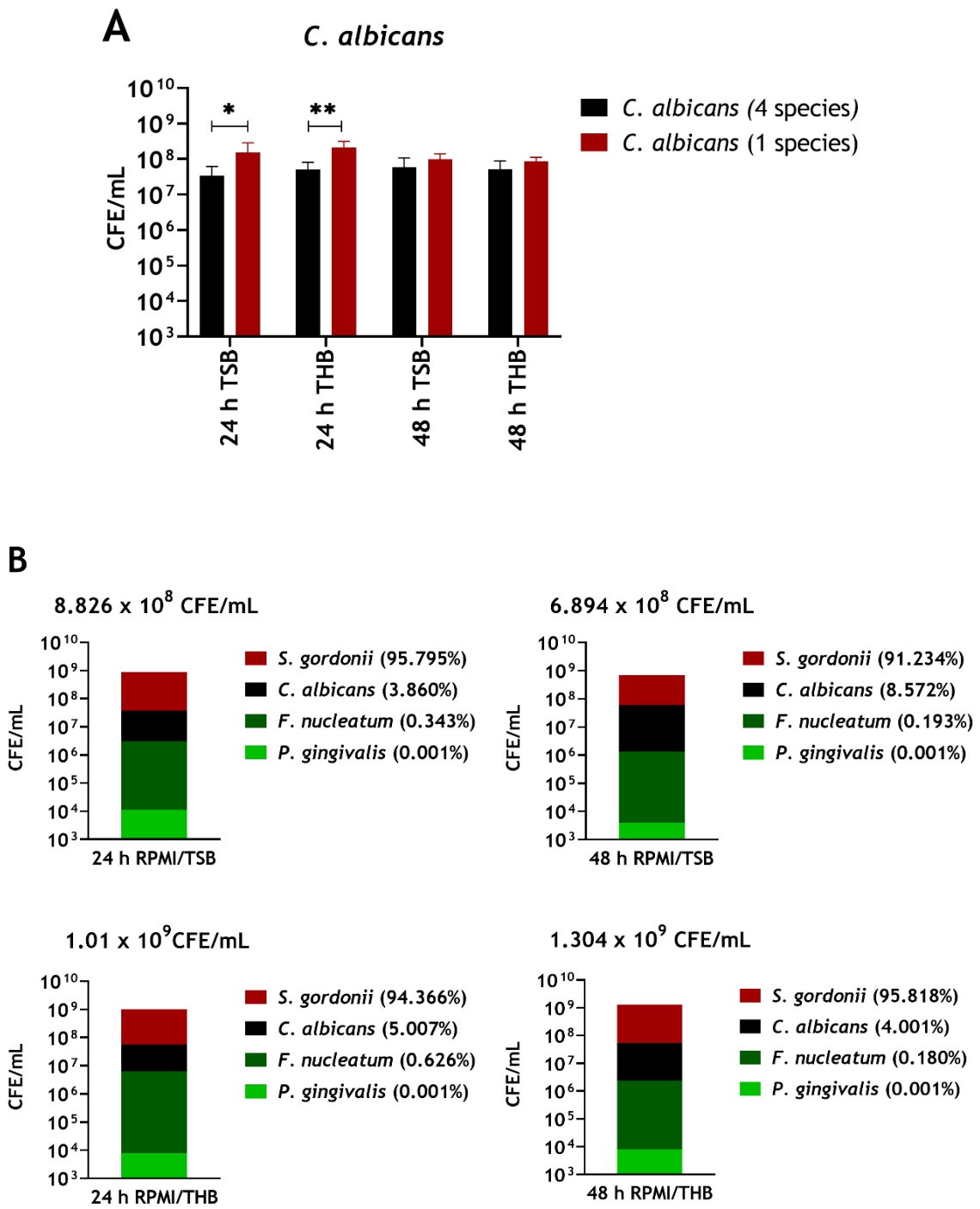

Figure 3.9. Compositional analysis of biofilms grown in two different media, supplemented with foetal bovine serum. *C. albicans* only biofilms and mixed biofilms (bacteria and *C. albicans*) were grown in a 1:1 mixture of either RPMI/TSB + 10% FBS (TSB) or RPMI/THB + 10% FBS (THB) in 6-well flat-bottom plates for 24 h and 48 h. **(A)** Colony forming equivalent (CFE/mL) of *C. albicans* mono-species biofilms (1 species) and *C. albicans* in multispecies biofilms (4 species). **(B)** Total CFE/mL for all four microorganisms in mixed-species biofilms are shown above each bar graph and percentages of each species within the biofilms are also shown. Each bar represents the mean of data obtained from triplicates of three independent repeats. Error bars represent the standard deviation. * Indicates statistically significant differences (* $p < 0.05$, ** $p < 0.01$). No significant differences were found between CFE/mL of *C. albicans* mono-species and *C. albicans* in multispecies biofilms at 48 h. No significant differences were found between total CFE/mL of mixed biofilms (4 species) in all conditions. Data were analysed by Kruskal-Wallis with Dunn's tests.

3.4.1.3 Scanning electron microscopy imaging

To further characterise model development, biofilm ultrastructure and architecture were observed using SEM at magnifications of ×1,000 and ×3,500. All biofilms imaged were grown on coverslips in either RPMI/THB or RPMI/TSB, supplemented with 10% FBS. The observations of *C. albicans* biofilms revealed filamentous cells predominantly formed under both media conditions. *C. albicans* biofilms are composed of an interlaced structure of a dense network of yeast, hyphae and pseudohyphae at 48 h of incubation (Figure 3.10A,B). *F. nucleatum* formed spindle-shaped rods of variable lengths (Figure 3.10C,D). *S. gordonii* formed chains of cocci (Figure 3.10E,F). Particularly noticeable, clusters of streptococci were observed in mono-species biofilms formed in THB (Figure 3.10F). However, it was not possible to observe *P. gingivalis* by SEM because of the very low abundance when grown as mono-species biofilms. In multispecies biofilm, germ tube formation was observed by *C. albicans* cells after 90 minutes of incubation (Figure 3.10G,H) and young hyphae of *C. albicans* was formed by 8 h (Figure 3.10I,J). All biofilms at 24 h and 48 h were dense, as shown (Figure 3.10K-N), with *C. albicans* yeast and hyphal cells co-aggregated with clusters of bacterial cells. These aggregates of bacterial cells were predominantly comprising of densely packed clumps of cocci-shaped colonies which were attached to the hyphae (highlighted in green in Figure inset). Sparse colonies of *P. gingivalis* were also seen (highlighted by blue arrows). Finally, *F. nucleatum* formed a scattered, loose filamentous network that was loosely scattered around the hyphae (highlighted by yellow arrows). The extracellular matrix was observed on the surfaces of some of these morphological forms. However, most of ECM was lost due to dehydration during sample processing. Combined with the results from Figure 3.9, the biofilms were comparable when grown in the two supplemented media tested.

Given the close similarities between the composition and architecture of the mixed-species biofilms grown for either 24 h or 48 h, in two types of FBS-supplemented media, RPMI/THB and one timepoint for biofilm formation (24 h) were selected for the next *in vitro* experiments as optimal growth conditions.

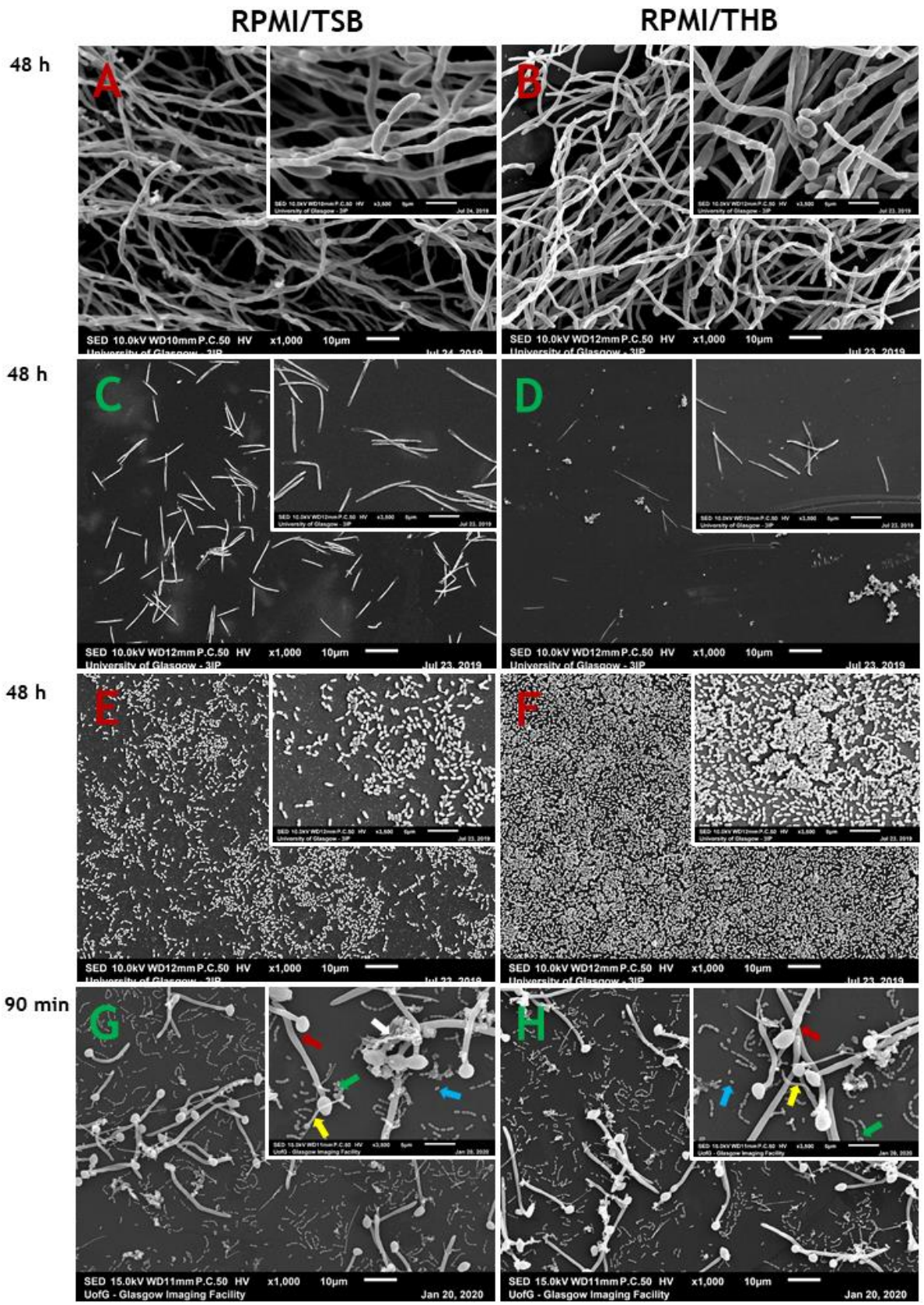
RPMI/TSB
RPMI/THB
48 h
48 h
48 h
90 min
A
B
C
D
E
F
G
H
SED 10.0kV WD10mm P.C.50 HV x1,000 10µm
SED 10.0kV WD12mm P.C.50 HV x1,000 10µm
SED 15.0kV WD11mm P.C.50 HV x1,000 10µm
UofG - Glasgow Imaging Facility
Jan 20, 2020

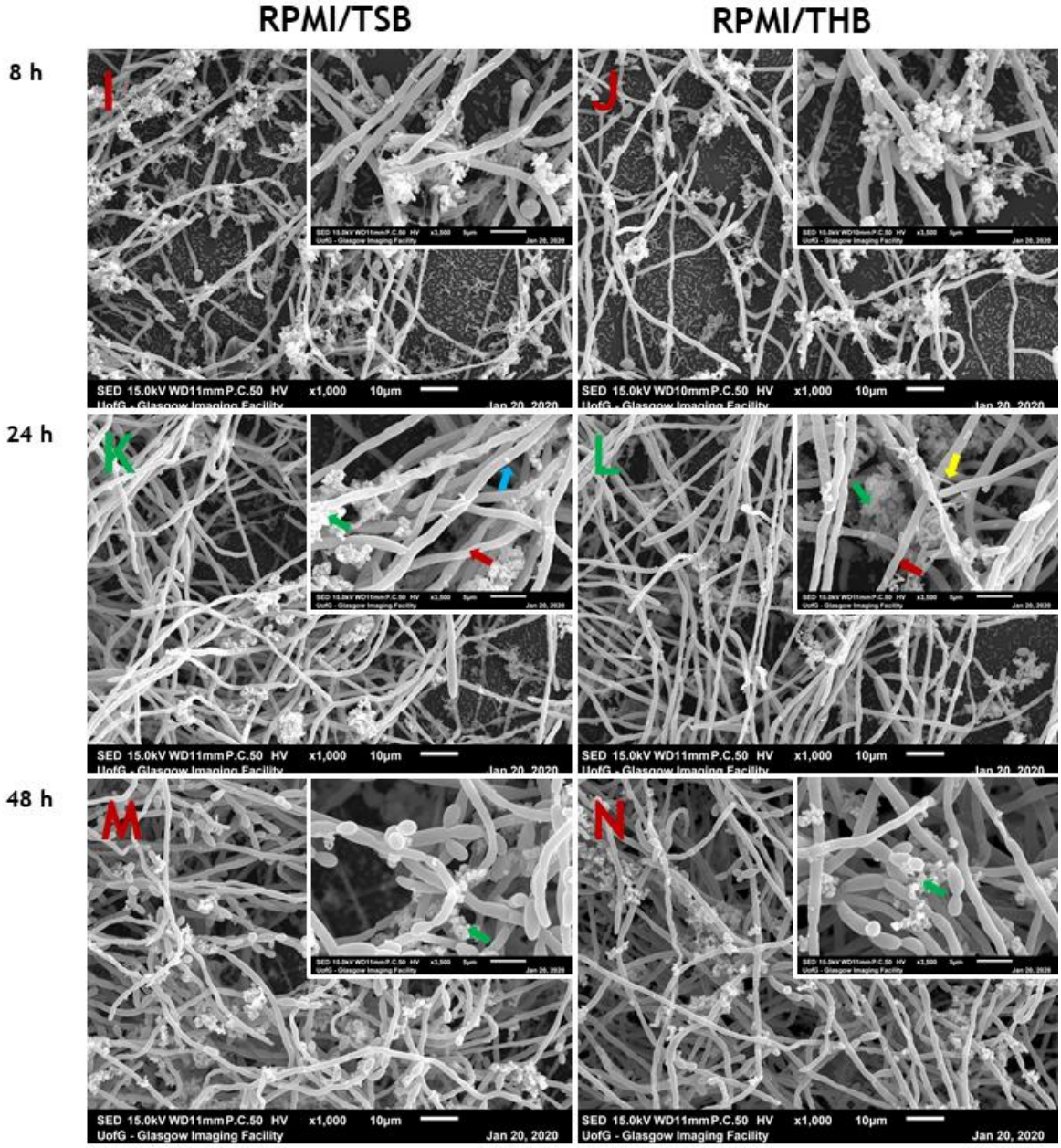

Figure 3.10. Scanning electron microscopy images of mono-and multispecies biofilms. The biofilms were grown in either 1:1 RPMI/THB + 10% FBS or in 1:1 RPMI/TSB + 10% FBS, before being fixed, processed and imaged, using a Jeol JSM-IT100 InTouch™ Scanning electron microscope. **(A & B)** *C. albicans* mono-species biofilms. **(C & D)** *F. nucleatum* mono-species biofilms. **(E & F)** *S. gordonii* mono-species biofilms. **(G-N)** SEM images show rich hyphal *C. albicans* growth within the mixed-species biofilms (red arrows), with clusters of bacteria adhering to the hyphae. These clusters of bacteria predominantly appear characteristic of morphological streptococci (green arrows). *F. nucleatum* (fusiform rods, highlighted by yellow arrows) and *P. gingivalis* (rod-shaped, blue arrows) were evident. Note: Most of ECM is lost due to dehydration during SEM processes. White arrows indicate the presence of ECM. Scale bar represents 10 µm and 5 µm at ×1,000 and ×3,500 magnifications, respectively. Samples were processed and imaged by Mr. Mark Butcher (Glasgow imaging facilities - University of Glasgow).

3.4.1.4 Fluorescent microscopy imaging

A live/dead cell imaging assay was then performed to assess whether the multispecies biofilm model was viable and functional before testing with conventional and novel endodontic therapeutics. For this, the optimised multispecies biofilm was grown on coverslips. Fluorescent microscopy with CFW (blue), SYTO™ 9 (green) and PI (red) revealed viable mixed-species biofilms. SYTO™ 9 stained total *C. albicans* and bacterial cells in green, while dead cells were stained in red by propidium iodide. CFW stained the cell wall of fungi in blue. Bacteria were seen as pale green colonies which were attached to the hyphae (Figure 3.11). However, the live/dead staining assay confirmed the viability of the biofilm model, before testing with antimicrobial agents.

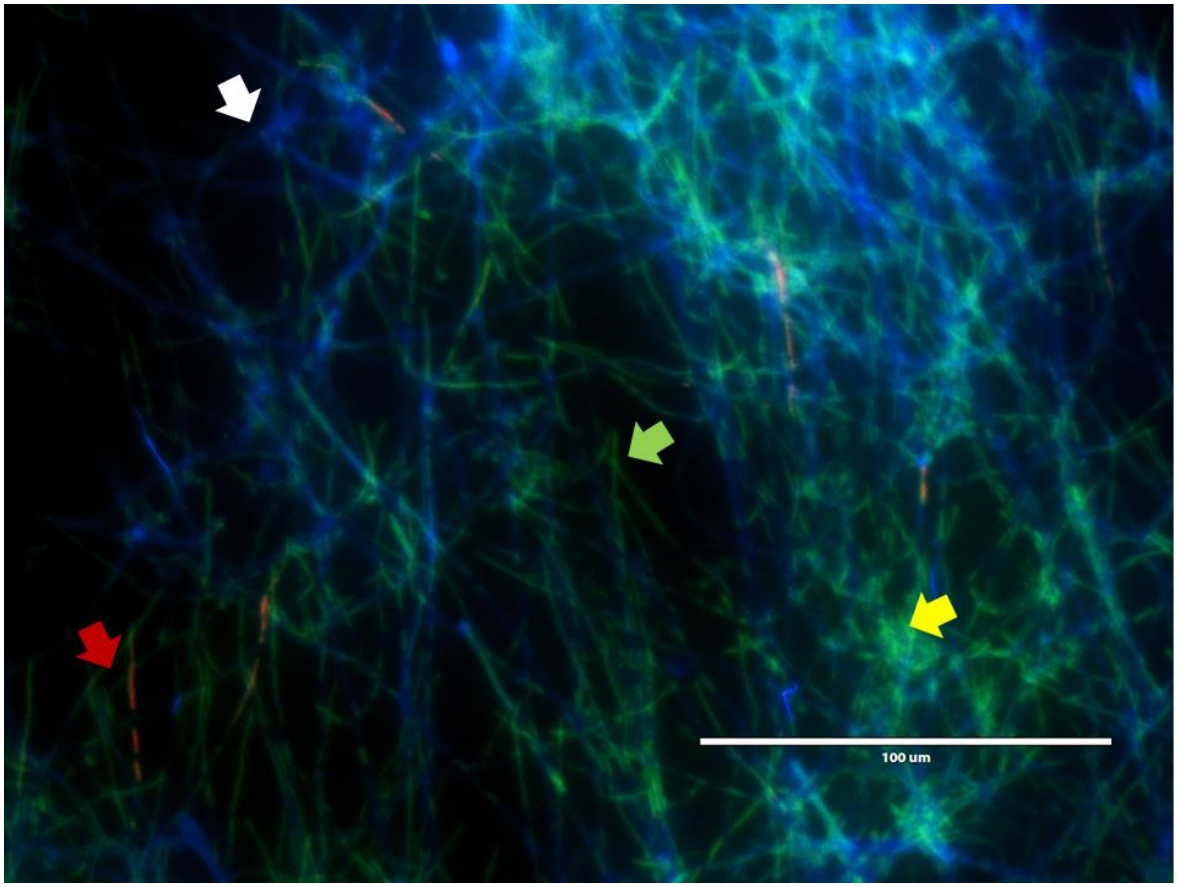

Figure 3.11. A fluorescent image of the 4-multispecies biofilm. Mixed-species biofilm (*F. nucleatum*, *P. gingivalis*, *S. gordonii* and *C. albicans*) was grown for 24 h in 1:1 RPMI/THB + 10% FBS, in 5% CO_2 at 37°C. Scale bar represents 100 µm at ×40 magnification. The hyphae of *C. albicans* appeared distinctly blue (stained by CFW, white arrow). Dead cells stained in red (stained by PI, red arrow). Total *C. albicans* and bacteria stained in green (stained by SYTO™ 9, green and yellow arrows, respectively).

3.4.2 Biofilm model characterisation on bovine dentine

The optimised mixed-species biofilm model was finally grown on a biological substrate (bovine dentine) to further mimic the interactions between host and microorganisms in endodontic infections. The ultrastructure of dentine (without biofilm) and biofilms were observed using SEM. The dentine was composed of dentinal tubules, peritubular dentine and intertubular dentine, as shown in Figure 3.12A. Rich hyphal growth of *C. albicans* was observed within mixed-species biofilms with clusters of bacteria attached to the hyphae, predominantly streptococci, similar to those formed on plastic coverslips (Figure 3.12B).

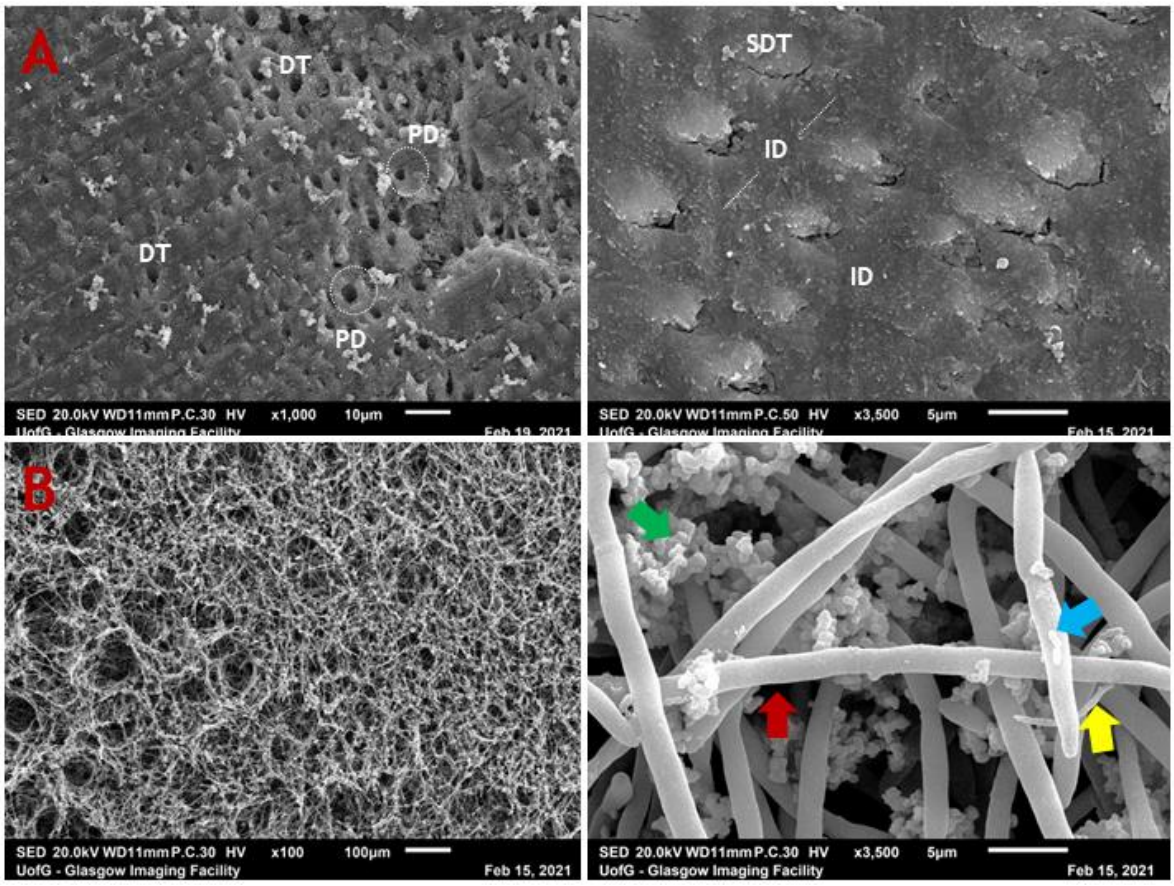

Figure 3.12. Scanning electron microscopy images of the ultrastructure of bovine dentine and the multispecies biofilm model grown on bovine dentine. (A) A transverse cross-section view of dentinal tubules through dentine. The dentine structure showing opened dentinal tubules (DT), obliterated (sclerotic) dentinal tubules (SDT), peritubular dentine (PD) and intertubular dentine (ID). **(B)** The optimised 4-species biofilm model was grown in 1:1 RPMI/THB with 10% FBS, in 5% CO_2 at 37°C for 24 h. The mixed biofilms (*F. nucleatum*, *P. gingivalis*, *S. gordonii* and *C. albicans*) were fixed, processed and imaged. A nest-like biofilm structure formed on dentine. Networks of *Candida* hypha (red arrow). Clusters of streptococci (green arrow). Yellow and blue arrows indicate *F. nucleatum* and *P. gingivalis*, respectively, adhering to the *Candida* hyphal network. Scale bar represents 100 µm, 10 µm and 5 µm at ×100, ×1,000 and ×3,500 magnifications, respectively. Samples were processed by Mr. Mark Butcher. Images were taken by Mrs. Margaret Mullin (University of Glasgow).

3.4.3 Interkingdom interaction within the optimised biofilm model

Next, *C. albicans* was co-cultured with either *F. nucleatum*, *P. gingivalis* or *S. gordonii* or all together for 6 h, 8 h and 24 h in RPMI/THB + FBS, to further assess the interkingdom interactions within dual- and mixed-species biofilms (4 species). *C. albicans* single species was also grown as a control to assess the effect of bacteria on *C. albicans*. The initial results indicating that the co-culture of *C. albicans* and *S. gordonii* exhibited the lowest metabolic activity when compared to *C. albicans* only at all timepoints (*** $p < 0.001$ and ** $p < 0.01$), while mixed-species biofilms displayed minimal metabolic activity with significant reductions at 6 h (*** $p < 0.001$). Conversely, the co-culture of *C. albicans* and *F. nucleatum* exhibited the highest metabolic activity compared to the control (*C. albicans* only) with a significant increase at 8 h (* $p < 0.05$), as shown (Figure 3.13A). For biomass, the highest increases in biomass were observed when *C. albicans* was co-cultured with *F. nucleatum* and *P. gingivalis* with no statistically significant changes. However, the lowest significant biomass (* $p < 0.05$) was observed at 24 h with mixed species (Figure 3.13B).

Based on the previous results, different bacterial species interact differently with *C. albicans*, although this needs further investigation.

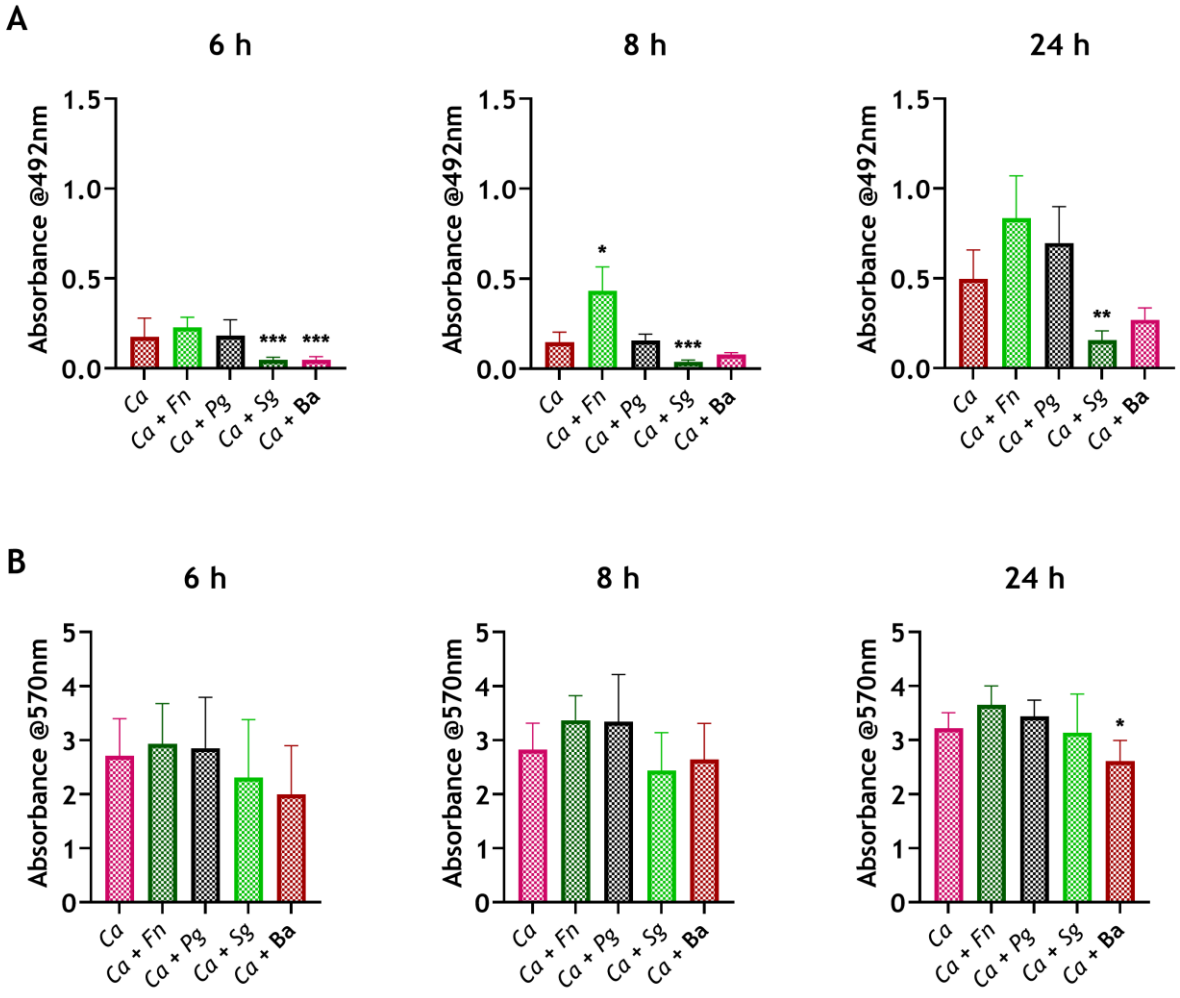

Figure 3.13. Metabolic activity measurement and biomass quantification of dual- and mixed-species biofilms. Biofilms were grown in a 1:1 mixture of RPMI/THB + 10% FBS in 24-well flat-bottom plates. Dual-species biofilms (*C. albicans* & *F. nucleatum* [*Ca* + *Fn*], *C. albicans* & *P. gingivalis* [*Ca* + *Pg*], *C. albicans* & *S. gordonii* [*Ca* + *Sg*]) and mixed biofilms (*C. albicans* & bacteria (*Ca* + Ba) were formed on 24-well plates. **(A)** Viability was measured by XTT. (B) Biomass was quantified by CV. Each bar represents the mean of data obtained from four technical repeats of three independent experiments. Error bars represent SD. Data were analysed by Kruskal-Wallis with Dunn's tests. * Indicates statistically significant differences compared to *C. albicans* mono-species biofilms (the control) (* $p < 0.05$, ** $p < 0.01$, *** $p < 0.001$).

To further investigate the effect of bacteria on *C. albicans* results, a quantitative PCR analysis was performed to firstly quantify the relative CFE/mL of *C. albicans* when co-cultured with bacterial species in dual- and mixed-species biofilms formed in RPMI/THB ± 10% FBS for 24 h. When *C. albicans* was co-cultured, in the serum-supplemented medium, with either *F. nucleatum* or *P. gingivalis*, the total CFE/mL counts increased by 9.8% and 68.9%, respectively compared to *C. albicans* (only). In contrast, *S. gordonii* and bacteria (3 species)

decreased the CFE/mL counts of *C. albicans* by 55% and 20%, respectively, relative to mono-species *C. albicans*. However, these changes were not statistically significant (Figure 3.14). Combined with the previous results in Figure 3.13, the results demonstrate interkingdom interactions, which may be synergistic as shown with *F. nucleatum* and *P. gingivalis*, or competitive as shown with *S. gordonii*.

In contrary, when the growth medium was not supplemented with FBS, co-culturing *C. albicans* with either *F. nucleatum*, *P. gingivalis*, *S. gordonii* or bacteria (all together) resulted in reduction of the CFE/mL counts of *C. albicans* by 15.1%, 37.5%, 71.8% and 52.7% respectively. Significant reductions were observed with *S. gordonii* (*** $p < 0.001$) and bacteria in the mixed (4 species) biofilm model (* $p < 0.05$), as shown in Figure 3.14. These results indicate that serum may modulate the inhibitory effects of bacteria on *C. albicans*.

Notably, total CFE/mL counts of *C. albicans* mono-species, grown without serum, reduced by 18% relative to *C. albicans* supplemented with serum, from 3.38×10^7 to 2.77×10^7 (Table 3.4 and Figure 3.14). The results demonstrate that serum enhances the growth of *C. albicans*. These results were in line with the previous metabolic activity and biomass results shown in Figure 3.5 and Figure 3.6.

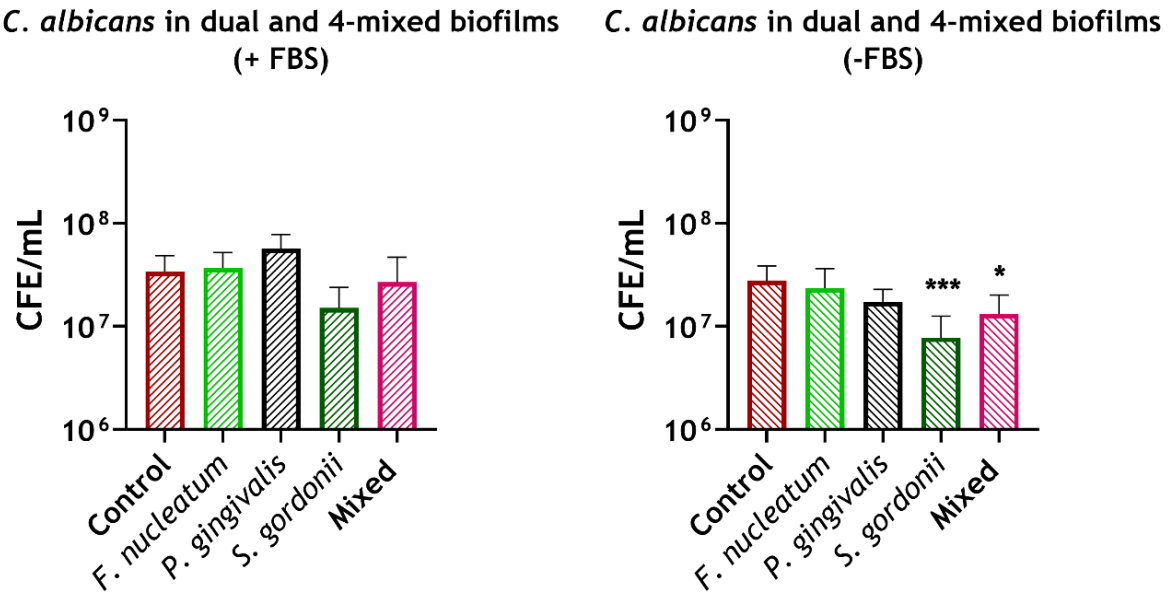

Figure 3.14. Colony forming equivalent per mL of *C. albicans* co-cultured with bacterial species, in the presence and absence of foetal bovine serum. *C. albicans* was co-cultured with either *F. nucleatum*, *P. gingivalis*, *S. gordonii* or all bacterial species together (mixed) in 1:1 RPMI/THB ± 10% FBS in 24-well flat-bottom plates for 24 h. Control; *C. albicans* mono-species biofilms. Each bar represents the mean of data obtained from triplicates of three independent repeats. Error bars represent the standard deviation. Data were analysed by Kruskal-Wallis with Dunn's tests. * Indicates statistically significant differences compared to the control (* $p < 0.05$, *** $p < 0.001$).

The previous experiment (Figure 3.14) was created in parallel with a biofilm model containing bacterial species only (*S. gordonii*, *P. gingivalis* and *F. nucleatum*). Compositional analyses were performed to assess the importance of *C. albicans* in supporting the growth of biofilms with and without FBS. A single species model (*S. gordonii*) was also run in parallel to further investigate the effect of *S. gordonii* on *C. albicans*. Based on the results, the CFE/mL counts of *C. albicans* decreased by 1.3- and 2-fold when grown with bacteria (3 species) in the presence and absence of FBS, respectively. While a 2-fold reduction was observed from bacteria in the presence of *C. albicans* co-cultured without serum. However, the scenario was reversed in the serum-supplemented medium with a 1.4-fold increase of bacterial numbers following inclusion of *C. albicans* (Figure 3.15A).

In contrast, 1.4- and 4-fold decreases were noted from *S. gordonii* when *C. albicans* was present, in the presence and absence of FBS, respectively, whereas

2- and 3.6-fold reductions were apparent from *C. albicans* when co-cultured with *S. gordonii*, in the presence and absence of FBS, respectively, as shown in Figure 3.15B.

Of interest, the qPCR reading illustrating CFE/mL showing that the total CFE/mL counts of bacteria grown in serum reduced by 24.8% relative to bacteria grown without serum, from 3.73×10^8 (- FBS) to 2.80×10^8 (+ FBS). Similarly, serum reduced CFE/mL counts of *S. gordonii* by 34.5% compared to *S. gordonii* grown in absence of serum, from 5.15×10^8 (- FBS) to 3.37×10^8 (+ FBS). Total CFE/mL counts for the biofilm models and biofilm composition (%) are shown in Table 3.4.

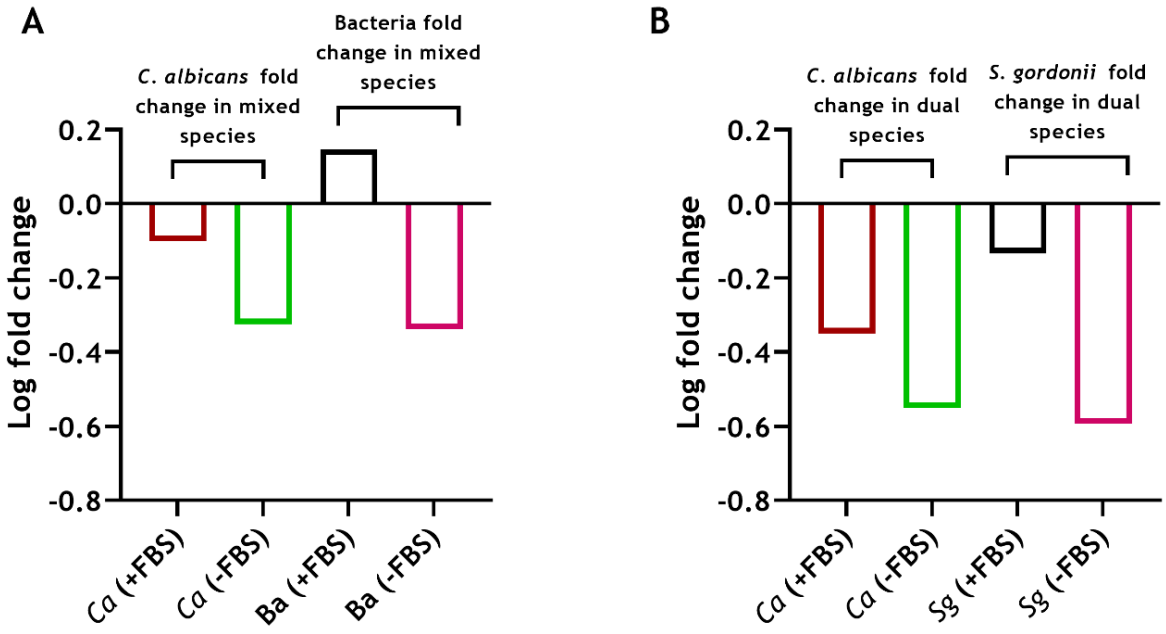

Figure 3.15. Log fold changes of *C. albicans* and bacteria in 4-species and dual-species biofilm models. (A) *C. albicans* and bacteria were quantified (CFE/mL) in mixed-species biofilms (4 species) and compared to simpler models of *C. albicans*-only biofilms (1 species) and bacterial-only biofilms (3 species), respectively. **(B)** *C. albicans* and *S. gordonii* were quantified in dual-species biofilms and compared to simpler models of *C. albicans*-only biofilms and *S. gordonii*-only biofilms, respectively. Log fold changes were calculated and presented graphically. Data are representative of biofilms from three independent repeats with three technical replicates. *Ca*; *C. albicans*, *Sg*; *S. gordonii*, Ba; bacteria, FBS; foetal bovine serum. Raw data are shown in Figure 3.14 and Table 3.4.

Taken together, our data suggested that the relation between *C. albicans* and bacterial species within the optimised 4-species biofilm model, when co-cultured simultaneously, is being competitive in nature where reductions of CFE/mL numbers were observed in both kingdoms. However, the inclusion of *C. albicans* may support bacterial biofilm formation in a serum-supplemented medium where a little increase in bacterial numbers were apparent (Figure 3.15).

Table 3.4. Total colony forming equivalent per mL of mono-, dual- and mixed biofilm models.

	4-species model				**3-species model**	**1-species model**
	Bacteria	(%)	*C. albicans*	(%)	Bacteria	*C. albicans*
+ FBS	3.92×10^8	93.6%	2.68×10^7	6.4%	2.80×10^8	3.38×10^7
- FBS	1.71×10^8	92.9%	1.31×10^7	7.1%	3.73×10^8	2.77×10^7
	Dual-species model				**1-species model**	**1-species model**
	S. gordonii	(%)	*C. albicans*	(%)	*S. gordonii*	*C. albicans*
+ FBS	2.48×10^8	94.3%	1.51×10^7	5.7%	3.37×10^8	3.38×10^7
- FBS	1.31×10^8	94.4%	7.81×10^6	5.6%	5.15×10^8	2.77×10^7
	***C. albicans* CFE counts in mono-, dual- and mixed-species (4 species) biofilms**					
	C. albicans (control)	*C. albicans* + *F. nucleatum*	*C. albicans* + *P. gingivalis*	*C. albicans* + *S. gordonii*	*C. albicans* + bacteria	
+ FBS	3.38×10^7	3.71×10^7	5.71×10^7	1.51×10^7	2.68×10^7	
- FBS	2.77×10^7	2.35×10^7	1.73×10^7	7.81×10^6	1.31×10^7	

Average CFE/mL and percentage composition (%) of biofilm models. Biofilms were grown in 1:1 RPMI/THB ± FBS for 24 h. Data representative of biofilms from three repeats with three technical replicates.

To further understand the interkingdom interactions, *C. albicans* was first grown for 4 h in 1:1 RPMI/THB, and sequential addition of standardised bacteria was then employed. Based on the previous results, FBS was not used in order to assess the effect of each bacterial species on *C. albicans* when sequentially added after initial *C. albicans* hyphal formation. Plates were incubated for an additional 20 h and compositional analyses were performed. In contrary to the previous results shown in Figure 3.14, the CFE/mL counts of *C. albicans* was increased by approximately 1 × $\log_{10}$, compared to *C. albicans* only, when co-cultured with bacterial species after initial hyphal formation (Figure 3.16A). The mixed-species biofilm was predominantly composed of *S. gordonii* followed by *C. albicans* (87.6 % and 11.7%, respectively), as previously shown in Figure 3.9.

Notably, *F. nucleatum* and *P. gingivalis* in mixed (4 species) biofilms were estimated to be approximately 2 $\log_{10}$ (0.6%) and 3 $\log_{10}$ (0.03%) lower than the total counts, respectively (Figure 3.16B).

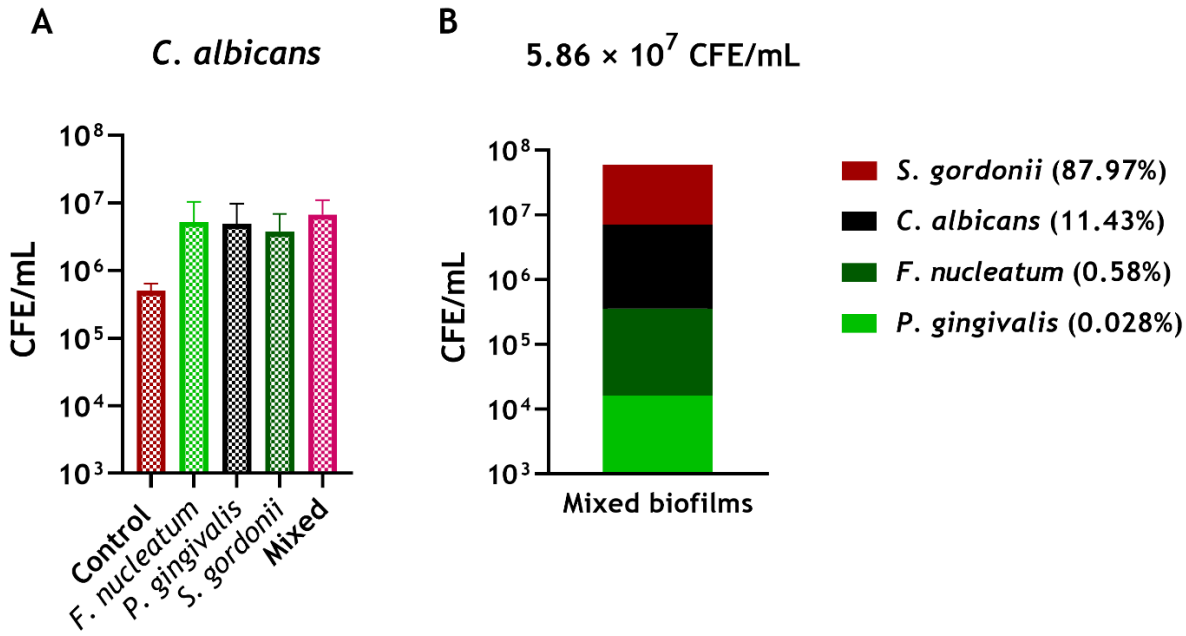

Figure 3.16. Compositional analyses of *C. albicans* co-cultured with bacterial species added sequentially. *C. albicans* was grown on Thermanox™ coverslips for 4 h in 24-well plates in 1:1 RPMI/THB. Sequential addition of standardised *F. nucleatum*, *P. gingivalis* and *S. gordonii* was then employed and incubated for additional 20 h. **(A)** *C. albicans* (CFE/mL) when co-cultured with *F. nucleatum*, *P. gingivalis*, *S. gordonii* and the three bacterial species. **(B)** Compositional analysis of mixed-species biofilms (4 species). Total CFE/mL for all four microorganisms in mixed-species biofilms are shown above the bar graph and percentages of each species within the biofilms are also displayed. Data distributions were assessed using Shapiro-Wilk normality test, and then analysed by ANOVA with Dunnett's tests to determine the P-value for multiple comparisons of normally distributed parametric data. No significant differences were found between *C. albicans* only (control) and *C. albicans* co-cultured with bacterial species. Each bar represents the mean of data obtained from one technical repeat of four independent experiments. Error bars represent the standard deviation.

3.5 Discussion

Within the field of endodontics, there has been a clear direction of travel toward model systems with more challenging complexity, both biologically and anatomically, to mirror the clinical reality more closely. Microbiological research fits within this ethos, with clear pointers from the literature highlighting inadequacies in biofilm models used for the development of better chemotherapeutic approaches. This is best illustrated in the quote from a recent systematic review that stated, "Because of substantial variation in experimental parameters, it is difficult to compare results between studies. This demonstrates the need for a more standardised approach and a validated endodontic biofilm model" (Swimberghe et al., 2019). To this end, we set out to tackle this research need with the aim of creating and then testing an optimised biofilm model that was both simple and reproducible, and importantly, being more representative of endodontic infections.

Whilst we appreciate the caveats on what represents the ideal and most representative model, there was clearly a need for a model with microbial complexity. In some studies, defined microbial species have been utilised, ranging from four to five single species (R Kim et al., 2015, Donyavi et al., 2017). Others have employed undefined microorganisms isolated from the human oral cavity, trying to simulate the complex *in vivo* situations. In the study by Jardine et al. (2019), human dentine blocks were worn intraorally by volunteers for 72 h to be infected in situ by oral microorganisms. In another study, root canals of extracted teeth were prepared, sterilised and then contaminated in situ with oral microorganisms for 1 week and incubated for 2 more weeks (O Peters et al., 2011). Extracted single-rooted teeth have also been inoculated with mixed human subgingival plaque samples (Lin et al., 2013), whereas, in another study, extracted teeth were inoculated with collected samples from infected root canals (Schaudinn et al., 2013). Growing a biofilm intraorally, or from an inoculum derived from an oral *ex vivo* sample is highly clinically relevant for an endodontic model. However, as mentioned above, these extremely diverse microbial populations are difficult to manipulate and imprecise to reproduce. Therefore, for the purpose of this study, a panel of four organisms were selected that represented diverse and relevant populations of

bacteria and yeast (Shin et al., 2018, Mergoni et al., 2018), with different atmospheric and nutritional requirements. Our model was purposely limited to four species, which reduces complexity, supports reproducibility, but importantly, limits costs for quantitative and compositional analyses.

Biofilm formation starts with surface attachment regardless of whether the substrate is biologic or non-biologic, though what defines the end of biofilm formation remains a challenge (Ren et al., 2018). The starter inoculum concentration of *C. albicans* significantly affects the growth rate of mature biofilms, possibly through quorum sensing mechanisms (Casalinuovo et al., 2017), where unnecessary overpopulation is controlled through a cell-cell communication strategy (Ramage et al., 2005). Thus, a significant increase in cell viability of mature biofilms was obtained by Casalinuovo et al. (2017) with a starter inoculum of 1×10^6 cells/mL. Augmenting the initial inoculum resulted in a proportional decrease of the metabolic activity of *C. albicans* cells. These results confirm that the development of biofilm is a coordinated process in which an optimal number of cells is needed for optimal growth (Casalinuovo et al., 2017). Therefore, *C. albicans* and bacterial species, in this study, were adjusted to the desired cellular density of 1×10^6 CFU/mL and 1×10^7 cells/mL, respectively, as previously shown (Montelongo-Jauregui et al., 2016, Montelongo-Jauregui et al., 2018, Alshanta et al., 2019, Alshanta et al., 2020). Along with optimised initial inoculums used, time was spent for optimising the biofilm model, using a range of experimental parameters, such as different atmospheric conditions, media and incubation times. Each of which were assessed to ensure optimal conditions that support growth of both *C. albicans* and the three bacterial species. There are numerous available media in the literature to grow microorganisms. Most microbial laboratory testing methods specify the use of a certain medium to grow any tested organism. This enables comparison of a specific organism's characteristics across studies and databases (Cleland et al., 2007). Although available laboratory methods cannot reflect the nutritional requirements that favour biofilm formation within the root canal environment with accuracy, the frequently used general growth media are highly nutritious, providing a source of carbohydrate, proteins and supplements that should optimally support and promote the biofilm formation of involved microorganisms, especially the fastidious species (Swimberghe et al., 2019). The

media selected contained a 1:1 ratio of RPMI and THB, as previously described by Montelongo-Jauregui et al. (2016) or RPMI and TSB. We deemed it pertinent to investigate different types of media for our model given that others have highlighted that variation in media constituents can impact fungi–bacteria biofilm growth *in vitro* (Arzmi et al., 2015, Montelongo-Jauregui et al., 2016, Leonhard et al., 2019). It has also been shown that changes in the composition of a growth medium can result in considerably different microbial growth characteristics (Wieme et al., 2014). Subtle phenotypic changes have also been observed between cultures grown on different media (Cleland et al., 2007). For *C. albicans*, a common protocol for induction of germ-tube formation is incubation of cells in the RPMI medium (Pierce et al., 2008). Therefore, RPMI was included to permit hyphal formation by *C. albicans*. FBS was also incorporated into the growth media to assess whether a rich variety of proteins such as albumin present in the FBS could aid *Candida* hyphal formation and bacterial growth in the biofilm model. It has been shown that germ-tube formation of *C. albicans* can be triggered by an effective induction medium such as serum (Hudson et al., 2004, Krom et al., 2007). In this study, FBS-supplemented media provided an increase in the metabolic activity and biomass formation in *C. albicans* and mixed-species biofilms (Figure 3.5 and Figure 3.6). These results have been further affirmed by qPCR where the *C. albicans* CFE counts, in the absence of serum, reduced by 18% relative to *C. albicans* supplemented with serum (Table 3.4). In contrast, reductions in the metabolic activity and CFE/mL counts of *S. gordonii* mono-species biofilms were observed with FBS (Figure 3.5 and Table 3.4). A previous study showed higher bacterial colonisation of *S. mutans* on uncoated hydroxylapatite (hydroxyapatite) beads than human serum-coated specimens (Nikawa et al., 1998). The inhibitory activity of FBS was also shown on biofilm formation of *Staphylococcus aureus*. It has been suggested that this inhibitory effect is due to inhibition of biofilm-related genes expression (Abraham and Jefferson, 2010). Nevertheless, regardless of the media used, all mixed-species biofilms possessed similar ultrastructure and architecture (Figure 3.10). Notably, the growth of *S. gordonii* mono-species biofilms was enhanced with THB. This could be attributed to the iron source in the THB medium supplemented by hemin. Oral streptococci were assumed to acquire iron for growth using hemin compounds (E Kim and Lee, 2019).

The compositional analyses of both serum-supplemented media showed that the biofilms were predominated by *C. albicans* and *S. gordonii*, making up more than 99% of the final composition, with the two anaerobes comprising of less than 1% (Figure 3.9). Importantly, the CFE/mL numbers of *P. gingivalis* were estimated to be approximately 5 $\log_{10}$ units lower than the total CFE/mL counts (0.001%). This relatively low number of *F. nucleatum* and *P. gingivalis* may be explained by the atmospheric conditions used (5% CO_2), which was selected, as this condition gave rise to mixed-species biofilms with the greatest biomass. This could be explained by the fact that CO_2 is one of the environmental stimuli that is known to promote the switch from yeast to hyphal growth (Hall et al., 2009). In contrary, the anaerobic condition was not the most favourable condition for *C. albicans* and the mixed biofilm formation. This was previously shown in other studies (Dumitru et al., 2004, Biswas and Chaffin, 2005). Being obligate anaerobes, *F. nucleatum* and *P. gingivalis* cannot survive in oxygenated microenvironments unless grown in the presence of oxygen-consuming species or in other oxygen-limiting conditions (Bradshaw et al., 1997, Bradshaw et al., 1998, Diaz et al., 2002, Diaz and Rogers, 2004).

Therefore, initially, we postulated that as *C. albicans* provides a hypoxic niche for anaerobic bacteria to survive and proliferate (Fox et al., 2014, Lambooij et al., 2017), allowing the anaerobic microorganisms to be more represented in the final composition. However, as the four microorganisms were added together, instead of sequentially as in other oral biofilm models (Sherry et al., 2016, Y Zhou et al., 2018, Brown et al., 2019a), the microenvironment itself may not have been suitably anoxic during the first few hours to allow survival of large quantities of *F. nucleatum* and *P. gingivalis*. This could explain the relatively higher quantity of *P. gingivalis* when bacterial species added sequentially, as shown (Figure 3.16). Nevertheless, we deemed the biofilm to be an accurate model given that, *in vivo*, microorganisms such as *P. gingivalis* were found similarly in very low quantities in disease (4-5 $\log_{10}$ lower than the total), consistent with our findings (Hajishengallis et al., 2011, Hajishengallis et al., 2012). Importantly, all four microorganisms could be detected by the scanning electron microscopy and observed within the biofilms (Figure 3.10).

Two colorimetric assays were used in this study, each of which describes biofilms differently. Crystal violet is known to be a good indicator of the amount of biomass formed, whereas XTT is bound to the metabolic activity of the cells forming the biofilm (Corte et al., 2019). XTT is a colorimetric-based assay that measures the metabolic activities of cells within the biofilm. A tetrazolium salt is reduced by metabolically active cells to water-soluble orange formazan compounds. The intensity of the colorimetric change is directly proportional to the number of living cells within the biofilm (Pierce et al., 2008). The XTT assay is non-invasive, non-destructive, requiring minimal processing and it is particularly useful for measuring the antimicrobial effect of drugs on biofilms (Pierce et al., 2008). However, it does not consider other biofilm components such as the extracellular matrix. The crystal violet staining method provides the total quantification of the biofilm biomass including ECM. It also allows for rapid, high-throughput processing of multiple samples. However, CV has a number of limitations such as the inability to differentiate subtle differences between samples (Kean et al., 2018), and between living and dead cells (Peeters et al., 2008). In addition, over- and under-estimation of biomass can occur due to the variability of the washing step of biofilms (Kean et al., 2018). Furthermore, CV is not useful specifically for quantifying biomass of biofilms treated with some antimicrobials. A good example of this is chlorhexidine as its precipitations would over-estimate the biofilm biomass. However, CV is easy to use and it showed a high reproducibility for most isolates, although it failed to give repeatable results for particular strains (Peeters et al., 2008).

On the other hand, scanning electron microscopy has been used in some *in vitro* models to analyse the morphological characteristics of biofilms formed in different media (Montelongo-Jauregui et al., 2016, Montelongo-Jauregui et al., 2018), and to evaluate biofilm morphological changes before and after antimicrobial treatment (O'Donnell et al., 2017). The SEM is an invaluable imaging tool for describing biofilms because of its ability to yield excellent-resolution images of topographic features at high magnifications (Schaudinn et al., 2009). Nevertheless, the obvious drawback of the conventional SEM is a significant loss of ECM through water loss due to the requirement of dehydration during sample processing (Alhede et al., 2012).

PCR methods have been widely used in various applications, encompassing molecular analysis of microbial pathogens, neoplasms and inheritable diseases and syndromes. Our understanding of medical microbiology has been revolutionised by the application of molecular based identification techniques (Y Kim et al., 2002). Molecular methods are based on the detection of specific genomic sequences for each microbial species (Shahi et al., 2018). Due to the progress of molecular techniques, it becomes possible to recognise uncultivable and fastidious microbial species and characterise the microflora associated with endodontic infections (Y Kim et al., 2002). For instance, the presence of *C. albicans* was detected in samples taken from infected root canals using PCR methods (Baumgartner et al., 2000). Another study employing qPCR has shown the high prevalence and abundance of *Tannerella forsythia* in endodontic infections (Saito et al., 2009). qPCR analyses were also utilised to quantify the composition of other oral biofilm models (Sherry et al., 2016, Young et al., 2021). The qPCR-based approach represents a robust, highly reproducible and sensitive method enabling the quantification of gene and/or transcript numbers under varying conditions. One main disadvantage of qPCR is the requirement for prior sequence data of the specific target gene of interest. So, it can only be used for detection of specific known genes (C Smith and Osborn, 2009).

On the other hand, different non-biological substrates on which biofilms were grown have been found to stimulate different emergent phenotypes during biofilm formation on these substratum materials (Ren et al., 2018). In a literature review by Swimberghe et al. (2019), it has been highlighted that 96% of endodontic studies used ‘dentine’ as a substrate for the biofilm growth. In fact, 68 articles made use of human dentine, six studies used bovine teeth and three studies used nonbiological substrates. However, Eick et al. (2017) highlighted that human dentine or moderately rough titanium discs coated with various protein layers do not significantly influence the adhesion of multispecies biofilm. Nevertheless, the dentine structure with its organic and inorganic components represents a distinctive substrate that is challenging to mimic or copy (Swimberghe et al., 2019). Due to the difficulty in obtaining human extracted teeth as substrates with sufficient quantity and quality, bovine teeth have been proposed as an alternative for *in vitro* dental experiments, as bovine enamel and dentine shows great similarity to human enamel and dentine with

regard to their chemical composition (de Dios Teruel et al., 2015). Notably, the SEM imaging, in this study, showed similarities between biofilms grown on dentine and coverslips (Figure 3.10L and Figure 3.12B).

Regarding interkingdom interactions, it was clear from the findings that inclusion of bacteria, particularly *S. gordonii*, reduced the CFE/mL counts of *C. albicans* grown on the microtiter plates in the presence and absence of FBS, while the addition of *C. albicans* showed a degree of reduction in bacterial growth, in the absence of FBS, when all microorganisms were added simultaneously. Interestingly, the inclusion of *C. albicans*, in the presence of FBS, showed an increase in the number of total bacteria by 1.4-fold (Figure 3.15). In a study by Kean et al. (2017), a strong interkingdom synergy was shown to exist through the physical scaffold of hyphae, providing a potential niche for *S. aureus* to colonise and form biofilms on the existing *C. albicans* biofilm, when co-cultured in 50% v/v foetal bovine serum, a phenomenon that has been termed "mycofilms". This could be explained by the fact that serum is one the factors that triggers hyphal formation of *Candida* species, which can be used thereafter as a scaffold for bacteria to colonise. Importantly and in contrary to the previous results, the fungal load in the oral biofilm model in dual- and mixed cultures increased by approximately 1 × $\log_{10}$ when bacteria were added sequentially. On the other hand, the CFE/mL numbers of *F. nucleatum* and *P. gingivalis* in mixed-species biofilms were estimated to be approximately 2 $\log_{10}$ and 3 $\log_{10}$ units, respectively, lower than the total CFE counts per mL, which seemed to be more represented in the final composition when added sequentially to *C. albicans* than those grown in the optimised endodontic biofilm model when all species were added together. Although this study did not determine the effect of *C. albicans* on each bacterial species when the sequential addition of bacteria was employed after initial *C. albicans* hyphal formation, a study by Young et al. (2021) highlighting that bacterial load was increased significantly, in oral biofilm models, with sequential additions when *C. albicans* was present.

Antagonistic interkingdom interactions have previously been reported by others, where *F. nucleatum* and a number of other bacterial species including *P. gingivalis* and streptococci have been shown to inhibit growth and hyphal morphogenesis of *C. albicans* (Thein et al., 2006, Bor et al., 2016). Other

researchers reported synergistic interactions between *S. gordonii* and *C. albicans* (Bamford et al., 2009), and between *P. gingivalis* and *C. albicans* (Nair et al., 2001), where hyphal production was enhanced. Different experimental methodologies between studies may explain the discrepancy between the results. However, it has been thought that the potential for interkingdom biofilm interactions in the root canal is likely to complicate the infection and require alternative treatment strategies (Persoon et al., 2017, Du et al., 2021).

CHAPTER FINDINGS

- A multispecies interkingdom biofilm model composed of key microorganisms is robust, reproducible and representative of endodontic infections.

- Robust methodologies are needed to establish robust biofilm systems that can be reproducible in different laboratories.

- Obtaining reproducible biofilm models with reproducible results is necessary to understand how altering one parameter could affect the growth and characteristics of biofilms.

- The interkingdom interactions may be synergistic or antagonistic and can be affected by different experimental setups and supplemented media.

- This model can be employed and used as a testbed to assess efficacy of novel endodontic therapeutics.

4 Assessing novel antimicrobial therapeutics in endodontic infections

4.1 Introduction

Microbial infections in the root canal system play the main role in endodontic failure (Yancheshmeh, 2020). It has been evidenced that root canal infections exist as a complex ecology involving heterogeneous polymicrobial communities of bacteria and fungi (Persoon et al., 2017). In spite of this, the contribution of fungi to endodontic infections has been extremely limited (O'Donnell et al., 2015, Persoon et al., 2017). Nonetheless, interkingdom interactions are highly relevant and should be considered in the development of effective treatment strategies (Persoon et al., 2017, Alshanta et al., 2020).

There has been a great interest in identifying a new natural compound that possesses antimicrobial properties against endodontic pathogens. The potential use of chitosan in endodontic treatment is not unheard of, with recent publications highlighting the potential development of chitosan-based endodontic materials. It has been shown that chitosan nanoparticles were effective in reducing the CFUs of an *E. faecalis* biofilm grown on human root canal dentin, when incorporated into $Ca(OH)_2$ pastes used as endodontic medicaments (del Carpio-Perochena et al., 2017). Additionally, the sustained release of calcium ions in the root canal system was obtained when chitosan gel was used as a vehicle for calcium hydroxide (Grover and Shetty, 2014). Other studies have shown that the antimicrobial effect of root-canal sealers was enhanced by the incorporation of CNPs (DaSilva et al., 2013, del Carpio-Perochena et al., 2015b, Pattanaik et al., 2019) and chitosan solution (Beshr and Abdelrahim, 2019a). The antimicrobial effectiveness of 0.25% and 0.5% chitosan, solubilised in acetic acid, has also been shown when used as a root canal irrigant (Yadav et al., 2017). Furthermore, chitosan is a natural and biocompatible chelating substance. Final irrigation of human root canals with either 15% EDTA or 0.2% chitosan had similar effects on dentine microhardness, push-out strength, sealer penetration into dentinal tubules (Antunes et al., 2019) and smear layer removal capacity (P Silva et al., 2013). Similarly, it has been found that final irrigation of bovine dentine with either 17% EDTA or 1.29 mg/mL CNPs has achieved a comparable chelating effect (del Carpio-Perochena et al., 2015a). In addition, the biofilm cell viability was found to be significantly lower in samples treated with chitosan, as a final irrigant, than samples treated with EDTA. Therefore, CNPs can be a useful alternative to EDTA due to its antibiofilm

activity and chelating effect on root dentine (del Carpio-Perochena et al., 2015a). Interestingly, in a study by Arnaud et al. (2010), it has been found by a chemical analysis and optical coherence tomography that chitosan solution possessed a remineralising property by inhibiting the release of phosphorus from enamel samples into a demineralising solution. It has been suggested that chitosan may inhibit the demineralisation process by acting as a potential barrier against acid penetration, optimally at concentrations between 2.5 mg/mL (0.25%) and 5.0 mg/mL (0.5%) and exposure between 60 and 90 seconds.

Despite chemo-mechanical disinfection, a significant challenge faced by dental cements used in the filling of the root canal space is the presence of infectious microorganisms lodged in the root canal system (Farrugia et al., 2017). Therefore, it is important to use dental materials that possess the greatest antimicrobial activities, but most importantly, not at the expense of their biological properties. In response to the challenges faced in sealing the root canal space, calcium-silicate-based materials have grown in prominence. Although considerable research has focused on the antimicrobial properties of these materials, as previously detailed in chapter 1, their antibiofilm efficacy has been scarcely investigated (Jardine et al., 2019, Ruiz-Linares et al., 2022). Therefore, in this chapter, the antimicrobial efficacy of chitosan, commercial calcium silicate materials and chitosan-modified calcium silicate materials was investigated against the optimised interkingdom biofilm model system, containing *C. albicans*, *S. gordonii*, *P. gingivalis* and *F. nucleatum*.

4.2 Hypothesis and aims

In vitro studies for management strategies of endodontic infections have been hampered by the lack of validated biofilm models. Therefore, this chapter aims to:

- Assess whether the optimised interkingdom biofilm model was a suitable system to be tested with conventional and novel therapeutics.
- Investigate the antibiofilm efficacy of ProRoot MTA and Biodentine materials against mono- and multispecies biofilm models, and whether the antimicrobial behaviour of these materials can be augmented by chitosan incorporation.
- Assess whether fungi could confer protection to bacterial species from active agents when grown in mixed microbial cultures.

Data from this chapter have been published in:

- **Abusrewil, S.**, Brown, J.L., Delaney, C.D., Butcher, M.C., Kean, R., Gamal, D., Scott, J.A., McLean, W. and Ramage, G., 2020. Filling the void: an optimized polymicrobial interkingdom biofilm model for assessing novel antimicrobial agents in endodontic infection. *Microorganisms*, 8(12): 1988. DOI: 10.3390/microorganisms8121988. Pub 2020 Dec 14. PMID: 33327403.
- **Abusrewil, S.**, Brown, J.L., Delaney, C., Butcher, M.C., Tiba, M., Scott, J.A., Ramage, G. and McLean, W., 2021. Chitosan enhances the anti-biofilm activity of Biodentine against an interkingdom biofilm model. *Antibiotics*, 10(11):1317. DOI: 10.3390/antibiotics10111317. Pub 2021 Oct 29. PMID: 34827255.

Work from this chapter has been presented at the annual Oral Microbiology and Immunology Group (OMIG) meeting, March 2021, UK.

4.3 Materials and methods

4.3.1 *In vitro* biofilm antimicrobial susceptibility testing

4.3.1.1 Preparation of test agents

To validate the previously optimised interkingdom biofilm model, the capacity of different antimicrobials to inhibit biofilm formation was assessed using this model. The antimicrobials tested and their stock concentrations were as follows: 20% chlorhexidine (v/v) (CHX [Sigma-Aldrich, Dorset, UK]), 17% (460 mM) Ethylenediaminetetraacetic acid (w/v) (EDTA [Sigma-Aldrich, Dorset, UK]) and medium molecular weight chitosan (CS-MMw [Sigma-Aldrich, St. Louis, MO, USA]), prepared to 1400 µg/mL. EDTA (17%) was prepared by adding 85 g of ethylenediaminetetraacetic acid disodium salt dihydrate to 400 mL of distilled water in a Duran bottle. The bottle was then placed on a magnetic stirrer to mix the solution using a small magnet. To dissolve the salt, the pH was adjusted at 8.0 by gradually adding 50 mL of sodium hydroxide solution (0.2 g/mL) to the EDTA disodium salt solution, using a calibrated pH meter (Mettler Toledo, Leicester, UK). The pH meter was calibrated before use, according to the buffer solutions (pH 4.0 and 7.0). When the salt was fully dissolved, the solution was topped up to 500 mL using distilled water, and then sterilised in the autoclave. For the conventional treatments, CHX and EDTA were diluted to 0.2% and 230 mM, respectively, in the relevant media. Chitosan was prepared as described previously (Vieira et al., 2019). Briefly, 1400 µg/mL chitosan was solubilised in 2% acetic acid under constant magnetic stirring for 24 h at room temperature. The stock solution was then diluted down to 0.7 mg/mL in the appropriate media prior to biofilm treatment.

4.3.1.2 Planktonic minimal inhibitory concentration (P-MIC)

The determination of the pathogens susceptibility to antimicrobials is vital in choosing the most appropriate compounds for treating microbial infections. Planktonic minimal inhibitory concentration susceptibility testing, based on Clinical and Laboratory Standards Institute (CLSI) methodologies (CLSI, 2008, CLSI, 2018), was performed to determine the MIC of different endodontically relevant antimicrobials against planktonic *C. albicans* mono-species and the co-culture of *C. albicans*, *F. nucleatum*, *P. gingivalis* and *S. gordonii*.

Briefly, yeast cells were adjusted to 2 x 10^4 CFU/mL while bacteria were adjusted to 2 x 10^5 cells/mL in 1:1 RPMI/THB. Two hundred microlitres of each drug were added to the appropriate wells of 96-well round-bottom microtiter plates (Corning Incorporated, NY, USA) and serial doubling-dilutions were performed in RPMI/THB, with concentrations starting from 0.025% (CHX), 4.25% (EDTA) and 1.4 mg/mL (CS-MMw). One hundred microlitres of standardised cell suspensions were added to each well containing the drug, to get a final volume of 200 µL. The plates were incubated in CO_2 for 24 h at 37°C. Appropriate positive and negative controls were also included. The MIC concentration was deemed to be the lowest concentration of the antimicrobial agent that prevents visible microbial growth.

4.3.1.3 *In vitro* biofilm susceptibility testing against biofilms grown in microtiter plates

The optimised interkingdom biofilm model system was used to assess the capacity of different antimicrobials to inhibit biofilm formation. The effect of each active was assessed against multispecies biofilms grown in optimal conditions in a 5% CO_2 incubator at 37°C. Three regimes were tested: the 'treatment' group, 'prevention' group and 'adsorption' group. The stock solution of CHX, EDTA and CS-MMw were diluted down to 0.2%, 230 mM and 0.7 mg/mL, respectively, in the appropriate media prior to biofilm treatment. In the 'treatment' group, biofilms were treated for 24 h at concentrations described above, prior to metabolic assessment. Conversely, to more effectively model endodontic protocols, the 'prevention' and 'adsorption' groups contained biofilms that were first mechanically disrupted, in order to assess the ability of the test antimicrobial agents to impede biofilm regrowth. Briefly, after biofilm maturation (24 h), the spent biofilm media were discarded, and biofilms were washed with 500 µL of PBS. The biofilms in the 'prevention' group were disrupted with a cell scraper into 1 mL of RPMI/THB ± FBS and diluted to 1:5 in fresh RPMI/THB ± FBS media. This new inoculum, representative of the 4-species biofilm consortia, was then inoculated into another 24-well tissue culture plate by pipetting 250 µL into wells, prior to treatment with 250 µL of each antimicrobial test agent adjusted to twice the desired concentrations described above. This was to get a 1:10 cell dilution and final concentrations of chlorhexidine (0.2%), chitosan (0.7 mg/mL), and EDTA (230 mM). For the

'adsorption' group, a new 24-well plate was pre-treated overnight with 500 µL of active agents in above mentioned concentrations. The biofilms were mechanically disrupted and diluted to 1:10 in the relevant media, as previously described. Cell seeding performed by adding 500 µL per well into the pre-treated wells, after drug discarding.

Plates were then incubated for an additional 24 h (a total of 48 h) in 5% CO_2 at 37°C to allow biofilm regrowth. Positive control biofilms were run in parallel for this experiment. These controls were disrupted as above, then replaced with fresh RPMI/THB ± FBS media excluding treatment. Negative control broths (minus inoculum) were included to assess for microbial contamination. Following incubation and washing with PBS, the metabolic activity was measured by the Alamar Blue™ (AB [Thermo Fisher Scientific, USA]) assay. For this, a 1:10 dilution of AB was prepared in RPMI/THB ± 10% FBS media. A volume of 250 µL of AB was added into each well and incubated for 1 h in the dark in the Classic incubator at 37°C. 100 microlitres were transferred to a new 96-well flat-bottom plate for fluorescence reading at 544/590 (excitation/emission), using the microtiter plate reader (FluoStar Omega, BMG Labtech, Aylesbury, UK). Next, the composition of the regrown mixed fungal/bacterial biofilms of the 'prevention' group, following treatment with CHX, EDTA and CS-MMw, was assessed using qPCR, as described in 3.3.2.3. The effect of the CS-MMw solution (0.7 mg/mL) was then assessed against mono- and multispecies biofilms grown in RPMI/THB as previously mentioned in the 'prevention' group. The metabolic activity was measured by Alamar Blue, and biomass was quantified using crystal violet.

4.3.2 Assessing the effect of chitosan on the optimised endodontic biofilm model upon dentine

The effect of the antimicrobial ability of chitosan was assessed against mixed-species biofilms regrowth on a biological substrate 'bovine dentine' and placed in pre-sterilised polystyrene 24-well flat-bottom plates. Due to the difficulty in obtaining human extracted teeth, bovine dentine has been used alternatively as a biologically relevant positive control, due to its great similarity to the human dentine (de Dios Teruel et al., 2015).

Bovine dentine discs (Modus laboratories, Reading, UK) were supplied in round cross-sections, approximately 7 mm in diameter and 1 mm in thickness, with transverse cross-sections. The 4-multispecies biofilm model was grown in RPMI/THB in 24-well plates. After 24 h, the biofilms were disrupted and inoculated into bovine dentine discs in a 24-well plate treated with CS-MMw (0.7 mg/mL) as previously mentioned in the 'prevention' biofilm model. Positive and negative controls broth were run in parallel as well. Pre-sterilised bovine dentine discs (negative control) were kept in media (minus inoculum) to assess for the sterilisation process. Following maturation and discarding spent media, each dentine disc was gently washed with 500 µL of PBS and then transferred into a bijoux tube containing 1 mL of PBS and sonicated at 35 kHz in a sonic bath for 10 minutes. The sonicate was then transferred into 1.5 mL Eppendorf tubes (Greiner Bio-one, Kremsmünster, Austria, UK) for DNA extraction. The structure and composition of the regrown biofilms on dentine discs were assessed using SEM and qPCR, respectively, as previously described in sections 3.3.2.3 and 3.3.3.

4.3.3 Investigating the antimicrobial properties of ProRoot MTA and Biodentine materials against the interkingdom biofilm model

4.3.3.1 Preparation of ProRoot MTA and Biodentine material discs

Two different types of calcium silicate materials, used in the management of endodontic diseases, were used in this current study to evaluate their antibiofilm efficacy: mineral trioxide aggregate (ProRoot MTA Root Repair Material [Dentsply Tulsa Dental Specialties, Johnson City, USA]) and Biodentine™ (BD [Septodont, Saint-Maur-des-fossés, Cedex, France]), as shown (Table 4.1). Moulds, 1 mm in height with 7 mm diameter corresponding to the size of the bovine dentine discs, were fabricated from dental silicone-based impression materials; putty soft (Coltene, altstätten, switzerland) and Polyvinyl siloxane impression material (Extrude, Romulus, USA). The moulds were then disinfected with 70% Ethanol. MTA and BD powders were mixed according to the manufacturers' instructions. MTA powder was mixed with a ProRoot liquid micro-dose ampoule with a stainless-steel spatula. The powder-containing capsule of Biodentine™ was mixed with five drops of the manufacturer Liquid component.

Materials were then placed into aseptic moulds and allowed to set in a moist atmosphere at 37°C for 3 h and 1 h, respectively.

Table 4.1. Composition of ProRoot MTA and Biodentine

Product	Composition	Manufacturer
White ProRoot Mineral Trioxide Aggregate	Powder: tricalcium silicate, dicalcium silicate, bismuth oxide, tricalcium aluminate, calcium sulfate dihydrate or gypsum. Liquid: water	Dentsply Tulsa Dental Specialties, Johnson City, USA
Biodentine	Powder: tricalcium silicate, dicalcium silicate, calcium carbonate, zirconium oxide, calcium oxide, iron oxide. Liquid: calcium chloride, a hydrosoluble (water-soluble) polymer, water.	Septodont, Saint-Maur-des-fossés, Cedex, France

4.3.3.2 Quantitative analysis of biofilms formed on ProRoot MTA and Biodentine materials using Live/Dead qPCR

The antimicrobial ability of ProRoot MTA and BD was assessed against biofilm regrowth on the materials placed in a 24-well plate. The four interkingdom mixed-species biofilm model was grown in a 1:1 mixture of RPMI/THB medium in 24-well plates for 24 h. After incubation, the spent biofilm media were discarded, and biofilms were washed with 500 µL of PBS. The biofilms were then mechanically disrupted in 1 mL of RPMI/THB and diluted to 1:10 in fresh RPMI/THB and then inoculated on MTA and BD discs into 24-well plates, as previously mentioned in the 'prevention' biofilm model. Bovine dentine discs were used as positive controls. Mechanical disruption of the biofilms serves the purpose of simulating mechanical debridement of the root canal. Plates were then incubated for an additional 24 h in 5% CO_2 at 37°C to allow biofilm growth. After incubation, discs were sonicated for 10 minutes, as previously described in 4.3.2. The composition of the regrown biofilms on dentine, MTA and BD discs was assessed using Live/dead PCR, a technique that uses propidium monoazide (PMA), which is a DNA-intercalating dye, to differentiate biofilm viable and dead microorganisms. Propidium monoazide is able to bind to DNA from dead cells or cells with compromised membranes following exposure to a bright light source, resulting in a permanent modification of the double stranded DNA, which

prevents DNA amplification in qPCR. Thus, only live cells can be detected (Nocker et al., 2006). Samples were prepared as previously described by Sherry et al. (2016). Briefly, each sonicated sample was equally split; samples to be treated with PMA and control samples without PMA. Following this, 5 µL/mL of 50 µM PMA dye was added to each sample. Treated and control samples were all incubated in the dark at room temperature for 10 minutes to allow cells to uptake the dye. Samples were then exposed to a 650 W halogen light and positioned 20 cm away from the sample tubes, for 5 minutes. During exposure, samples were placed on a bed of ice, to avoid excessive heating. Following this, DNA extraction and real-time quantitative analyses were carried out, as previously described in 3.3.2.3, for bacteria and *C. albicans* and then for each bacterial species. Primers used for bacteria and *Candida* were 16S and 18S, respectively.

4.3.3.3 Visualisation of biofilms formed on materials and dentine using confocal laser scanning microscopy

1-species (*C. albicans*) and 4-species (mixed) 'prevention' models were grown on bovine dentine, MTA and BD discs. A qualitative CLSM microbiology technique was utilised to vision live/dead microorganisms present on the surface of substrates. Staining of biofilms for each disc was carried out using PI, SYTO™ 9 and CFW fluorescent dyes, as previously described in 3.3.2.5. Stained and fixed biofilms were washing once with PBS, dried overnight in the dark. Following drying, the discs containing biofilms were carefully removed from the 24-well plate using sterilised tweezers. These were transferred to microscope slides for viewing and kept in place using superglue on the underside of the disc prior to imaging on the confocal microscope (Upright Zeiss LSM 880). Slides were maintained in the dark before imaging. 488ex/500em$_{nm}$, 532ex/635em$_{nm}$ and 365ex/435em$_{nm}$ were used for excitation/emission wavelengths for visualising SYTO 9, PI and CFW, respectively. Images were compiled using the ZEN Blue software (Zeiss LSM780, Germany).

4.3.4 Investigating the antimicrobial efficacy of ProRoot MTA and Biodentine materials ± chitosan against single- and mixed-species biofilm models

4.3.4.1 Preparation of ProRoot MTA and Biodentine materials + CS-MMw, biofilm growth and enumeration

To investigate the effect of chitosan on the antimicrobial properties of tested materials, chitosan powder (microparticles) was incorporated into MTA and BD. Medium molecular weight chitosan (CS-MMw) was used throughout this study. Briefly, chitosan powder was disinfected using the ultraviolet light (UV) for 15 minutes. Following this, the chitosan powder was mixed with the manufacturer powder of Biodentine™ and MTA using two different concentrations (2.5% and 5% by weight). According to the manufacturer, the weight of commercial MTA and BD powder was claimed to be 0.5 g and 0.7 g, respectively. The weight of CS-MMw powder incorporated into the powder of both materials was calculated, using the following equation: material powder weight (g) × CS% (2.5 or 5) / 100. The powder-containing capsule of Biodentine™ was opened and chitosan powder was added to Biodentine™ powder and then 6 drops of the Biodentine™ Liquid were added into the capsule. The capsule was mixed with a mixing machine for 30 seconds. The new-mixed powder of MTA was mixed with distilled water. Unmodified materials were prepared in parallel. Materials were then filled into the aseptic moulds and allowed to set, as previously described in 4.3.3.1. Notably, in this study, the chitosan powder was not solubilised in acetic acid, to avoid replacement of the manufacturer BD liquid (BD-L) with the solubilised form of CS in the diluted acetic acid with water. It has been thought that replacement of BD-L with water may compromise the compaction and adaptation of the material (Pires et al., 2021). To keep consistency, both materials were prepared similarly.

Two derived biofilm models were used in parallel with the 4-species model, one of which contained bacterial species only (*F. nucleatum*, *P. gingivalis* and *S. gordonii*) and one contained *C. albicans* only, grown in the optimised conditions. This was to assess the importance of *C. albicans* in maintaining biofilm tolerance or otherwise. The composition of the regrown biofilms on materials and bovine dentine was enumerated using live/dead qPCR, as previously described in 4.3.3.2.

4.3.4.2 Evaluation of pH of MTA and Biodentine leachate

To investigate the effect of chitosan on the pH measurements of MTA and BD, material discs ± CS of 1 mm in thickness and 7 mm diameter were prepared of both materials. CS-MMw powder was incorporated into both materials at concentrations of 2.5 wt%, 5 wt%, 10 wt% and 20 wt%. MTA and BD were mixed with distilled water and the Biodentine™ Liquid, respectively, as shown (Table 4.2). The materials were allowed to set in a moist atmosphere at 37°C for roughly 3 h and 1 h, respectively. Each disc was placed in a bijoux tube containing 3 mL of sterile water. All samples were kept in a 5% CO_2 incubator at 37°C. Measurements of pH change of the storage solution was taken using a calibrated pH meter (Mettler Toledo, Leicester, UK) at 1 h, 3 h, 24 h, 7 days and 28 days. The pH of the manufacturer's BD liquid was also recorded.

Table 4.2. Chitosan percentages (%) incorporated into ProRoot MTA and Biodentine materials.

Test group	BD-P (g)	CS-P (g)	BD-L (µL)	MTA-P (g)	CS-P (g)	MTA-L (µL)
Control	0.7	—	180	0.5	—	150
0.5 wt%	0.6965	0.0035	180	—	—	—
1 wt%	0.693	0.007	180	—	—	—
2.5 wt%	0.6825	0.0175	180	0.4875	0.0125	150
5 wt%	0.665	0.035	200	0.475	0.025	150
10 wt%	0.63	0.07	270	0.45	0.05	180
20 wt%	0.56	0.14	400	0.4	0.1	340

To assure consistency between samples, the dry powder of MTA and BD was reweighed, before mixing, to exact 0.5 g and 0.7 g, respectively, as weight variations between MTA pouches and BD capsules were observed. The manufacturer liquid for both materials was measured and dispensed in microlitres. Powder weighing 0.7 g of the unmodified Biodentine™ (BD-P) was mixed with 180 µL of the manufacturer Biodentine liquid (BD-L [5 drops of Biodentine liquid = 180 µL]). While 0.5 g of ProRoot MTA powder (MTA-P) was mixed with 150 µL of sterile water (MTA-L [1 ampoule of water = 150 µL]). Incorporating 10 wt% and 20 wt% of chitosan powder (CS-P) required higher volumes of MTA-L and BD-L to triturate the new composite. Control; unmodified commercial materials.

4.3.5 Investigating the antimicrobial efficacy of Biodentine ± chitosan with different molecular weights against the interkingdom biofilm model

The effect of 0.5 wt% and 1 wt% of high, medium and low molecular weights of chitosan powder (Sigma-Aldrich, St. Louis, MO, USA) on the antimicrobial efficacy of BD were assessed against the regrowth of 4-species biofilms (Table 4.3). The material discs were prepared, as shown in Table 4.2, and then disinfected using the UV for 15 minutes. The composition of the regrown biofilms on BD discs was assessed using live/dead PCR, and the pH measurements of the material leachate were taken, as previously described in 4.3.4.2.

Table 4.3. Chitosan with low, medium and high molecular weights used in this study.

Description	Biological source	Molecular weight	DDA
CS-LMW	Animal origin	50,000-190,000 Da	75-85%
CS-MMW	Animal origin	190,000-310,000 Da	75-85%
CS-HMW	Animal origin	310,000-375,000 Da	>75%

DDA; Degree of deacetylation.

4.3.6 Statistical analysis

Graphs, data distribution and statistical analysis were performed using GraphPad Prism version 9. Data distributions were assessed before analysis using a D' Agostino-Pearson omnibus normality test. Kruskal-Wallis with Dunn's tests were used to determine the p values for multiple comparisons when data weren't normally distributed. Mann-Whitney test was used to determine the p values for two comparisons with non-parametric data. Differences were considered statistically significant if $p < 0.05$. Error bars represent standard deviations.

4.4 Results

4.4.1 Assessing antimicrobials within the optimised endodontic biofilm model in microtiter plates

The susceptibility of planktonic *C. albicans* mono-species and co-cultured microorganisms to the active compounds was assessed, and the MICs of the antimicrobials were determined as shown (Table 4.4).

Table 4.4. Effect of different actives on planktonic *C. albicans* and mixed (4 species) microorganisms.

	CHX (%)	EDTA (%)	CS-MMw (mg/mL)
C. albicans	0.0004	0.266	0.35
4-species (mixed)	0.0004	0.266	0.35

Susceptibility of planktonic *C. albicans* and mixed microorganisms (bacteria + *C. albicans*) to CHX, EDTA and chitosan (MMw). Data are representative of three technical repeats from three independent repeats. Numbers represent P-MIC values.

The optimised biofilm model was assessed with three antimicrobials: two conventional endodontic compounds and one novel therapeutic (CS-MMw). For these sets of *in vitro* antimicrobial testing experiments, a 1:1 mixture of RPMI/THB was supplemented with and without 10% FBS to ensure that FBS did not adversely affect the efficacy of the antimicrobial challenge. In an attempt to mimic endodontic treatment regimens, biofilm testing involved either direct treatment of a biofilm with the chosen compound (termed 'treatment'), or mechanical disruption of the biofilm, prior to regrowth experiments in pre-treated culture plates containing the actives (termed 'prevention'), or mechanical disruption of the biofilm, prior to regrowth experiments in pre-treated culture plates after discarding the active compounds (termed 'adsorption'). In the 'treatment' studies, the metabolic activity results indicated that both CHX and CS-MMw were equally effective and significantly reduced the metabolic activity of biofilms grown in the RPMI/THB media supplemented with and without FBS (> 99%, **** $p < 0.0001$), when compared to the positive control. In contrast, EDTA did not significantly reduce the metabolic activity of the biofilm following treatment (Figure 4.1A,D). All the three compounds, in the 'prevention' studies, were effective in reducing the metabolic activity of the regrown biofilms in the presence and absence of FBS (CHX and CS-MMw **** p <

0.0001; EDTA ** $p < 0.01$), as shown (Figure 4.1B,E). Notably, no detectable fluorescens were recorded for chitosan-treated biofilms in the presence of FBS. In the 'adsorption' studies, CS-MMw was not effective in reducing the level of metabolic activities. In contrast, CHX and EDTA reduced the metabolic activity, significantly (CHX **** $p < 0.0001$) as shown (Figure 4.1C,F). All reductions percentages are presented in Table 4.5.

Assessment of antimicrobial activity showed significant effectiveness of each antimicrobial, irrespective of serum. The three actives were most efficient against the prevention biofilm model, where the greatest reduction was observed for chitosan-treated biofilms.

Table 4.5. Percentage reductions of the metabolic activity of the regrown biofilms treated with CHX (0.2%), EDTA (230 mM) and CS-MMw (0.7 mg/mL).

Reduction	**Treatment**			**Prevention**			**Adsorption**		
(%) *	CHX	EDTA	CS	CHX	EDTA	CS	CHX	EDTA	CS
+ FBS	99.73	72.64	99.67	99.86	99.18	100	99.79	94.13	4.07
- FBS	99.87	57.32	99.99	99.21	98.77	99.65	96.04	77.08	0

Biofilms were grown in 1:1 RPMI/THB ± FBS. * Average reduction % of mixed-species biofilms treated with different actives. Data are representative of three technical repeats from three independent repeats.

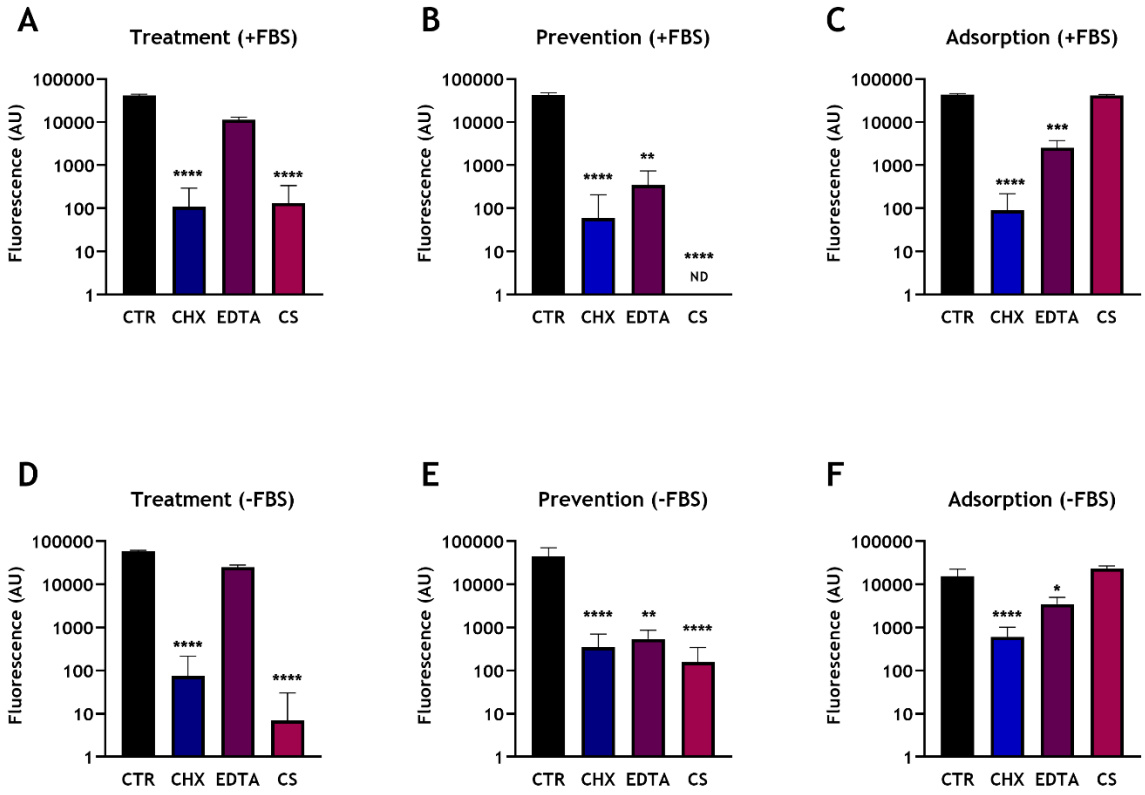

Figure 4.1. Assessing biofilm viability following treatment with conventional and novel endodontic therapies. Biofilms were grown for 24 h in 1:1 RPMI/THB ± 10% FBS in 24-well flat-bottom plates. After incubation, biofilms grown in the 'treatment' group **(A & D)** were treated with CHX (0.2%), CS-MMw (0.7 mg/mL) and EDTA (230 mM). Biofilms in the 'prevention' group **(B & E)** were disrupted first by scraping into RPMI/THB ± 10% FBS media, then diluted to 1:5 with fresh media. The diluted samples were then inoculated into a new 24-well tissue culture plate containing each antimicrobial test agent adjusted to twice the desired above concentrations to obtain a 1:10 cell dilution and final concentrations of chlorhexidine (0.2%), chitosan (0.7 mg/mL) and EDTA (230 mM). For the 'adsorption' group **(C & F)**, a new 24-well plate was pre-treated overnight of active agents in the desired above concentrations. The biofilms were disrupted and then diluted to 1:10 in the relevant media. The diluted samples were then inoculated into the pre-treated 24-well tissue culture plate after discarding antimicrobial test agents. After 24 h incubation, the metabolic activity was measured by the Alamar Blue assay. Each bar represents the mean of data obtained from three technical repeats of three independent experiments. The mean of each column was compared with the mean of the control group (CTR). Data were analysed by Kruskal–Wallis with Dunn's tests. * Indicates statistically significant differences (** $p < 0.01$, **** $p < 0.0001$). Error bars represent standard deviations.

Based on the previous results, the regrowth 'prevention' model was chosen from the above platforms for future experiments, to recapitulate biofilm regrowth following chemo-mechanical means of disinfections. The antimicrobial effect of the three therapeutics on the regrown mixed-species biofilms were further assessed using qPCR. The results indicating that all treated and untreated biofilms were dominated by *S. gordonii* followed by *C. albicans* (Figure 4.2). However, it seems that regrowth of *C. albicans* was most affected following treatment with the three actives. Total CFE counts for the treated biofilms were all reduced compared to the positive control (untreated biofilms). The greatest reduction was observed for chitosan-treated biofilms (**** $p < 0.0001$). Chitosan (0.7 mg/mL) reduced the total CFE by 99.82% in media supplemented with FBS from 2.15×10^8 CFE/mL to 3.75×10^5 CFE/mL. A reduction in CFE counts by 99.94% was also observed for chitosan-treated biofilms in media without FBS supplementation, with treatment reducing the microbial burden from 4.37×10^8 CFE/mL in untreated to 2.74×10^5 CFE/mL in treated biofilm. Following treatment with CHX (0.2%), the microbial burden was reduced to 6.67×10^6 CFE/mL (96.89%) in media supplemented with FBS (** $p < 0.01$). A similar reduction was also observed for CHX-treated biofilms in media without FBS (97.48%). Treatment with EDTA (230 mM) showed the lowest reduction. The total CFE was reduced to 3.17×10^7 CFE/mL (85.24%) and 3.03×10^7 CFE/mL (93.07%) in the presence and absence of FBS, respectively (Figure 4.2), with no significant differences compared to the control. All % changes of the four microorganisms are shown (Table 4.6).

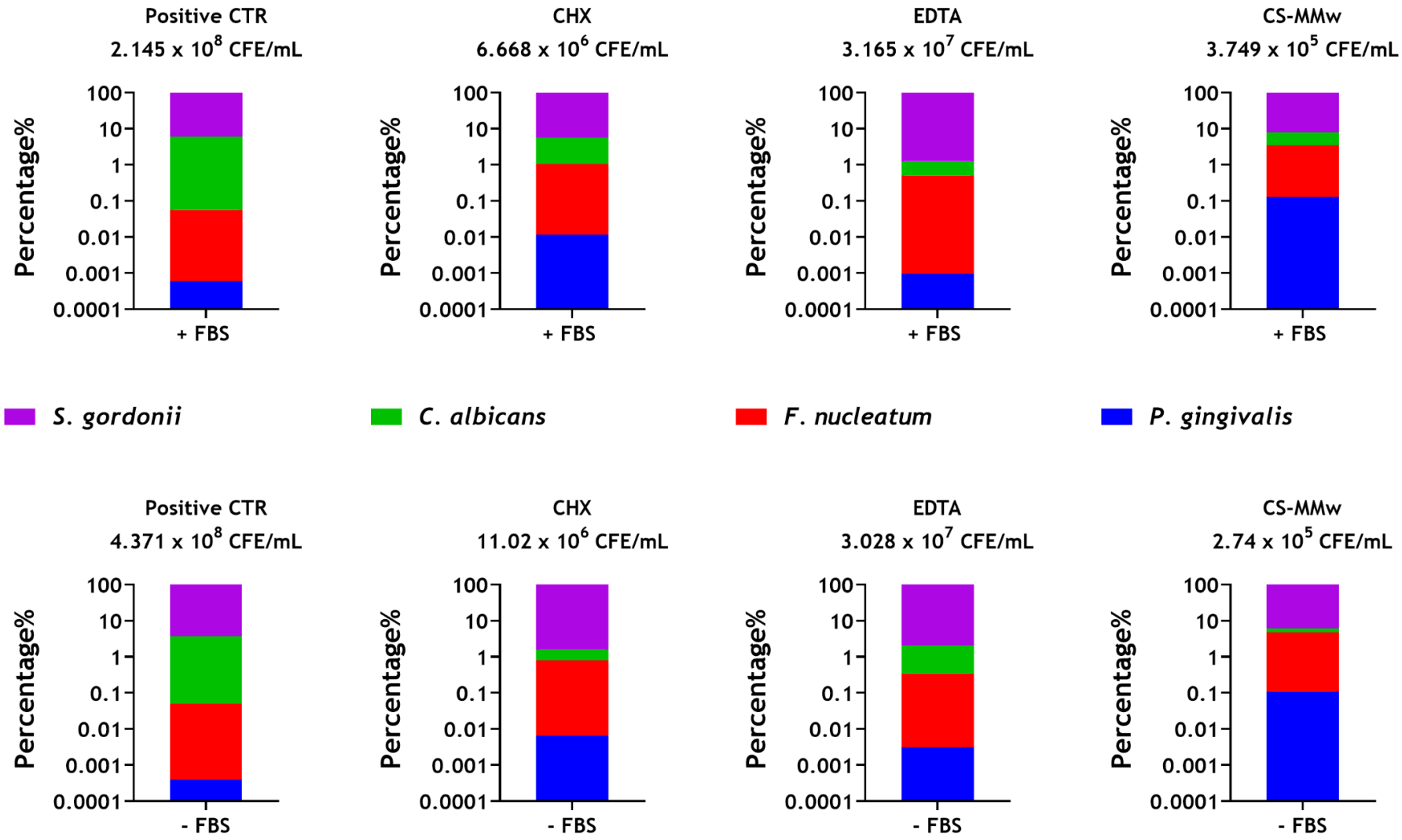
Positive CTR
2.145 x 10^8 CFE/mL
CHX
6.668 x 10^6 CFE/mL
EDTA
3.165 x 10^7 CFE/mL
CS-MMw
3.749 x 10^5 CFE/mL
Percentage%
100
10
1
0.1
0.01
0.001
0.0001
+ FBS
S. gordonii
C. albicans
F. nucleatum
P. gingivalis
Positive CTR
4.371 x 10^8 CFE/mL
CHX
11.02 x 10^6 CFE/mL
EDTA
3.028 x 10^7 CFE/mL
CS-MMw
2.74 x 10^5 CFE/mL
- FBS

Figure 4.2. Compositional analyses of re-grown multispecies biofilms in RPMI/THB ± 10% FBS. Biofilms in the 'prevention' group as described in Figure 4.1 were processed for DNA extraction prior to composition analyses via qPCR. In brief, once biofilms formed in 6-well culture plates after 24 h incubation, biofilms were disrupted, diluted to 1:5, then transferred to fresh 6-well plates containing test agents adjusted to twice the desired concentrations, to obtain a 1:10 cell dilution and final concentrations of CHX (0.2%), CS-MMw (0.7 mg/mL), and EDTA (230 mM). Plates were cultured for 24 h to permit biofilm regrowth before DNA extraction. Average % composition is shown in the bar graphs. Raw data were analysed by Kruskal–Wallis with Dunn's tests. The mean of each treatment was compared with the mean of the control group (CTR). Positive control biofilms (CTR) received no treatment during regrowth. CHX and CS-MMw, in both media, inhibited the biofilms significantly (** $p < 0.01$; **** $p < 0.0001$), respectively, compared to the control. Data are representative of biofilms from three independent repeats (three technical replicates in each experiment).

Table 4.6. Percentage composition of the mixed-species biofilm model following 'prevention' treatment.

	Percentage composition (%)*							
	S. gordonii		*C. albicans*		*F. nucleatum*		*P. gingivalis*	
	- FBS	+ FBS	- FBS	+ FBS	- FBS	+ FBS	- FBS	+ FBS
Positive CTR	96.30	93.98	3.65	5.96	0.05	0.06	0.0004	0.001
CHX	98.41	94.36	0.78	4.61	0.79	1.02	0.006	0.011
EDTA	97.91	98.73	1.74	0.76	0.38	0.51	0.003	0.001
CS-MMw	93.85	92.10	1.35	4.42	4.68	3.36	0.110	0.130

* Average percentage composition of each of the four microorganisms shown in Figure 4.2.

These compositional analyses showed subtle fluctuations in the proportion of each microorganism in the mixed-species biofilms following treatment (Figure 4.2), where *C. albicans* was most affected to treatment with the three actives, and chitosan was the most effective active (3 log reduction). From here, the chitosan biomaterial was selected for further investigation using the regrowth 'prevention' model.

Next, we examined the susceptibility properties of mixed fungal/bacterial species (4 species) as compared to mono-species biofilms formed on microtiter 24-well plates, grown in RPMI/THB and mechanically disrupted, against the previously prepared solubilised chitosan, as described above in the 'prevention' model, using Alamar blue and crystal violet assays. The results indicated that both *F. nucleatum* and *P. gingivalis* positive control biofilms displayed minimal metabolic activity and biomass. However, significant reductions in the reading of both assays (**** $p < 0.0001$) were observed in mono-species (*S. gordonii* and *C. albicans*) and mixed species (4 species) when compared to the positive controls (Figure 4.3).

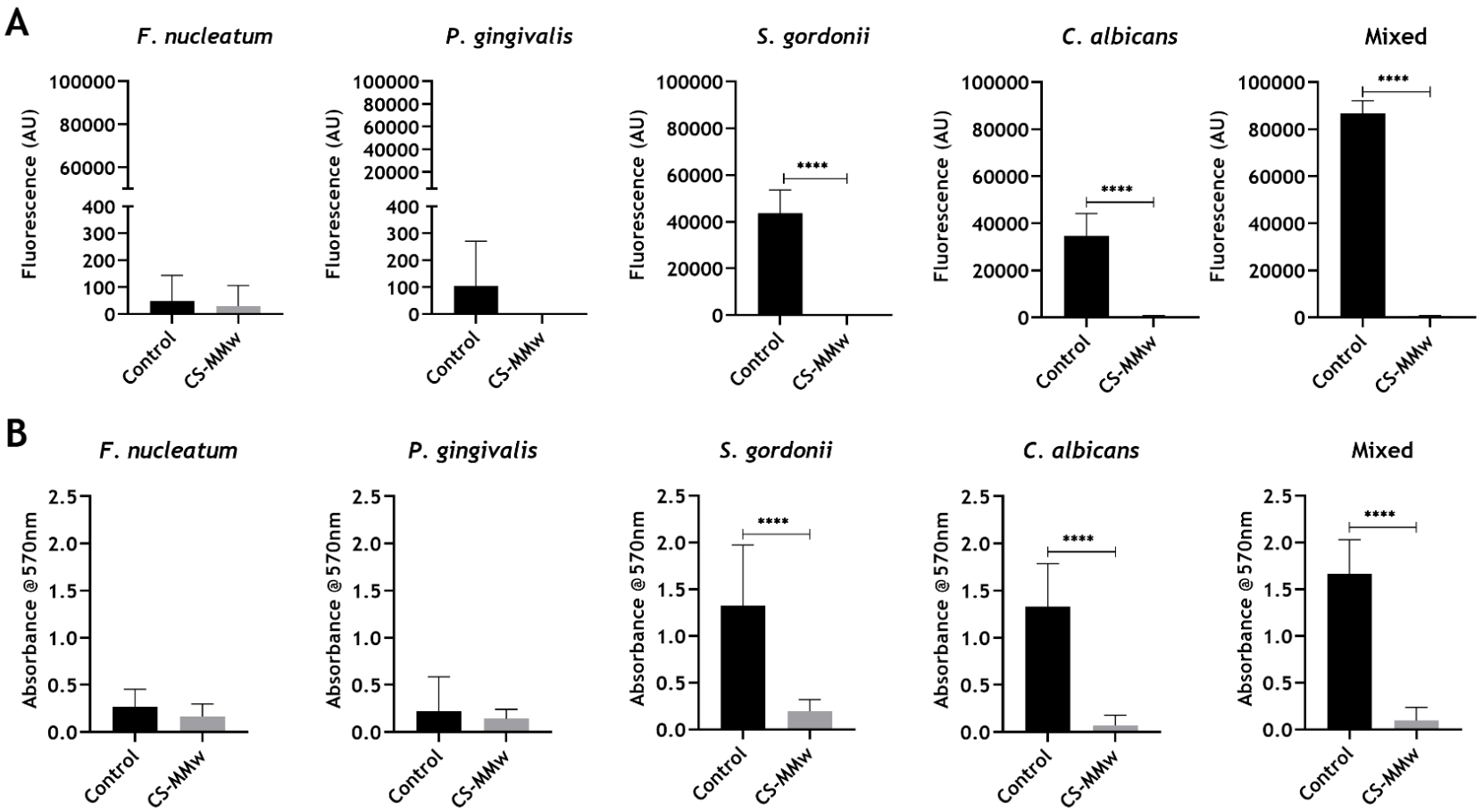

Figure 4.3. Metabolic activity and biomass of the regrown biofilms of single and multispecies biofilms after 24 h of chitosan treatment. (A) Metabolic activity was measured by Alamar Blue. **(B)** Biomass was quantified by crystal violet. Each bar represents the mean of data. Error bars represent standard deviations. Data were analysed by Mann-Whitney test. * Indicates statistically significant differences (**** $p < 0.0001$). Data are representative of three technical repeats from three independent experiments. CS-MMw; chitosan medium molecular weight (0.7 mg/mL).

4.4.2 *In vitro* biofilm susceptibility testing on bovine dentine discs

The optimised biofilm model was grown on a biologically relevant substrate (bovine dentine) to further mimic interactions between microorganisms and the host in endodontic infections. A similar experimental setup was used, as described for the 'prevention' studies. Results indicated that biofilms were similarly dominated by *S. gordonii* followed by *C. albicans*. The solubilised chitosan was similarly effective in inhibiting biofilm regrowth on the dentine substrate. There were significant reductions in the total CFE/mL of the mixed-species biofilms compared to the control (**** $p < 0.0001$). The compositional changes of the biofilm indicated that chitosan preferentially targeted and reduced the level of *C. albicans* from 14.45% to 3.48% (Figure 4.4), which is in line with the previous results in Figure 4.2.

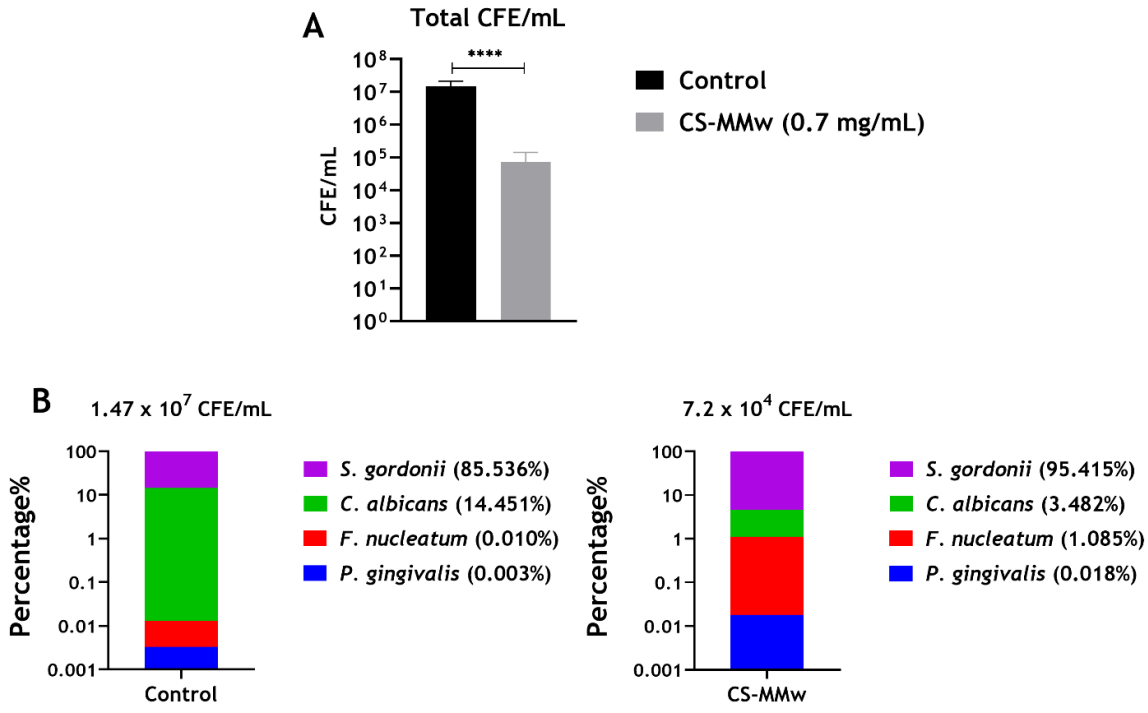

Figure 4.4. Compositional analysis of regrown multispecies biofilms on bovine dentine discs following treatment with chitosan. Biofilms were grown in 1:1 RPMI/THB in 24-well plates for 24 h. After incubation, the biofilms were disrupted and diluted to 1:5 with fresh media and then seeded on pre-sterilised bovine dentine discs, placed in a 24-well plate and treated with chitosan adjusted to twice the desired concentration, to get a concentration of chitosan at 0.7 mg/mL. Following additional 24 h incubation, the total CFE/mL **(A)** and the composition of the regrown biofilms **(B)** were assessed using qPCR. Data are representative of three technical repeats from three independent experiments. Data were analysed by the Mann-Whitney test. * Indicates statistically significant differences (**** $p < 0.0001$). Each bar represents the mean of data. Error bars represent standard deviations. CS-MMw; chitosan medium molecular weight.

The results in Figure 4.4 were further demonstrated by SEM analysis (Figure 4.5). No microorganisms were evident within the dentine after sterilisation. Biofilm ultrastructure and architecture of the regrowth biofilm on dentine following chitosan treatment were observed using SEM. The positive control showing a network of yeast and hyphal elements, co-aggregated with clusters of bacterial cells. These aggregates were predominantly comprising of cocci-shaped colonies of streptococci. For a chitosan-treated sample, a great reduction of biofilms was observed compared to the positive control.

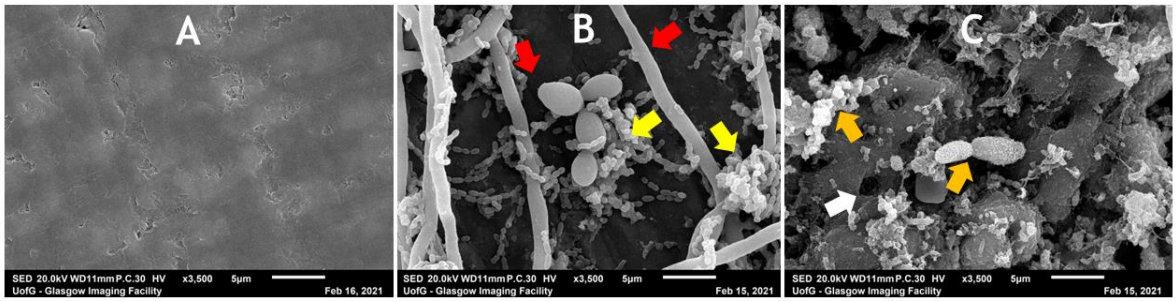

Figure 4.5. Scanning electron microscopy images of regrowth mixed-species biofilms on bovine dentine discs. The biofilms grown in the previous experiment (Figure 4.4) were imaged. Biofilms were fixed, processed and imaged. **(A)** A transverse cross-section of bovine dentine (negative control). **(B)** Biofilm model untreated (positive control). Networks of yeast and hyphal elements (red arrows). Clusters of bacteria predominantly streptococci (yellow arrows). **(C)** Biofilm model treated with chitosan (0.7 mg/mL). Orange arrows indicate biofilm remains. Scale bar represents 5 µm at ×3,500 magnification. Samples were processed by Mr. Mark Butcher. Images were taken by Mrs. Margaret Mullin (University of Glasgow).

4.4.3 Unmodified calcium silicate-based materials demonstrate no antibiofilm activity in comparison to dentine against 4-species biofilms

The regrowth of four mixed-species (*S. gordonii*, *P. gingivalis*, *F. nucleatum* and *C. albicans*) biofilms on ProRoot MTA and BD discs were explored using live-dead qPCR. These were compared to regrowth on dentine discs.

The results highlighting that neither material showed the ability to inhibit the regrowth of the biofilms, after 24 h of incubation (Figure 4.6). The results also indicated that Biodentine substrate retained the highest microbial CFE/mL numbers, followed by MTA. All biofilms grown on dentine and the materials were

dominated by *S. gordonii*, followed by *C. albicans*. Percentage composition (%) of the mixed-species biofilm model is shown in Table 4.7.

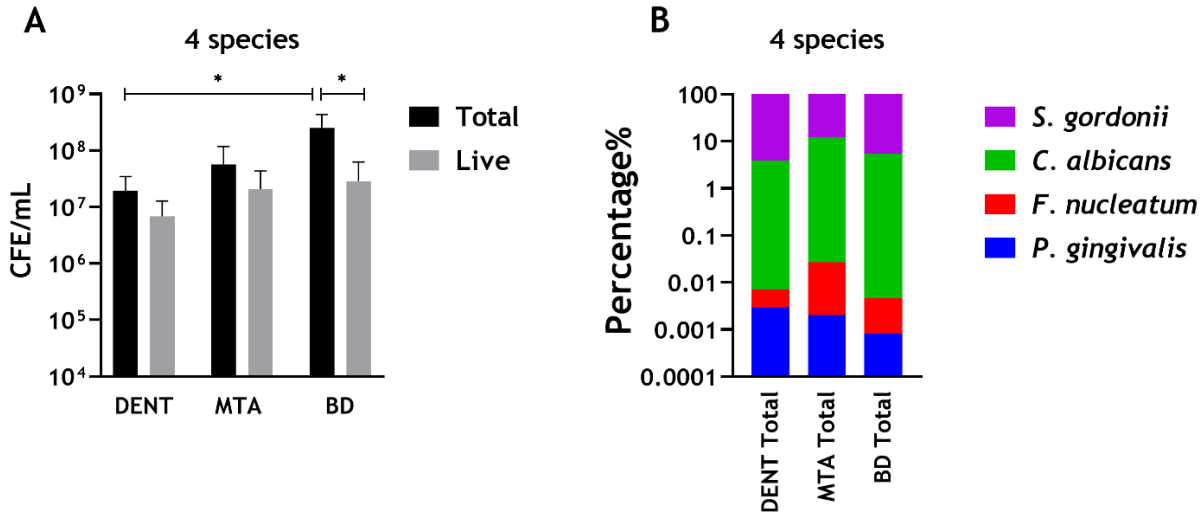

Figure 4.6. Compositional analysis of regrown mixed-species biofilms on MTA, Biodentine and pre-sterilised bovine dentine discs. All biofilms were formed in RPMI/THB in 24-well plates for 24 h. Following incubation, biofilms were mechanically disrupted and diluted to 1:10 and then inoculated on the three substrates. Plates were then incubated for additional 24 h to allow biofilm regrowth. After incubation, the composition of the regrown biofilms was assessed using live/dead qPCR. **(A)** Total and live CFE/mL of mixed biofilms (the bacterial and fungal loads were quantified using 16S and 18S primers, respectively). **(B)** The composition (%) for each microbial species was also calculated. Data were analysed by Kruskal–Wallis with Dunn's tests to determine the p values for non-parametric multiple comparisons. * Indicates statistically significant differences (* $p < 0.05$). Each bar represents the mean of data. Error bars represent the standard deviations. Data are representative of biofilms from three independent repeats with three technical replicates. DENT; Dentine, MTA; ProRoot mineral trioxide aggregate, BD; Biodentine.

Table 4.7. Percentage composition (%) of 4-species biofilms grown on dentine, MTA and Biodentine.

	Percentage composition % *			
	P. gingivalis	*F. nucleatum*	*C. albicans*	*S. gordonii*
Dentine	0.003	0.004	3.849	96.144
MTA	0.002	0.025	12.089	87.884
Biodentine	0.001	0.004	5.425	94.571

* Average percentage composition of each of the four microorganisms in the mixed-species biofilm model (total CFE/mL) shown in Figure 4.6.

The 1-species (*C. albicans*) and 4-species (mixed) models were grown on bovine dentine, MTA and BD discs. Confocal microscopy was used to explore the biofilm regrowth on different substrates. Mixed biofilm grown on a dentine surface showed a network of hyphae with aggregates of bacteria scattered around the hyphae (Figure 4.7A). For *C. albicans* mono-species, fewer hyphae appeared on dentine substrate when compared to the *C. albicans* co-culture (Figure 4.7C). With the MTA substrate, a dense network of fungal hyphae and bacterial aggregates were visualised within the mixed-species biofilms (Figure 4.7B). However, contrastingly, the picture for mono-species *C. albicans* demonstrated a distinctly denser *C. albicans* biofilm colonising the MTA surface (Figure 4.7D). It was not possible to image the biofilms formed on a Biodentine substrate. Heavy precipitates observed on the BD surface after incubation may have prevented visualisation of formed biofilms. However, the live/dead staining assay confirmed the ineffective ability of both materials in inhibiting biofilm regrowth.

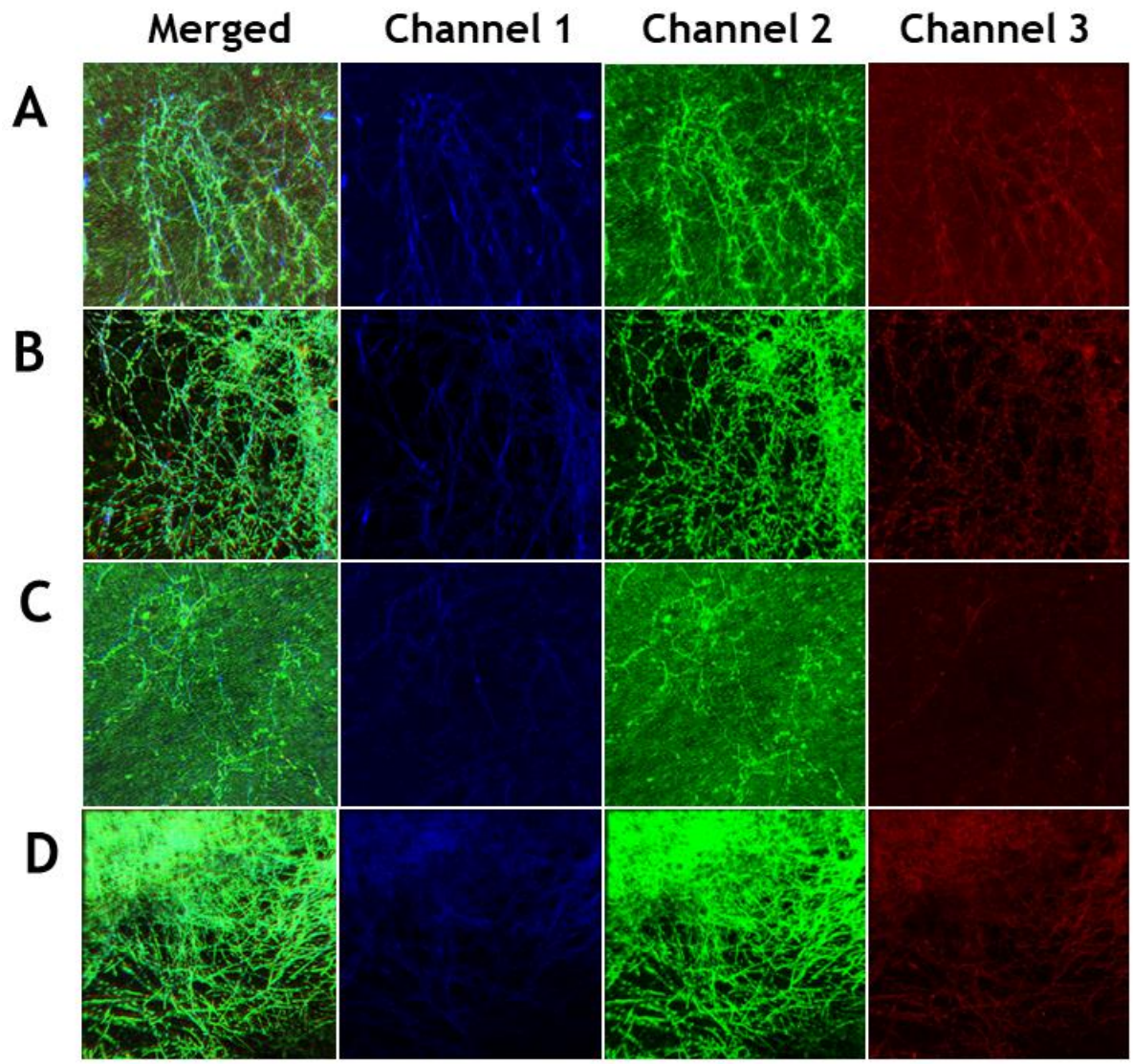

Figure 4.7. Confocal imaging for biofilms grown on dentine and MTA discs. (A) 4-species model—Dentine, **(B)** 4-species model—MTA, **(C)** 1-species model—Dentine, **(D)** 1-species model—MTA. Calcofluor white stained the cell wall of fungi in blue (Channel 1), SYTO™ 9 stained total *Candida* and bacterial cells in green (Channel 2), and dead cells were stained by propidium iodide in red (Channel 3). 1-species model (*C. albicans*), 4-species model (*F. nucleatum*, *P. gingivalis*, *S. gordonii* and *C. albicans*). Samples were imaged by Dr Jason Brown (University of Glasgow).

4.4.4 Addition of chitosan microparticles confers antimicrobial properties on Biodentine, but not MTA, against 4-species biofilms

The effects on regrowth of three biofilm models were assessed following the addition of CS-MMw powder to each calcium-silicate cement (ProRoot MTA and Biodentine), using live/dead qPCR techniques. Firstly, biofilm regrowth on the unmodified materials and interkingdom interactions were assessed. It was evident that neither unmodified MTA nor BD showed an ability to inhibit biofilm regrowth of any of the biofilm models after 24 h of incubation, compared to the control dentine discs (Figure 4.8A-C). Notably, the colony-forming equivalent (CFE) for *C. albicans* and bacteria formed on controls (dentine discs) were approximately 1 × $\log_{10}$ less, when compared with colonies formed on the tested materials, although this did not reach statistical significance for viable cells.

When determining the potential effect of interkingdom interactions, there was approximately a 3.5-fold increase in viable bacteria when *C. albicans* was present on a dentine substrate (4.28 × 10^5 compared to 1.48 × 10^6), while on BD, a much smaller 1.4-fold increase was apparent with respect to bacterial numbers in the absence of *C. albicans*. Meanwhile, no change was noted for bacterial loads on an MTA substrate (Figure 4.8D). The results indicate that inclusion of *C. albicans* may support bacterial biofilm formation on a biological substrate. However, there were no or little supportive effects of *C. albicans* on bacterial numbers on abiotic surfaces. In contrast, on a dentine substrate, viable *C. albicans* showed a slight 1.2-fold increase when bacteria were incorporated, while an approximate 2–fold decrease was found in *C. albicans* CFE when grown on MTA and BD in the presence of bacteria (Figure 4.8D). These findings are in agreement with the confocal images (Figure 4.7) whereby bacteria might support hyphae formation on dentine while inhibiting *C. albicans* hyphae on an MTA substrate. These results might suggest some level of interkingdom antagonistic interactions with bacteria inhibiting *C. albicans* on abiotic surfaces. Total and live CFE counts for all biofilms and biofilm composition (%) for bacteria and *C. albicans* in each mixed biofilm are shown in Table 4.8.

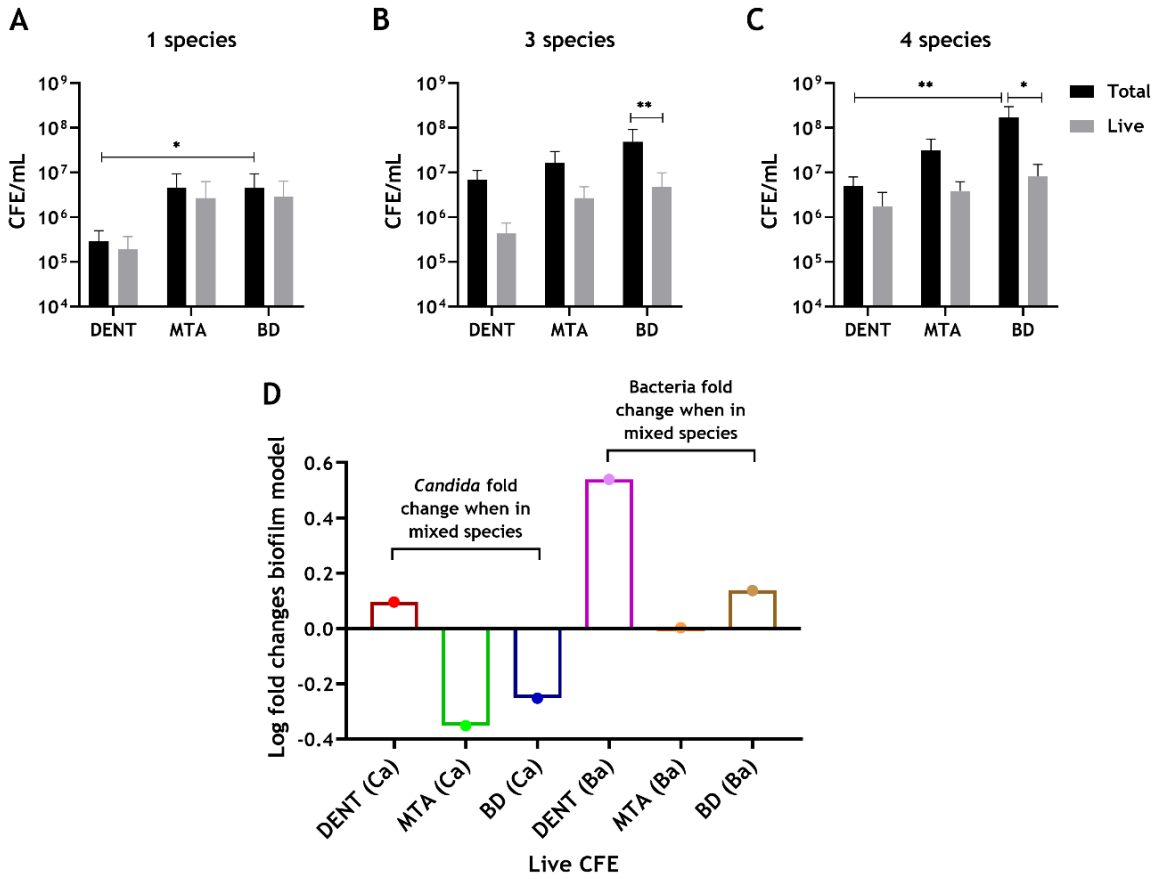

Figure 4.8. Compositional analysis of regrown mono-species, bacterial and mixed biofilms on MTA, Biodentine and dentine discs. All biofilms were grown and assessed using live/dead qPCR. **(A)** Total and live CFE/mL of *C. albicans*-only biofilms. **(B)** Total and live CFE/mL of 3-species bacterial-only biofilms (*S. gordonii*, *P. gingivalis* and *F. nucleatum*). **(C)** Total and live CFE/mL of mixed biofilms (bacteria and *C. albicans*). **(D)** Log fold changes of live yeast and bacteria in the complex 4-species biofilm model on three different substrates. *C. albicans* and bacteria were quantified (CFE/mL) in mixed-species biofilms (4 species) and compared to simpler models of *C. albicans*-only biofilms (1 species) and bacterial-only biofilms (3 species), respectively. Log fold changes were calculated and presented graphically. Data were analysed by Kruskal–Wallis with Dunn's tests. Differences were considered statistically significant when $p < 0.05$. * Indicates statistically significant differences (* $p < 0.05$, ** $p < 0.01$). Each bar represents the mean of data. Error bars represent the standard deviations. Data are representative of biofilms from three independent repeats with three technical replicates. *Ca*; *C. albicans*, Ba; bacteria, DENT; Dentine. MTA; ProRoot mineral trioxide aggregate, BD; Biodentine.

Table 4.8. Total and live CFE/mL for biofilms and the percentage composition for bacteria and *C. albicans*.

	4-species model				**3-species model**	**1-species model**
	Bacteria	(%) *	*C. albicans*	(%) *	Bacteria	*C. albicans*
Dentine (Total)	4.54×10^6	90.21	4.92×10^5	9.79	6.84×10^6	2.85×10^5
Dentine (Live)	1.48×10^6	86.04	2.40×10^5	13.96	4.28×10^5	1.93×10^5
MTA (Total)	2.90×10^7	92.0	2.53×10^6	8.0	1.63×10^7	4.62×10^6
MTA (Live)	2.696×10^6	69.17	1.20×10^6	30.83	2.68×10^6	2.70×10^6
BD (Total)	1.66×10^8	97.01	5.10×10^6	2.99	4.90×10^7	4.52×10^6
BD (Live)	6.60×10^6	80.16	1.63×10^6	19.84	4.81×10^6	2.92×10^6

***** Average percentage composition of bacteria and *C. albicans* in the mixed-species (4 species) biofilms, shown in Figure 4.8.

The potential for the use of enhanced filling materials to modify biofilm regrowth is a promising strategy. This study aimed to evaluate the antibiofilm efficacy of calcium silicate cements modified with chitosan. The addition of CS-MMw to MTA imparted no or little antimicrobial enhancement against the biofilm models used (Figure 4.9A-C). Interestingly, in multispecies biofilms, CFE counts increased by 54.5% and 22% with the addition of 2.5% and 5% CS-MMw, respectively, when compared to unaltered MTA (Figure 4.9C).

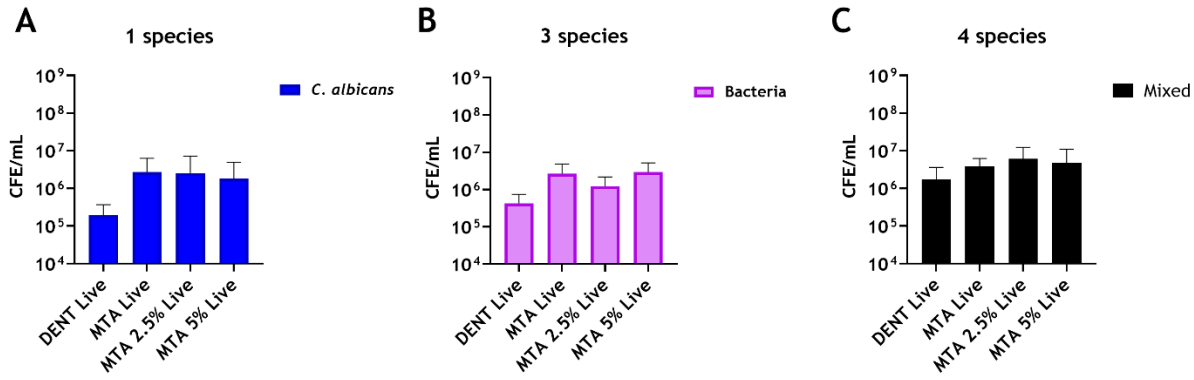

Figure 4.9. Compositional analysis of biofilms on MTA material discs incorporated with chitosan. Live/dead qPCR was conducted following incorporation of 2.5 wt% and 5 wt% of CS-MMw. **(A)** Live CFE/mL of *C. albicans*-only biofilms. **(B)** Live CFE/mL of bacterial-only biofilms. **(C)** Live CFE/mL of mixed biofilms (biofilms containing bacteria and *C. albicans*). The bacterial and fungal loads were quantified using 16S and 18S primers, respectively. Data were analysed by Kruskal-Wallis with Dunn's tests. No significant differences were found between the test groups. Each bar represents the mean of data. Error bars represent the standard deviations. Data are representative of biofilms from three independent repeats with three technical replicates. DENT; Dentine.

In contrast, for Biodentine, when *C. albicans* was grown as a mono-species biofilm, the live CFE/mL following 2.5 wt% and 5 wt% chitosan incorporations was reduced by 83% and 71%, respectively, compared to the unmodified BD. However, this reduction was not to a degree considered statistically significant (Figure 4.10A). In contrast, the addition of 2.5% and 5% CS-MMw reduced the live CFE/mL of three species biofilm model (bacteria only) by 85% and 97%, respectively, from 4.81×10^6 CFE/mL (unmodified material) to 7.12×10^5 and 1.42×10^5 CFE/mL. The microbial reduction was dose-dependent, and the greatest reduction observed at 5% chitosan was significant (** $p < 0.01$). A decrease in bacterial load ($p > 0.05$) by 67% was also observed at 5% compared to the control (bovine dentine) (Figure 4.10B). For the four-species biofilm model, adding 2.5% and 5% CS-MMw to Biodentine was able to effectively reduce live CFE by 56% and 90.5%, respectively, compared to the unaltered BD (Figure 4.10C). The reduction from 8.24×10^6 CFE/mL, in the unaltered material, to 3.6×10^6 and 7.8×10^5 CFE/mL, in the chitosan treated material (2.5% and 5%, respectively) was significant in the 5% added material (** $p < 0.01$). A decrease in the live CFE/mL of the mixed fungal/bacterial biofilm ($p > 0.05$) by 55% was also observed at 5% compared to the control (bovine dentine). Of interest, addition

of chitosan preferentially targeted *C. albicans* in mixed-species biofilms (Figure 4.10D), and a concomitant significant (** $p < 0.01$) inhibition of regrowth of 4-species biofilms was shown. In contrast, at 5% CS-MMw, the reduction of bacterial CFE number was not significant ($p > 0.05$) when *C. albicans* was present (Figure 4.10E). However, in biofilms omitting *C. albicans*, a significant decrease in bacterial load was observed (** $p < 0.01$) at 5% CS-MMw (Figure 4.10B).

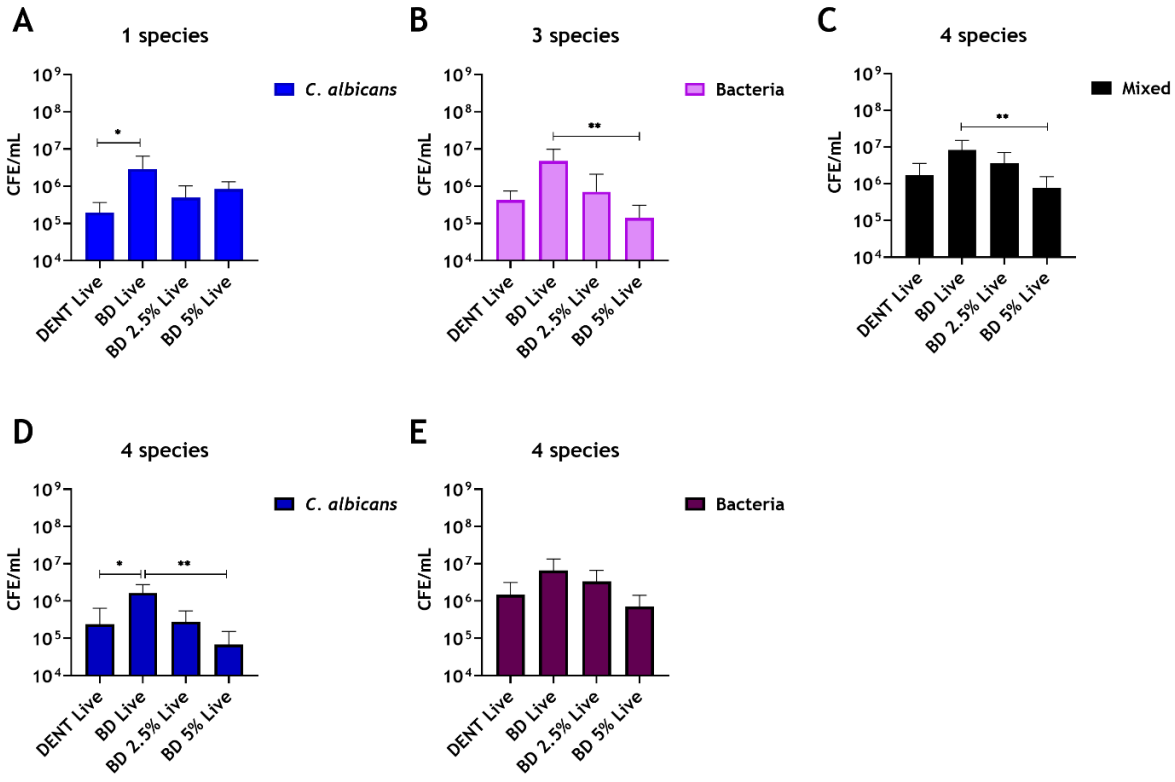

Figure 4.10. Compositional analysis of regrown biofilms on Biodentine incorporated with chitosan. Chitosan (CS-MMw) amounts of 2.5 wt% and 5 wt% were incorporated into Biodentine material, and live/dead qPCR was performed. **(A)** Live CFE/mL of *C. albicans* biofilms. **(B)** Live CFE/mL of bacterial biofilms. **(C)** Live CFE/mL of mixed biofilms (bacteria & *Candida*). **(D)** Live CFE/mL of *C. albicans* in mixed-species biofilms. **(E)** Live CFE/mL of bacteria in mixed-species biofilms. Bovine dentine and unaltered Biodentine discs were used as controls. Data were analysed by Kruskal-Wallis with Dunn's tests. * Indicates statistically significant differences (* $p < 0.05$, ** $p < 0.01$). Data are obtained from three technical repeats of three independent experiments. Each bar represents the mean of data. Error bars represent the standard deviations.

Similarly, the CFE counts of *C. albicans* grown on Biodentine with 2.5% CS-MMw was decreased by approximately 2-fold when the three bacterial species were added. While an approximate 12-fold reduction was noted for *C. albicans* on BD with 5% CS-MMw (8.39×10^5 compared to 6.79×10^4), compared to *C. albicans*

mono-species biofilm, in the presence of bacteria (Figure 4.11). However, the scenario was reversed with 4.7- and 5-fold increases in bacterial numbers observed at 2.5% and 5% CS-MMw, respectively, following inclusion of *C. albicans* (Figure 4.11). Live CFE counts for biofilms grown on BD with 2.5% and 5% chitosan and biofilm composition (%) for bacteria and *C. albicans* in each mixed biofilm are shown in Table 4.9.

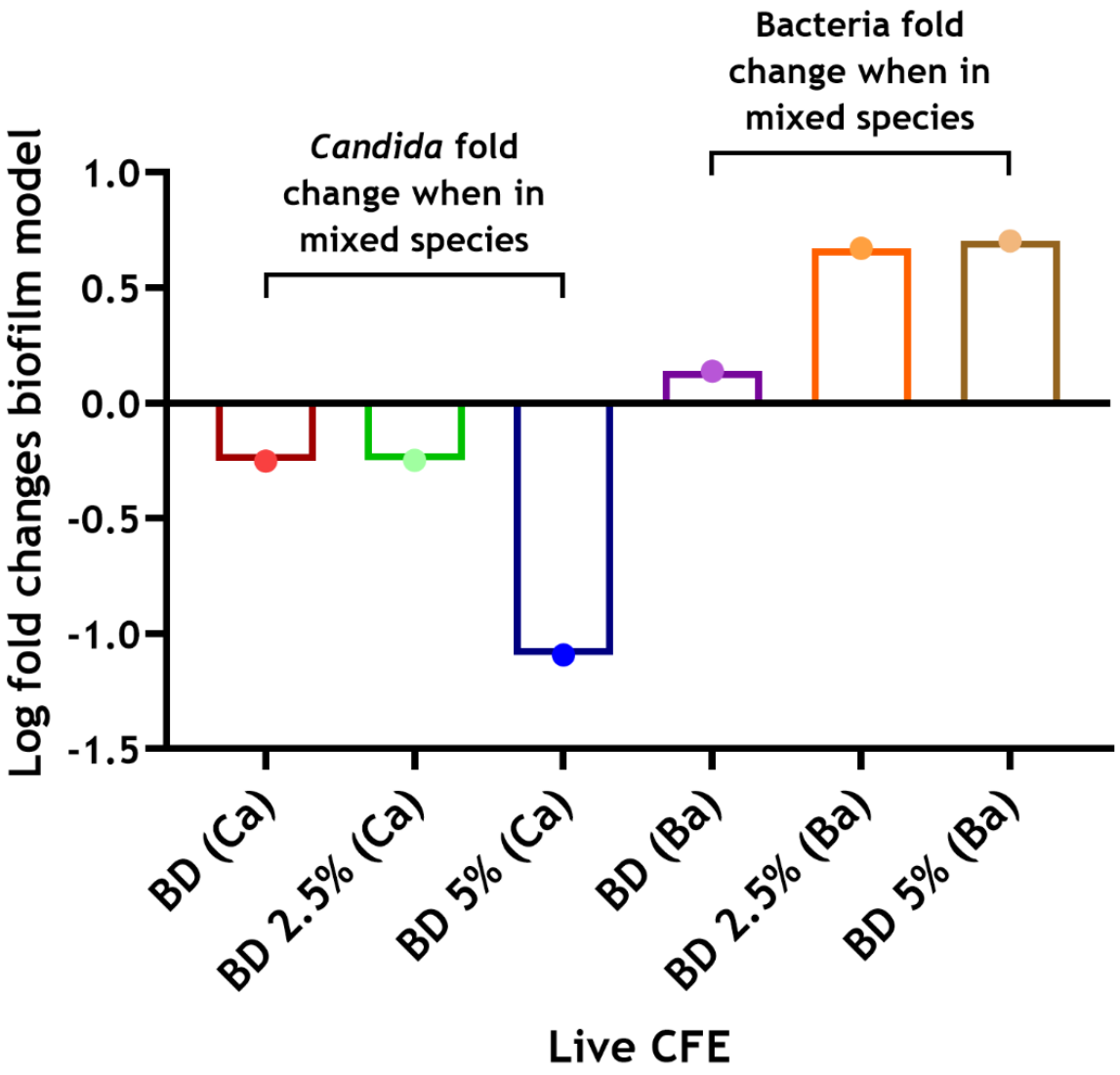

Figure 4.11. Log fold changes of live yeast and bacteria in the 4-species biofilm model on Biodentine discs ± chitosan. *C. albicans* and bacteria were quantified (CFE/mL) in mixed-species biofilms (4 species) and compared to simpler models of *C. albicans*-only biofilms (1 species) and bacterial-only biofilms (3 species), respectively. Log fold changes were calculated and presented graphically. Data are representative of biofilms from three independent experiments with three technical replicates. Each bar represents the mean of data. *Ca*; *C. albicans*, Ba; bacteria.

Table 4.9. Live CFE/mL counts for *C. albicans* and bacteria and percentage composition in all biofilms following biofilm growth on Biodentine discs.

	4-species model				3-species model	1-species model
	Bacteria	(%) *	*C. albicans*	(%) *	Bacteria	*C. albicans*
BD Control	6.60×10^6	80.16	1.63×10^6	19.84	4.81×10^6	2.92×10^6
BD + 2.5 wt% CS	3.33×10^6	92.22	2.8×10^5	7.78	7.124×10^5	4.98×10^5
BD + 5 wt% CS	7.120×10^5	91.30	6.79×10^4	8.70	1.42×10^5	8.39×10^5

***** Average percentage composition of bacteria and *C. albicans* in the mixed-species (4 species) biofilms, shown in Figure 4.10.

4.4.5 Low molecular weight chitosan confers the greatest antimicrobial properties on Biodentine

The quantitative analysis revealed decreases in the live CFE counts of mixed biofilms following incorporation of chitosan powder into BD, compared to the control (unmodified BD). At 0.5 wt% CS, reductions in CFE counts were observed by 79.2%, 89.9% and 90.6% with HMw, MMw and LMw, respectively. Similarly, the live CFE/mL following the addition of 1 wt% CS-HMw, CS-MMw and CS-LMw was reduced by 86.1% and 86.4% and 96.2%, respectively. Notably, the addition of 1 wt% CS-LMw reduced the CFE counts significantly (** $p < 0.01$) from 1.57×10^6 to 5.9×10^4 CFE/mL (Figure 4.12). These data suggest that chitosan low molecular weight showing the greatest antibiofilm potential when compared with the medium and high molecular weights.

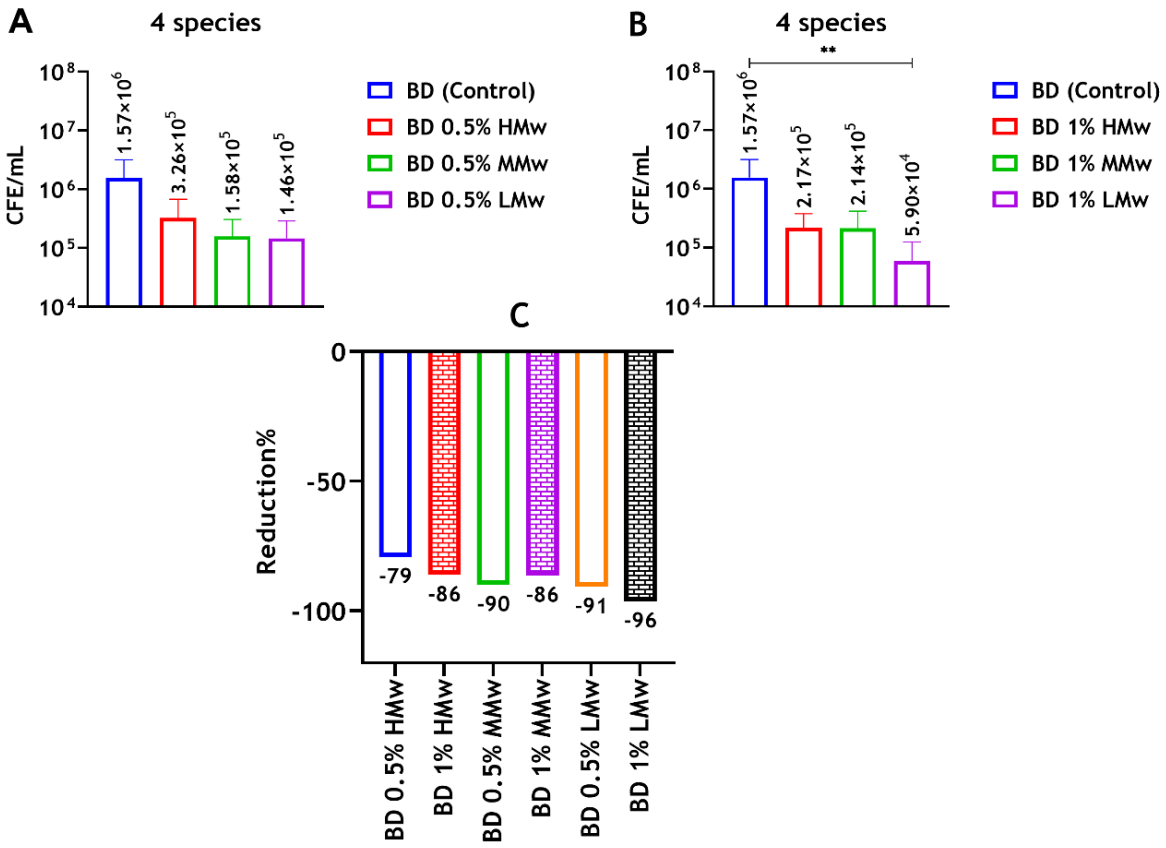

Figure 4.12. Compositional analysis of regrown biofilms on Biodentine incorporated with different molecular weights of chitosan. Chitosan amounts of 0.5 wt% and 1 wt% of high molecular weight (HMw), medium molecular weight (MMw) and low molecular weight (LMw) were incorporated into Biodentine material, and live/dead qPCR was performed. **(A)** Live CFE/mL of 4-species biofilms grown on BD ± 0.5 wt% CS. **(B)** Live CFE/mL of 4-species biofilms grown on BD ± 1 wt% CS. **(C)** Reduction (%) of CFE/mL for each test group compared to the control (unmodified BD). Data were analysed by Kruskal-Wallis with Dunn's tests. * Indicates statistically significant differences between the control and each test group (** $p < 0.01$). Data are representative of biofilms from three repeats with three technical replicates.

4.4.6 Addition of chitosan drives an increase in pH for Biodentine but not MTA

Analysis of pH of leachate was determined for all modified materials and compared with their unmodified counterparts. It has been observed that both unmodified MTA and BD cements exhibited a time-related gradual increase in alkalinity as setting proceeds. The pH values for MTA and BD at 24 h were 12.7 and 11.5, respectively. Elevated pH was determined, particularly, for BD when CS-MMw (2.5-20 wt%) was incorporated, at 1 h, 3 h, 24 h and 7 days. However, the addition of CS-MMw to BD made no difference in pH at 28 days (Figure 4.13).

In contrast, the addition of CS-MMw did not increase the alkalinity of MTA leachate, at timepoints assessed (Figure 4.13). It was also established that the addition of small amounts of different molecular weights of CS (0.5-1 wt%) to BD made no appreciable increase in pH at timepoints assessed (Figure 4.14). The pH of the manufacturer-supplied liquid component was also assessed for BD and was determined to be 3.7. All pH values are presented in Table 4.10.

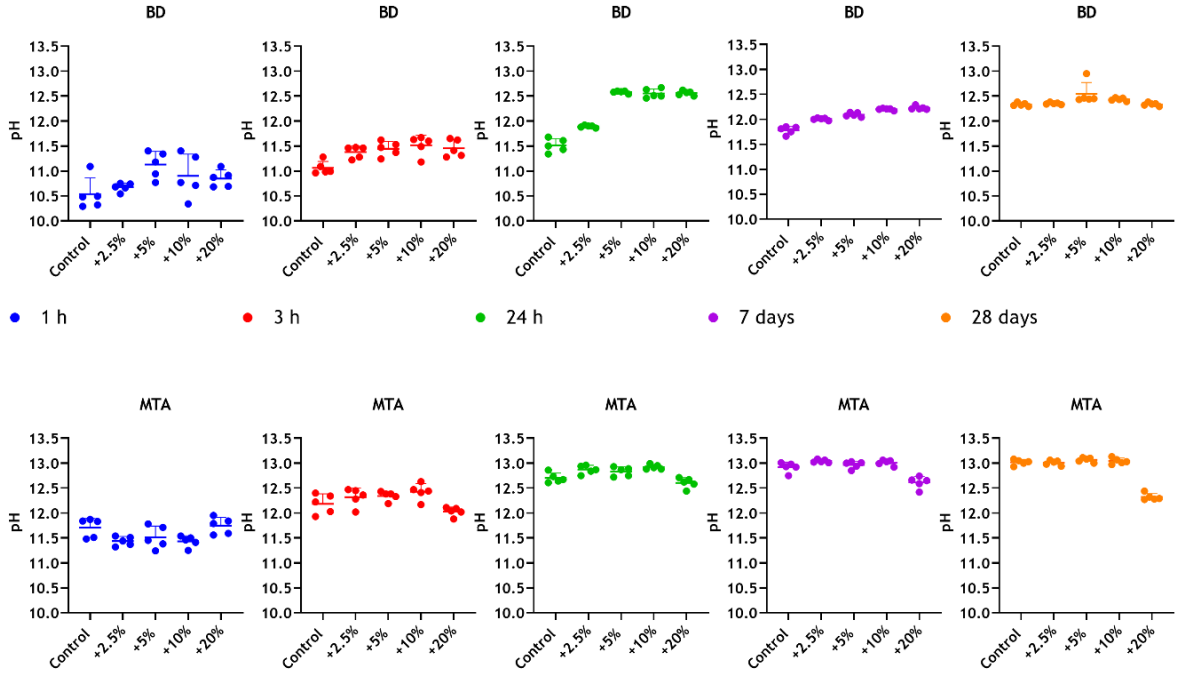

Figure 4.13. pH evaluation of leachate from different calcium silicate materials ± CS-MMw. pH values for distilled water in contact with MTA and Biodentine + 2.5-20 wt% CS-MMw, were determined at 1 h, 3 h, 24 h, 7 days and 28 days. Unmodified materials were used as controls. Each dot represents a material replicate (a total of five replicates per group). Each error bar represents SD.

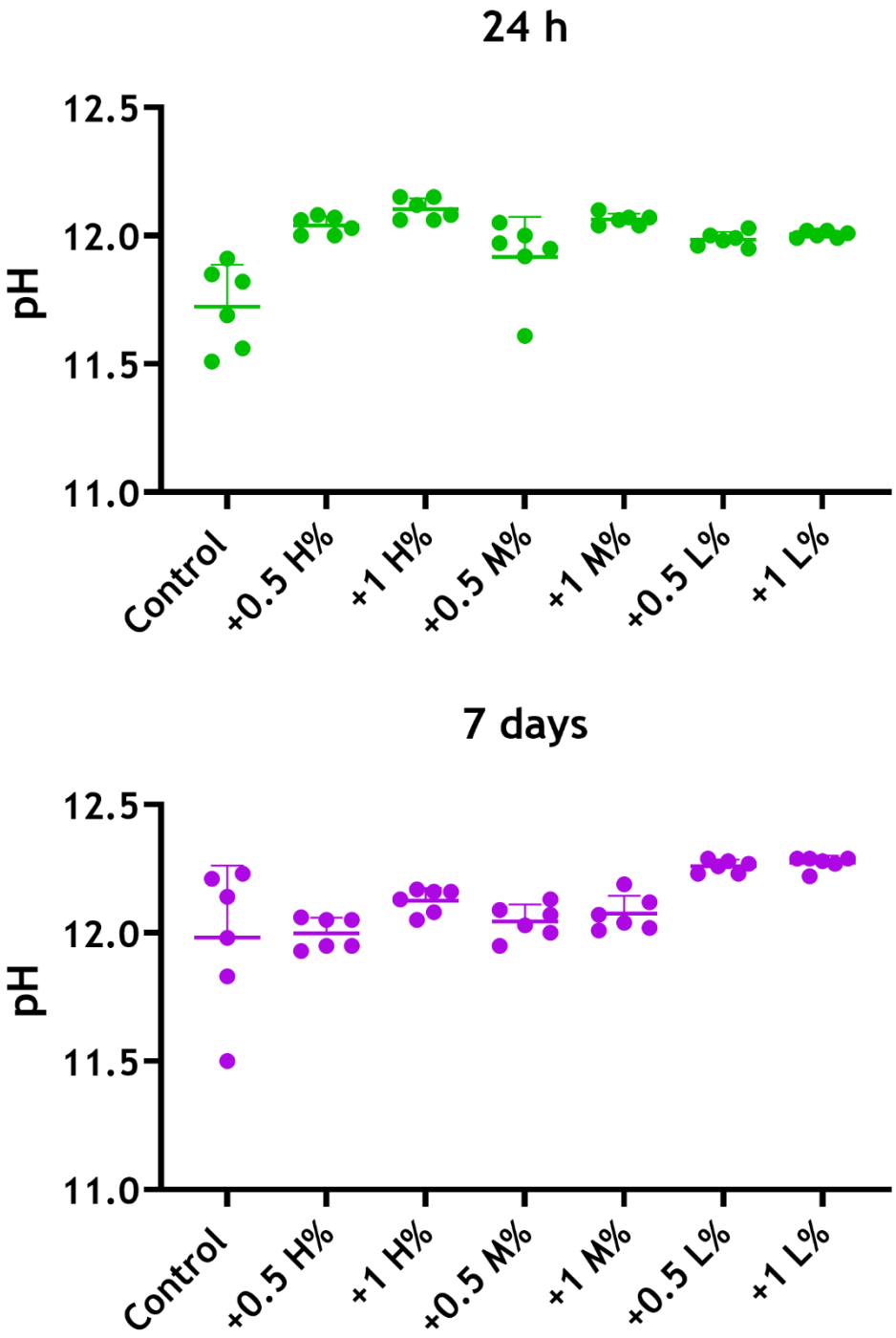

Figure 4.14. pH evaluation of leachate from Biodentine ± chitosan with high, medium and low molecular weights. pH values for distilled water in contact with BD + 0.5-1 wt% CS, were determined at 24 h and 7 days. Unmodified Biodentine was used as a control. Each dot represents a replicate (a total of six replicates per group). Each error bar represents SD. H; CS-HMw, M; CS-MMw, L; CS-LMw.

Table 4.10. pH values of leachate from MTA and Biodentine materials ± chitosan

Materials ± CS-MMw	Biodentine liquid pH = 3.7				
	1 h	**3 h**	**24 h**	**7 days**	**28 days**
MTA Control	11.71	12.18	12.70	12.92	13.02
MTA + 2.5 wt% CS-MMw	11.44	12.32	12.87	13.04	13.01
MTA + 5 wt% CS-MMw	11.51	12.34	12.83	12.97	13.07
MTA + 10 wt% CS-MMw	11.43	12.42	12.92	13.01	13.04
MTA + 20 wt% CS-MMw	11.75	12.03	12.60	12.61	12.32
BD Control	10.53	11.06	11.51	11.78	12.33
BD + 2.5 wt% CS-MMw	10.67	11.38	11.89	12.01	12.35
BD + 5 wt% CS-MMw	11.13	11.45	12.58	12.09	12.55
BD + 10 wt% CS-MMw	10.9	11.51	12.55	12.20	12.43
BD + 20 wt% CS-MMw	10.85	11.45	12.56	12.23	12.34
Biodentine ± CS			**24 h**	**7 days**	
BD Control			11.72	11.98	
BD + 0.5 wt% CS-HMw			12.04	12.00	
BD + 1 wt% CS-HMw			12.10	12.13	
BD + 0.5 wt% CS-MMw			11.92	12.05	
BD + 1 wt% CS-MMw			12.06	12.08	
BD + 0.5 wt% CS-LMw			11.99	12.26	
BD + 1 wt% CS-LMw			12.01	12.27	

Each value represents the mean of data. HMw; high molecular weight, MMw; medium molecular weight, LMw; low molecular weight.

4.5 Discussion

In this study, the optimised biofilm model provided a useful testbed for assessing the therapeutic effects of two conventional endodontic treatments (CHX and EDTA) and a novel antimicrobial compound (chitosan). For these *in vitro* studies, 'treatment', 'prevention' and 'adsorption', biofilm models were used with the latter two providing an *in vitro* imitation for root canal debridement, by mechanical disruption of grown biofilms, followed by antimicrobial applications to prevent biofilm regrowth. From these results, it was clear that all compounds tested, within this optimised endodontic biofilm model, were effective in reducing the microbial load and/or metabolic activity of the regrown biofilm in the 'prevention' group, in the presence and absence of serum. A study has shown that bovine serum albumin (BSA) did not interfere substantially with the antimicrobial activity of NaOCl and CHX irrigation (Sassone et al., 2003). Another study showed no inhibitory effect of BSA on the antimicrobial activity of NaOCl and no substantial effect on the bactericidal activity of CHX (Khedmat et al., 2009). However, the presence of BSA substantially inhibited the antimicrobial effectiveness of calcium hydroxide (Portenier et al., 2001). It was also found that tissue inhibitors, standing within the root canal, such as pulp tissue and serum albumin have significantly inhibited the antimicrobial properties of CNPs when tested on planktonic *E. faecalis* (Shrestha and Kishen, 2012).

In contrast to the 'prevention' model, EDTA (230 mM) was ineffective against preformed biofilms in the 'treatment' group. An inhibitory effect of EDTA was shown upon adherent *C. albicans* cells by Ramage et al. (2007) at 1, 2 and 4 h in a concentration dependant manner. However, in agreement with our results, preformed 24 h biofilms were minimally affected by EDTA at 250 mM (Ramage et al., 2007). In another study by Casalinuovo et al. (2017), EDTA at 2.5 and 25 mM significantly reduced the preformed 72 h biofilm viability. In contrast to EDTA and CHX, chitosan was ineffective in the 'adsorption' groups (Figure 4.1), which indicates the lack of substantivity. However, chitosan is shown to possess antimicrobial activity against the nosocomial pathogens *C. albicans* and *C. auris*, both *in vitro* and *in vivo* (Arias et al., 2020b). Another study also showed that acetic acid-solubilised chitosan was effective in reducing the viability of three single-species biofilms containing *Streptococcus mutans*, *Actinomyces*

naeslundii, and *Enterococcus faecalis* (Gu et al., 2019). Chitosan within a nanocarrier system has been shown to be effective against interkingdom biofilms representing caries (five species), gingivitis (seven species), and denture stomatitis (11 species) (Arias et al., 2020a).

It was deemed pertinent to include the regrowth 'prevention' biofilm model, from these platforms, to particularly replicate an endodontist's clinical treatment plan of an infected root canal following chemo-mechanical means of root canal disinfection. Of note, the solubilised chitosan was particularly effective in reducing the CFE counts of the mixed-species biofilm in the regrowth experiments in pre-treated culture plates 'prevention'. This was also reaffirmed on a biological substrate, bovine dentine, to further validate our model and antimicrobial results for the chitosan solution (Figure 4.4). Bovine dentine is very similar to human dentine with regard to morphology, physical properties and chemical composition (de Dios Teruel et al., 2015). Interestingly, others have shown that chitosan particles were able to deposit on the surface of bovine dentine slabs and within the dentinal tubules (Ururahy et al., 2017), which likely prevents recolonisation of the biofilm. However, due to the financial implications related to the use of bovine dentine, we were restricted to select one therapeutic arm to test in this biological system. Future studies merit consideration of repeating this biological system with different therapeutics.

The antimicrobial properties of calcium silicate-based materials have been widely investigated, though these studies are limited by their exploration of only single-species microbial models and the use of traditional microbiological techniques (R Kim et al., 2015, Donyavi et al., 2017, Atom et al., 2021). The potential for the use of antimicrobial filling or obturation materials following chemo-mechanical disinfection to inhibit biofilm regrowth is of interest. Therefore, the present study aims to close the gap in the literature, creating an understanding of the antimicrobial activities of these materials within a more relevant microbiological model system.

Our results indicated that neither material in an unmodified state shows an ability to inhibit biofilm regrowth of the three biofilm models after 24 h of

incubation, compared to the control substrate of bovine dentine. The number of live *C. albicans* and bacterial colonies formed on both MTA and BD were increased by approximately one log compared to those formed on dentine discs (Figure 4.8), albeit without reaching statistical significance. This finding is interesting and raises the question as to whether dentine is demonstrating an antimicrobial effect in comparison to the cements, or if calcium silicate cements are supportive of microbial growth. Previous studies have demonstrated that dentine can enhance the antimicrobial effects of some materials, including calcium silicate materials, and it has been hypothesised this is a result of changing the physicochemical nature of the materials with which dentine is combined (Zehnder et al., 2006, H Zhang et al., 2009). However, in the present study, dentine was not combined with the materials. Therefore, it is not inconceivable that dentine itself as a biologically active substrate may have a weak antimicrobial capacity of its own. A previous study has demonstrated that extracellular matrix isolated from the pulp and dentine of freshly extracted teeth demonstrated some level of antibacterial activity. This indicates that the release of bioactive molecules from the matrix of the pulp and dentine may contribute to immune responses during dental disease (J Smith et al., 2012). However, in a separate study, it was shown that the addition of a sterilised crushed human dentine to a suspension of *E. faecalis* did not exhibit any antibacterial activity after 24 h of exposure (H Zhang et al., 2009). Another possibility is related to microbial adhesion. Type I collagen is the main organic component of dentine (Arana-Chavez and Massa, 2004). It has been suggested that collagen-rich substrates, such as dentine, can act as an ideal substrate for colonisation by streptococci (Miller et al., 2015, Love and Jenkinson, 2002). The preparation of dentine used in microbiological studies may have an effect on microbial adhesion (Swimberghe et al., 2019). In the present study, the high temperature steam sterilisation used may have resulted in collagen denaturation, which has previously been suggested to reduce microbial adhesion (Chivatxaranukul et al., 2008). In contrast, it has been demonstrated that dentinal collagen of bovine dentine slices, despite being partially denatured at high temperatures (≤ 175°C), can revert to its original confirmation (Bachmann et al., 2005). However, despite the potential confounding factors, it is felt that the use of dentine as a control substrate is appropriate. Previous studies have dispensed with biologically relevant substrates and used cell culture plastics as

control surfaces for establishing the antimicrobial effect of this group of materials (Lovato and Sedgley, 2011, Damlar et al., 2014). Although such *in vitro* biofilm systems have greatly enhanced our understanding of biofilm biology, their lack of biological and clinical relevance limits the understanding gleaned (Roberts et al., 2015).

As stated, it was evident from the results that both unmodified ProRoot MTA and Biodentine were readily colonised by *C. albicans* and bacterial biofilms after 24 h of incubation. Neither material demonstrated antimicrobial properties against *C. albicans*, bacterial or interkingdom biofilms compared to the dentine control. It was clear from the findings that inclusion of bacteria inhibits *C. albicans* growth on both materials, whilst the addition of *C. albicans* showed a degree of enhancement of bacterial growth on these materials. Antagonistic interkingdom interactions have previously been highlighted where *F. nucleatum* and a number of other bacterial species including streptococci and *P. gingivalis* inhibit growth and hyphal morphogenesis of *C. albicans* (Thein et al., 2006, Bor et al., 2016). On the other hand, on the dentine substrate, the inclusion of *C. albicans* increased the number of viable bacteria by approximately 3.5-fold, while the addition of bacteria showed a small 1.2-fold increase in viable *C. albicans*. Microbial interactions differ according to the substrate on which the interaction occurs. Such substrate-dependent phenomena have been described in other interkingdom interactions. Antagonistic interactions between *E. faecalis* and *C. albicans* in *in vitro* and *in vivo* models have been previously described (Graham et al., 2017, Alshanta et al., 2020, Alshanta et al., 2022). Contrastingly, Krishnamoorthy et al. (2020) highlighted synergistic interactions between these species in an oral epithelium model.

The addition of CS-MMw to MTA provided no enhancement against the mixed biofilm models after 24 h of incubation. In contrast, the combination of CS-MMw and Biodentine reduced the live colony-forming equivalent of the bacterial and mixed-species biofilms significantly. Notably, chitosan affected the composition of the evaluated four-species biofilms, causing a significant reduction in the viable fungal load in the mixed culture. Interestingly, in the presence of *C. albicans*, bacterial load was decreased, but not significantly. In contrast, bacteria were decreased significantly when *C. albicans* was absent. These results

indicate that fungi may confer protection to bacteria from active agents when grown in mixed microbial culture. This is in line with that described by Young et al. (2021), where protection to antimicrobial challenge is conferred upon bacterial species in the presence of *C. albicans* (Young et al., 2021). It has also been shown that *C. albicans* ECM protected *S. aureus* against vancomycin treatment, possibly by limiting or delaying drug diffusion to *S. aureus* (Harriott and Noverr, 2009).

It is clear from the findings that ProRoot MTA and Biodentine exhibited different antimicrobial behaviours when dry chitosan powder was added. One mechanism by which calcium silicate cements have been said to exert an antimicrobial effect is through modifying environmental pH. It has been postulated that increased alkalinity, resulting from the release of calcium hydroxide upon setting of MTA preparations and its subsequent dissociation into calcium and hydroxide ions, may be responsible for any observed antimicrobial action (Al-Hezaimi et al., 2006, Abou ElReash et al., 2019). The effect of $Ca(OH)_2$ on microbial biofilms, however, is still controversial (Mohammadi et al., 2012). It has been shown that $Ca(OH)_2$ was not effective against *C. albicans* and *E. faecalis* biofilms (Zancan et al., 2019). The impact of chitosan on Biodentine is interesting. To understand if the addition of chitosan modified pH, measurements of both materials' leachate were taken. The unmodified MTA exhibited greater alkalinity than unmodified Biodentine at all timepoints assessed. This could be a result of differences observed in the pH of the manufacturer-supplied liquid components of both MTA (pH 7) and Biodentine (pH 3.7). It was also established that the addition of chitosan to MTA made no appreciable difference in pH at 24 h. However, at 24 h, upon addition of chitosan to Biodentine, an increase in pH was observed. Given that the pH change merely brings it in line with that of MTA, at 24 h, it is unlikely that pH accounts for the antimicrobial activity differences seen between the two materials. However, in contrast to MTA, the increase in pH observed for modified Biodentine cement indicates that there may be an interaction between the cement components and the chitosan microparticles.

One of the factors that affect the antimicrobial activity of chitosan is pH. It has been shown that acidic chitosan solution displays a stronger antibacterial

activity against *E. coli* than that of more alkaline solutions (Tsai and Su, 1999). It has been suggested that the surrounding acidic medium leads to protonation of amino groups (-NH_2) of chitosan, which subsequently favours electrostatic interactions between the formed positively charged chitosan molecules and negative residues at biological sites (Tsai and Su, 1999, Wani et al., 2021). Other studies have shown higher antimicrobial activities when pH values of the chitosan solution ranged between 5 and 6.5–7; however, the inhibitory effect was completely abolished at pHs greater than 7 (Kong et al., 2008, Aleanizy et al., 2018). In fact, regardless of form or quantity, antimicrobial compounds typically need water for their activity. Samples that are completely dry are incapable of releasing their stored energy in chemical bonding to begin interactions (Kong et al., 2010). Accordingly, it is believed that the poor solubility of chitosan in water has limited the compound's biological applications (Kaczmarek et al., 2019). Therefore, it is understandable that the powdered chitosan blended with MTA was no longer bactericidal because of the poor solubility of chitosan in the manufacturer liquid of MTA (water) at pH 7. In contrast, the antimicrobial effect of chitosan on Biodentine is interesting. The solid undissolved chitosan microparticles exhibited unique inhibitory effects among the material. Although the mechanism is not clear, a possible explanation is that the acidic pH of the manufacturer liquid of Biodentine or its components may have interacted with chitosan, resulting in enhanced antimicrobial activity of the new compound. These results indicate that the powdered chitosan in its insoluble form is not totally inactive. Meanwhile, a correlation between antimicrobial activity and chitosan Mw was also reported. It has been shown that decreasing chitosan Mw lead to strengthening chitosan antimicrobial activity (Ye et al., 2008, Chávez de Paz et al., 2011), while in other studies, the antimicrobial effect was enhanced as the molecular weight of chitosan increased (Ikinci et al., 2002, Akca et al., 2018). The data of this study suggested that chitosan with LMw showed the highest antimicrobial effect, while the antibiofilm effect was decreased with the increased chitosan molecular weight.

The present study demonstrates limited intrinsic antimicrobial abilities for the tested calcium silicate cements. This contrasts with previous studies but is likely a result of the use of biofilm models. This further highlights the need for the use of appropriate model systems in assessment of therapeutics to account for the

often synergistic/protective relationships that exist in complex microbiological systems. The present study highlights the potential to enhance the antimicrobial properties of an existing calcium silicate cement (Biodentine), which may serve to reduce the likelihood of persistence or re-establishment of infections within the treated root canal space.

CHAPTER FINDINGS

- Chitosan solution can be employed in root canal treatment as an alternative treatment strategy.
- Calcium silicate materials tested have a limited antibiofilm activity.
- The addition of chitosan powder to MTA shows no antimicrobial enhancement against the mixed-species biofilm model.
- Biodentine incorporated with chitosan powder displays a dose-dependent reduction in multispecies biofilm regrowth.
- Bacteria grown in the presence of *C. albicans* on Biodentine show a higher level of tolerance to chitosan compared to bacteria grown in the absence of *C. albicans*.
- *C. albicans* grown in the presence of bacteria on Biodentine demonstrates a lower level of tolerance to chitosan treatment compared to *C. albicans* only biofilm.
- The antibiofilm effect of chitosan increases with the decreased chitosan molecular weight.

5 The effect of chitosan incorporation on material characteristics of Biodentine™

5.1 Introduction

Biodentine™ is a novel hydraulic calcium silicate material, recognised for its high bioactivity, biocompatibility (Widbiller et al., 2022), outstanding sealing properties (Solanki et al., 2018) and physicochemical characteristics superior to those of mineral trioxide aggregate (Pradeep et al., 2018, Rahimi et al., 2018). Such properties allow its use as a permanent dentine substitute in teeth. Its uses include vital pulp therapy, apexification, retrograde root filling, management of root resorption and perforation repair (Septodont, 2010, Dammaschke, 2012b). *In vitro* testing of Biodentine, like other bioceramics, showed good antimicrobial activity against planktonic microbes (Hiremath et al., 2015, Fathy et al., 2019, Çırakoğlu et al., 2020, Esteki et al., 2021). However, Biodentine was much less effective when tested against multispecies biofilms (Farrugia et al., 2018, Jardine et al., 2019). Although Biodentine has been shown to give good clinical success, across multiple treatments when used in vital pulp therapy; for example 94.4% at a 2-year follow-up (Rahman and Goswami, 2021) and 91.7% at a 3-year follow-up (Awawdeh et al., 2018a), there remains scope for improving the antimicrobial effects of these materials.

Studies have been conducted with various types of additives incorporated into Biodentine in an attempt to improve the material properties. For example, incorporation of 5% glass fiber powder into Biodentine was found to significantly improve the fracture resistance of obturated roots with the modified material, when the material was used as an intra-orifice barrier (Nagas et al., 2016). In another study, surface microhardness, fracture resistance and antimicrobial properties of Biodentine-incorporating titanium tetrafluoride (TiF4) powder were significantly enhanced when compared with the control group (Elsaka et al., 2019). It has been also found that the incorporation of bioactive glass nanoparticles improved the nanocomposite bioactivity, expressed by an accelerated apatite formation on the Biodentine surface after short-term immersion in a simulated body fluid (Corral Nuñez et al., 2017). Aidaros et al. evaluated the pulp response to direct pulp capping with Biodentine conjugated with calcium phosphate nanoparticles (NPs), where the thickness of dentine bridge formed by the new mixture was significantly greater than the one formed by Biodentine alone (Aidaros et al., 2018). Silver NPs have also been trialled with *Rosmarinus officinalis* leaf extract (ROE) and Cefuroxime. The antibiofilm

efficacy of Cefuroxime-ROE-AgNPs nano-antibiotic in Biodentine displayed a significantly higher efficiency than the unmodified Biodentine, Cefuroxime or ROE-AgNPs alone (Gad El-Rab et al., 2021). In the previous chapter, Biodentine has displayed antibiofilm activity when integrated with chitosan powder. Accordingly, it is essential that material properties are maintained regardless of the additions to allow the material to function as designed clinically. Therefore, this chapter aims to investigate the effect of chitosan addition on the physico-mechanical and biological properties of Biodentine.

5.2 Hypothesis and aims

Adding any substance, such as chitosan powder, may affect some material properties of the cement. This potential for diminution of the physico-mechanical and biological properties requires further investigation. Therefore, the following chapter aims to investigate the effect of the incorporation of chitosan on some of the physico-mechanical and biological properties of Biodentine. This is to assess any alterations that could have detrimental effects on the clinical efficacy of Biodentine.

5.3 Materials and methods

Commercially available Biodentine™ is a powder and liquid system, available in pre-set capsules with 0.7 g of powder, in which five drops of BD liquid are placed prior to mixing (Septodont, 2010) (Table 5.1). In this study, Biodentine powder was mixed with four different proportions of chitosan MMw (2.5 wt%, 5 wt%, 10 wt% and 20 wt%), and then with two different proportions of chitosan LMw (0.5 wt% and 1 wt%). The weight of BD powder in each capsule was found ranging between 0.67 g and 0.73 g. Therefore, to assure consistency between samples, Biodentine powder was reweighed and kept to 0.7 g, as the manufacturer claimed, and then mixed with 180 µL of the manufacturer liquid (five drops of Biodentine liquid = 180 µL). Incorporating higher concentrations of chitosan (> 2.5 wt%) required higher volumes of BD liquid to triturate the new composite, as previously described (Table 4.2). The resultant powder was mixed with the manufacturer Biodentine™ liquid component (measured in µL) in a mixing machine at 4000-4200 rpm for 30 seconds, as shown (Figure 5.1 and Table 4.2). After mixing, BD was compacted into assigned moulds and each specimen was kept at 37°C in a humid environment for the specified time. Specification tests of the International Organisation for Standardisation (ISO) 6876 (ISO, 2012) was adapted for material tests, unless otherwise stated.

The setting time was determined using a Vicat apparatus, solubility was assessed by calculating weight variation following immersion in water, radiopacity was assessed and expressed in thickness of aluminium, the compressive strength (CSI) was assessed using an Instron testing machine and the microhardness (MH) was evaluated using a Vickers microhardness tester. Additionally, surface topography was analysed using scanning electron microscopy, the effect of the incorporated chitosan on the viability of human embryonic kidney (HEK 293) cells was investigated using a colorimetric MTT assay. Finally, the cytotoxicity effect of the material on human dental pulp stem cells (h-DPSCs) was evaluated using an LDH cytotoxicity assay.

Figure 5.1. Mixing Biodentine with chitosan. (A) Biodentine powder was mixed with four different proportions of chitosan powder of MMw (2.5 wt%, 5 wt%, 10 wt% and 20 wt%) and with two different proportions of LMw (0.5 wt% and 1 wt%). To ensure consistency between samples, the powder in each capsule was reweighed and kept to 700 mg, as the manufacturer claimed for the unmodified formula, using a digital scale. The manufacturer liquid was added into BD capsules by a pipette (five drops of BD liquid, as the manufacturer claimed, was replaced by 180 µL of BD liquid). Incorporating higher concentrations of chitosan (> 2.5 wt%) required higher volume of the manufacturer liquid to triturate the new composite. **(B)** Each BD capsule was mixed in the mixing machine for 30 seconds. **(C)** Following mixing, a line of BD paste shown along the capsule indicates the correct consistency of the unmodified Biodentine. **(D)** The cement paste became stiffer when chitosan powder was integrated as a filler.

Table 5.1. Composition of Biodentine material, according to the manufacturer (Septodont, 2010).

Powder	
Tricalcium silicate	Main core material
Dicalcium silicate	Second core material
Calcium carbonate and oxide	Filler
Iron oxide	Shade
Zirconium oxide	Radiopacifier
Liquid	
Calcium chloride	Accelerator
Hydrosoluble (water-soluble) polymer	Water reducing agent
Water	

5.3.1 Setting time

Biodentine samples were mixed and compacted into a stainless-steel ring mould, with an internal diameter of 13 mm and a height of 2 mm. Prior to the testing, the ring moulds were kept in a humid cabinet at 37°C. Each ring mould was placed on a glass plate and filled with the allocated material group and the excess material was removed to obtain a flat surface. The assembly was stored in the cabinet at 37°C in a moist atmosphere for 9 minutes. Ten minutes after mixing, the assembly was taken out of the cabinet and the test was performed using a Vicat apparatus E055N ([Matest, Caerphilly, UK], a sliding rod weighing 300 g with a removable needle with a cylindrical tip and a flat end [1.13 mm in diameter]), as shown (Figure 5.2). The needle was carefully lowered vertically onto the horizontal surface of the cement, without exerting further pressure. The cement was tested for setting initially at 10 minutes time intervals. As the final setting time approached, the process was repeated every approximately 30 seconds until a mark was no longer visible. The final setting time was calculated as the time taken from the end of mixing to the time at which the needle failed to leave an indentation on the set material surface. Seven and five replicates for MMw and LMw experimental groups, respectively, were prepared.

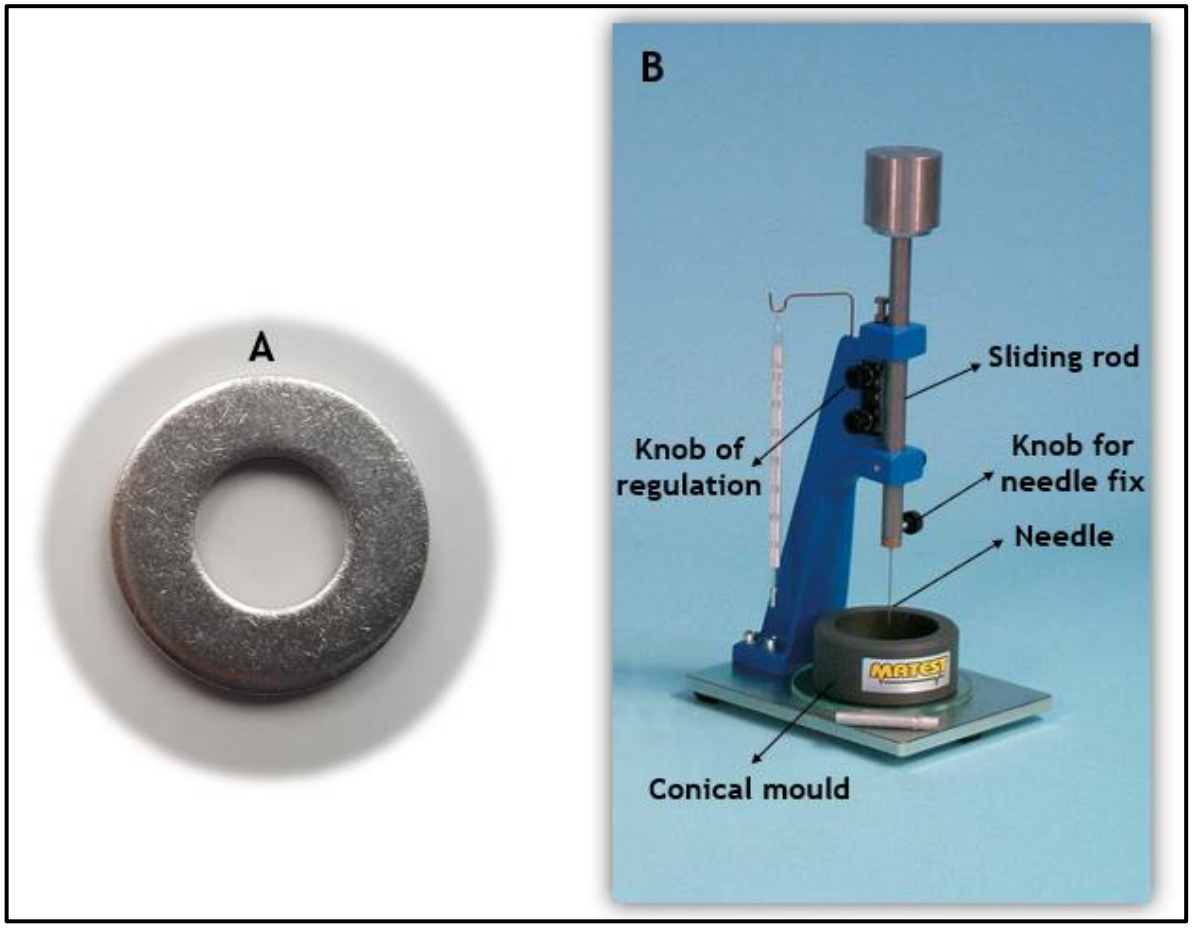

Figure 5.2. The setting time test. (A) A stain-less steel mould with an internal diameter of 13 × 2 mm. **(B)** A Vicat apparatus E055N for testing the setting time. Each assembly was placed on a glass slab on the conical mould, and the needle was carefully lowered vertically onto the horizontal surface of the BD cement. The final setting time was counted as the time taken from the end of mixing to the time at which the needle failed to leave an indentation on the set material surface.

5.3.2 Solubility

The solubility test determined weight loss of the test samples. Six replicates for each experimental group were prepared. Test specimens were prepared using ring metal moulds with a height of 2 mm and an internal diameter of 13 mm. Prior to use, all moulds were individually weighted (W_0). The moulds were filled with the allocated material group on a glass slab, and excess material was removed. The specimens were left to set in a humid atmosphere at 37°C for 24 h. All samples were then weighted individually in their ring moulds before immersion in water (W_1). The differences found between W_1 and W_0 were recorded as initial dry weight (IDW). The specimens were individually immersed in a clean glass tube containing a fresh aliquot of 20 mL of sterile distilled

water. Before use, all glass tubes were individually weighted (W_2) and autoclave adhesive strips were attached to each ring mould to hang a sample in the glass tube such that both surfaces of the cement were freely accessible to the immersing water and not contacting the walls of the containers. The glass tubes, with specimens inside, were then transferred into the incubator at 37°C where they were kept for one day. After 24 h, the specimens were removed from the glass tubes and rinsed with 1 mL of distilled water recollected in the same tubes, to remove loose debris of decomposition. The autoclave tape was then removed from each ring and the samples were left for complete drying at 37°C for 48 h and then reweighed with their ring moulds (W_3). The differences found between W_3 and W_0 were recorded as final wet weight (FWW). The water was then evaporated in an oven at 95°C. The dried glass tubes and residues were then weighed when they cooled down (W_4). The differences found between W_4 and the original glass tube weight (W_2) were recorded as dry precipitant weight (DPW). All measurement readings were in grams and recorded to four decimal places to the nearest 0.0001 g. The amount of solubility was calculated to the nearest 0.001% using the following equations:

$$\text{Solubility A } (\%) = \frac{\text{DPW}}{\text{IDW}} \times 100 \text{ (Residue method)}$$

$$\text{Solubility B } (\%) = \frac{\text{IDW} - \text{FWW}}{\text{IDW}} \times 100$$

5.3.3 Radiopacity

Cement specimens were prepared, using silicon moulds with a diameter of 7 mm and a thickness of 1 mm. Specimens were stored in a humid incubator at 37°C. Sample were digitally radiographed after, 24 h and 30 days, with an aluminium step wedge (aluminium purity at 96%, 30 mm long × 15 mm wide, having 5 steps with a thickness of 2.5, 3.5, 4.75, 7 and 9 mm). The digital X-ray machine (Gendex 765DC) is operating at 65 kV, a current of 7 mA and an exposure time of 0.020 seconds (Figure 5.3). All radiographic images were exported in JPG format. Using the ImageJ program (National Institutes of Health, Bethesda, Maryland, USA), a rectangular region of interest was established on the centre of each aluminium step, using the 'rectangular' tool. The mean grey pixel values of various thickness of the aluminium stepwedge were obtained and plotted against

their thickness, and a calibration curve was constructed automatically. After calibration, a circular area was established on the centre of the material images using the 'Oval tool', and the mean grey pixel value for each material disc was automatically expressed in millimetres of aluminium (mm Al). Six and five replicates for MMw and LMw experimental groups, respectively, were prepared.

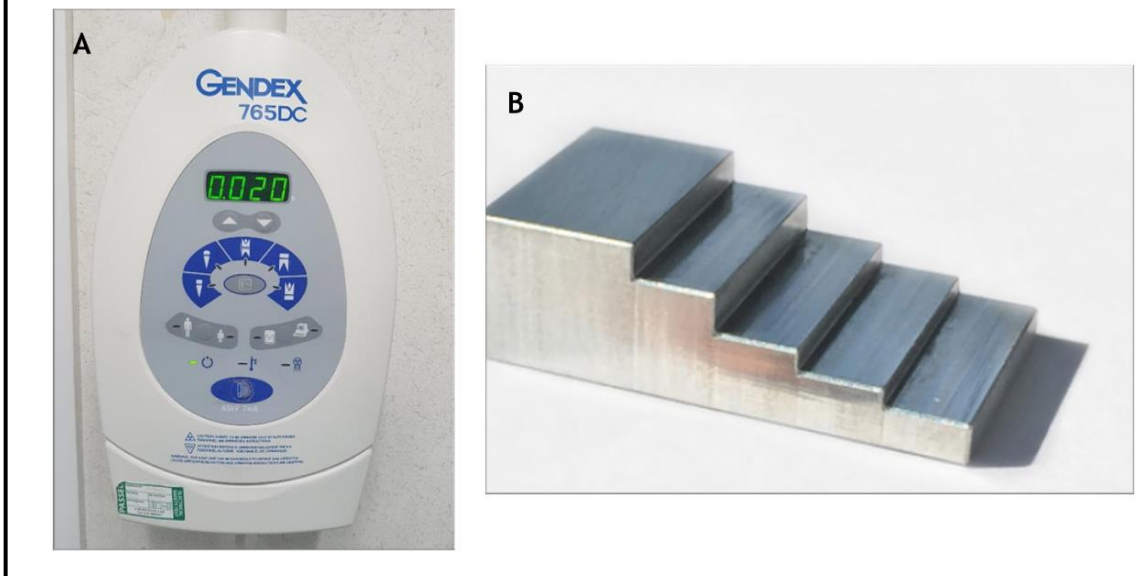

Figure 5.3. Radiopacity evaluation. (A) The digital X-ray machine (Gendex 765DC). **(B)** An aluminium stepwedge with various thickness of 2.5, 3.5, 4.75, 7 and 9 mm was used for radiopacity evaluation. Each sample was digitally radiographed with the aluminium step wedge. Using the ImageJ software, the radiopacity was assessed and expressed in thickness of aluminium.

5.3.4 Cell proliferation

Human embryo kidney cells (HEK 293) were cultured, and the cells were seeded in 75-cm^2 flasks at 5,000-6,000 cells/cm^2 in Knock-out Dulbecco's modified Eagle's medium (DMEM-KO [Gibco, Loughborough, UK]) supplemented with 10% foetal bovine serum, 200 mM L-Glutamine and Penicillin-Streptomycin solution. Medium was refreshed every three days, and when flasks were approximately 90% confluency, cells were passaged by detaching with 0.25% trypsin–EDTA (Gibco™, Loughborough, UK).

Cultures were maintained at sub-confluent levels at 37°C in a humid atmosphere with 5% CO_2. Biodentine ± CS-MMw discs (7 mm in diameter × 2 mm in thickness) were prepared and left in a humid atmosphere at 37°C for 24 h. Discs were then disinfected by UV for 30 minutes. Material discs were placed in a 24-well plate submerged in 1 mL of DMEM-KO and maintained at 37°C and 5% CO_2 overnight. HEK 293 cells were plated into a 96-well plate at a seeding density of 10^4 in DMEM-KO and allowed to adhere overnight. The following day, the cell's medium was replaced with the material leachates. To observe a dose-response relationship, the material extracts were serially diluted with DMEM-KO, as described by H Zhou et al. (2013), to achieve a total of three concentrations of each extract used to treat the cells. HEK 293 cells in normal culture were used as control. To evaluate the effect of chitosan on proliferation, cell metabolism was assessed using a colorimetric MTT assay (Sigma-Aldrich, Gillingham, UK) after 72 h of incubation. For each well, media were replaced with 100 µL MTT solution (0.5 mg/mL diluted in PBS) and incubated for 4 hours at 37°C and 5% CO_2. Subsequently, the solution was replaced with 100 µL of dimethyl sulfoxide (DMSO [Sigma-Aldrich, Gillingham, UK]) per well and further incubated for 1 hour at 37°C and 5% CO_2. Finally, plates were shaken at 250 rpm for 5 minutes and absorbance readings were performed on a microplate reader (FluoStar Omega, BMG Labtech, Aylesbury, UK) at 545 nm wavelength and 630 nm as a reference wavelength. Three biological repeats for each condition were performed in triplicate.

5.3.5 Cytotoxicity

To evaluate the cytotoxicity of CS-LMw, levels of Lactate dehydrogenase (LDH, a stable enzyme in all cell types released from dead cells when membrane is damaged) in supernatants were measured. Biodentine ± CS-LMw discs were prepared and submerged in 1 mL of DMEM-KO for 24 h, as previously described in 5.3.4. Before seeding, the pH readings of DMEM-KO and the material leachates in the cell culture medium were recorded. Human dental pulp stem cells (h-DPSCs [Lonza Inc, Bornem, Belgium]) were cultured, as previously described (5.3.4). The DPSCs that were used for the following experiment are between passages four and five as the supplier guarantee viability of ten population doublings.

An LDH cytotoxicity assay kit (CyQUANT™ LDH Cytotoxicity Assay [Thermo Scientific, Loughborough, UK]) was used according to manufacturer's instructions. Briefly, 50 µL of cell supernatant were plated in a 96-well plate with a positive control (lysed cells). Then, 50 µL of LDH reaction mix was added to each well and incubated in the dark for 30 minutes at room temperature. After incubation, the reaction was terminated by adding 50 µL of a stop solution provided by the manufacturer. Absorbance was read at 490 nm with a reference wavelength of 680 nm using a FluoStar Omega microplate reader. Three biological repeats were performed in duplicate.

5.3.6 Surface topography

Biodentine microstructure was observed using scanning electron microscopy (SEM). Cement specimens were prepared (7 mm in diameter × 1 mm in thickness). The specimens were kept at the humid cabinet for a month before being imaged. Samples were then taken for gold/palladium sputter coating and mounting. Digital images were acquired using Jeol JSM-IT100 InTouch™ Scanning electron microscope. Representative images were taken at a magnification of ×800.

5.3.7 Microhardness

For Vickers microhardness (HV), BD disc-shaped specimens were prepared by compacting the material into stainless-steel ring moulds (13 mm in diameter and 2 mm in thickness), 30 days before the test. The surface microhardness testing was performed using a Vickers microhardness tester [Krautkramer TIV, (GE Inspection Technologies, Coventry, UK)] with a Vicker diamond indenter point (Figure 5.4). Three indentations were made on one polished cement surface of each sample and the image of each indentation was transferred and evaluated automatically. The mean Vickers hardness number (VHN) value for each group was recorded. Five replicates for each experimental group were prepared.

Figure 5.4. The TIV hardness tester with a probe and a hardness reference block. The probe contains special optics and a CCD camera. The hardness is measured with the TIV method (Through Indenter Viewing) which enables to view and determine the test indentation of the Vickers diamond, that grows on the test object's surface under load, through the optical system.

5.3.8 Compressive strength

A test of ISO 9917-1 (ISO, 2007) was adapted for testing the compressive strength. Cylindrical specimens (6 mm in diameter × 6 mm in height) were prepared (n =10) using silicon moulds. All Biodentine cylinders were stored at 37°C in a humid atmosphere for 30 days. Prior to the compressive testing, each material cylinder was replaced into the mould (Figure 5.5) and the two circular faces of each cylindrical specimen were polished by a stainless-steel dental polishing strip, to create two smooth flat surfaces parallel to each other. Test samples were checked, and defective specimens were discarded. The CSI for each specimen was measured using an Instron 3367 Universal Testing Machine [30 KN Static Load Cell (Instron, Buckinghamshire, UK)] at a speed of 1 mm/minute (Figure 5.5). Each cylinder with its flat ends was placed between the platens of the apparatus and the load was applied in the direction parallel to the long axis of the material until the samples were crushed. The maximum load needed to break each test sample was recorded. The mean of ten and six replicates for MMw and LMw experimental group, respectively, were recorded.

The CSI were calculated in Megapascals (MPa) using the following formula, where F is the maximum force applied (N), and d is the mean diameter of the specimen in mm.

$$\sigma_c\,(\mathrm{MPa}) = \frac{4F}{\pi d^2}\,(\mathrm{N/mm^2})$$

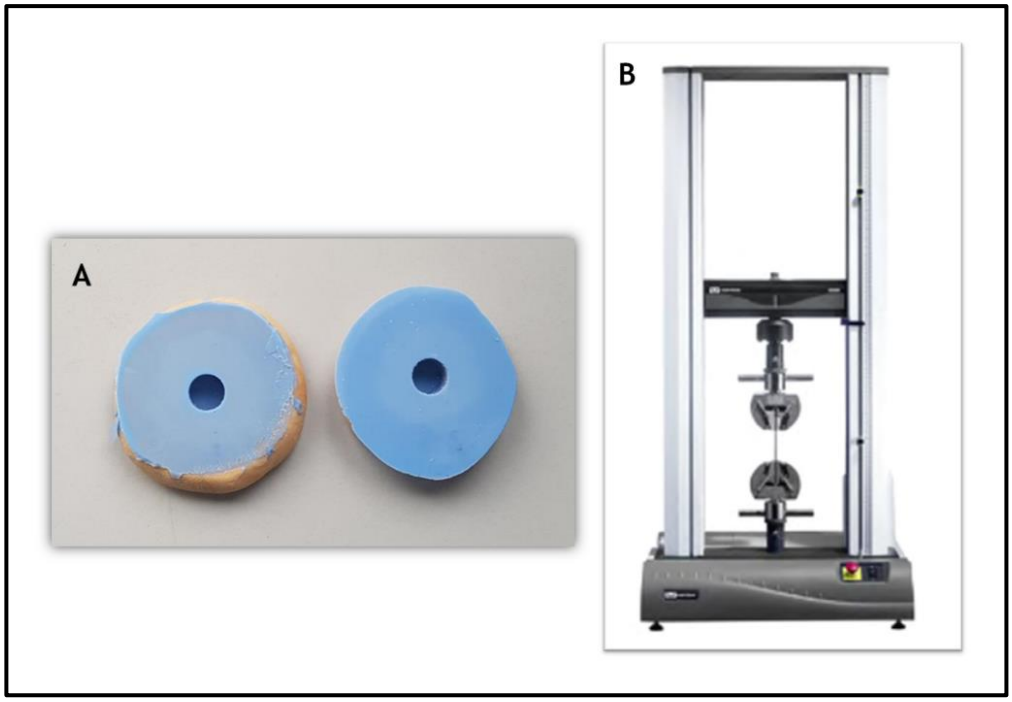

Figure 5.5. The compressive strength testing. (A) Moulds, 6 mm in height with 6 mm diameter were fabricated from dental silicone-based impression materials. The test material was filled into the cylindrical hole with a slight excess. A glass slap was then placed on top of the filled moulds and pressed down to remove the material excess. Before the test, each cylinder of test groups was placed back into the mould and its two circular sides were trimmed, by a stainless-steel polishing strip, to create two smooth parallel surfaces. **(B)** Instron 3367 Universal Testing Machine.

5.3.9 Statistical analysis

All graphs, data distribution and statistical analysis were performed using GraphPad Prism version 9 (GraphPad, San Diego, CA, USA). Before analysis, data distributions were assessed using a D'Agostino-Pearson omnibus normality test (samples ≥ 8) and Shapiro-Wilk normality test (samples < 8). Kruskal-Wallis with Dunn's tests were used to determine the p values for multiple comparisons for non-parametric data. ANOVA with Tukey's tests were used for multiple comparisons of normally distributed parametric data. Differences were considered statistically significant if $p < 0.05$.

5.4 Results

5.4.1 Setting time

The final setting time of unmodified BD was determined to be 31 minutes (Figure 5.6A,C). Slight decreases in setting time by 25.7% and 27.1% were seen following the inclusion of 2.5 wt% and 5 wt% CS-MMw, respectively. In contrast, the mean setting times for BD mixed with 10 wt% and 20 wt% CS-MMw increased by 43% and 82%, respectively, compared to the unmodified Biodentine (Figure 5.6B). However, the setting times for the unmodified material and modified BD incorporated with 0.5 wt% CS-LMw were comparable. Only 6% reduction in the final setting time was observed when 1 wt% of CS-LMw was integrated into the material. No statistically significant differences were found between the 0.5 wt% and 1 wt% groups (Figure 5.6C,D).

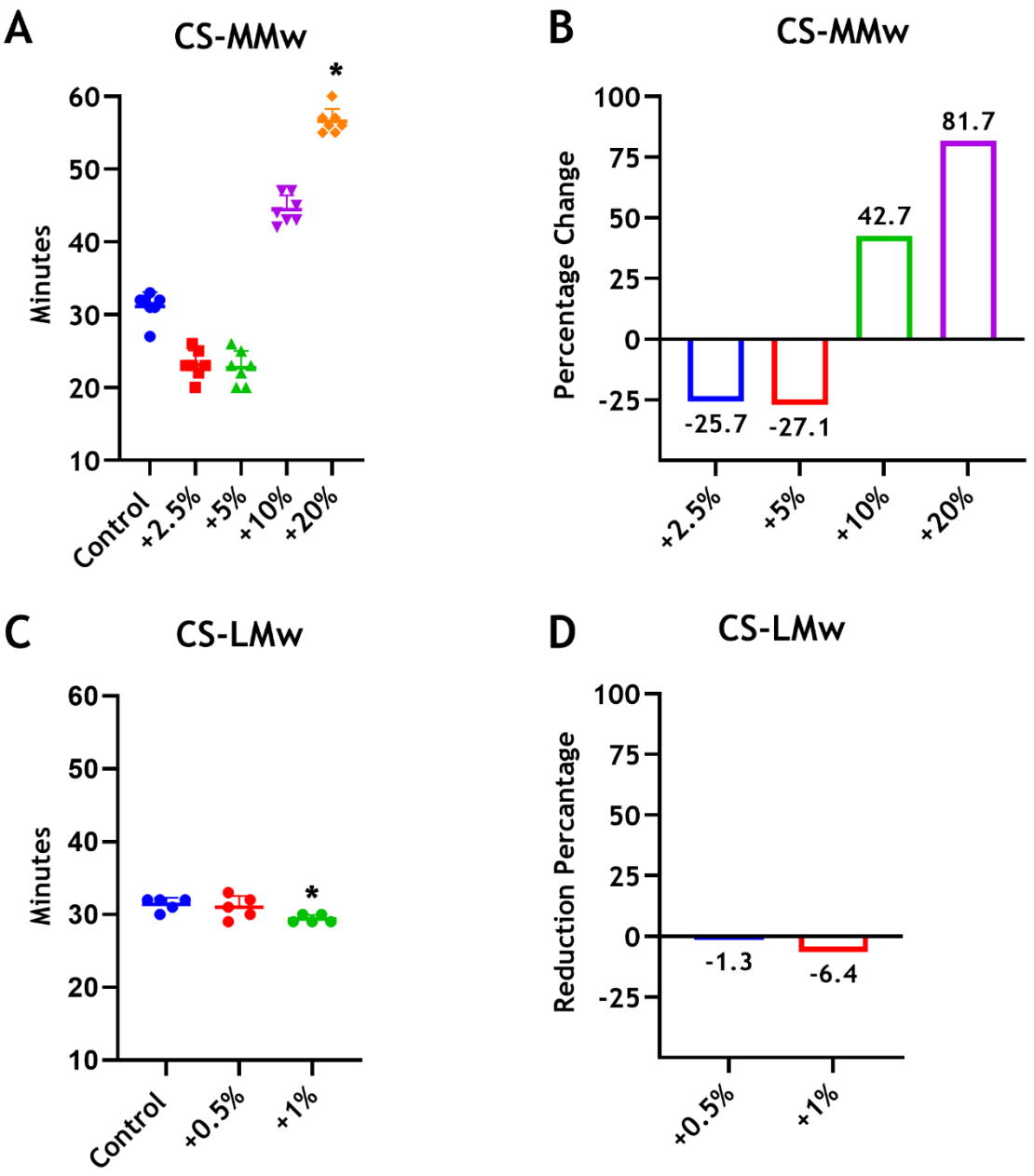

Figure 5.6. Setting time evaluation of Biodentine after incorporation of chitosan, using a Vicat apparatus. (A) Setting time of BD following incorporation of 2.5 wt%, 5 wt%, 10 wt% and 20 wt% of CS-MMw (n = 7). **(B)** The percentages of reduction and increase in setting time of MMw groups compared to the control group. **(C)** Setting times of BD ± CS-LMw after incorporation of 0.5 wt% and 1 wt% (n = 5). **(D)** The percentages of reduction in setting time of LMw groups compared to the control (unmodified Biodentine) group. Data were analysed by Kruskal-Wallis with Dunn's tests. Differences between the control and chitosan groups were considered statistically significant when $p < 0.05$. * Indicates statistically significant differences (* $p < 0.05$). No statistically significant differences were found between the 0.5 wt% and 1 wt% groups. Each dot/shape represents a replicate. Each error bar represents SD. Each bar, in the graphs B and D, represents the mean of data obtained from seven and five replicates (material discs), respectively.

5.4.2 Solubility

The amount of weight loss was calculated using the residue method (Figure 5.7A,C) or by measuring weight changes of the cement specimens after immersion (Figure 5.7B,D). The results showing that the solubility/disintegration of the unmodified control and modified BD incorporated with 0.5 wt% and 1 wt% CS-LMw were comparable with no significant differences found between the test groups, after 24 h of immersion in sterile water (Figure 5.7C,D). In contrast, the weight loss of BD blended with 2.5 wt% CS-MMw was slightly higher than the control whereas incorporation of 5 wt%, 10 wt% and 20 wt% CS-MMw were significantly higher than the control in a dose-dependent manner (Figure 5.7A,B). Notably, the material loss calculated in either way demonstrated similar trends where the greater amount of chitosan incorporation, the more disintegration the material will be. Regardless, when the weight loss was calculated according to the weight differences recorded before and after immersion, the test groups of BD supplemented with smaller amounts of CS-LMw (0.5 wt% and 1 wt%) and CS-MMw (2.5 wt%) showed a weight loss of less than 3% by weight (Figure 5.7B,D), which is in agreement with the ISO standard.

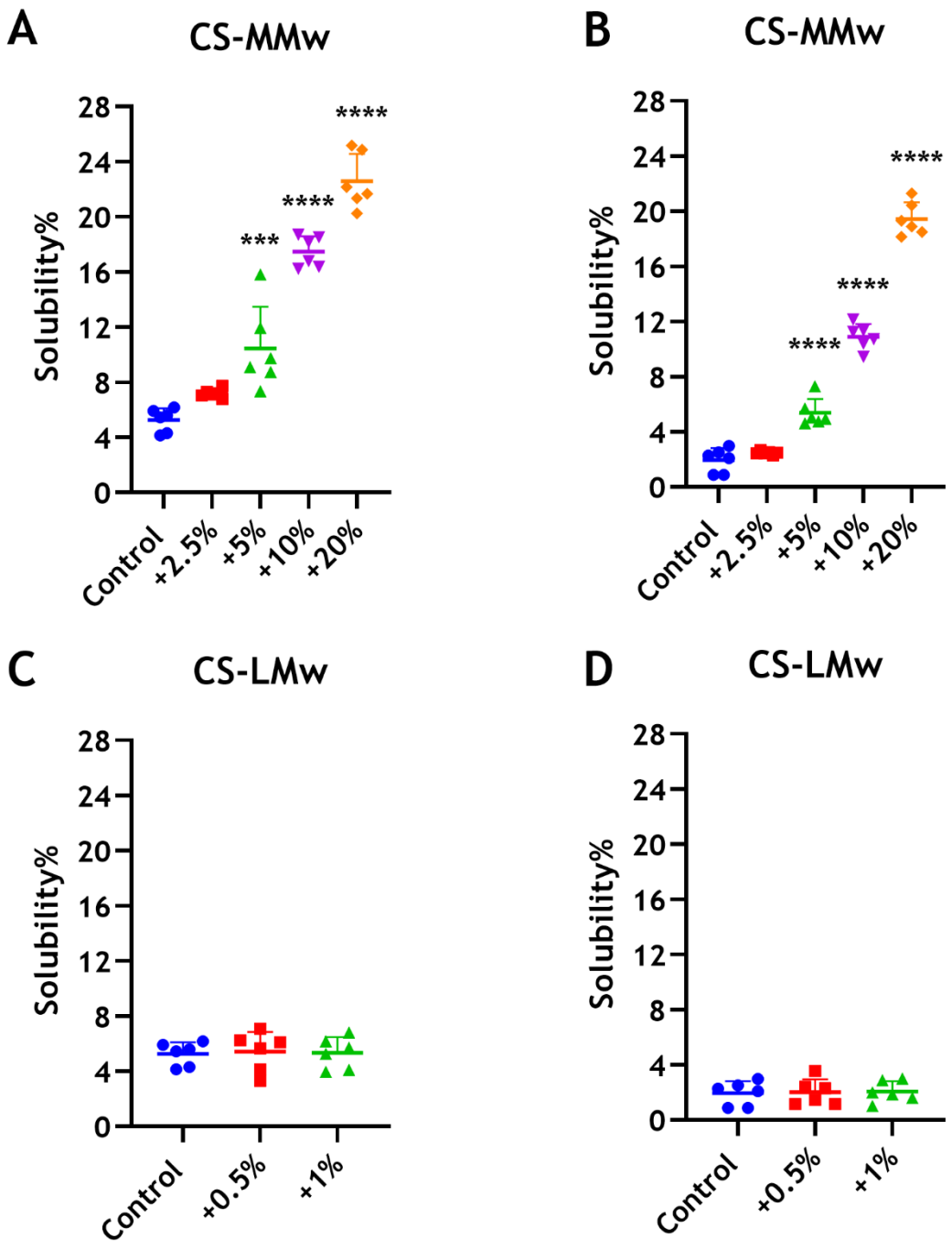

Figure 5.7. Solubility percentages recorded for Biodentine ± chitosan following immersion in sterile distilled water for 24 h. (A & C) The amount of Biodentine removed from the specimens (residue method) was calculated as a percentage of the original weight (n = 6). **(B & D)** The difference in Biodentine weight before and after immersion was calculated as a percentage of the original weight (n = 6). Data were analysed by ANOVA with Tukey's tests. Differences between the control (unmodified Biodentine) and chitosan groups were considered statistically significant when $p < 0.05$. * Indicates statistically significant differences (*** $p < 0.001$, **** $p < 0.0001$). Each dot/shape represents a replicate. Each error bar represents SD. Six replicates (material discs) of each group were tested.

5.4.3 Radiopacity

The radiopacity of unmodified BD was equivalent to 2.6 mm Al at 24 h and 30 days. The radiopacity of BD mixed with 2.5 wt% and 5 wt% CS-MMw decreased, but not significantly, by 6% and 13%, respectively, compared to the control. However, the 10% and 20% groups were significantly less radiopaque than the control group (** $p < 0.01$, *** $p < 0.001$) with 34.7% and 41.1% reductions in radiopacity, respectively after 24 h of being maintained at 37°C (Figure 5.8A,B). Similar values of radiopacity were seen after 30 days of storing the samples in the humid incubator (Figure 5.8C). In contrast, the radiopacity of BD supplemented with small portions of CS-LMw (0.5 wt% and 1 wt%) demonstrated a negligible decrease by approximately 3%, with no statistically significant differences between the test groups (Figure 5.8D). A representative radiographic image for each group is shown in Figure 5.9.

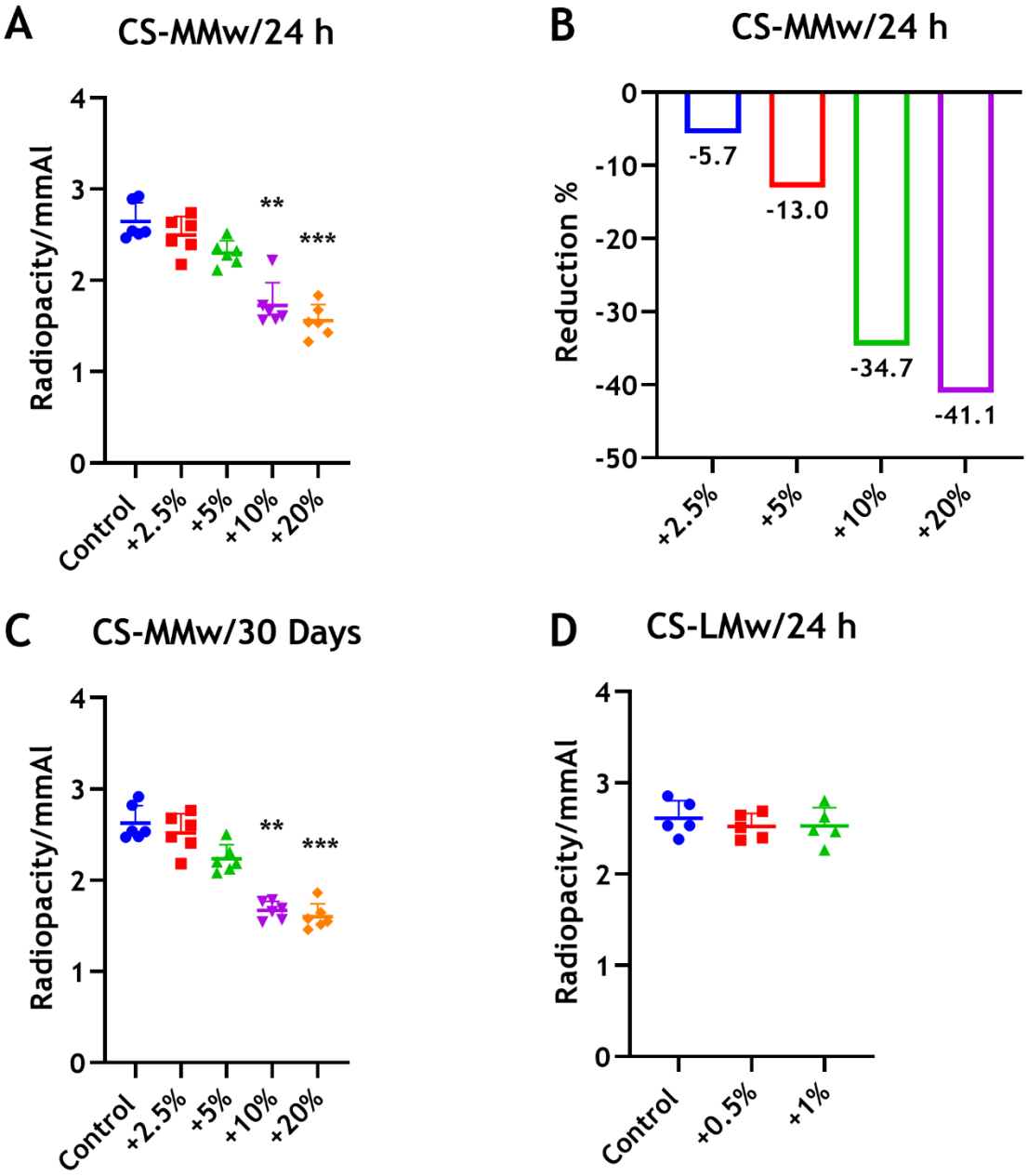

Figure 5.8. Radiopacity assessment of Biodentine following incorporation of chitosan. (A & C) Radiopacity of BD assessed after 24 h and 30 days of storing samples at 37°C, respectively, following incorporation of 2.5 wt%, 5 wt%, 10 wt% and 20 wt% of CS-MMw (n = 6). **(B)** The percentages of reduction in radiopacity with CS-MMw compared to the control unmodified Biodentine. **(D)** Radiopacity of BD with 0.5 wt% and 1 wt% CS-LMw (n = 5). Data were analysed by Kruskal-Wallis with Dunn's tests. * Indicates statistically significant differences between the control and chitosan groups (** $p < 0.01$, *** $p < 0.001$). Each dot/shape represents a replicate. Each error bar represents SD. Each bar, in the graph B, represents the mean of data obtained from six replicates.

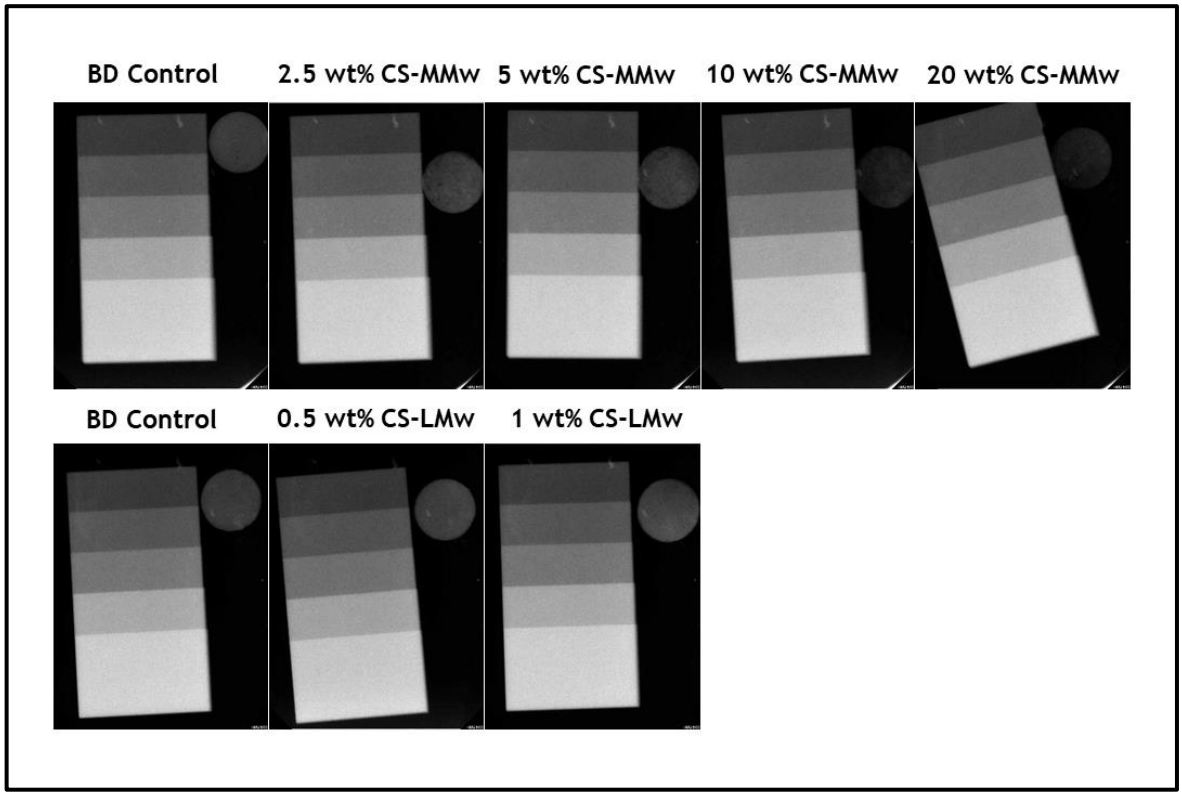

Figure 5.9. Digital radiographic images of Biodentine discs. Each replicate (material disc) was digitally radiographed with the aluminium step wedge. The material mean grey value was expressed in mm of aluminium thickness. A representative image is shown for each group.

5.4.4 Cell viability

After culturing for 72 h, results of the viability assay on the cell viability of HEK 293 cells showing high cell viability of BD-treated cells at all extract concentrations, with no statistically significant differences found compared to the positive control (cells cultured without material extracts). The undiluted extract (100%) from BD presented viable cells at 98.5%, whereas cells cultured with undiluted extracts derived from BD-CS-MMw, at all chitosan concentrations, showed significant decreases in viability compared to the control group (**** $p < 0.0001$). Cells viability of BD-chitosan extract at 2.5 wt% was 42.2%, whereas cells exposed to undiluted BD-CS-MMw extracts with 5 wt%, 10 wt% and 20 wt% displayed the lowest viabilities at 2.4%, 1.5% and 1.8%, respectively (Figure 5.10A). With extract dilutions in DMEM, higher percentages of cell viability cultured with all BD-CS-MMw groups were observed. Accordingly, half-diluted extracts of 2.5 wt% chitosan showing no significant viability reduction. The CS-MMw groups of 5 wt%, 10 wt% and 20 wt% showing statistically significant

viability reductions in comparison with the positive control (**** $p < 0.0001$), at 52.6%, 8.2% and 7.5%, respectively (Figure 5.10B). With 25% dilution, significant reductions in viability were only found with 10 wt% and 20 wt% (* $p < 0.05$), at 51.2% and 46.5%, respectively (Figure 5.10C). All absorbance values (OD) are presented (Table 5.2)

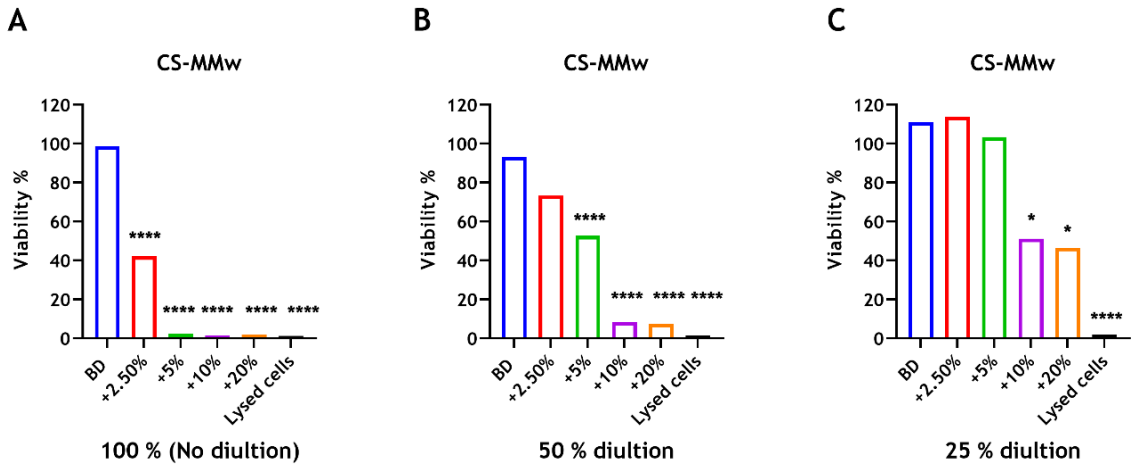

Figure 5.10. Evaluation of cell viability treated with extracts derived from Biodentine following incorporation of chitosan. Original (undiluted) extracts derived from Biodentine were serially diluted with DMEM. The MTT assay was used to measure the metabolic activity of HEK 293 cells treated with undiluted and diluted extracts of BD ± CS-MMw, cultured for 72 h. The percentage of cell viability of each test group was calculated relative to the untreated positive control. **(A)** No dilution (100%). **(B)** 50% dilution **(C)** 25% dilution. Data were analysed by ANOVA with Tukey's tests. * Indicates statistically significant differences between the control (untreated cells) and test groups (* $p < 0.05$, **** $p < 0.0001$). Note: statistical analyses were performed on raw data. Each bar represents average percentages of cell viability obtained from three parallel experiments with three technical replicates. Mr. Saeed Alqahtani contributed to this work (University of Glasgow).

Table 5.2. Absorbance values with standard deviations.

Group	100% (undiluted)	50% dilution	25% dilution
Positive control	0.355 (±0.075)	0.372 (±0.080)	0.298 (±0.132)
BD (unmodified)	0.350 (±0.102)	0.346 (±0.112)	0.331 (±0.095)
BD + 2.5 wt% CS-MMw	0.150 (±0.073)	0.273 (±0.079)	0.339 (±0.115)
BD + 5 wt% CS-MMw	0.009 (±0.003)	0.196 (±0.083)	0.308 (±0.108)
BD + 10 wt% CS-MMw	0.005 (±0.001)	0.031 (±0.013)	0.153 (±0.077)
BD + 20 wt% CS-MMw	0.006 (±0.002)	0.028 (±0.010)	0.139 (±0.072)
Lysed cells	0.004 (±0.002)	0.005 (±0.002)	0.006 (±0.002)

Average OD values of raw data representative of three technical repeats from three biological repeats, as shown in Figure 5.10.

5.4.5 Cytotoxicity

The pH of the DMEM-KO medium was determined to be 8.4 while the pH readings of the material leachates of unmodified BD, BD + 0.5 wt% LMw and BD + 1 wt% LMw were 8.1, 8.0 and 7.9, respectively. However, the results indicated that BD ± CS-LMw presented no cytotoxic effect on stem cells, in undiluted extracts at 72 h. The LDH release from the treated h-DPSCs was significantly lower (**** $p < 0.0001$) when compared to the maximum release of the LDH achieved by the lysis solution. No significant differences were found between the test groups (Figure 5.11).

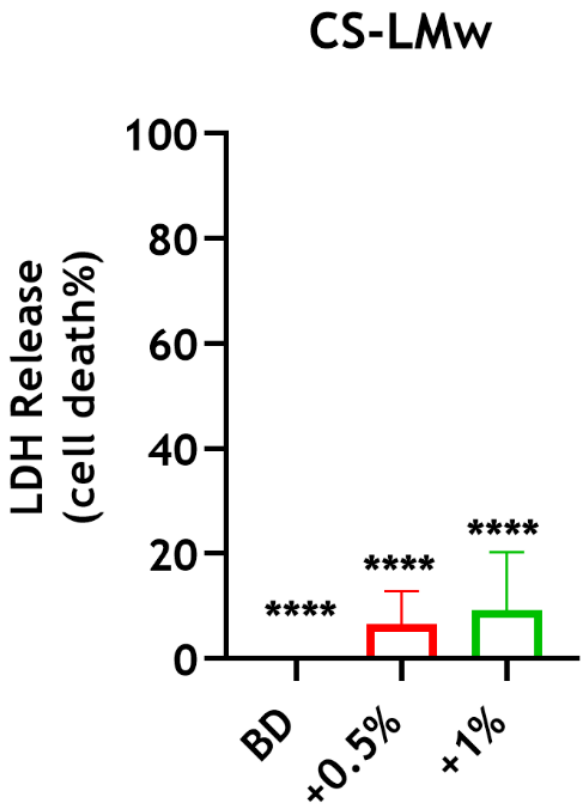

Figure 5.11. Evaluation of the cytotoxic effect of Biodentine on h-DPSCs following incorporation of chitosan. LDH release% was measured from h-DPSCs treated with 100% extract of BD ± CS-LMw. The percentage of cytotoxicity of test groups was calculated relative to the control (lysed cells). Data were analysed by ANOVA with Tukey's tests. * Indicates statistically significant differences between lysed cells and test groups (**** $p < 0.0001$). No significant differences were found between the test groups. Note: statistical analyses were performed on raw data. Each bar represents the mean of data obtained from two technical repeats of three independent experiments. Mr. Saeed Alqahtani contributed to this work (University of Glasgow).

5.4.6 Surface topography

The microstructure of BD surface showing superficial small intergrowth structures and needle-shaped crystals appeared to form in thin bundles (Figure 5.12A). In the chitosan-incorporated material, small particles of chitosan at 2.5 wt% are seen dispersed within the needle-shaped structures (Figure 5.12B). From 5 wt% and onwards, clusters or larger aggregations of CS-MMw are observed. The modified form of the material with larger amount of CS-MMw showing fewer crystalline structures, compared to the commercial BD material (Figure 5.12C-E).

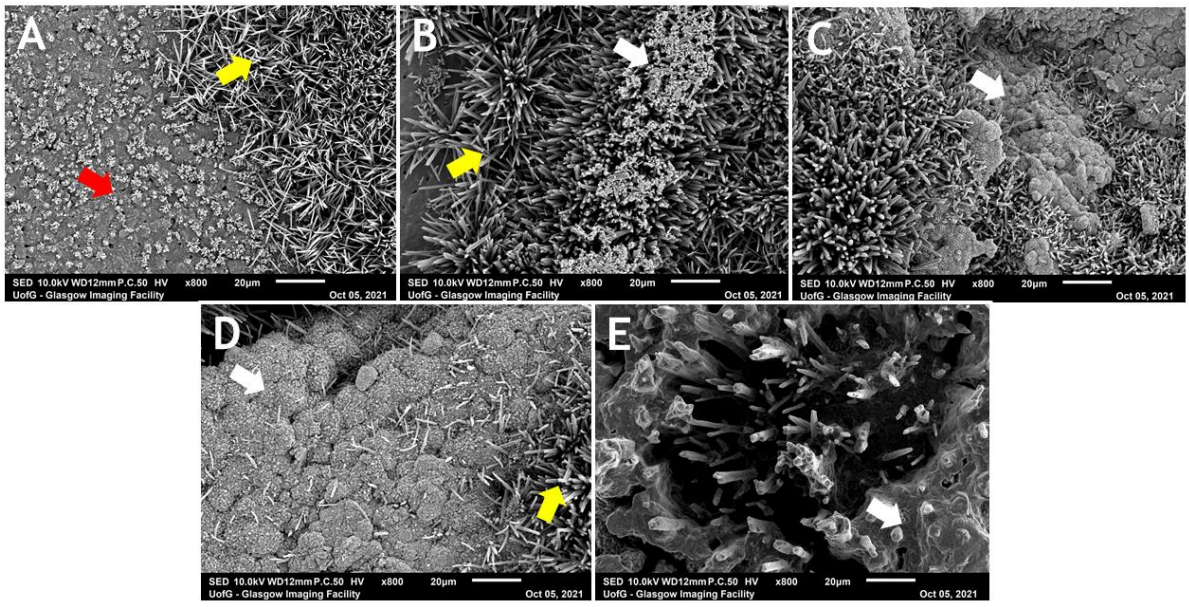

Figure 5.12. Scanning electron microscopy of Biodentine specimens ± chitosan. (A) Unmodified BD (control). **(B)** BD + 2.5 wt% CS-MMw. **(C)** BD + 5 wt% CS-MMw. **(D)** BD + 10 wt% CS-MMw. **(E)** BD + 20 wt% CS-MMw. SEM images show chitosan clumps (white arrows). Red and yellow arrows indicate intergrowth structures and needle-like structures, respectively. Representative images were taken at magnifications of ×800. Samples were processed and imaged by Mr. Mark Butcher (University of Glasgow).

5.4.7 Microhardness

The mean unmodified BD Vickers microhardness was 113.6 HV. Adding 2.5 wt%, 5 wt%, 10 wt% and 20 wt% CS-MMw to BD was found to decrease the microhardness of the material significantly (**** $p < 0.0001$) by 32%, 47%, 51% and 67%, respectively (Figure 5.13A,B). Furthermore, the microhardness of BD decreased significantly (**** $p < 0.0001$) by 16% and 29% when mixed with 0.5 wt% and 1

wt% CS-LMw, respectively, compared to the control (Figure 5.13C,D). A significant difference was also found between 0.5% and 1% groups (# $p < 0.05$).

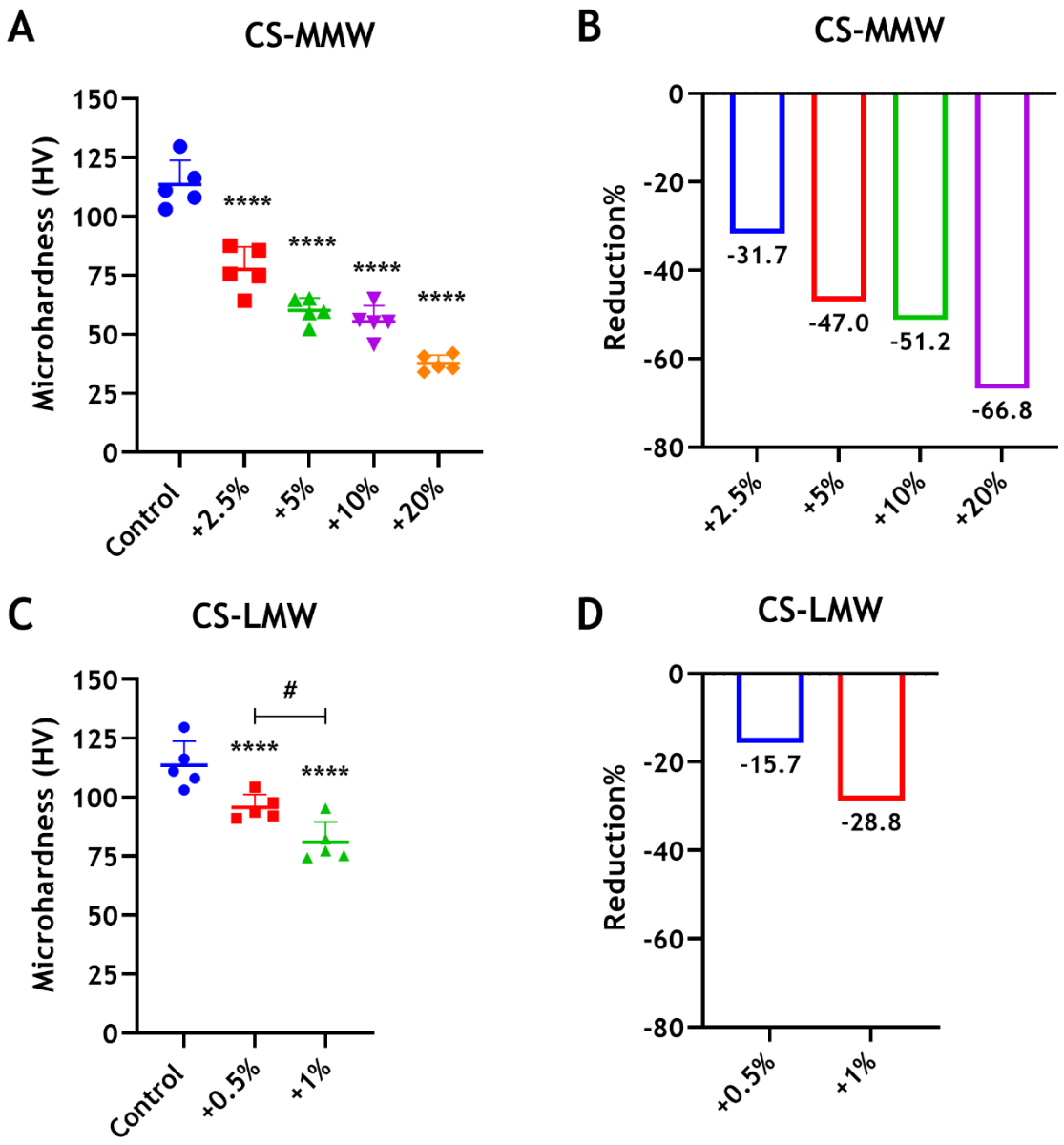

Figure 5.13. Microhardness assessment of Biodentine following incorporation of chitosan. (A) Microhardness of BD was assessed following incorporation of 2.5 wt%, 5 wt%, 10 wt% and 20 wt% of CS-MMw, using a Vickers diamond indenter point. **(B)** The percentages of reduction in microhardness compared to the control. **(C & D)** The graphs demonstrate microhardness of BD ± CS-LMw and the reduction percentages compared to the control unmodified material, respectively (n = 5). Data were analysed by ANOVA with Tukey's tests. * Indicates statistically significant differences between the control and chitosan groups (**** $p < 0.0001$). # Indicates statistically significant differences between the chitosan test groups (# $p < 0.05$). Each dot/shape represents a replicate. Each error bar represents SD. Each bar, in the graphs B and D, represents the mean of data obtained from five replicate tests per group.

5.4.8 Compressive strength

Based on the results shown, the addition of CS-MMw significantly reduced the CSI of BD in all groups in a dose-dependent manner (**** $p < 0.0001$). Adding 2.5 wt%, 5 wt%, 10 wt% and 20 wt% CS-MMw, decreased the strength by 55%, 81%, 90% and 92% respectively, compared to the control (unmodified BD), which showed a significant superior strength (Figure 5.14A,B). Similarly, the compressive strength of BD declined significantly (**** $p < 0.0001$) when only small amount of CS-LMw (0.5 wt% and 1 wt%) integrated into the cement, compared to the unmodified formula which showed a superior strength (182.88 MPa). No significant difference was observed between the 0.5% and 1% groups (Figure 5.14C,D).

The mean values of all tested groups with standard deviations are summarised below (Table 5.3 and Table 5.4).

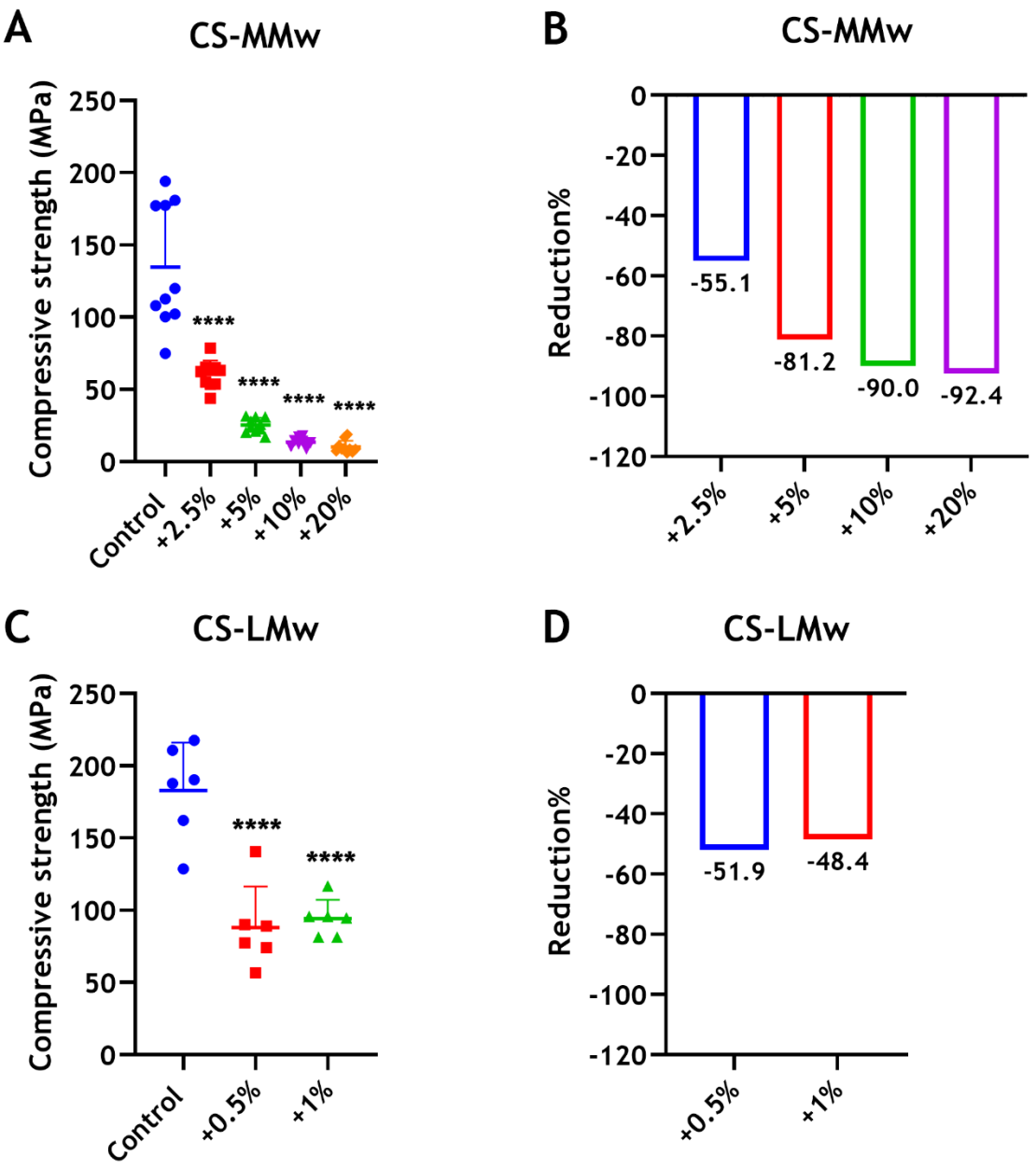

Figure 5.14. Compressive strength testing of Biodentine following incorporation of chitosan. **(A)** Compressive strength of BD was evaluated following the addition of CS-MMw, using Instron Testing Machine (n = 10). Measurements were carried out on 30-day-old cylinders in each test group, stored in a humid atmosphere at 37°C. **(B)** The percentages of reduction in CSI compared to the control unmodified material. **(C & D)** The graphs illustrate compressive strength of BD ± CS-LMw and the reduction percentages compared to the control, respectively (n = 6). Data were analysed by ANOVA with Tukey's tests. * Indicates statistically significant differences between the control and chitosan groups (**** $p < 0.0001$). No significant difference was observed between the 0.5% and 1% groups. Each dot/shape represents a replicate. Each error bar represents SD. The mean of replicates per group was recorded and presented as reduction percentages, compared to the control.

Table 5.3. Mean values of data obtained from Biodentine samples ± CS-MMw, with standard deviations.

Test Group	Setting time (n = 7)	Solubility-A: Residue method (n = 6)	Solubility-B (n = 6)	Radiopacity at 24 h (n = 6)	Compressive Strength (n = 10)	Microhardness (n = 5)
BD Control	31.14 (±1.95 min)	5.27 (±0.85%)	1.94 (±0.87%)	2.64 (±0.21 mmAl)	134.78 (±42.84 MPa)	113.60 (±10.20 HV)
BD + 2.5 wt% CS	23.14 (±1.95 min)	7.19 (±0.32%)	2.47 (±0.13%)	2.49 (±0.20 mmAl)	60.56 (±9.43 MPa)	77.60 (±9.42 HV)
BD + 5 wt% CS	22.71 (±2.29 min)	10.45 (±3.03%)	5.38 (±1.01%)	2.30 (±0.14 mmAl)	25.27 (±5.05 MPa)	60.20 (±5.24 HV)
BD + 10 wt% CS	44.43 (±1.99 min)	17.46 (±1.12%)	10.88 (±0.93%)	1.73 (±0.25 mmAl)	13.48 (±3.60 MPa)	55.40 (±6.85 HV)
BD + 20 wt% CS	56.57 (±1.72 min)	22.57 (± 2.0%)	19.42 (±1.21%)	1.56 (±0.18 mmAl)	10.20 (±4.34 MPa)	37.73 (±3.43 HV)

Table 5.4. Mean values of data obtained from Biodentine samples ± CS-LMw, with standard deviations.

Test Group	Setting time (n = 5)	Solubility-A: Residue method (n = 6)	Solubility-B (n = 6)	Radiopacity at 24 h (n = 5)	Compressive Strength (n = 6)	Microhardness (n = 5)
BD Control	31.40 (±0.89 min)	5.27 (±0.85%)	1.94 (±0.87%)	2.61 (±0.19 mmAl)	182.88 (±32.96 MPa)	113.60 (±10.20 HV)
BD + 0.5 wt% CS	31.0 (±1.58 min)	5.42 (±1.42%)	2.01 (±0.94%)	2.52 (±0.14 mmAl)	87.98 (±28.45 MPa)	95.73 (±5.44 HV)
BD + 1 wt% CS	29.40 (±0.55 min)	5.33 (±1.14%)	2.06 (±0.77%)	2.53 (±0.20 mmAl)	94.31 (±12.98 MPa)	80.93 (±8.62 HV)

5.5 Discussion

5.5.1 Setting time

The setting time is defined as the length of time for a material to shift from a fluid state into a solidified state (Wang, 2015). Long setting times are seen as one of the most problematic features of calcium silicate materials. These prolonged setting times cause difficulty in placement of the material, where it will not maintain its shape and is susceptible to be washed out before it is fully set (Shen et al., 2015). Biodentine has a reduced setting time when compared with other calcium silicate materials such as MTA (Careddu and Duncan, 2018) and this is perceived as one of its main clinical advantages (H Singh et al., 2014). Biodentine liquid contains calcium chloride as a setting accelerator. The cement powder includes calcium carbonate, which acts as a nucleation site for calcium silicate hydrate, which shortens the induction period and subsequently the setting reaction (Camilleri et al., 2013).

Measurement of setting time has been conducted using various methods. However, the main principle remains based upon the resistance of a needle to penetrate the material surface, either when the needle fails to make a trace on the surface of the cement (ISO, 2012) or when it fails to create a complete circular indentation in the cement (ISO, 2007). Measuring elastic modules was another method applied by the manufacturer, based on the method used by Nonat and Franquin (2006). The final setting time, according to the manufacturer, was determined at around 10-12 minutes, when the elastic modulus reached 100 MPa (Septodont, 2010). In our study, the final setting of BD was approximately three times longer than that described by the manufacturer. This increase in setting time has been observed before. Grech et al. (2013), Kaup et al. (2015) and Elsaka et al. (2019) evaluated the final setting time to be 45 minutes, 85.66 minutes and 44 minutes, respectively, when an impression on the BD surface was no longer visible. These differences in setting time are probably attributable to slightly different experimental methodologies. These prolonged times could be because that the assembly was not stored at 37°C in a humid cabinet before testing. Dawood et al. (2015), however, placed the assembly at 37°C and reported the final setting time to be 13.1 minutes.

Another study reported the initial setting time to be 6.5 minutes (Butt et al., 2014). The initial setting time was recorded when a Vicat needle did not make an indentation of 1 mm in depth. This is not the same as measured in this study or in other studies where the final setting time was recorded (Grech et al., 2013, Kaup et al., 2015, Elsaka et al., 2019).

The results in this study show some decreases in the setting time when small amounts of CS-MMw (2.5 wt% and 5 wt%) were added. However, from 10% onwards there was a retardation in setting. It was observed that the addition of CS-MMw increased the stiffness of the BD paste, equating to a reduced water-to-powder ratio, during mixing as shown in Figure 5.1. An increase in water-to-powder ratio has been shown to increase Biodentine's setting time (Pires et al., 2021). Thus, reductions in set times could have been achieved by the decreasing the amount of the free mixing BD liquid, which subsequently led to acceleration in the setting time with the 2.5% and 5% samples. Accordingly, when BD integrated with small amount of CS-LMw (0.5 wt% and 1 wt%), the flowability of the cement reduced only slightly compared to the unmodified formula, which may explain the negligible reductions in the setting time of the CS-LMw groups. Paradoxically, increasing CS-MMw content up to 10 wt% and 20 wt% retarded the setting reactions. It has been shown that Biodentine sets through a hydration reaction (Camilleri, 2014). The addition of larger amounts of CS-MMw seemed to affect the hydration reaction of the cement adversely, by interrupting the connectivity between the cement grains, as shown in the SEM images, which results in an extended setting time.

5.5.2 Solubility

One of the most important properties determining the durability of dental cements is resistance against disintegration or dissolution (Nomoto and McCabe, 2001). The procedure which determines solubility and disintegration according to the ISO 6876:2012 standard (ISO, 2012) suggests measuring the increase in weight of the dish in which the material specimens have been kept after the final drying of the residue (the amount of BD removed from the material samples) by evaporating the free water (residue method, equation A). According to ISO, the solubility of the set material shall not exceed 3.0% of the initial

weight of the material following immersion in water for 24 h. In this study, the weight loss of Biodentine specimens was also recorded by measuring the weight changes of the test samples after storage in distilled water (equation B), as described in other publications (Zeid et al., 2015, Kaup et al., 2015, Alazrag et al., 2020).

It is worth mentioning that the solubility of a solid, as a physicochemical term, "can only be applied to the situation where a pure chemical compound is in thermodynamic equilibrium with its solution" (Wilson, 1976). It can be argued that the solubility test used, records the elution of water-soluble material, not the solubility in terms of its strict definition (Kaup et al., 2015). It can also measure disintegration of the cement particles that fall out during storage in water. Nevertheless, recording the weight loss after storage in water may result in water uptake that may compensate for dissolved materials (Kaup et al., 2015). The samples, therefore, were left to dry for 48 h to avoid an underestimation of weight loss due to water uptake. According to the results, the commercial BD showed a weight loss of less than 3%. Other authors reported a solubility of 2.65% (Kaup et al., 2015) and 3.36% (Alazrag et al., 2020) for BD after 24 h. The unmodified BD and the chitosan groups of 0.5%, 1% and 2.5% attained the ISO standard by showing a weight loss, in water, of less than 3%, whereas the modified groups with chitosan from 5 wt% and onwards showed higher disintegration (> 3%). Interestingly, the dissolution/disintegration of Biodentine in distilled water, calculated according to the formula (B), was lower than that recorded using the equation (A), as Biodentine (unmodified) exhibited a weight loss of 5% when cement residue was calculated as a percentage of the Biodentine original weight. These results may be of clinical relevance, as body fluid uptake from surrounding environment may result in growing Biodentine crystals that could partially compensate for a dissolved/disintegrated material.

Irrespective of the different calculation methods, the more chitosan in the sample, the greater its weight loss. This may have been attributed to the reducing in the connectivity of the cement network structure by increasing the gaps between the cement particles when more chitosan particles were incorporated into the material, where a chemical bond between the chitosan additives and the cement was not evident.

On the other hand, although lack of solubility has been considered as a favorable property for a root-end filling material (Torabinejad et al., 1993), a cement like Biodentine which produces calcium hydroxide through a hydration process (Camilleri, 2014) should present a certain level of solubility to enhance the mineralisation process (Kaup et al., 2015). It has been found that Biodentine leached more calcium ions than MTA (Zeid et al., 2015) and Theracal (a light curable resin modified Portland cement-based material) (Camilleri, 2014). On the other hand, it is unclear whether the high solubility recorded in '*in vitro*' studies has an adverse effect, clinically (E Silva et al., 2021). According to a systematic review and meta-analysis, calcium silicate-based sealers, in terms of solubility, have shown "worrying results" for clinical use (E Silva et al., 2021). Nevertheless, the overall clinical success rate of root canal treatment using calcium silicate sealer has been shown to be over 90% (Chybowski et al., 2018).

5.5.3 Radiopacity

Highly-radiopaque materials are recommended for root canals and filling bone defects, to allow better definition of the filling quality and levels of resorption (Pekkan, 2016). It is known that the radiopacity of 1 mm of dentine is equivalent to that of an equal thickness of aluminium, while enamel is twice as radiopaque as aluminium (Williams and Billington, 1987, Devito et al., 2004).

Therefore, use of an aluminium step wedge was recommended by the ISO standard (ISO, 2012) which established a minimum radiopacity corresponding to 3 mm Al for root canal sealing materials in clinical use. The ImageJ software determined the radiopacity in a simple and easily reproducible manner. Radiopacity of the unaltered Biodentine, was found to be 2.6 mm Al, regardless of the storage time at 37°C. This is different from the manufacturer's claims that BD possess a radiopacity of 3.5 mm of aluminium complying with the ISO standard. The results are, nonetheless, in agreement with a number of other studies which reported similar radiopacity values for this material. Biodentine, in different studies, display a radiopacity of 2.8 mm Al (Tanalp et al., 2013, Corral et al., 2018, Milutinović-Smiljanić et al., 2021), 2.9 mm Al (El-Din and El-Helbawy, 2016), and 2.06-2.52 mm Al, using conventional and digital radiography systems (Ochoa-Rodríguez et al., 2019). Lower results were

obtained by others who found an average radiopacity of 1.5 mm Al (Kaup et al., 2015). In contrast Farrugia et al. (2018) and Elsaka et al. (2019) reported a higher radiopacity values of 5.8 mm Al and 4.2 mm Al, respectively. Additionally, BD was found to yield radiopacity values of 4.1 to 3.3 mm Al (Grech et al., 2013) and approximately 4.8 to 4.3 mm Al (Camilleri et al., 2013) for 1 day and 28 days, respectively, following immersion in gelatinised Hank's balanced salt solution.

According to Camilleri et al. (Camilleri et al., 2013), 5.1 wt% of zirconium oxide has been detected in BD powder as radiopacifier to facilitate detection on radiographs. Nevertheless, clinicians have reported inadequate contrast between BD and surrounded structures when assessed radiographically, which compromises radiographic assessment of outcomes and follow-up (Bachoo et al., 2013). Integration of chitosan showed a decrease in BD radiopacity compared to the control in a dose-dependent manner. Biodentine incorporated with 0.5 wt% and 1 wt% of CS-LMw showed a negligible decrease by only 3%. Although the reductions with 2.5 wt% (6%) and 5 wt% (13%) of CS-MMw were not statistically significant, compared to the unmodified material, such small decreases in radiopacity may have an impact, clinically.

To get better understanding, one of the physical principles of the radiopacity of a substance is related, in part, to the atomic numbers of the object. The greater the atomic number (Z), the more radiopaque the object will be (Patil and Patil, 2009). Biodentine is made up mainly of calcium (Z=20), whereas the organic chitosan filler contains low atomic number elements such as carbon (Z=6), hydrogen (Z=1), nitrogen (Z=7) and oxygen (Z=8). It is therefore not surprising that incorporation of chitosan into Biodentine results in a reduction in radiopacity in a dose-dependent manner. In fact, an endodontic material with low radiopacity is a significant clinical problem, resulting in lack of clarity and misinterpretation that could lead to difficulties in diagnosis and assessment of technical outcomes of treatment or encountering unnecessary retreatment.

5.5.4 Cell viability and cytotoxicity

Materials used as a retrograde filling, such as Biodentine, are placed in intimate contact with apical bone and periodontal tissues. It is therefore essential that they should be biocompatible with these living host tissues (H Zhou et al., 2013). The biocompatible materials (tolerable biomaterials) may not be entirely "inert". In fact, a bioactive material is the one that elicits a specific biological response in the adjacent cells which results in promoting the healing process (Schmalz and Arenholt-Bindslev, 2009). However, the biocompatibility tests of dental materials generally assess the cytotoxicity of a material relative to certain cell lines. In the present study, the human embryonic kidney cell was selected as an *in vitro* model to assess cell viability. This cell line is a widely used model to assess cytotoxicity (Kulshrestha et al., 2016, Barma et al., 2021). Cell viability was determined by using MTT-based colorimetric assay. The MTT assay measures cellular metabolic activity as an indicator of cell viability and proliferation (Vistica et al., 1991). This colorimetric assay is based on the reduction of a yellow tetrazolium salt [3-(4,5-dimethylthiazol-2-yl)-2,5-diphenyltetrazolium bromide], by metabolically active cells, to coloured formazan derivatives that can be quantitated spectrophotometrically (Vistica et al., 1991).

Based on the results of this study, the high cell viability of BD-treated cells, at all extract concentrations, could be attributed to the constituents of the material itself, which is mainly composed of tricalcium silicate and dicalcium silicate (Margunato et al., 2015). The biocompatibility and bioactivity of Biodentine and its capacity to stimulate the mineralisation process have been reported by other researchers (Margunato et al., 2015, Escobar-García et al., 2016, Widbiller et al., 2016, Widbiller et al., 2022). In contrast, the addition of chitosan powder into BD significantly reduced the metabolic activity of cultured cells in a dose-dependent manner. As expected, diluted extracts from modified Biodentine, in DMEM, showing higher percentages of cell viability with a similar trend observed amongst undiluted and diluted extracts. This is relevant clinically as when a root canal filling material is placed as an orthograde or a retrograde filling *in vivo*, leached substances may be diluted by tissue fluids. Thus, material

extracts were performed to simulate a possible dose-response effect occurring *in vivo* (Yoshino et al., 2013).

Reduced metabolic activity of the cells shown might be a precondition to cellular cytotoxicity. Although the MTT assay has been widely used as a 'gold standard' for testing the cytotoxicity of root filling materials (Jagtap et al., 2018, Ferreira et al., 2019, Nabavizadeh et al., 2022), it was not found to be sensitive in detecting small changes in cell number and not robust enough to generate reproducible results (Van Tonder et al., 2015). Therefore, to determine cytotoxicity on a more relevant cell line (h-DPSCs), an alternative and more sensitive assay has been used; the LDH assay. This is a widely used method for determining cytotoxicity based on measuring the activity of cytoplasmic enzyme released by damaged cells. Lactate dehydrogenase is a cytosolic enzyme that is found in many different cell types. Damage to the plasma membrane rapidly releases LDH into the cell culture supernatant; a reliable indicator of cytotoxicity (Kumar et al., 2018). Based on the results, the undiluted extracts of Biodentine with small concentrations of CS-LMw (0.5 wt% and 1 wt%) showed no cytotoxic effect on h-DPSCs at 72 h.

The cytotoxicity in human liver cells has been delineated by Loh et al. (2010), following exposure to higher concentrations (above 0.5% w/v) of MMw chitosan nanoparticles, where cellular uptake of CSNPs was visualised into the nucleus, at a nanoparticle concentration of 1% w/v, and the integrity of the cell membrane was compromised, as evidenced by enzyme leakage (Loh et al., 2010). The findings of another study suggested that CSNPs, were relatively non-toxic to mouse hematopoietic stem cells, at low concentrations (10 and 100 µg/mL), and the toxicity was concentration dependent (Omar Zaki et al., 2015). However, in a study by VandeVord et al. (2002), chitosan scaffold (prepared from a 2 wt% chitosan solution) showed a high degree of biocompatibility in a mouse implantation model. Although the material leachate was used in this study, these results may indicate that the use of chitosan in dental materials could be applicable in low concentrations, where the material antimicrobial property can be beneficial against microbial biofilms.

5.5.5 Surface topography

Scanning electron microscopic analysis of the surface of hydrated BD revealed intergrowth of fibers accompanied and covered by needle-like crystals. The former was thought to be a form of C-S-H; one of the main products of the hydration process of tricalcium silicate (Camilleri et al., 2013). The lack of superficial deposition of hexagonal plate-like crystals of $Ca(OH)_2$ (Portlandite) is thought to be due to the low porosity of BD that discourages crystal deposition and attachment (Camilleri, 2014). These needle-like structures on the BD surface, kept in a humid environment, were observed in other studies (Elnaghy, 2014b) when BD was exposed to different acidic pH values (Elnaghy, 2014a). These crystals are believed to be calcium carbonate (calcite) (H Singh et al., 2014). Chitosan microparticles have been observed in dispersion within the material, in clumps that seemed to interfere with the crystalline formation, particularly at 10 wt% and 20 wt% CS-MMw. Highly disturbed crystalline structures could explain the significant decrease in the material mechanical properties. In relation to this, the formation of needle-shaped crystals in MTA is believed to be important in interlocking the entire material mass, and their absence can decrease the material hardness (Lee et al., 2004).

5.5.6 Compressive strength and microhardness

While compressive strength and microhardness of BD are not of primary concern, when placed as a root-end filling or perforation repair where it does not bear any direct pressure nor penetration, the CSI is relevant when used as a direct pulp capping agent where it must be able to withstand forces generated during mastication. The samples were measured at 30 days because the compressive strength of the material has been shown to rise up over time until reaching a maximum strength after one month, when compared to 1 and 7 days (Butt et al., 2014).

In this study, the compressive strength of the commercial BD, at 30 days, was determined to be 182.88 ±32.96 MPa and 134.78 ±42.84 MPa. However, in other studies, the CS of Biodentine was 304.78 ±2.59 MPa (Butt et al., 2014) and 60.17 ±37.51 MPa (Atmeh, 2020). In the previous two studies, although BD samples were stored in water for 28 days, there was a significant difference between the

results (304.78 MPa vs 60.17 MPa). It has also been affirmed that Biodentine, at 28 days, following immersion in HBSS, had a compressive strength and microhardness of 67.18 MPa and 48.4 HV, respectively (Grech et al., 2013). In another study, microhardness of Biodentine, at 1 month, was determined to be 79.8 ±3.97 HV (Bayraktar et al., 2021). In contrast, the microhardness in this study was found to be 113.60 ±10.20 HV. Different experimental setups between studies and different testing Machines used may explain the discrepancy between these results.

Biodentine has been shown to be less porous than other tricalcium materials (Camilleri et al., 2014). The reduction of the manufacturer water quantity due to the presence of the hydrosoluble polymer “water reducing agent” (Septodont, 2010), reduces the material porosity. Biodentine sets through a hydration process that produces calcium silicate hydrate (CSH) and calcium hydroxide (Camilleri, 2014). The porosity of BD is mainly filled by C-S-H, and by $Ca(OH)_2$, to a lesser extent (Camilleri et al., 2013). Thus, Biodentine gains strength and becomes denser through the hydration reaction. The reductions in both compressive strength and microhardness shown by increasing the amount of chitosan incorporation occur in a dose-dependent manner. These observations suggest that the interface between chitosan particles and the hydration products of Biodentine was weak. Chitosan addition seemed to disturb the hydration reaction and crystalline structure of BD which results in compromising the cement’s mechanical properties greatly. According to Luković et al. (2015), the development and propagation of microcracks within a cement are controlled by local stress distribution and weak links in the structure. If the cement has high heterogeneity, this leads to microcracking almost through the whole specimen (Luković et al., 2015). In relation to this concept, it has been shown that the inter-connections and the strong chemical bonding between C-S-H and the limestone filler, resulting in strength development and a very high resistance of the cement to crack propagation, after applying a mechanical load (Ouyang et al., 2017). This is the same as in the composite material where non-silanated filler particles reduced the strength of the material, whereas particles coated with a silane agent increased the strength of resin composites by enhancing the adhesion between the filler and resin matrix (McCool et al., 2001, Ferracane and Palin, 2013).

However, the compressive strength of the 0.5% group was 88 MPa, which is greater than those obtained for Glass Ionomer (47 MPa) (Ezz et al., 2018), Super ethoxybenzoic acid (60-78 MPa) and intermediate restorative material (52-57 MPa) (Torabinejad et al., 1995). All of these materials have been used successfully as lining and in load bearing areas for decades. In fact, compressive strength and microhardness are not important factors to consider when a filling material does not bear a direct pressure nor scratching, such as root-end fillings and liners. Thus, the clinical use of the modified BD with smaller amount of chitosan could be limited to those applications where the material bioactivity can be beneficial, but a high compressive strength is not necessarily required. However, even with the addition of 0.5% CS-LMw, the compressive strength of the modified Biodentine material was superior to ProRoot MTA (40-67 MPa) (Torabinejad et al., 1995). Thus, this new composite would still be applicable for use in any situation where MTA might be considered.

CHAPTER FINDINGS

- Incorporation of 2.5 wt% and 5 wt% chitosan MMw delivers an advantage by accelerating the setting time of the material.
- Chitosan MMw (2.5 wt% to 20 wt%) incorporation compromises material properties and the crystalline structure in a dose dependent manner, which is likely to reduce its clinical value.
- The addition of small proportions of chitosan LMw (0.5 wt% and 1 wt%) shows no detrimental effects on the physical properties (setting, radiopacity and solubility) of the material nor cytotoxic effect on human stem cells.
- Incorporation of 0.5 wt% and 1 wt% chitosan LMw into Biodentine reduces the mechanical properties of the material. Despite these reductions, such a new composite could still be utilised in various endodontic applications.

6 Final discussion

The principal goal of this thesis was to establish an interkingdom biofilm model that can be utilised in assessing different endodontic therapeutics. An interkingdom multispecies model can offer a more appropriate and relevant biofilm for continued investigation of different approaches, instruments and materials used in endodontic practice. This final chapter aims to address questions related to the major findings, highlight the limitations and discuss the potential areas of future research.

6.1 What is the keystone pathogen in endodontic infections?

In architecture, the keystone is the central supporting stone at the summit of an arch, locking the other pieces together in place. The term "keystone" has been introduced in the ecological literature to characterise species that were thought to be the keystone of the community's structure, because of their disproportionately large effects on their communities (Paine, 1969). Looking at the ecology of our own body, the complexity of the oral cavity represents a challenge for microbiologists, with diverse environments in which highly complex microbial communities of hundreds of microbial species communicate and interact. This, of course, raises the question: "what are all these species doing there?" (Janus et al., 2016). The concept of "keystone" has been expanded as a keystone pathogen in human microbiota. It has been hypothesised that *P. gingivalis* might be a keystone pathogen in periodontal disease by using sophisticated strategies to disturb the normally homeostatic host-microbiota, thereby creating dysbiosis of the periodontal microbiota leading to inflammation (Hajishengallis et al., 2012). This was supported by a study in a mouse model showing the ability of *P. gingivalis*, at very low colonisation level, to induce significant alterations in the amount and composition of the oral commensal bacteria that drive inflammatory periodontal bone loss (Hajishengallis et al., 2011). Similarly, it has been postulated that yeasts in general, and *C. albicans* specifically, may act as potential keystone components of oral biofilms (Young et al., 2021). This postulation was based on the findings of Young et al. (2021) where *C. albicans* conferred protection upon bacterial species against different antimicrobials. In the endodontic literature, *E. faecalis* has been identified as a keystone player in endodontic infections (Sahar-Helft et al., 2019). This

assumption was based upon the high detection rate of *E. faecalis* in root canals with persistent intraradicular infections (C Zhang et al., 2015). Recently, Korona-Glowniak et al. (2021) stated that all species detected in teeth with apical periodontitis were important and contributing to the entire microbial community. Korona-Glowniak et al. (2021), whilst dismissing the contribution of fungi to endodontic infections, considered bacterial species such as *Propionibacterium acnes*, *F. nucleatum*, *Streptococcus* spp., *Lactobacillus* spp. and *E. faecalis*, as possible keystone pathogens. Thus, the body of work in this thesis does not exonerate *E. faecalis* by its exclusion, but instead acknowledges the emerging postulations that there are many other potential important or 'keystone' pathogens in endodontic infections rather than a single pathogen.

6.2 Do interkingdom interactions modify microbial tolerance against endodontic antimicrobials?

Bacteria and fungi have adopted many mechanisms of resistance to help them evade antimicrobials (McKeegan et al., 2002). The growing problem of antibiotic resistance is a significant threat that makes infectious diseases harder, or even impossible to treat with existing antibiotics (English and Gaur, 2010). The terms "resistance" and "tolerance" are often used interchangeably in the literature. This may lead to misclassification of resistant strains as tolerant, and vice versa (Rapacka-Zdonczyk et al., 2021). To make a clear distinction, resistance refers to an inherited or acquired insensitivity of microorganisms to a drug, as a result of inherent structural characteristics or via mutations in genes (Scholar et al., 2000, Blair et al., 2015). In other words, resistance is defined as a decline in effectiveness of a given antibiotic at high concentrations against microorganisms, irrespective of the duration of treatment. Resistance is determined using MIC testing. Tolerance, unlike resistance, is a more general term used to describe the ability of microbial populations to survive temporary exposure to concentrations of an antibiotic that would otherwise be lethal, without a change in the MIC (Scholar et al., 2000, Brauner et al., 2016). Thus, it is been thought that tolerant strains require a longer exposure to a drug rather than a high concentration in order to produce the required level of killing (Brauner et al., 2016). Tolerance may be conferred by cross-kingdom interactions. For instance, *C. albicans* was shown to enhance the tolerance of

Pseudomonas aeruginosa biofilm to an antibiotic (meropenem) at a clinically relevant concentration. The findings revealed that *P. aeruginosa* tolerance was afforded by the protective effect of *Candida*-derived ECM (Alam et al., 2020). In contrast, the finding by D Kim et al. (2018) indicated that *Streptococcus mutans* enhanced *C. albicans* biofilm tolerance to fluconazole. Secreted bacterial extracellular polysaccharides (EPS) were shown to have the protective effect by reducing the efficacy of the antifungal drug (D Kim et al., 2018). These shielding effects shown were biofilm specific. This could result in acquiring true drug resistance, clinically (Alam et al., 2020). Similarly, bacterial species, in this work, showed higher levels of tolerance to chitosan when co-cultured with *C. albicans*, whereas the tolerance of *C. albicans* to chitosan reduced when co-cultured with bacteria. Although one of the limitations of this study is that the microbial burden was quantified after a relatively short-term exposure (24 h) to treatment, these data provide new insights for treatment of polymicrobial endodontic infections. Hence, a better understanding of interkingdom and interspecies interactions and how these impact antimicrobial tolerance which is potentially of great importance to our clinical practice.

6.3 How do calcium silicate materials behave in the real world?

It is challenging to predict what the biological behaviour of calcium silicate materials is, in clinical situations, where many biological factors cannot adequately be presented *in vitro*. It may be possible, however, to speculate their behavior in the host environment, based on the existing knowledge. It is known that the main remaining elements in an empty root canal before obturation are dentine, moisture and potentially some residual surviving microorganisms left after treatment. Following the root canal disinfection procedures, the root canal is filled with a calcium silicate material that comes into contact with dentine and surrounding tissues. Tricalcium silicate hydrates into calcium silicate hydrate and calcium hydroxide, which can result in a crystalline deposition of calcium phosphate when the hydrated cement is in contact with a physiological fluid (Camilleri, 2011). The deposition of hydroxyapatite is also aided by the calcium silicate hydrate which produces a good surface for the nucleation of the crystals (Camilleri, 2011). Initially, the

presence of dentine moisture (Papa et al., 1994) in contact with the material may sustain the chemical dissociation of calcium hydroxide and the release of calcium ions (Gandolfi et al., 2012). These would likely penetrate the surrounding dentine (Hosoya et al., 2001) and neutralise acids, thus creating a healing environment (Qadiri and Mustafa, 2019). It has been thought that the initial antimicrobial effect of calcium silicate materials may be achieved by their high alkalinity (Al-Hezaimi et al., 2006, Abou ElReash et al., 2019). However, the work in this thesis showed that increased alkalinity did not show an antimicrobial effect against biofilm regrowth in optimised *in vitro* conditions. The antimicrobial effect of calcium silicate-based materials could initially be achieved, clinically, by their excellent physical sealing ability, when applied to seal the portals of the root canal system, thus preventing microleakage and fluid penetration. Having said that, it is difficult to draw the conclusion that these unmodified calcium silicate materials do not possess an antimicrobial activity in '*in vivo*' conditions. In fact, these materials may possess antimicrobial properties against a low microbial load of residual microorganisms that do not exceed the threshold/capacity of their antimicrobial action. Interestingly, the hydration reactions and structure maturation of a calcium silicate cement can continue over a one-year period (Chedella and Berzins, 2010). Meanwhile, the hydroxyapatite crystals can nucleate and grow into the root canals and fill the microscopic space between the cement and the dentinal wall (Sarkar et al., 2003), creating mechanical and chemical bonds (Sarkar et al., 2005). Importantly, the material could entomb the remaining intracanal bacteria within the dentinal tubules (Yoo et al., 2014). The calcium silicate materials can also stimulate dentinal bridge formation (Nasri et al., 2022). The first member of the calcium silicate material (MTA) was found to promote regeneration of the periradicular periodontium when used as a root-end filling. A complete cemental coverage was formed over the root end and the root-end filling, incorporating both a physical and biological covering or "a double seal" of the resected root end (Regan et al., 2002). Calcium silicate materials were shown to have high success rates of 91.6% at a 4-year follow-up (S Kim et al., 2016), 91.7% at a 3-year follow-up (Awawdeh et al., 2018a), 93.1% and 94.4% at a 1-year follow-up (W Zhou et al., 2017), across multiple treatments. As these materials did not show a 100% success rate, there is still room to improve the success rates,

possibly by augmenting their antimicrobial activity with suitable antimicrobial additives, against persistent microorganisms.

6.4 How to interpret statistical significance in its logical context?

A randomised clinical study by Rôças et al. (2016) compared the antibacterial efficacy of irrigation with either 2.5% NaOCl or 2% CHX as the main irrigant of infected root canals with apical periodontitis. The results indicated that both irrigants reduced total bacterial counts effectively. No statistically significant difference was found between the two irrigations. Regardless of these results, Rôças et al. (2016) did not define the long-term treatment outcomes when using both irrigation protocols. This would raise the inevitable question: what is the statistically significant/insignificant mean?

One of the common pitfalls faced by readers of scientific literature is the misinterpretation of the concept of "significance". According to the Scientific Committee (SC), "Statistical significance is considered as just one part of an appropriate statistical analysis of a well-designed experiment or study" (SC, 2011). Statistical significance is a concept associated with the use of a specific statistical test to test a null hypothesis of no difference between two or more variables. This significance, when $p < 0.05$, is unlikely to have occurred by chance alone (Andrade, 2019). The concept of biological relevance, in clinical trials, refers to a biological effect of interest, based on expert judgement, that is considered important and meaningful (SC, 2011). In other words, the term "significant" does not necessarily mean that the difference is large or biologically/clinically relevant; it could be smaller than the pre-defined relevant biological/clinical effect, and vice versa (SC, 2011).

In fact, a problem can also arise in the interpretation of statistical anaysis of *in vitro* studies, especially when standards designated to define the clinical relevance do not exist. According to ISO (ISO, 2012), the weight loss of a set material shall not exceed 3.0% of the initial weight. Although the ISO standards are still the cornerstone in assessing root canal sealing materials, it is unknown whether highly significant solubility results, *in vitro*, have an adverse effect

clinically (E Silva et al., 2021). On the other hand, the ISO standard established a minimum radiopacity of root filling materials, for clinical use, corresponding to 3 mm thickness of aluminium, to allow adequate contrast between the material and surrounding structures on radiographs. Therefore, and regardless of "statistically insignificant results", a material demonstrating a radiopacity of less than 3 mm Al *in vitro* may hinder its detection on radiographs, as shown by other clinicians with the Biodentine material (Dammaschke, 2012a, Bachoo et al., 2013). Therefore, it may be crucial to use pre-defined relevant standards when initiating a study, though it may be difficult to define the clinical relevance in each situation.

6.5 Future work

In this body of work, chitosan microparticles were incorporated into the calcium silicate materials. A microparticle is defined to have a physical dimension in the range of 0.1 to 100 μm, although the lower limit between micro- and nano-sizing is still debatable (Vert et al., 2012). These particles have displayed an exceptional improvement to the antimicrobial properties of Biodentine, particularly when the low molecular weight was used. This could be due to size effects (Ye et al., 2008), as the molecular particle size decreases with a decrease in the molecular weight.

Various additives have been used, in the literature, to investigate the effects upon the antimicrobial, physicochemical, mechanical and biological properties of current commercial calcium silicate materials. In recent years, nanoparticles have received increasing attention in dentistry. It is been thought that these tiny particles have the great potential to improve diagnosis, treatment and prevention of many oral diseases because of their unique physicochemical and biological characteristics (Bapat et al., 2019, Moraes et al., 2021). Therefore, future studies may merit consideration of incorporating pure chitosan nanoparticles into Biodentine and other calcium silicate materials, produced by a chemical bottom-up method, as outlined in chapter 1.

In fact, in this work, we were also limited to use insoluble chitosan from crustacean sources, due to financial implications and product availability. There

may be merit in considering a repeat of the current work with water soluble chitosan that could be dissolved easily in the manufacturers' liquid of MTA and Biodentine materials, without the aid of solvents. Using fungal chitosan, which has received less research interest, could be another novel approach to be considered.

Importantly, such work should not be limited to chitosan microparticle and nanoparticle technologies. There is a burgeoning field that show distinct promise and open potential applications in endodontics. For instance, modifying MTA and Biodentine, by adding a natural substance such as 1 wt% of eggshell powder, was found to improve their bioactivity and sealing ability through mineral deposition at root dentine/material interface (Beshr and Abdelrahim, 2019b). However, the antimicrobial efficacy of the new composites has not been investigated yet. In addition, modifying MTA with AgNPs (Bahador et al., 2015), bismuth lipophilic NPs (Hernandez-Delgadillo et al., 2017) and copper iodide NPs (Atchison, 2018) were shown to significantly enhance the antimicrobial properties of the material. Therefore, further research is needed, using an appropriate biofilm model where interspecies and interkingdom interactions that may modify microbial tolerance are not dismissed.

The current work paves the way for greater understanding and further advancements in endodontic research and knowledge. A general overview of thesis' chapters has been summarised below in Figure 6.1.

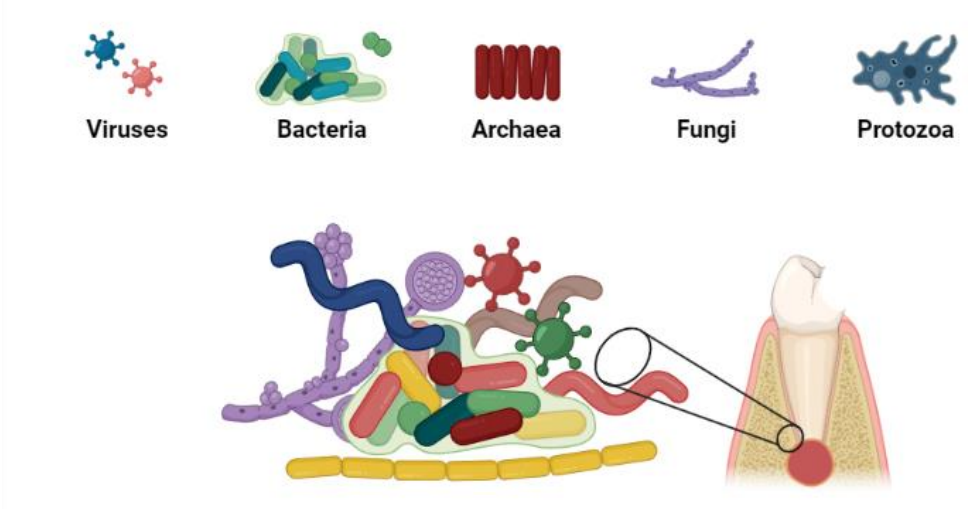

Chapter 1: A general overview – endodontic microbiology

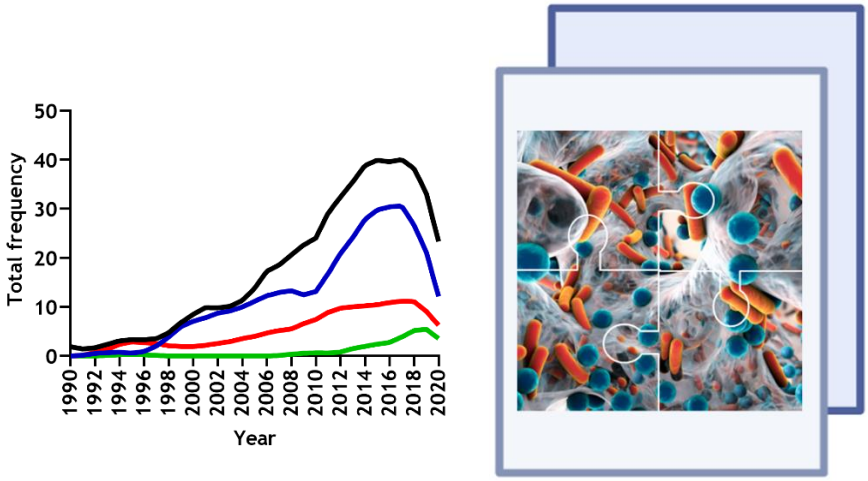

Chapter 2: Analysis of scientific research outputs

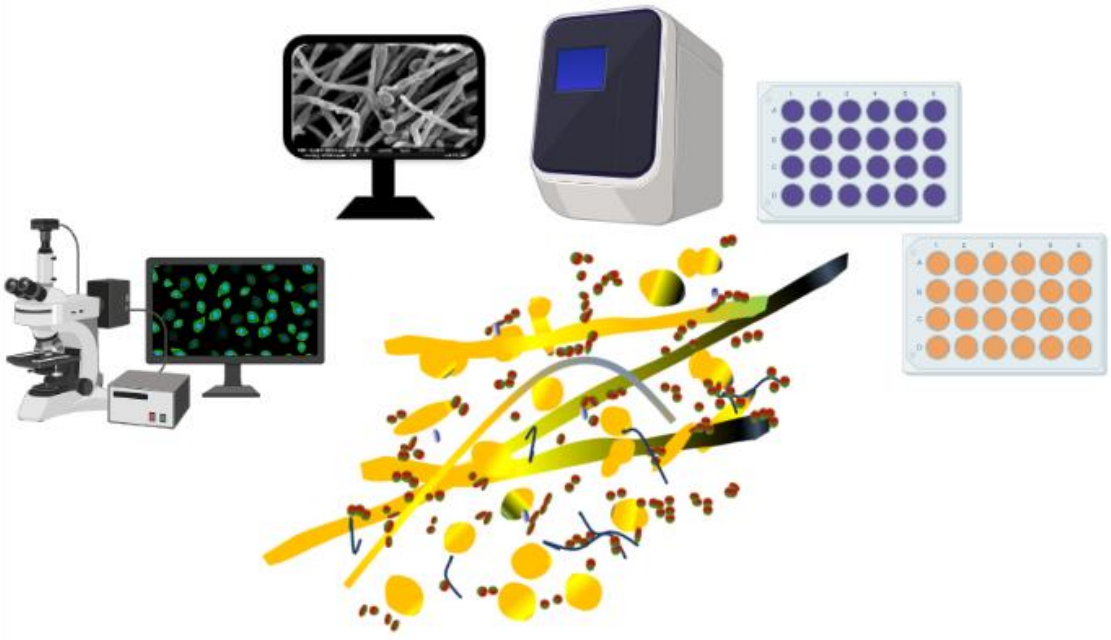

Chapter 3: Developing a polymicrobial interkingdom biofilm model

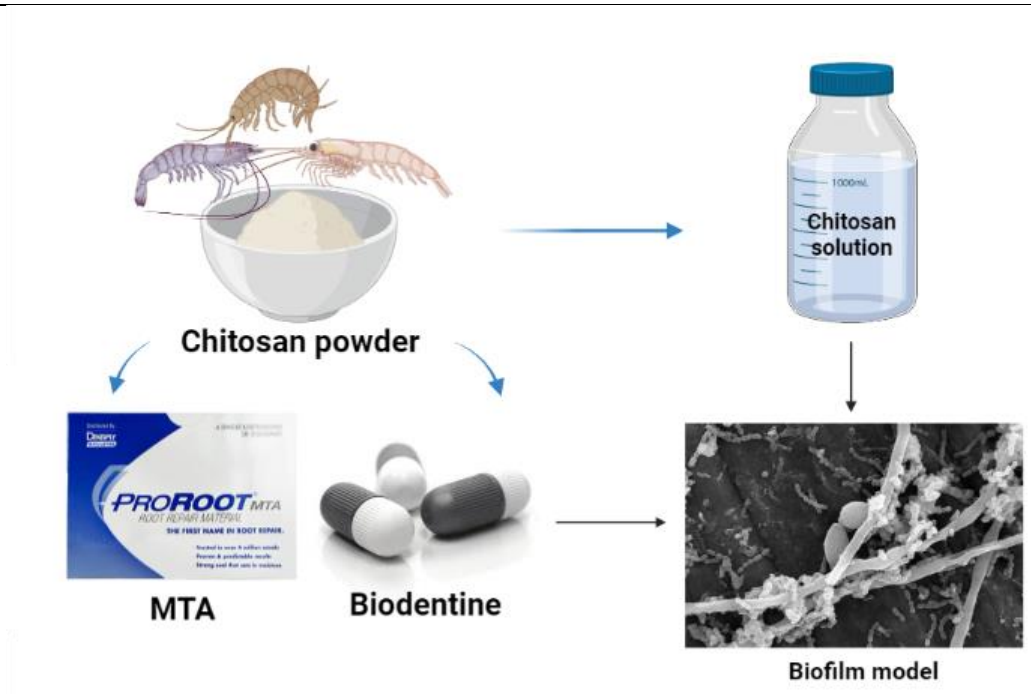

Chapter 4: Assessing antimicrobial properties of chitosan and calcium silicate materials ± chitosan

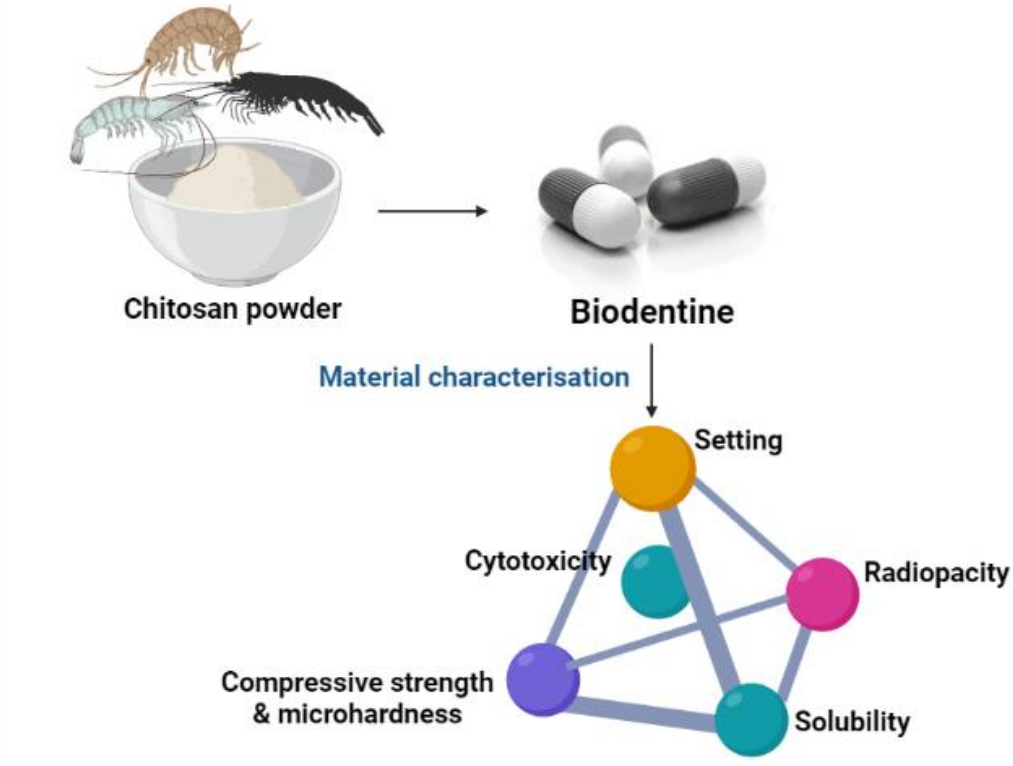

Chapter 5: Assessing the effect of chitosan incorporation on material characteristics of Biodentine™

Figure 6.1. A graphical overview of thesis's chapters. Diagram was created in Microsoft PowerPoint and BioRender.com.

7 References

A SINGH, A. & PUROHIT, K. 2011. Chemical synthesis, characterization and bioactivity evaluation of hydroxyapatite prepared from garden snail (helix aspersa). *Journal of Biotechnology & Biomaterials,* 1, 104-109.

A SMITH, A., TOBIAS, R., PLANT, C., BROWNE, R., LESOT, H. & RUCH, J. 1990. In vivo morphogenetic activity of dentine matrix proteins. *Journal de Biologie Buccale,* 18, 123-129.

AAE 2002. American Association of Endodontists - Clinical and Biological Implications in Endodontic Success. *ENDODONTICS: Colleagues for Excellence*, 1-6.

AAE 2009. American Association of Endodontists - Obturation of Root Canal Systems. *ENDODONTICS: Colleagues for Excellence*, 1-8.

AAE 2013. American Association of Endodontists - Endodontic Diagnosis *ENDODONTICS: Colleagues for Excellence*, 1-6.

AAE 2020. American Association of Endodontists - glossary of endodontic terms. 1-47.

AAE 2021. American Association of Endodontists - Clinical Considerations for a Regenerative Procedure. *ENDODONTICS: Colleagues for Excellence*, 1-8.

ABOU ELREASH, A., HAMAMA, H., ELDARS, W., LINGWEI, G., EL-DIN, A. M. Z. & XIAOLI, X. 2019. Antimicrobial activity and pH measurement of calcium silicate cements versus new bioactive resin composite restorative material. *BMC Oral Health,* 19, 235.

ABRAHAM, N. M. & JEFFERSON, K. K. 2010. A low molecular weight component of serum inhibits biofilm formation in Staphylococcus aureus. *Microbial Pathogenesis,* 49, 388-391.

ADNAN, S. & ULLAH, R. 2018. Top-cited articles in regenerative endodontics: a bibliometric analysis. *Journal of Endodontics,* 44, 1650-1664.

ADUNLIN, G., DIABY, V. & XIAO, H. 2015. Application of multicriteria decision analysis in health care: a systematic review and bibliometric analysis. *Health Expectations,* 18, 1894-1905.

AFKHAMI, F., POURHASHEMI, S. J., SADEGH, M., SALEHI, Y. & FARD, M. J. K. 2015. Antibiofilm efficacy of silver nanoparticles as a vehicle for calcium hydroxide medicament against Enterococcus faecalis. *Journal of Dentistry,* 43, 1573-1579.

AGARWAL, A., DURAIRAJANAYAGAM, D., TATAGARI, S., ESTEVES, S. C., HARLEV, A., HENKEL, R., ROYCHOUDHURY, S., HOMA, S., PUCHALT, N. G. & RAMASAMY, R. 2016. Bibliometrics: tracking research impact by selecting the appropriate metrics. *Asian Journal of Andrology,* 18, 296-309.

AHANGARI, Z., ALBORZI, S., YADEGARI, Z., DEHGHANI, F., AHANGARI, L. & NASERI, M. 2013. The effect of propolis as a biological storage media on periodontal ligament cell survival in an avulsed tooth: an in vitro study. *Cell Journal (Yakhteh),* 15, 244-249.

AHMADI, F., OVEISI, Z., SAMANI, S. M. & AMOOZGAR, Z. 2015. Chitosan based hydrogels: characteristics and pharmaceutical applications. *Research in Pharmaceutical Sciences,* 10, 1-16.

AIDAROS, N. H., NIAZY, M. A. & EL-YASSAKY, M. A. 2018. The Effect of Incorporating Nanocalcium Phosphate Particles into Biodentine on Pulpal Tissue Response (In Vitro Study). *Al-Azhar Dental Journal for Girls,* 5, 181-186.

AKCA, G., ÖZDEMIR, A., ÖNER, Z. G. & ŞENEL, S. 2018. Comparison of different types and sources of chitosan for the treatment of infections in the oral cavity. *Research on Chemical Intermediates,* 44, 4811-4825.

AKSNES, D. W. 2008. When different persons have an identical author name. How frequent are homonyms? *Journal of the American Society for Information Science and Technology,* 59**,** 838-841.

AL-HEZAIMI, K., AL-SHALAN, T. A., NAGHSHBANDI, J., OGLESBY, S., SIMON, J. H. & ROTSTEIN, I. 2006. Antibacterial effect of two mineral trioxide aggregate (MTA) preparations against Enterococcus faecalis and Streptococcus sanguis in vitro. *Journal of Endodontics,* 32**,** 1053-1056.

ALAM, F., CATLOW, D., DI MAIO, A., BLAIR, J. M. & HALL, R. A. 2020. Candida albicans enhances meropenem tolerance of Pseudomonas aeruginosa in a dual-species biofilm. *Journal of Antimicrobial Chemotherapy,* 75**,** 925-935.

ALAZRAG, M., ABU-SEIDA, A. M., EL-BATOUTY, K. M. & EL ASHRY, S. H. 2020. Marginal adaptation, solubility and biocompatibility of TheraCal LC compared with MTA-angelus and biodentine as a furcation perforation repair material. *BMC Oral Health,* 20**,** 1-12.

ALCALDE, M. P., BRAMANTE, C. M., VIVAN, R. R., AMORSO-SILVA, P. A., ANDRADE, F. B. D. & DUARTE, M. A. H. 2017. Intradentinal antimicrobial action and filling quality promoted by ultrasonic agitation of epoxy resin-based sealer in endodontic obturation. *Journal of Applied Oral Science,* 25**,** 641-649.

ALEANIZY, F. S., ALQAHTANI, F. Y., SHAZLY, G., ALFARAJ, R., ALSARRA, I., ALSHAMSAN, A. & ABDULHADY, H. G. 2018. Measurement and evaluation of the effects of pH gradients on the antimicrobial and antivirulence activities of chitosan nanoparticles in Pseudomonas aeruginosa. *Saudi Pharmaceutical Journal,* 26**,** 79-83.

ALEXANDER, J. W. 2009. History of the medical use of silver. *Surgical Infections,* 10**,** 289-292.

ALGHAMDI, F. & SHAKIR, M. 2020. The influence of Enterococcus faecalis as a dental root canal pathogen on endodontic treatment: A systematic review. *Cureus,* 12**,** e7257.

ALHEDE, M., QVORTRUP, K., LIEBRECHTS, R., HØIBY, N., GIVSKOV, M. & BJARNSHOLT, T. 2012. Combination of microscopic techniques reveals a comprehensive visual impression of biofilm structure and composition. *FEMS Immunology & Medical Microbiology,* 65**,** 335-342.

ALLKJA, J., BJARNSHOLT, T., COENYE, T., COS, P., FALLARERO, A., HARRISON, J. J., LOPES, S. P., OLIVER, A., PEREIRA, M. O. & RAMAGE, G. 2020. Minimum information guideline for spectrophotometric and fluorometric methods to assess biofilm formation in microplates. *Biofilm,* 2**,** 100010.

ALMADI, E. M. & ALMOHAIMEDE, A. A. 2018. Natural products in endodontics. *Saudi Medical Journal,* 39**,** 124-130.

ALSHANTA, O. A., ALBASHAIREH, K., MCKLOUD, E., DELANEY, C., KEAN, R., MCLEAN, W. & RAMAGE, G. 2022. Candida albicans and Enterococcus faecalis biofilm frenemies: When the relationship sours. *Biofilm,* 4**,** 100072.

ALSHANTA, O. A., ALQAHTANI, S., SHABAN, S., ALBASHAIREH, K., MCLEAN, W. & RAMAGE, G. 2020. Comparison of Three Endodontic Irrigant Regimens against Dual-Species Interkingdom Biofilms: Considerations for Maintaining the Status Quo. *Antibiotics,* 9**,** 634.

ALSHANTA, O. A., SHABAN, S., NILE, C. J., MCLEAN, W. & RAMAGE, G. 2019. Candida albicans Biofilm Heterogeneity and Tolerance of Clinical Isolates: Implications for Secondary Endodontic Infections. *Antibiotics,* 8**,** 204.

ANDRADE, C. 2019. The P value and statistical significance: misunderstandings, explanations, challenges, and alternatives. *Indian Journal of Psychological Medicine,* 41, 210-215.

ANTUNES, P. V. S., FLAMINI, L. E. S., CHAVES, J. F. M., SILVA, R. G. & CRUZ FILHO, A. M. D. 2019. Comparative effects of final canal irrigation with chitosan and EDTA. *Journal of Applied Oral Science,* 28, e20190005.

ARANA-CHAVEZ, V. E. & MASSA, L. F. 2004. Odontoblasts: the cells forming and maintaining dentine. *The International Journal of Biochemistry & Cell biology,* 36, 1367-1373.

ARENS, D. E., GLUSKIN, A. H., PETERS, C. I. & PETERS, O. A. 2009. Practical lessons in endodontic treatment, Quintessence, 213-220.

ARIA, M. & CUCCURULLO, C. 2017. bibliometrix: An R-tool for comprehensive science mapping analysis. *Journal of Informetrics,* 11, 959-975.

ARIAS, L. S., BROWN, J. L., BUTCHER, M. C., DELANEY, C., MONTEIRO, D. R. & RAMAGE, G. 2020a. A nanocarrier system that potentiates the effect of miconazole within different interkingdom biofilms. *Journal of Oral Microbiology,* 12, 1771071.

ARIAS, L. S., BUTCHER, M. C., SHORT, B., MCKLOUD, E., DELANEY, C., KEAN, R., MONTEIRO, D. R., WILLIAMS, C., RAMAGE, G. & BROWN, J. L. 2020b. Chitosan ameliorates Candida auris virulence in a Galleria mellonella infection model. *Antimicrobial Agents and Chemotherapy,* 64, e00476-00420.

ARNAUD, T. M. S., DE BARROS NETO, B. & DINIZ, F. B. 2010. Chitosan effect on dental enamel de-remineralization: an in vitro evaluation. *Journal of Dentistry,* 38, 848-852.

ARROUZE, F., ESSAHLI, M., RHAZI, M., DESBRIERES, J. & TOLAIMATE, A. 2017. Chitin and chitosan: study of the possibilities of their production by valorization of the waste of crustaceans and cephalopods rejected in Essaouira. *Journal of Materials and Environmental Science,* 8, 2251-2258.

ARSLAN, H., AHMED, H. M. A., ŞAHIN, Y., YıLDıZ, E. D., GÜNDOĞDU, E. C., GÜVEN, Y. & KHALILOV, R. 2019. Regenerative Endodontic Procedures in Necrotic Mature Teeth with Periapical Radiolucencies: A Preliminary Randomized Clinical Study. *Journal of Endodontics,* 45, 863-872.

ARZMI, M. H., DASHPER, S., CATMULL, D., CIRILLO, N., REYNOLDS, E. C. & MCCULLOUGH, M. 2015. Coaggregation of Candida albicans, Actinomyces naeslundii and Streptococcus mutans is Candida albicans strain dependent. *FEMS Yeast Research,* 15, fov038.

ATCHISON, C. A. 2018. *The Efficacy of Copper Iodide Nanoparticle-Augmented MTA against Enterococcus Faecalis: A Confocal Microscopy Study*. Medical University of South Carolina.

ATLAS, A., GRANDINI, S. & MARTIGNONI, M. 2019. Evidence-based treatment planning for the restoration of endodontically treated single teeth: importance of coronal seal, post vs no post, and indirect vs direct restoration. *Quintessence International,* 50, 772-781.

ATMEH, A. R. 2020. Investigating the effect of bicarbonate ion on the structure and strength of calcium silicate-based dental restorative material—Biodentine. *Clinical Oral Investigations,* 24, 4597-4606.

ATOM, J., DEVI, N. R., LAIRENLAKPAM, R., AL WADEI, M. H. D., HAKAMI, A. R. & BINSHAYA, A. S. 2021. Antimicrobial efficacy of different pulp-capping materials against Enterococcus faecalis: An In vitro study. *Journal of Pharmacy and Bioallied Sciences,* 13, 608-611.

ATTUR, K., JOY, M. T., KARIM, R., KUMAR, V. A., DEEPIKA, C. & AHMED, H. 2016. Comparative analysis of endodontic smear layer removal efficacy of 17% ethylenediaminetetraacetic acid, 7% maleic acid, and 2% chlorhexidine using scanning electron microscope: An in vitro study. *Journal of International Society of Preventive & Community Dentistry,* 6**,** S160-S165.

AUSTIN, P., BRINE, C., CASTLE, J. & ZIKAKIS, J. 1981. Chitin: New facets of research. *Science,* 212**,** 749-753.

AWAWDEH, L., AL-QUDAH, A., HAMOURI, H. & CHAKRA, R. J. 2018a. Outcomes of vital pulp therapy using mineral trioxide aggregate or Biodentine: a prospective randomized clinical trial. *Journal of Endodontics,* 44**,** 1603-1609.

AWAWDEH, L., JAMLEH, A. & AL BEITAWI, M. 2018b. The antifungal effect of propolis endodontic irrigant with three other irrigation solutions in presence and absence of smear layer: an in vitro study. *Iranian Endodontic Journal,* 13**,** 234–239.

BACHMANN, L., GOMES, A. S. & ZEZELL, D. M. 2005. Collagen absorption bands in heated and rehydrated dentine. *Spectrochimica Acta Part A: Molecular and Biomolecular Spectroscopy,* 62**,** 1045-1049.

BACHOO, I., SEYMOUR, D. & BRUNTON, P. 2013. Clinical case reports using a novel calcium-based cement. *British Dental Journal,* 214**,** 61-64.

BAHADOR, A., POURAKBARI, B., BOLHARI, B. & HASHEMI, F. B. 2015. In vitro evaluation of the antimicrobial activity of nanosilver-mineral trioxide aggregate against frequent anaerobic oral pathogens by a membrane-enclosed immersion test. *Biomedical Journal,* 38**,** 77-83.

BAMFORD, C. V., D'MELLO, A., NOBBS, A. H., DUTTON, L. C., VICKERMAN, M. M. & JENKINSON, H. F. 2009. Streptococcus gordonii modulates Candida albicans biofilm formation through intergeneric communication. *Infection and Immunity,* 77**,** 3696-3704.

BAPAT, R. A., JOSHI, C. P., BAPAT, P., CHAUBAL, T. V., PANDURANGAPPA, R., JNANENDRAPPA, N., GORAIN, B., KHURANA, S. & KESHARWANI, P. 2019. The use of nanoparticles as biomaterials in dentistry. *Drug discovery today,* 24**,** 85-98.

BARMA, M. D., MUTHUPANDIYAN, I., SAMUEL, S. R. & AMAECHI, B. T. 2021. Inhibition of Streptococcus mutans, antioxidant property and cytotoxicity of novel nano-zinc oxide varnish. *Archives of Oral Biology,* 126**,** 105132.

BARNES, C. 2017. The h-index debate: an introduction for librarians. *The Journal of Academic Librarianship,* 43**,** 487-494.

BARSNESS, B. D. & ROACH, S. H. 2016. Endodontic Considerations for the Restoration of Endodontically Treated Teeth. In Restoration of Root Canal-Treated Teeth. Springer, 1-24.

BAUMGARTNER, J. C. & FALKLER, W. A. 1991. BACTERIA IN THE APICAL 5 MM OF INFECTED ROOT CANALS. *Journal of Endodontics,* 17**,** 380-383.

BAUMGARTNER, J. C., WATTS, C. M. & XIA, T. 2000. Occurrence of Candida albicans in infections of endodontic origin. *Journal of Endodontics,* 26**,** 695-698.

BAYRAKTAR, K., BASTURK, F. B., TURKAYDIN, D. & GUNDAY, M. 2021. Long-term effect of acidic pH on the surface microhardness of ProRoot mineral trioxide aggregate, Biodentine, and total fill root repair material putty. *Dental Research Journal,* 18**,** 2021.

BECERRA, P., RICUCCI, D., LOGHIN, S., GIBBS, J. L. & LIN, L. M. 2014. Histologic study of a human immature permanent premolar with chronic apical

abscess after revascularization/revitalization. *Journal of Endodontics,* 40**,** 133-139.

BECK, B. H., YILDIRIM-AKSOY, M., SHOEMAKER, C. A., FULLER, S. A. & PEATMAN, E. 2019. Antimicrobial activity of the biopolymer chitosan against Streptococcus iniae. *Journal of Fish Diseases,* 42**,** 371-377.

BEDIER, M. M. A. 2017. ANTIBACTERIAL EFFICACY OF MINERAL TRIOXIDE AGGREGATE COMBINED WITH NANO-SILVER ADDITIVES. *Egyptian Dental Journal,* 63**,** 1833-1841.

BELTZ, R. E., TORABINEJAD, M. & POURESMAIL, M. 2003. Quantitative analysis of the solubilizing action of MTAD, sodium hypochlorite, and EDTA on bovine pulp and dentin. *Journal of Endodontics,* 29**,** 334-337.

BERBER, V., GOMES, B., SENA, N., VIANNA, M., FERRAZ, C., ZAIA, A. & SOUZA-FILHO, F. 2006. Efficacy of various concentrations of NaOCl and instrumentation techniques in reducing Enterococcus faecalis within root canals and dentinal tubules. *International Endodontic Journal,* 39**,** 10-17.

BERGENHOLTZ, G. 2016. Assessment of treatment failure in endodontic therapy. *Journal of Oral Rehabilitation,* 43**,** 753-758.

BERGENHOLTZ, G., TORNECK, C. & KISHEN, A. 2015. Inter-appointment Medication with Calcium Hydroxide in Routine Cases of Root Canal Therapy. In The Root Canal Biofilm. Springer, 303-325.

BESHR, K. A. & ABDELRAHIM, R. A. 2019a. Antibacterial efficacy of Allium sativum (garlic) and chitosan incorporated into two root canal sealers against Enterococcus faecalis: comparative study. *Tanta Dental Journal,* 16**,** 94-98.

BESHR, K. A. & ABDELRAHIM, R. A. 2019b. Enhanced bioactivity and interfacial marginal adaptation of mineral trioxide aggregate and Biodentine materials modified by eggshell powder at root dentine. *Tanta Dental Journal,* 16**,** 136–141.

BESINIS, A., DE PERALTA, T. & HANDY, R. D. 2014. Inhibition of biofilm formation and antibacterial properties of a silver nano-coating on human dentine. *Nanotoxicology,* 8**,** 745-754.

BISWAS, S. K. & CHAFFIN, W. L. 2005. Anaerobic growth of Candida albicans does not support biofilm formation under similar conditions used for aerobic biofilm. *Current Microbiology,* 51**,** 100-104.

BJÖRK, E. & WU, J. 2018. PCR Analysis as a Method of Microbiological Control in Endodontic Treatment Is there a Correlation to Healing? A pilot study. OAI: DiVA.org:umu-153622.

BLAIR, J., WEBBER, M. A., BAYLAY, A. J., OGBOLU, D. O. & PIDDOCK, L. J. 2015. Molecular mechanisms of antibiotic resistance. *Nature Reviews Microbiology,* 13**,** 42-51.

BLAKE, J. 2004. Bio-ontologies—fast and furious. *Nature Biotechnology,* 22**,** 773-774.

BO, M., BAVESTRELLO, G., KUREK, D., PAASCH, S., BRUNNER, E., BORN, R., GALLI, R., STELLING, A. L., SIVKOV, V. N. & PETROVA, O. V. 2012. Isolation and identification of chitin in the black coral Parantipathes larix (Anthozoa: Cnidaria). *International Journal of Biological Macromolecules,* 51, 129-137.

BOR, B., CEN, L., AGNELLO, M., SHI, W. & HE, X. 2016. Morphological and physiological changes induced by contact-dependent interaction between Candida albicans and Fusobacterium nucleatum. *Scientific Reports,* 6**,** 27956.

BOSAID, F., AKSEL, H. & AZIM, A. A. 2022. Influence of acidic pH on antimicrobial activity of different calcium silicate based–endodontic sealers. *Clinical Oral Investigations,* 26**,** 5369–5376.

BOSSÙ, M., MANCINI, P., BRUNI, E., UCCELLETTI, D., PREZIOSI, A., RULLI, M., RELUCENTI, M., DONFRANCESCO, O., IACULLI, F. & DI GIORGIO, G. 2021. Biocompatibility and Antibiofilm Properties of Calcium Silicate-Based Cements: An In Vitro Evaluation and Report of Two Clinical Cases. *Biology,* 10**,** 470.

BRADFORD, S. C. 1934. Sources of information on specific subjects. *Engineering,* 137**,** 85-86.

BRADSHAW, D., MARSH, P., WATSON, G. & ALLISON, C. 1997. Oral anaerobes cannot survive oxygen stress without interacting with facultative/aerobic species as a microbial commmunity. *Letters in Applied Microbiology,* 25**,** 385-387.

BRADSHAW, D. J., MARSH, P. D., WATSON, G. K. & ALLISON, C. 1998. Role of Fusobacterium nucleatum and coaggregation in anaerobe survival in planktonic and biofilm oral microbial communities during aeration. *Infection and Immunity,* 66**,** 4729-4732.

BRAUNER, A., FRIDMAN, O., GEFEN, O. & BALABAN, N. Q. 2016. Distinguishing between resistance, tolerance and persistence to antibiotic treatment. *Nature Reviews Microbiology,* 14**,** 320-330.

BROSCO, V. H., BERNARDINELI, N., TORRES, S. A., CONSOLARO, A., BRAMANTE, C. M., DE MORAES, I. G., ORDINOLA-ZAPATA, R. & GARCIA, R. B. 2010. Bacterial leakage in obturated root canals—part 2: a comparative histologic and microbiologic analyses. *Oral Surgery, Oral Medicine, Oral Pathology, Oral Radiology, and Endodontology,* 109**,** 788-794.

BROWN, J. L., JOHNSTON, W., DELANEY, C., RAJENDRAN, R., BUTCHER, J., KHAN, S., BRADSHAW, D., RAMAGE, G. & CULSHAW, S. 2019a. Biofilm-stimulated epithelium modulates the inflammatory responses in co-cultured immune cells. *Scientific Reports,* 9**,** 1-14.

BROWN, J. L., JOHNSTON, W., DELANEY, C., SHORT, B., BUTCHER, M. C., YOUNG, T., BUTCHER, J., RIGGIO, M., CULSHAW, S. & RAMAGE, G. 2019b. Polymicrobial oral biofilm models: simplifying the complex. *Journal of Medical Microbiology,* 68**,** 1573-1584.

BROWN, J. L., SHORT, B., WARE, A., SHERRY, L., KEAN, R. & RAMAGE, G. 2022. Cell viability assays for Candida auris. In Candida auris: Methods and Protocols. Springer, 129-153.

BRZEZIŃSKA-BŁASZCZYK, E., PAWŁOWSKA, E., PŁOSZAJ, T., WITAS, H., GODZIK, U. & AGIER, J. 2018. Presence of archaea and selected bacteria in infected root canal systems. *Canadian Journal of Microbiology,* 64**,** 317-326.

BURKOVSKI, A. & KARL, M. 2019. Lack of evidence for the necessity of root canal obturation. *Quintessence International,* 50**,** 22-28.

BUTT, N., TALWAR, S., CHAUDHRY, S., NAWAL, R. R., YADAV, S. & BALI, A. 2014. Comparison of physical and mechanical properties of mineral trioxide aggregate and Biodentine. *Indian Journal of Dental Research,* 25**,** 692-697.

C SMITH, C. J. & OSBORN, A. M. 2009. Advantages and limitations of quantitative PCR (Q-PCR)-based approaches in microbial ecology. *FEMS Microbiology Ecology,* 67**,** 6-20.

C TAN, C. H., LEE, K. W. K., BURMØLLE, M., KJELLEBERG, S. & RICE, S. A. 2017. All together now: experimental multispecies biofilm model systems. *Environmental Microbiology,* 19, 42-53.

C ZHANG, C., DU, J. & PENG, Z. 2015. Correlation between Enterococcus faecalis and persistent intraradicular infection compared with primary intraradicular infection: a systematic review. *Journal of Endodontics,* 41, 1207-1213.

CABREIRA, L. J., GOMINHO, L. F., RÔÇAS, I. N., DESSAUNE-NETO, N., SIQUEIRA JR, J. F. & ALVES, F. R. 2019. Quantitative analysis of apically extruded bacteria following preparation of curved canals with three systems. *Australian Endodontic Journal,* 45, 79-85.

CALVO, P., REMUNAN-LOPEZ, C., VILA-JATO, J. L. & ALONSO, M. 1997. Novel hydrophilic chitosan-polyethylene oxide nanoparticles as protein carriers. *Journal of Applied Polymer Science,* 63, 125-132.

CAMILLERI, J. 2007. Hydration mechanisms of mineral trioxide aggregate. *International Endodontic Journal,* 40, 462-470.

CAMILLERI, J. 2011. Characterization and hydration kinetics of tricalcium silicate cement for use as a dental biomaterial. *Dental Materials,* 27, 836-844.

CAMILLERI, J. 2014. Hydration characteristics of Biodentine and Theracal used as pulp capping materials. *Dental Materials,* 30, 709-715.

CAMILLERI, J. 2015. Mineral trioxide aggregate: present and future developments. *Endodontic Topics,* 32, 31-46.

CAMILLERI, J. 2021a. Characterization and Properties of Bioceramic Materials for Endodontics. In Bioceramic Materials in Clinical Endodontics. Springer, 7-18.

CAMILLERI, J. 2021b. Current Classification of Bioceramic Materials in Endodontics. In Bioceramic Materials in Clinical Endodontics. Springer, 1-6.

CAMILLERI, J., GRECH, L., GALEA, K., KEIR, D., FENECH, M., FORMOSA, L., DAMIDOT, D. & MALLIA, B. 2014. Assessment of porosity and sealing ability of tricalcium silicate-based root-end filling materials. *Clinical Oral Investigations,* 2014.

CAMILLERI, J., SORRENTINO, F. & DAMIDOT, D. 2013. Investigation of the hydration and bioactivity of radiopacified tricalcium silicate cement, Biodentine and MTA Angelus. *Dental Materials,* 29, 580-593.

CARBAJAL MEJÍA, J. B. 2014. Antimicrobial effects of calcium hydroxide, chlorhexidine, and propolis on E nterococcus faecalis and C andida albicans. *Journal of Investigative and Clinical Dentistry,* 5, 194-200.

CARD, S. J., SIGURDSSON, A., ØRSTAVIK, D. & TROPE, M. 2002. The effectiveness of increased apical enlargement in reducing intracanal bacteria. *Journal of Endodontics,* 28, 779-783.

CAREDDU, R. & DUNCAN, H. 2018. How does the pulpal response to Biodentine and ProRoot mineral trioxide aggregate compare in the laboratory and clinic? *British Dental Journal,* 225, 743-749.

CARROTTE, P. 2004. Endodontics: Part 4 Morphology of the root canal system. *British Dental Journal,* 197, 379-383.

CASALINUOVO, I. A., SORGE, R., BONELLI, G. & DI FRANCESCO, P. 2017. Evaluation of the antifungal effect of EDTA, a metal chelator agent, on Candida albicans biofilm. *European Review for Medical and Pharmacological Sciences,* 21, 1413-1420.

CASTELLUCCI, A. 2019. Internal Tooth Anatomy and Root Canal Obturation. In The Root Canal Anatomy in Permanent Dentition. Springer, 323-341.

CERI, H., OLSON, M., STREMICK, C., READ, R., MORCK, D. & BURET, A. 1999. The Calgary Biofilm Device: new technology for rapid determination of antibiotic susceptibilities of bacterial biofilms. *Journal of Clinical Microbiology,* 37, 1771-1776.

CHAN, H.-K. & KWOK, P. C. L. 2011. Production methods for nanodrug particles using the bottom-up approach. *Advanced Drug Delivery Reviews,* 63, 406-416.

CHANDY, T. & SHARMA, C. P. 1990. Chitosan-as a Biomaterial. *Biomaterials, Artificial Cells and Artificial Organs,* 18, 1-24.

CHÁVEZ DE PAZ, L. E., RESIN, A., HOWARD, K. A., SUTHERLAND, D. S. & WEJSE, P. L. 2011. Antimicrobial effect of chitosan nanoparticles on Streptococcus mutans biofilms. *Applied and Environmental Microbiology,* 77, 3892-3895.

CHEDELLA, S. & BERZINS, D. 2010. A differential scanning calorimetry study of the setting reaction of MTA. *International Endodontic Journal,* 43, 509-518.

CHIEGO, D. J., JR. 2019. Essentials of oral histology and embryology: a clinical approach, St. Louis, Missouri, Elsevier, 88-109.

CHIVATXARANUKUL, P., DASHPER, S. & MESSER, H. 2008. Dentinal tubule invasion and adherence by Enterococcus faecalis. *International Endodontic Journal,* 41, 873-882.

CHOW, L., JOHNSON, V., IMPASTATO, R., COY, J., STRUMPF, A. & DOW, S. 2019. Antibacterial activity of human mesenchymal stem cells mediated directly by constitutively secreted factors and indirectly by activation of innate immune effector cells. *Stem cells Translational Medicine,* 9, 235–249.

CHRISTENSEN, C. E., MCNEAL, S. F. & ELEAZER, P. 2008. Effect of lowering the pH of sodium hypochlorite on dissolving tissue in vitro. *Journal of Endodontics,* 34, 449-452.

CHYBOWSKI, E. A., GLICKMAN, G. N., PATEL, Y., FLEURY, A., SOLOMON, E. & HE, J. 2018. Clinical outcome of non-surgical root canal treatment using a single-cone technique with endosequence bioceramic sealer: a retrospective analysis. *Journal of Endodontics,* 44, 941-945.

ÇıRAKOĞLU, S., BADDAL, B. & İSLAM, A. 2020. The effectiveness of laser-activated irrigation on the apical microleakage qualities of MTA repair HP and NeoMTA plus in simulated immature teeth: A comparative study. *Materials,* 13, 3287.

CLELAND, D., JASTRZEMBSKI, K., STAMENOVA, E., BENSON, J., CATRANIS, C., EMERSON, D. & BECK, B. 2007. Growth characteristics of microorganisms on commercially available animal-free alternatives to tryptic soy medium. *Journal of Microbiological Methods,* 69, 345-352.

CLSI 2008. Reference Method for Broth Dilution Antifungal Susceptibility Testing of Yeasts. 3rd ed. CLSI standard M27-A3. Wayne, PA: Clinical and Laboratory Standards Institute; 2008.

CLSI 2018. Methods for Dilution Antimicrobial Susceptibility Tests for Bacteria that Grow Aerobically. 11th ed. CLSI standard M07. Wayne, PA: Clinical and Laboratory Standards Institute; 2018.

COBANKARA, F. K., OZKAN, H. B. & TERLEMEZ, A. 2010. Comparison of organic tissue dissolution capacities of sodium hypochlorite and chlorine dioxide. *Journal of Endodontics,* 36, 272-274.

COELHO, T., NOGUEIRA, E., STEIMACHER, A., MEDINA, A., WEINAND, W., LIMA, W., BAESSO, M. & BENTO, A. 2006. Characterization of natural

nanostructured hydroxyapatite obtained from the bones of Brazilian river fish. *Journal of Applied Physics,* 100**,** 094312.

COLMAN, G. & WILLIAMS, R. 1965. The cell walls of streptococci. *Microbiology,* 41**,** 375-387.

COMA, V., MARTIAL-GROS, A., GARREAU, S., COPINET, A., SALIN, F. & DESCHAMPS, A. 2002. Edible antimicrobial films based on chitosan matrix. *Journal of Food Science,* 67**,** 1162-1169.

COOPER, P. R., TAKAHASHI, Y., GRAHAM, L. W., SIMON, S., IMAZATO, S. & SMITH, A. J. 2010. Inflammation–regeneration interplay in the dentine–pulp complex. *Journal of Dentistry,* 38**,** 687-697.

CORRAL, C., NEGRETE, P., ESTAY, J., OSORIO, S., COVARRUBIAS, C., DE OLIVEIRA JUNIOR, O. B., BARUD, H., CORRAL, C., NEGRETE, P. & ESTAY, J. 2018. Radiopacity and chemical assessment of new commercial calcium silicate-based cements. *Journal of Odontostomatology,* 12**,** 262-268.

CORRAL NUÑEZ, C., COVARRUBIAS, C., FERNANDEZ, E. & OLIVEIRA, O. B. D. 2017. Enhanced bioactive properties of biodentine TM modified with bioactive glass nanoparticles. *Journal of Applied Oral Science,* 25**,** 177-185.

CORTE, L., CASAGRANDE PIERANTONI, D., TASCINI, C., ROSCINI, L. & CARDINALI, G. 2019. Biofilm specific activity: a measure to quantify microbial biofilm. *Microorganisms,* 7**,** 73.

COYKENDALL, A. L., KACZMAREK, F. S. & SLOTS, J. 1980. Genetic Heterogeneity in Bacteroides asaccharolyticus (Holdeman and Moore 1970) Finegold and Barnes 1977 (Approved Lists, 1980) and Proposal of Bacteroides gingivalis sp. nov. and Bacteroides macacae (Slots and Genco) comb. nov. *International Journal of Systematic and Evolutionary Microbiology,* 30**,** 559-564.

CUERO, R., OSUJI, G. & WASHINGTON, A. 1991. N-carboxymethylchitosan inhibition of aflatoxin production: role of zinc. *Biotechnology Letters,* 13**,** 441-444.

D KIM, D., LIU, Y., BENHAMOU, R. I., SANCHEZ, H., SIMÓN-SORO, Á., LI, Y., HWANG, G., FRIDMAN, M., ANDES, D. R. & KOO, H. 2018. Bacterial-derived exopolysaccharides enhance antifungal drug tolerance in a cross-kingdom oral biofilm. *The ISME Journal,* 12**,** 1427-1442.

D WU, D., FAN, W., KISHEN, A., GUTMANN, J. L. & FAN, B. 2014. Evaluation of the antibacterial efficacy of silver nanoparticles against Enterococcus faecalis biofilm. *Journal of Endodontics,* 40**,** 285-290.

DAMLAR, I., OZCAN, E., ERKAN, Y., YALCIN, M. & CELIK, S. 2014. Antimicrobial effects of several calcium silicate-based root-end filling materials. *Dental Materials Journal,* 33**,** 453-457.

DAMMASCHKE, T. 2012a. Biodentine™ - an overview. *Septodont Case Studies Collection.* No. 03 - October 2012.

DAMMASCHKE, T. 2012b. Biodentine™ a new bioactive cement for direct pulp capping. Septodont case studies collection, March (2012)[cited 2013 Jun 28].

DASILVA, L., FINER, Y., FRIEDMAN, S., BASRANI, B. & KISHEN, A. 2013. Biofilm formation within the interface of bovine root dentin treated with conjugated chitosan and sealer containing chitosan nanoparticles. *Journal of Endodontics,* 39**,** 249-253.

DAVIES, A., BENTLEY, M. & FIELD, B. S. 1968. Comparison of the action of vantocil, cetrimide and chlorhexidine on Escherichia coli and its

spheroplasts and the protoplasts of gram positive bacteria. *Journal of Applied Bacteriology,* 31, 448-461.

DAWOOD, A., MANTON, D., PARASHOS, P., WONG, R., PALAMARA, J., STANTON, D. & REYNOLDS, E. 2015. The physical properties and ion release of CPP-ACP-modified calcium silicate-based cements. *Australian Dental Journal,* 60, 434-444.

DE ARAUJO, W. C., VARAH, E. & MERGENHAGEN, S. E. 1963. Immunochemical analysis of human oral strains of Fusobacterium and Leptotrichia. *Journal of Bacteriology,* 86, 837-844.

DE DIOS TERUEL, J., ALCOLEA, A., HERNÁNDEZ, A. & RUIZ, A. J. O. 2015. Comparison of chemical composition of enamel and dentine in human, bovine, porcine and ovine teeth. *Archives of Oral Biology,* 60, 768-775.

DE PAZ, L. C., SVENSÄTER, G., DAHLÉN, G. & BERGENHOLTZ, G. 2005. Streptococci from root canals in teeth with apical periodontitis receiving endodontic treatment. *Oral Surgery, Oral Medicine, Oral Pathology, Oral Radiology, and Endodontology,* 100, 232-241.

DE PAZ VILLANUEVA, L. E. C. 2002. Fusobacterium nucleatum in endodontic flare-ups. *Oral Surgery, Oral Medicine, Oral Pathology, Oral Radiology, and Endodontology,* 93, 179-183.

DEBELIAN, G. & TROPE, M. 2016. The use of premixed bioceramic materials in endodontics. *Giornale Italiano di Endodonzia,* 30, 70-80.

DEL CARPIO-PEROCHENA, A., BRAMANTE, C. M., DUARTE, M. A. H., DE MOURA, M. R., AOUADA, F. A. & KISHEN, A. 2015a. Chelating and antibacterial properties of chitosan nanoparticles on dentin. *Restorative Dentistry & Endodontics,* 40, 195-201.

DEL CARPIO-PEROCHENA, A., KISHEN, A., FELITTI, R., BHAGIRATH, A. Y., MEDAPATI, M. R., LAI, C. & CUNHA, R. S. 2017. Antibacterial properties of chitosan nanoparticles and propolis associated with calcium hydroxide against single-and multispecies biofilms: an in vitro and in situ study. *Journal of Endodontics,* 43, 1332-1336.

DEL CARPIO-PEROCHENA, A., KISHEN, A., SHRESTHA, A. & BRAMANTE, C. M. 2015b. Antibacterial properties associated with chitosan nanoparticle treatment on root dentin and 2 types of endodontic sealers. *Journal of Endodontics,* 41, 1353-1358.

DELANEY, C., KEAN, R., SHORT, B., TUMELTY, M., MCLEAN, W., NILE, C. J. & RAMAGE, G. 2018. Fungi at the Scene of the Crime: Innocent Bystanders or Accomplices in Oral Infections? *Current Clinical Microbiology Reports,* 5, 190-200.

DEVITO, K. L., ORTEGA, A. I. & HAITER-NETO, F. 2004. Radiopacity of calcium hydroxide cement compared with human tooth structure. *Journal of Applied Oral Science,* 12, 290-293.

DIAZ, P. & ROGERS, A. 2004. The effect of oxygen on the growth and physiology of Porphyromonas gingivalis. *Oral Microbiology and Immunology,* 19, 88-94.

DIAZ, P., ZILM, P. & ROGERS, A. 2002. Fusobacterium nucleatum supports the growth of Porphyromonas gingivalis in oxygenated and carbon-dioxide-depleted environments. *Microbiology,* 148, 467-472.

DISTEL, J. W., HATTON, J. F. & GILLESPIE, M. J. 2002. Biofilm formation in medicated root canals. *Journal of Endodontics,* 28, 689-693.

DIVIA, A. R., NAIR, M. G., VARUGHESE, J. M. & KURIEN, S. 2018. A comparative evaluation of Morinda citrifolia, green tea polyphenols, and Triphala with

5% sodium hypochlorite as an endodontic irrigant against Enterococcus faecalis: An in vitro study. *Dental Researh Journal,* 15**,** 117-122.

DONALDSON, M. & GOODCHILD, J. 2019. Chlorhexidine allergy: raising awareness about rare but potentially life-threatening reactions. *General Dentistry,* 67**,** 7-10.

DONYAVI, Z., HEIDARI, N., KHOSHBIN, E., SHAHRIARI, S., FARHADIAN, M., MASHOUF, R. Y. & ESMAEILZADEH, M. 2017. Antibacterial activity of mineral trioxide aggregate, new endodontic cement, Retro MTA and Ortho MTA against common endodontic pathogens. *Indo American Journal of Pharmaceutical Sciences,* 4**,** 4720-4728.

DOS REIS-PRADO, A. H., ABREU, L. G., FAGUNDES, R. R., OLIVEIRA, S. D. C., BOTTINO, M. C., RIBEIRO-SOBRINHO, A. P. & BENETTI, F. 2022. Influence of ethylenediaminetetraacetic acid on regenerative endodontics: A systematic review. *International Endodontic Journal,* 55**,** 579-612.

DU, Q., YUAN, S., ZHAO, S., FU, D., CHEN, Y., ZHOU, Y., CAO, Y., GAO, Y., XU, X. & ZHOU, X. 2021. Coexistence of Candida albicans and Enterococcus faecalis increases biofilm virulence and periapical lesions in rats. *Biofouling,* 37**,** 964-974.

DUMITRU, R., HORNBY, J. M. & NICKERSON, K. W. 2004. Defined anaerobic growth medium for studying Candida albicans basic biology and resistance to eight antifungal drugs. *Antimicrobial Agents and Chemotherapy,* 48**,** 2350-2354.

DUMMER, P. M., MCGINN, J. & REES, D. G. 1984. The position and topography of the apical canal constriction and apical foramen. *International Endodontic Journal,* 17**,** 192-198.

DUMONT, J. E. 1989. The bias of citations. *Trends in biochemical sciences,* 14**,** 327-328.

E KIM, E. J. & LEE, S. Y. 2019. Identification of Hemin-binding Protein of Oral Streptococci via Electrophoresis in SDS Polyacrylamide Gel. *Journal of Advances in Microbiology,* 15**,** 1-5.

E SILVA, E. J., CARDOSO, M. L., RODRIGUES, J. P., DE-DEUS, G. & FIDALGO, T. K. D. S. 2021. Solubility of bioceramic-and epoxy resin-based root canal sealers: A systematic review and meta-analysis. *Australian Endodontic Journal,* 47**,** 690-702.

EGUSA, H., SONOYAMA, W., NISHIMURA, M., ATSUTA, I. & AKIYAMA, K. 2012. Stem cells in dentistry–part I: stem cell sources. *Journal of Prosthodontic Research,* 56**,** 151-165.

EICK, S., KINDBLOM, C., MIZGALSKA, D., MAGDOŃ, A., JURCZYK, K., SCULEAN, A. & STAVROPOULOS, A. 2017. Adhesion of Porphyromonas gingivalis and Tannerella forsythia to dentin and titanium with sandblasted and acid etched surface coated with serum and serum proteins - An in vitro study. *Archives of Oral Biology,* 75**,** 81-88.

EL-DIN, N. G. & EL-HELBAWY, D. 2016. Evaluation of radiopacity changes of Biodentine as a root-end filling material within soft and hard tissue simulation using digital radiography. *ENDO (Lond Engl),* 10**,** 77-82.

ELIZABETH, P.-S., NÉSTOR, M.-M. & DAVID, Q.-G. 2019. Nanoparticles as dental drug-delivery systems. In Nanobiomaterials in Clinical Dentistry. Elsevier, 567-593.

ELLEGAARD, O. & WALLIN, J. A. 2015. The bibliometric analysis of scholarly production: How great is the impact? *Scientometrics,* 105**,** 1809-1831.

ELNAGHY, A. M. 2014a. Influence of acidic environment on properties of biodentine and white mineral trioxide aggregate: a comparative study. *Journal of Endodontics,* 40**,** 953-957.

ELNAGHY, A. M. 2014b. Influence of QMix irrigant on the micropush-out bond strength of Biodentine and white mineral trioxide aggregate. *Journal of Adhesive Dentistry,* 16**,** 277-283.

ELSAKA, S. E., ELNAGHY, A. M., MANDORAH, A. & ELSHAZLI, A. H. 2019. Effect of titanium tetrafluoride addition on the physicochemical and antibacterial properties of Biodentine as intraorfice barrier. *Dental Materials,* 35**,** 185-193.

ENGLISH, B. K. & GAUR, A. H. 2010. The use and abuse of antibiotics and the development of antibiotic resistance. In Hot topics in infection and immunity in children VI. 73-82.

ERLANDSEN, S. L., KRISTICH, C. J., DUNNY, G. M. & WELLS, C. L. 2004. High-resolution visualization of the microbial glycocalyx with low-voltage scanning electron microscopy: dependence on cationic dyes. *Journal of Histochemistry & Cytochemistry,* 52**,** 1427-1435.

ESCOBAR-GARCÍA, D. M., AGUIRRE-LÓPEZ, E., MÉNDEZ-GONZÁLEZ, V. & POZOS-GUILLÉN, A. 2016. Cytotoxicity and Initial Biocompatibility of Endodontic Biomaterials (MTA and Biodentine™) Used as Root-End Filling Materials. *BioMed Research International,* 2016**,** 2016.

ESTEKI, P., JAHROMI, M. Z. & TAHMOURESPOUR, A. 2021. In vitro antimicrobial activity of mineral trioxide aggregate, Biodentine, and calcium-enriched mixture cement against Enterococcus faecalis, Streptococcus mutans, and Candida albicans using the agar diffusion technique. *Dental Research Journal,* 18**,** 2021.

EUROPEAN COMMISSION 2011. Recommendations: commission recommendation of 18 October 2011 on the definition of nanomaterial. The European Commission Brussels, 275/238-275/240.

EYRE-WALKER, A. & STOLETZKI, N. 2013. The assessment of science: the relative merits of post-publication review, the impact factor, and the number of citations. *PLoS Biol,* 11**,** e1001675.

EZZ, A., SHABAN, A., M ABDALLA, M. & ABBAS, M. 2018. Bonding ability and mechanical strength of recently formulated glass ionomer cements. *Al-Azhar Journal of Dental Science,* 21**,** 147-154.

FARDI, A., KODONAS, K., GOGOS, C. & ECONOMIDES, N. 2011. Top-cited articles in endodontic journals. *Journal of Endodontics,* 37**,** 1183-1190.

FARINHA, I. & FREITAS, F. 2020. Chapter 2 - Chemically modified chitin, chitosan, and chitinous polymers as biomaterials. In: GOPI, S., THOMAS, S. & PIUS, A. (eds.) In Handbook of Chitin and Chitosan. Elsevier, 43-69.

FARRUGIA, C., BACA, P., CAMILLERI, J. & MOLIZ, M. A. 2017. Antimicrobial activity of ProRoot MTA in contact with blood. *Scientific Reports,* 7**,** 41359.

FARRUGIA, C., LUNG, C. Y., WISMAYER, P. S., ARIAS-MOLIZ, M. T. & CAMILLERI, J. 2018. The relationship of surface characteristics and antimicrobial performance of pulp capping materials. *Journal of Endodontics,* 44**,** 1115-1120.

FATHY, S. M., ABD EL-AZIZ, A. M. & LABAH, D. A. 2019. Cellular interaction and antibacterial efficacy of two hydraulic calcium silicate-based cements: Cell-dependent model. *Journal of Conservative Dentistry,* 22**,** 17-22.

FERRACANE, J. L. & PALIN, W. M. 2013. Effects of particulate filler systems on the properties and performance of dental polymer composites. In Non-

Metallic Biomaterials for Tooth Repair and Replacement. Elsevier, 294-335.

FERRAZ, J., DE CARVALHO JUNIOR, J. R., SAQUY, P. C., PÉCORA, J. D. & SOUSA-NETO, M. D. 2001. Dental anomaly: dens evaginatus (talon cusp). *Brazilian Dental Journal,* 12**,** 132-134.

FERREIRA, C., SASSONE, L. M., GONÇALVES, A. S., DE CARVALHO, J. J., TOMÁS-CATALÁ, C. J., GARCÍA-BERNAL, D., OÑATE-SÁNCHEZ, R. E., RODRÍGUEZ-LOZANO, F. J. & SILVA, E. J. N. L. 2019. Physicochemical, cytotoxicity and in vivo biocompatibility of a high-plasticity calcium-silicate based material. *Scientific Reports,* 9**,** 1-11.

FIELD, J., STEELE, J. & WASSELL, R. 2019. Managing Tooth Surface Loss. In Extra-Coronal Restorations. Springer, 147-160.

FIGINI, L., LODI, G., GORNI, F. & GAGLIANI, M. 2008. Single versus multiple visits for endodontic treatment of permanent teeth: a Cochrane systematic review. *Journal of Endodontics,* 34**,** 1041-1047.

FOUAD, A. F., BARRY, J., CAIMANO, M., CLAWSON, M., ZHU, Q., CARVER, R., HAZLETT, K. & RADOLF, J. D. 2002. PCR-based identification of bacteria associated with endodontic infections. *Journal of Clinical Microbiology,* 40**,** 3223-3231.

FOX, E., COWLEY, E., NOBILE, C., HARTOONI, N., NEWMAN, D. & JOHNSON, A. 2014. Anaerobic bacteria grow within Candida albicans biofilms and induce biofilm formation in suspension cultures. *Current Biology,* 24**,** 2411-2416.

FRANCI, G., FALANGA, A., GALDIERO, S., PALOMBA, L., RAI, M., MORELLI, G. & GALDIERO, M. 2015. Silver nanoparticles as potential antibacterial agents. *Molecules,* 20**,** 8856-8874.

FREILICH, S., ZARECKI, R., EILAM, O., SEGAL, E. S., HENRY, C. S., KUPIEC, M., GOPHNA, U., SHARAN, R. & RUPPIN, E. 2011. Competitive and cooperative metabolic interactions in bacterial communities. *Nature Communications,* 2**,** 589.

GAD EL-RAB, S. M., ASHOUR, A. A., BASHA, S., ALYAMANI, A. A., FELEMBAN, N. H. & ENAN, E. T. 2021. Well-Orientation Strategy Biosynthesis of Cefuroxime-Silver Nanoantibiotic for Reinforced Biodentine™ and Its Dental Application against Streptococcus mutans. *Molecules,* 26**,** 6832.

GALLER, K., KRASTL, G., SIMON, S., VAN GORP, G., MESCHI, N., VAHEDI, B. & LAMBRECHTS, P. 2016. European Society of Endodontology position statement: Revitalization procedures. *International Endodontic Journal,* 49**,** 717-723.

GANDOLFI, M., SIBONI, F. & PRATI, C. 2012. Chemical–physical properties of TheraCal, a novel light-curable MTA-like material for pulp capping. *International Endodontic Journal,* 45**,** 571-579.

GAO, L., XU, T., HUANG, G., JIANG, S., GU, Y. & CHEN, F. 2018. Oral microbiomes: more and more importance in oral cavity and whole body. *Protein & Cell,* 9**,** 488-500.

GARFIELD, E. 1955. Citation indexes for science: a new dimension in documentation through association of ideas. *Science,* 122**,** 108-111.

GARFIELD, E. 1964. " Science Citation Index"—A New Dimension in Indexing: This unique approach underlies versatile bibliographic systems for communicating and evaluating information. *Science,* 144**,** 649-654.

GARFIELD, E. 1977. Introducing citation classics-human side of scientific reports. *Current Contents,* 1**,** 5-7.

GAZZANEO, I., VIEIRA, G. C., PÉREZ, A. R., ALVES, F. R., GONÇALVES, L. S., MDALA, I., SIQUEIRA JR, J. F. & RÔÇAS, I. N. 2019. Root canal disinfection by single-and multiple-instrument systems: effects of sodium hypochlorite volume, concentration, and retention time. *Journal of Endodontics,* 45**,** 736-741.

GEORGE, R. 2019. Evaluation of the evidence of effectiveness of ultrasonic activated irrigation for root canal treatment. *Evidence-Based Dentistry,* 20**,** 83-84.

GEORGE, S., KISHEN, A. & SONG, P. 2005. The role of environmental changes on monospecies biofilm formation on root canal wall by Enterococcus faecalis. *Journal of Endodontics,* 31**,** 867-872.

GHANNOUM, M. A., JUREVIC, R. J., MUKHERJEE, P. K., CUI, F., SIKAROODI, M., NAQVI, A. & GILLEVET, P. M. 2010. Characterization of the oral fungal microbiome (mycobiome) in healthy individuals. *PLOS Pathogens,* 6**,** 1-8.

GHISALBERTI, E., JEFFERIES, P., LANTERI, R. & MATISONS, J. 1978. Constituents of propolis. *Experientia,* 34**,** 157-158.

GIANA, H. E., SILVEIRA, L., ZÂNGARO, R. A. & PACHECO, M. T. T. 2003. Rapid identification of bacterial species by fluorescence spectroscopy and classification through principal components analysis. *Journal of Fluorescence,* 13**,** 489-493.

GILLEN, B. M., LOONEY, S. W., GU, L.-S., LOUSHINE, B. A., WELLER, R. N., LOUSHINE, R. J., PASHLEY, D. H. & TAY, F. R. 2011. Impact of the quality of coronal restoration versus the quality of root canal fillings on success of root canal treatment: a systematic review and meta-analysis. *Journal of Endodontics,* 37**,** 895-902.

GILLUM, A. M., TSAY, E. Y. & KIRSCH, D. R. 1984. Isolation of the Candida albicans gene for orotidine-5′-phosphate decarboxylase by complementation of S. cerevisiae ura3 and E. coli pyrF mutations. *Molecular and General Genetics,* 198**,** 179-182.

GODIN, B. 2006. On the origins of bibliometrics. *Scientometrics,* 68**,** 109-133.

GOLDBERG, M. 2014. Dental Pulp, Springer, 3-34.

GOMES, B., FERRAZ, C., ME, V., BERBER, V., TEIXEIRA, F. & SOUZA-FILHO, F. 2001. In vitro antimicrobial activity of several concentrations of sodium hypochlorite and chlorhexidine gluconate in the elimination of Enterococcus faecalis. *International Endodontic Journal,* 34**,** 424-428.

GOMES, B. P., FRANCISCO, P. A., GODOI JR, E. P., ENDO, M. S., BARBOSA-RIBEIRO, M., DELBONI, M. G. & PECORARI, V. G. 2021. Identification of culturable and nonculturable microorganisms, lipopolysaccharides, and lipoteichoic acids from root canals of teeth with endodontic failure. *Journal of Endodontics,* 47**,** 1075-1086.

GOMES, B. P., JACINTO, R. C., PINHEIRO, E. T., SOUSA, E. L., ZAIA, A. A., FERRAZ, C. C. & SOUZA-FILHO, F. J. 2006. Molecular analysis of Filifactor alocis, Tannerella forsythia, and Treponema denticola associated with primary endodontic infections and failed endodontic treatment. *Journal of Endodontics,* 32**,** 937-940.

GOMES, B. P., PINHEIRO, E. T., GADÊ-NETO, C., SOUSA, E. L., FERRAZ, C. C., ZAIA, A. A., TEIXEIRA, F. & SOUZA-FILHO, F. 2004. Microbiological examination of infected dental root canals. *Oral Microbiology and Immunology,* 19**,** 71-76.

GONÇALVES, C., FERREIRA, N. & LOURENÇO, L. 2021. Production of low molecular weight chitosan and chitooligosaccharides (COS): A review. *Polymers,* 13**,** 2466.

GOPAL, J., MUTHU, M., DHAKSHANAMURTHY, T., KIM, K. J., HASAN, N., KWON, S. J. & CHUN, S. 2019. Sustainable ecofriendly phytoextract mediated one pot green recovery of chitosan. *Scientific Reports,* 9**,** 13832.

GOY, R. C., MORAIS, S. T. & ASSIS, O. B. 2016. Evaluation of the antimicrobial activity of chitosan and its quaternized derivative on E. coli and S. aureus growth. *Revista Brasileira de Farmacognosia,* 26**,** 122-127.

GRAHAM, C. E., CRUZ, M. R., GARSIN, D. A. & LORENZ, M. C. 2017. Enterococcus faecalis bacteriocin EntV inhibits hyphal morphogenesis, biofilm formation, and virulence of Candida albicans. *Proceedings of the National Academy of Sciences,* 114**,** 4507-4512.

GRAWEHR, M., SENER, B., WALTIMO, T. & ZEHNDER, M. 2003. Interactions of ethylenediamine tetraacetic acid with sodium hypochlorite in aqueous solutions. *International Endodontic Journal,* 36**,** 411-415.

GRAWISH, M. E., GRAWISH, L. M., GRAWISH, H. M., GRAWISH, M. M., HOLIEL, A. A., SULTAN, N. & EL-NEGOLY, S. A. 2022. Demineralized Dentin Matrix for Dental and Alveolar Bone Tissues Regeneration: An Innovative Scope Review. *Tissue Engineering and Regenerative Medicine,* 19**,** 687-701.

GRECH, L., MALLIA, B. & CAMILLERI, J. 2013. Investigation of the physical properties of tricalcium silicate cement-based root-end filling materials. *Dental Materials,* 29**,** e20-e28.

GROVER, C. & SHETTY, N. 2014. Evaluation of calcium ion release and change in pH on combining calcium hydroxide with different vehicles. *Contemporary Clinical Dentistry,* 5**,** 434.

GU, L., CAI, X., GUO, J., PASHLEY, D., BRESCHI, L., XU, H., WANG, X., TAY, F. & NIU, L. 2019. Chitosan-based extrafibrillar demineralization for dentin bonding. *Journal of Dental Research,* 98**,** 186-193.

GULER, A. T., WAAIJER, C. J., MOHAMMED, Y. & PALMBLAD, M. 2016. Automating bibliometric analyses using Taverna scientific workflows: A tutorial on integrating Web Services. *Journal of Informetrics,* 10**,** 830-841.

GUTMANN, J. L. & MANJARRÉS, V. 2018. Historical and contemporary perspectives on the microbiological aspects of endodontics. *Dentistry Journal,* 6**,** 49.

H SINGH, H., KAUR, M., MARKAN, S. & KAPOOR, P. 2014. Biodentine: A promising dentin substitute. *Journal of Interdisciplinary Medicine and Dental Science,* 2.

H ZHANG, H., PAPPEN, F. G. & HAAPASALO, M. 2009. Dentin enhances the antibacterial effect of mineral trioxide aggregate and bioaggregate. *Journal of Endodontics,* 35**,** 221-224.

H ZHOU, H.-M., SHEN, Y., WANG, Z.-J., LI, L., ZHENG, Y.-F., HÄKKINEN, L. & HAAPASALO, M. 2013. In vitro cytotoxicity evaluation of a novel root repair material. *Journal of Endodontics,* 39**,** 478-483.

HAAPASALO, H., SIRÉN, E., WALTIMO, T., ORSTAVIK, D. & HAAPASALO, M. 2000. Inactivation of local root canal medicaments by dentine: an in vitro study. *International Endodontic Journal,* 33**,** 126-131.

HACKMAN, R. & GOLDBERG, M. 1981. A method for determinations of microgram amounts of chitin in arthropod cuticles. *Analytical Biochemistry,* 110**,** 277-280.

HAGHGOO, R., AHMADVAND, M., NYAKAN, M. & JAFARI, M. 2017. Antimicrobial Efficacy of Mixtures of Nanosilver and Zinc Oxide Eugenol against Enterococcus faecalis. *The Journal of Contemporary Dental Practice,* 18**,** 177-181.

HAJISHENGALLIS, G., DARVEAU, R. P. & CURTIS, M. A. 2012. The keystone-pathogen hypothesis. *Nature Reviews Microbiology,* 10**,** 717-725.

HAJISHENGALLIS, G., LIANG, S., PAYNE, M. A., HASHIM, A., JOTWANI, R., ESKAN, M. A., MCINTOSH, M. L., ALSAM, A., KIRKWOOD, K. L. & LAMBRIS, J. D. 2011. Low-abundance biofilm species orchestrates inflammatory periodontal disease through the commensal microbiota and complement. *Cell Host & Microbe,* 10**,** 497-506.

HALL-STOODLEY, L., COSTERTON, J. W. & STOODLEY, P. 2004. Bacterial biofilms: from the natural environment to infectious diseases. *Nature Reviews Microbiology,* 2**,** 95-108.

HALL-STOODLEY, L. & STOODLEY, P. 2009. Evolving concepts in biofilm infections. *Cellular Microbiology,* 11**,** 1034-1043.

HALL, R. A., COTTIER, F. & MÜHLSCHLEGEL, F. A. 2009. Molecular networks in the fungal pathogen Candida albicans. *Advances in Applied Microbiology,* 67**,** 191-212.

HANCOCK III, H., SIGURDSSON, A., TROPE, M. & MOISEIWITSCH, J. 2001. Bacteria isolated after unsuccessful endodontic treatment in a North American population. *Oral Surgery, Oral Medicine, Oral Pathology, Oral Radiology, and Endodontology,* 91**,** 579-586.

HARRIOTT, M. M. & NOVERR, M. C. 2009. Candida albicans and Staphylococcus aureus form polymicrobial biofilms: effects on antimicrobial resistance. *Antimicrobial Agents and Chemotherapy,* 53**,** 3914-3922.

HEGDE, A., SHETTY, P. & BHAT, R. 2021. Insight on the Use and Abuse of Sodium Hypochlorite in Endodontics: A Review. *International Journal of Dentistry & Oral Science,* 8**,** 4028-4031.

HENCH, L. L. 1993. Introduction. In An introduction to bioceramics. World scientific, 1-12.

HERNANDEZ-DELGADILLO, R., DEL ANGEL-MOSQUEDA, C., SOLÍS-SOTO, J. M., MUNGUIA-MORENO, S., PINEDA-AGUILAR, N., SÁNCHEZ-NÁJERA, R. I., CHELLAM, S. & CABRAL-ROMERO, C. 2017. Antimicrobial and antibiofilm activities of MTA supplemented with bismuth lipophilic nanoparticles. *Dental Materials Journal,* 36**,** 503-510.

HERZOG, D., HOSNY, N., NIAZI, S., KOLLER, G., COOK, R., FOSCHI, F., WATSON, T., MANNOCCI, F. & FESTY, F. 2017. Rapid bacterial detection during endodontic treatment. *Journal of Dental Research,* 96**,** 626-632.

HIREMATH, G. S., KULKARNI, R. D. & NAIK, B. D. 2015. Evaluation of minimal inhibitory concentration of two new materials using tube dilution method: An in vitro study. *Journal of Conservative Dentistry,* 18**,** 159-162.

HIRSCH, J. E. 2005. An index to quantify an individual's scientific research output. *Proceedings of the National Academy of Sciences,* 102**,** 16569-16572.

HOMAYONI, H., RAVANDI, S. A. H. & VALIZADEH, M. 2009. Electrospinning of chitosan nanofibers: Processing optimization. *Carbohydrate Polymers,* 77**,** 656-661.

HOSOYA, N., TAKAHASHI, G., ARAI, T. & NAKAMURA, J. 2001. Calcium concentration and pH of the periapical environment after applying calcium hydroxide into root canals in vitro. *Journal of Endodontics,* 27**,** 343-346.

HUANG, X., SUN, Y., NIE, J., LU, W., YANG, L., ZHANG, Z., YIN, H., WANG, Z. & HU, Q. 2015. Using absorbable chitosan hemostatic sponges as a promising surgical dressing. *International Journal of Biological Macromolecules,* 75**,** 322-329.

HUDSON, D. A., SCIASCIA, Q. L., SANDERS, R. J., NORRIS, G. E., EDWARDS, P. J., SULLIVAN, P. A. & FARLEY, P. C. 2004. Identification of the dialysable serum inducer of germ-tube formation in Candida albicans. *Microbiology,* 150, 3041-3049.

HÜLSMANN, M. 1997. Dens invaginatus: aetiology, classification, prevalence, diagnosis, and treatment considerations. *International Endodontic Journal,* 30, 79-90.

HÜLSMANN, M., PETERS, O. A. & DUMMER, P. M. 2005. Mechanical preparation of root canals: shaping goals, techniques and means. *Endodontic Topics,* 10, 30-76.

IKINCI, G., ŞENEL, S., AKıNCıBAY, H., KAŞ, S., ERCIŞ, S., WILSON, C. & HıNCAL, A. 2002. Effect of chitosan on a periodontal pathogen Porphyromonas gingivalis. *International Journal of Pharmaceutics,* 235, 121-127.

ISO 2007. 9917-1:2007 Dentistry — Water-based cements — Part 1: Powder/liquid acid-base cements. International organization for Standardization. British Standards Institution.

ISO 2012. 6876: 2012 Dentistry — Root Canal Sealing Materials. International Organization for Standardization. British Standards Institution.

J SMITH, J., SMITH, A., SHELTON, R. & COOPER, P. 2012. Antibacterial activity of dentine and pulp extracellular matrix extracts. *International Endodontic Journal,* 45, 749-755.

J YANG, J., YUAN, G. & CHEN, Z. 2016. Pulp regeneration: current approaches and future challenges. *Frontiers in Physiology,* 7, 58.

JAFARZADEH, H., NABAVI, S., SHAKERI, M., BIDAR, M. & ZAMANPOUR, M. 2018. The Comparison of Apical Leakage between Two Obturation Techniques (Cold Lateral Condensation and Obtura II) by Using Fluid Filtration Method. *Razavi International Journal of Medicine,* 6, 42-45.

JAGTAP, P., SHETTY, R., AGARWALLA, A., WANI, P., BHARGAVA, K. & MARTANDE, S. 2018. Comparative Evaluation of Cytotoxicity of Root Canal Sealers on Cultured Human Periodontal Fibroblasts: In vitro Study. *The Journal of Contemporary Dental Practice,* 19, 847-852.

JANUS, M. M., WILLEMS, H. M. & KROM, B. P. 2016. Candida albicans in multispecies oral communities; a keystone commensal? In Fungal Biofilms and related infections. 13-20.

JARDINE, A. P., MONTAGNER, F., QUINTANA, R. M., ZACCARA, I. M. & KOPPER, P. M. P. 2019. Antimicrobial effect of bioceramic cements on multispecies microcosm biofilm: a confocal laser microscopy study. *Clinical Oral Investigations,* 23, 1367-1372.

JAYAKUMAR, R., REIS, R. & MANO, J. 2006. Phosphorous containing chitosan beads for controlled oral drug delivery. *Journal of Bioactive and Compatible Polymers,* 21, 327-340.

JEANSONNE, M. J. & WHITE, R. R. 1994. A comparison of 2.0% chlorhexidine gluconate and 5.25% sodium hypochlorite as antimicrobial endodontic irrigants. *Journal of endodontics,* 20, 276-278.

JEEVANANDAM, J., BARHOUM, A., CHAN, Y. S., DUFRESNE, A. & DANQUAH, M. K. 2018. Review on nanoparticles and nanostructured materials: history, sources, toxicity and regulations. *Beilstein Journal of Nanotechnology,* 9, 1050-1074.

JEREZ-OLATE, C., ARAYA, N., ALCÁNTARA, R., LUENGO, L., BELLO-TOLEDO, H., GONZÁLEZ-ROCHA, G. & SÁNCHEZ-SANHUEZA, G. 2021. In vitro antibacterial activity of endodontic bioceramic materials against dual and

multispecies aerobic-anaerobic biofilm models. *Australian Endodontic Journal*, doi: 10.1111/aej.12587.

JIA, Z. & SHEN, D. 2002. Effect of reaction temperature and reaction time on the preparation of low-molecular-weight chitosan using phosphoric acid. *Carbohydrate Polymers,* 49, 393-396.

JONAIDI-JAFARI, N., IZADI, M. & JAVIDI, P. 2016. The effects of silver nanoparticles on antimicrobial activity of ProRoot mineral trioxide aggregate (MTA) and calcium enriched mixture (CEM). *Journal of Clinical and Experimental Dentistry,* 8, e22-e26.

JORTH, P., TURNER, K. H., GUMUS, P., NIZAM, N., BUDUNELI, N. & WHITELEY, M. 2014. Metatranscriptomics of the human oral microbiome during health and disease. *mBio,* 5, e01012-01014.

K TAN, K. S., YU, V. S. H., QUAH, S. Y. & BERGENHOLTZ, G. 2015. Rapid method for the detection of root canal bacteria in endodontic therapy. *Journal of Endodontics,* 41, 447-450.

KACZMAREK, M. B., STRUSZCZYK-SWITA, K., LI, X., SZCZĘSNA-ANTCZAK, M. & DAROCH, M. 2019. Enzymatic modifications of chitin, chitosan, and chitooligosaccharides. *Frontiers in Bioengineering and Biotechnology,* 7, 243.

KAKEHASHI, S., STANLEY, H. & FITZGERALD, R. 1965. The effects of surgical exposures of dental pulps in germ-free and conventional laboratory rats. *Oral Surgery, Oral Medicine, Oral Pathology,* 20, 340-349.

KAMATH, U., SHETH, H., RAMESH, S. & SINGLA, K. 2013. Comparison of the antibacterial efficacy of tea tree oil with 3% sodium hypochlorite and 2% Chlorhexidine against E. faecalis: An in vitro study. *Journal of Contemporary Dentistry,* 3, 117-120.

KANGARLOU, A., SOFIABADI, S., ASGARY, S., MAHJOUR, F., DIANAT, O., YADEGARI, Z. & YOUNESSIAN, F. 2012. Assessment of antifungal activity of Proroot mineral trioxide aggregate and mineral trioxide aggregate-Angelus. *Dental Research Journal,* 9, 256-260.

KANGARLOU, A., SOFIABADI, S., YADEGARI, Z. & ASGARY, S. 2009. Antifungal effect of calcium enriched mixture cement against Candida albicans. *Iranian Endodontic Journal,* 4, 101-105.

KAUP, M., SCHÄFER, E. & DAMMASCHKE, T. 2015. An in vitro study of different material properties of Biodentine compared to ProRoot MTA. *Head & Face Medicine,* 11, 16.

KEAN, R., DELANEY, C., RAJENDRAN, R., SHERRY, L., METCALFE, R., THOMAS, R., MCLEAN, W., WILLIAMS, C. & RAMAGE, G. 2018. Gaining insights from Candida biofilm heterogeneity: one size does not fit all. *Journal of Fungi,* 4, 12.

KEAN, R., RAJENDRAN, R., HAGGARTY, J., TOWNSEND, E. M., SHORT, B., BURGESS, K. E., LANG, S., MILLINGTON, O., MACKAY, W. G. & WILLIAMS, C. 2017. Candida albicans mycofilms support Staphylococcus aureus colonization and enhances miconazole resistance in dual-species interactions. *Frontiers in Microbiology,* 8, 258.

KELEŞ, A., KESKIN, C., ÇIFTÇIOĞLU, E. & ALAK, G. 2022. Evaluation of the band-shaped isthmuses in the mesiobuccal root canal system using micro-computed tomography. *Clinical Oral Investigations*, doi: 10.1007/s00784-00022-04548-00780.

KFIR, A., GOLDENBERG, C., METZGER, Z., HÜLSMANN, M. & BAXTER, S. 2020. Cleanliness and erosion of root canal walls after irrigation with a new HEDP-based solution vs. traditional sodium hypochlorite followed by

EDTA. A scanning electron microscope study. *Clinical Oral Investigations,* 24, 3699-3706.

KHAN, I., SAEED, K. & KHAN, I. 2019. Nanoparticles: Properties, applications and toxicities. *Arabian Journal of Chemistry,* 12, 908-931.

KHEDMAT, S., ALIGHOLI, M. & SADEGHI, S. 2009. Influence of Bovine Serum Albumin on the Antibacterial Activity of Endodontic Irrigants against Enterococcus Faecalis. *Iranian Endodontic Journal,* 4, 139-143.

KISHEN, A., SUM, C.-P., MATHEW, S. & LIM, C.-T. 2008. Influence of irrigation regimens on the adherence of Enterococcus faecalis to root canal dentin. *Journal of Endodontics,* 34, 850-854.

KOCH, K. & BRAVE, D. 2012. Bioceramics, part I: the clinician's viewpoint. *Dentistry Today,* 31, 130-135.

KOCI, O., LOGAN, M., SVOLOS, V., RUSSELL, R. K., GERASIMIDIS, K. & IJAZ, U. Z. 2018. An automated identification and analysis of ontological terms in gastrointestinal diseases and nutrition-related literature provides useful insights. *PeerJ,* 6, e5047.

KONG, M., CHEN, X.-G., XUE, Y.-P., LIU, C.-S., YU, L.-J., JI, Q.-X., CHA, D. S. & PARK, H. J. 2008. Preparation and antibacterial activity of chitosan microshperes in a solid dispersing system. *Frontiers of Materials Science in China,* 2, 214-220.

KONG, M., CHEN, X. G., XING, K. & PARK, H. J. 2010. Antimicrobial properties of chitosan and mode of action: a state of the art review. *International Journal of Food Microbiology,* 144, 51-63.

KORONA-GLOWNIAK, I., PIATEK, D., FORNAL, E., LUKOWIAK, A., GERASYMCHUK, Y., KEDZIORA, A., BUGLA-PŁOSKONSKA, G., GRYWALSKA, E., BACHANEK, T. & MALM, A. 2021. Patterns of oral microbiota in patients with apical periodontitis. *Journal of Clinical Medicine,* 10, 2707.

KRASNER, P. & RANKOW, H. J. 2004. Anatomy of the pulp-chamber floor. *Journal of Endodontics,* 30, 5-16.

KRISHNAMOORTHY, A. L., LEMUS, A. A., SOLOMON, A. P., VALM, A. M. & NEELAKANTAN, P. 2020. Interactions between Candida albicans and Enterococcus faecalis in an Organotypic Oral Epithelial Model. *Microorganisms,* 8, 1771.

KROM, B. P., COHEN, J. B., FESER, G. E. M. & CIHLAR, R. L. 2007. Optimized candidal biofilm microtiter assay. *Journal of Microbiological Methods,* 68, 421-423.

KUJUMGIEV, A., TSVETKOVA, I., SERKEDJIEVA, Y., BANKOVA, V., CHRISTOV, R. & POPOV, S. 1999. Antibacterial, antifungal and antiviral activity of propolis of different geographic origin. *Journal of Ethnopharmacology,* 64, 235-240.

KULSHRESTHA, S., KHAN, S., HASAN, S., KHAN, M. E., MISBA, L. & KHAN, A. U. 2016. Calcium fluoride nanoparticles induced suppression of Streptococcus mutans biofilm: an in vitro and in vivo approach. *Applied Microbiology and Biotechnology,* 100, 1901-1914.

KUMAR, H. 2013. An in vitro evaluation of the antimicrobial efficacy of Curcuma longa, Tachyspermum ammi, chlorhexidine gluconate, and calcium hydroxide on Enterococcus faecalis. *Journal of Conservative Dentistry,* 16, 144-147.

KUMAR, M. R., MUZZARELLI, R. A., MUZZARELLI, C., SASHIWA, H. & DOMB, A. 2004. Chitosan Chemistry and Pharmaceutical Perspectives. *Chemical reviews,* 104, 6017-6084.

KUMAR, P., NAGARAJAN, A. & UCHIL, P. D. 2018. Analysis of cell viability by the lactate dehydrogenase assay. *Cold Spring Harbor Protocols,* 2018**,** doi: 10.1101/pdb.prot095497.

KUROPATNICKI, A. K., SZLISZKA, E. & KROL, W. 2013. Historical aspects of propolis research in modern times. *Evidence-Based Complementary and Alternative Medicine,* 2013**,** 964149.

L PETERS, L., WESSELINK, P., BUIJS, J. & VAN WINKELHOFF, A. 2001. Viable bacteria in root dentinal tubules of teeth with apical periodontitis. *Journal of Endodontics,* 27**,** 76-81.

L PETERS, L., WESSELINK, P. & MOORER, W. 1995. The fate and the role of bacteria left in root dentinal tubules. *International Endodontic Journal,* 28**,** 95-99.

L SMITH, L. C. 1981. CITATION ANALYSIS. *Library Trends,* 30**,** 83-106.

L YANG, L., LU, W., PANG, Y., HUANG, X., WANG, Z., QIN, A. & HU, Q. 2016. Fabrication of a novel chitosan scaffold with asymmetric structure for guided tissue regeneration. *RSC advances,* 6**,** 71567-71573.

L ZHANG, L., LI, Q.-L., CAO, Y. & WANG, Y. 2018. Regenerating a monoblock to obturate root canalsvia a mineralising strategy. *Scientific Reports,* 8**,** 13356.

LAMBOOIJ, J. M., HOOGENKAMP, M. A., BRANDT, B. W., JANUS, M. M. & KROM, B. P. 2017. Fungal mitochondrial oxygen consumption induces the growth of strict anaerobic bacteria. *Fungal Genetics and Biology,* 109**,** 1-6.

LEACH, S. 1977. Mode of action of chlorhexidine in the mouth. In The borderland between caries and periodontal disease. Academic Press, 105-128.

LEE, Y.-L., LEE, B.-S., LIN, F.-H., LIN, A. Y., LAN, W.-H. & LIN, C.-P. 2004. Effects of physiological environments on the hydration behavior of mineral trioxide aggregate. *Biomaterials,* 25**,** 787-793.

LEONARDO, M. R., TANOMARU FILHO, M., SILVA, L. A. B. D., NELSON FILHO, P., BONIFACIO, K. & ITO, I. Y. 1999. In vivo antimicrobial activity of 2% chlorhexidine used as a root canal irrigating solution. *Journal of Endodontics,* 25**,** 167-171.

LEONHARD, M., ZATORSKA, B., MOSER, D. & SCHNEIDER-STICKLER, B. 2019. Growth media for mixed multispecies oropharyngeal biofilm compositions on silicone. *BioMed Research International,* 2019**,** 8051270.

LEWISON, G., ROE, P., WEBBER, R. & SULLIVAN, R. 2016. Lung cancer researchers, 2008–2013: their sex and ethnicity. *Scientometrics,* 106**,** 105-117.

LIMA, A. R., GANGULY, T., WALKER, A. R., ACOSTA, N., FRANCISCO, P. A., PILEGGI, R., LEMOS, J. A., GOMES, B. P. & ABRANCHES, J. 2020. Phenotypic and genotypic characterization of Streptococcus mutans strains isolated from endodontic infections. *Journal of Endodontics*.

LIN, J., SHEN, Y. & HAAPASALO, M. 2013. A comparative study of biofilm removal with hand, rotary nickel-titanium, and self-adjusting file instrumentation using a novel in vitro biofilm model. *Journal of Endodontics,* 39**,** 658-663.

LOH, J. W., YEOH, G., SAUNDERS, M. & LIM, L.-Y. 2010. Uptake and cytotoxicity of chitosan nanoparticles in human liver cells. *Toxicology and Applied Pharmacology,* 249**,** 148-157.

LOTKA, A. J. 1926. The frequency distribution of scientific productivity. *Journal of the Washington Academy of Sciences,* 16**,** 317-323.

LOVATO, K. F. & SEDGLEY, C. M. 2011. Antibacterial activity of endosequence root repair material and proroot MTA against clinical isolates of Enterococcus faecalis. *Journal of Endodontics,* 37**,** 1542-1546.

LOVE, R. 2001. Enterococcus faecalis–a mechanism for its role in endodontic failure. *International Endodontic Journal,* 34**,** 399-405.

LOVE, R. & JENKINSON, H. 2002. Invasion of dentinal tubules by oral bacteria. *Critical Reviews in Oral Biology & Medicine,* 13**,** 171-183.

LUKOVIĆ, M., SCHLANGEN, E. & YE, G. 2015. Combined experimental and numerical study of fracture behaviour of cement paste at the microlevel. *Cement and Concrete Research,* 73**,** 123-135.

M WU, M.-K., WESSELINK, P. R. & WALTON, R. E. 2000. Apical terminus location of root canal treatment procedures. *Oral Surgery, Oral Medicine, Oral Pathology, Oral Radiology, and Endodontology,* 89**,** 99-103.

M WU, M. K., DUMMER, P. & WESSELINK, P. 2006. Consequences of and strategies to deal with residual post-treatment root canal infection. *International Endodontic Journal,* 39**,** 343-356.

MACHA, I. J., OZYEGIN, L., CHOU, J., SAMUR, R., OKTAR, F. & BEN-NISSAN, B. 2013. An alternative synthesis method for di calcium phosphate (Monetite) powders from mediterranean mussel (Mytilus galloprovincialis) shells. *Journal of the Australian Ceramic Society,* 49**,** 122-128.

MACROBERTS, M. H. & MACROBERTS, B. R. 1989. Problems of citation analysis: A critical review. *Journal of the American Society for information Science,* 40**,** 342-349.

MANFREDI, M., FIGINI, L., GAGLIANI, M. & LODI, G. 2016. Single versus multiple visits for endodontic treatment of permanent teeth. *Cochrane Database of Systematic Reviews***,** doi: 10.1002/14651858.CD14005296.pub14651853.

MANOIL, D., AL-MANEI, K. & BELIBASAKIS, G. N. 2020. A Systematic Review of the Root Canal Microbiota Associated with Apical Periodontitis: Lessons from Next-Generation Sequencing. *Proteomics - Clinical Applications,* 14**,** 1900060.

MARGUNATO, S., TAŞLı, P. N., AYDıN, S., KAZANDAĞ, M. K. & ŞAHIN, F. 2015. In vitro evaluation of ProRoot MTA, Biodentine, and MM-MTA on human alveolar bone marrow stem cells in terms of biocompatibility and mineralization. *Journal of Endodontics,* 41**,** 1646-1652.

MARSH, P. D. 1995. The role of continuous culture in modelling the human microflora. *Journal of Chemical Technology & Biotechnology,* 64**,** 1-9.

MARTIN, M. P. & PILEGGI, R. 2004. A quantitative analysis of Propolis: a promising new storage media following avulsion. *Dental Traumatology,* 20**,** 85-89.

MARTINEZ-ANDRADE, J. M., AVALOS-BORJA, M., VILCHIS-NESTOR, A. R., SANCHEZ-VARGAS, L. O. & CASTRO-LONGORIA, E. 2018. Dual function of EDTA with silver nanoparticles for root canal treatment–A novel modification. *PlOS One,* 13**,** e0190866.

MASIC, I. & BEGIC, E. 2016. Scientometric Dilemma: Is H-index adequate for scientific validity of academic's work? *Acta Informatica Medica,* 24**,** 228–232.

MATICA, M. A., AACHMANN, F. L., TØNDERVIK, A., SLETTA, H. & OSTAFE, V. 2019. Chitosan as a Wound Dressing Starting Material: Antimicrobial Properties and Mode of Action. *International Journal of Molecular Sciences,* 20**,** 1-33.

MATTIGATTI, S., RATNAKAR, P., MOTURI, S., VARMA, S. & RAIRAM, S. 2012. Antimicrobial effect of conventional root canal medicaments vs propolis

against Enterococcus faecalis, Staphylococcus aureus and Candida albicans. *The Journal of Contemporary Dental Practice,* 13**,** 305-309.

MCCOOL, J. I., BOBERICK, K. G. & BARAN, G. R. 2001. Lifetime predictions for resin-based composites using cyclic and dynamic fatigue. *Journal of Biomedical Materials Research,* 58**,** 247-253.

MCKEEGAN, K. S., BORGES-WALMSLEY, M. I. & WALMSLEY, A. R. 2002. Microbial and viral drug resistance mechanisms. *Trends in Microbiology,* 10**,** s8-s14.

MENG, D., GARBA, B., REN, Y., YAO, M., XIA, X., LI, M. & WANG, Y. 2020. Antifungal activity of chitosan against Aspergillus ochraceus and its possible mechanisms of action. *International Journal of Biological Macromolecules,* 158**,** 1063-1070.

MERGONI, G., PERCUDANI, D., LODI, G., BERTANI, P. & MANFREDI, M. 2018. Prevalence of Candida Species in Endodontic Infections: Systematic Review and Meta-analysis. *Journal of Endodontics,* 44**,** 1616-1625.

MI, F.-L., SHYU, S.-S., WU, Y.-B., LEE, S.-T., SHYONG, J.-Y. & HUANG, R.-N. 2001. Fabrication and characterization of a sponge-like asymmetric chitosan membrane as a wound dressing. *Biomaterials,* 22**,** 165-173.

MILES, A. A., MISRA, S. S. & IRWIN, J. O. 1938. The estimation of the bactericidal power of the blood. *The Journal of Hygiene,* 38**,** 732-749.

MILLER, J. H., AVILÉS-REYES, A., SCOTT-ANNE, K., GREGOIRE, S., WATSON, G. E., SAMPSON, E., PROGULSKE-FOX, A., KOO, H., BOWEN, W. H. & LEMOS, J. A. 2015. The collagen binding protein Cnm contributes to oral colonization and cariogenicity of Streptococcus mutans OMZ175. *Infection and Immunity,* 83**,** 2001-2010.

MILUTINOVIĆ-SMILJANIĆ, S., ILIĆ, D., DANILOVIĆ, V. & ANTONIJEVIĆ, Đ. 2021. The advantages and disadvantages of biodentine: satisfactory mechanical properties and radiopacity not meeting ISO standard. *Vojnosanitetski Pregled,* 78**,** 973-980.

MITTAL, R., TANDAN, M. & KAUSHIK, G. 2022. Antimicrobial efficacy of commercially available ozonated olive oil and sodium hypochlorite with and without ultrasonic activation in primary endodontic infections: A randomized clinical trial. *Endodontology,* 34**,** 102-107.

MOED, H. F. 2009. New developments in the use of citation analysis in research evaluation. *Archivum Immunologiae et Therapiae Experimentalis,* 57**,** 13-18.

MOHAMMADI, Z. & ABBOTT, P. 2009. The properties and applications of chlorhexidine in endodontics. *International Endodontic Journal,* 42**,** 288-302.

MOHAMMADI, Z., SHALAVI, S. & YAZDIZADEH, M. 2012. Antimicrobial activity of calcium hydroxide in endodontics: a review. *Chonnam Medical Journal,* 48**,** 133-140.

MOHMMED, S., VIANNA, M., PENNY, M., HILTON, S., MORDAN, N. & KNOWLES, J. 2018. Investigations into in situ Enterococcus faecalis biofilm removal by passive and active sodium hypochlorite irrigation delivered into the lateral canal of a simulated root canal model. *International Endodontic Journal,* 51**,** 649-662.

MOHMMED, S. A., VIANNA, M. E., PENNY, M. R., HILTON, S. T., MORDAN, N. & KNOWLES, J. C. 2017. Confocal laser scanning, scanning electron, and transmission electron microscopy investigation of Enterococcus faecalis biofilm degradation using passive and active sodium hypochlorite irrigation within a simulated root canal model. *Microbiologyopen,* 6**,** e00455.

MOLANDER, A., REIT, C., DAHLEN, G. & KVIST, T. 1998. Microbiological status of root-filled teeth with apical periodontitis. *International Endodontic Journal,* 31, 1-7.

MONTEIRO, D. R., GORUP, L. F., TAKAMIYA, A. S., RUVOLLO-FILHO, A. C., DE CAMARGO, E. R. & BARBOSA, D. B. 2009. The growing importance of materials that prevent microbial adhesion: antimicrobial effect of medical devices containing silver. *International Journal of Antimicrobial Agents,* 34, 103-110.

MONTELONGO-JAUREGUI, D., SRINIVASAN, A., RAMASUBRAMANIAN, A. K. & LOPEZ-RIBOT, J. L. 2016. An in vitro model for oral mixed biofilms of Candida albicans and Streptococcus gordonii in synthetic saliva. *Frontiers in Microbiology,* 7, 686.

MONTELONGO-JAUREGUI, D., SRINIVASAN, A., RAMASUBRAMANIAN, A. K. & LOPEZ-RIBOT, J. L. 2018. An in vitro model for Candida albicans–Streptococcus gordonii biofilms on titanium surfaces. *Journal of Fungi,* 4, 66.

MORAES, G., ZAMBOM, C. & SIQUEIRA, W. L. 2021. Nanoparticles in Dentistry: A Comprehensive Review. *Pharmaceuticals,* 14, 752.

MORAGO, A., ORDINOLA-ZAPATA, R., FERRER-LUQUE, C. M., BACA, P., RUIZ-LINARES, M. & ARIAS-MOLIZ, M. T. 2016. Influence of smear layer on the antimicrobial activity of a sodium hypochlorite/etidronic acid irrigating solution in infected dentin. *Journal of Endodontics,* 42, 1647-1650.

MUBARAKALI, D., LEWISOSCAR, F., GOPINATH, V., ALHARBI, N. S., ALHARBI, S. A. & THAJUDDIN, N. 2018. An inhibitory action of chitosan nanoparticles against pathogenic bacteria and fungi and their potential applications as biocompatible antioxidants. *Microbial pathogenesis,* 114, 323-327.

MUNIZ, F. W. M., MONTAGNER, F., JACINTO, R. C., RÖSING, C. K. & GOMES, B. P. 2018. Correlation between crestal alveolar bone loss with intracanal bacteria and apical lesion area in necrotic teeth. *Archives of Oral Biology,* 95, 1-6.

MUNSON, M., PITT-FORD, T., CHONG, B., WEIGHTMAN, A. & WADE, W. 2002. Molecular and cultural analysis of the microflora associated with endodontic infections. *Journal of Dental Research,* 81, 761-766.

MURAD, C., SASSONE, L., FAVERI, M., HIRATA JR, R., FIGUEIREDO, L. & FERES, M. 2014. Microbial diversity in persistent root canal infections investigated by checkerboard DNA-DNA hybridization. *Journal of Endodontics,* 40, 899-906.

NABAVIZADEH, M. R., MOAZZAMI, F., GHOLAMI, A., MEHRABI, V. & GHAHRAMANI, Y. 2022. Cytotoxic Effect of Nano Fast Cement and ProRoot Mineral Trioxide Aggregate on L-929 Fibroblast Cells: an in vitro Study. *Journal of Dentistry,* 23, 13.

NAENNI, N., THOMA, K. & ZEHNDER, M. 2004. Soft tissue dissolution capacity of currently used and potential endodontic irrigants. *Journal of Endodontics,* 30, 785-787.

NAGAS, E., CEHRELI, Z. C., UYANIK, O., VALLITTU, P. K. & LASSILA, L. V. 2016. Reinforcing Effect of Glass Fiber–incorporated ProRoot MTA and Biodentine as Intraorifice Barriers. *Journal of Endodontics,* 42, 1673-1676.

NAIR, P. 2004. Pathogenesis of apical periodontitis and the causes of endodontic failures. *Critical Reviews in Oral Biology & Medicine,* 15, 348-381.

NAIR, P., HENRY, S., CANO, V. & VERA, J. 2005. Microbial status of apical root canal system of human mandibular first molars with primary apical periodontitis after "one-visit" endodontic treatment. *Oral Surgery, Oral*

Medicine, Oral Pathology, Oral Radiology, and Endodontology, 99**,** 231-252.

NAIR, P. R., SJÖGREN, U., KREY, G., KAHNBERG, K.-E. & SUNDQVIST, G. 1990. Intraradicular bacteria and fungi in root-filled, asymptomatic human teeth with therapy-resistant periapical lesions: a long-term light and electron microscopic follow-up study. *Journal of Endodontics,* 16**,** 580-588.

NAIR, R., ANIL, S. & SAMARANAYAKE, L. 2001. The effect of oral bacteria on Candida albicans germ-tube formation. *Acta Pathologica, Microbiologica, et Immunologica Scandinavica,* 109**,** 147-154.

NARDELLO, L. C., AMADO, P. P., FRANCO, D. C., CAZARES, R. X., NOGALES, C. G., MAYER, M. P., KARYGIANNI, L., THURNHEER, T. & PINHEIRO, E. T. 2020. Next-Generation sequencing to assess potentially active bacteria in endodontic infections. *Journal of Endodontics,* 46**,** 1105-1112.

NARIN, F. 1976. Evaluative Bibliometrics: The Use of Publication and Citation Analysis in the Evaluation of Scientific Activity, Computer Horizons.

NASRI, Z., JAHROMI, M. Z. & AMINZADEH, A. 2022. Clinical and histological response of human pulp tissue to direct pulp capping with mineral trioxide aggregate, Biodentine and propolis. *Dental Research Journal,* 19**,** 2022.

NATERA, M., PILEGGI, R. & NAIR, U. 2011. A comparison of two gutta-percha obturation techniques to replicate canal irregularities in a split-tooth model. *Oral Surgery, Oral Medicine, Oral Pathology, Oral Radiology, and Endodontology,* 112**,** e29-e34.

NAVYA, P. & DAIMA, H. K. 2016. Rational engineering of physicochemical properties of nanomaterials for biomedical applications with nanotoxicological perspectives. *Nano Convergence,* 3**,** 1.

NEELAKANTAN, P., HERRERA, D., PECORARI, V. & GOMES, B. 2019. Endotoxin levels after chemomechanical preparation of root canals with sodium hypochlorite or chlorhexidine: a systematic review of clinical trials and meta-analysis. *International Endodontic Journal,* 52**,** 19-27.

NEELAKANTAN, P., ROMERO, M., VERA, J., DAOOD, U., KHAN, A. U., YAN, A. & CHEUNG, G. S. P. 2017. Biofilms in endodontics—current status and future directions. *International Journal of Molecular Sciences,* 18**,** 1748.

NIKAWA, H., HAMADA, T., YAMASHIRO, H., MURATA, H. & SUBIWAHJUDI, A. 1998. The effect of saliva or serum on Streptococcus mutans and Candida albicans colonization of hydroxylapatite beads. *Journal of Dentistry,* 26**,** 31-37.

NIKIFORUK, G. & SREEBNY, L. 1953. Demineralization of hard tissues by organic chelating agents at neutral pH. *Journal of Dental Research,* 32**,** 859-867.

NÓBREGA, L. M., DELBONI, M. G., MARTINHO, F. C., ZAIA, A. A., FERRAZ, C. C. & GOMES, B. P. 2013. Treponema diversity in root canals with endodontic failure. *European Journal of Dentistry,* 7**,** 061-068.

NOCKER, A., CHEUNG, C. Y. & CAMPER, A. K. 2006. Comparison of propidium monoazide with ethidium monoazide for differentiation of live vs. dead bacteria by selective removal of DNA from dead cells. *Journal Microbiol Methods,* 67**,** 310-320.

NOMOTO, R. & MCCABE, J. 2001. A simple acid erosion test for dental water-based cements. *Dental Materials,* 17**,** 53-59.

NONAT, A. & FRANQUIN, J.-C. 2006. Unnouveaumatériau de restaurationdentaire à base minérale. *Matériaux*.

NOSRAT, A., KOLAHDOUZAN, A., HOSSEINI, F., MEHRIZI, E. A., VERMA, P. & TORABINEJAD, M. 2015. Histologic outcomes of uninfected human

immature teeth treated with regenerative endodontics: 2 case reports. *Journal of Endodontics,* 41**,** 1725-1729.

O'DONNELL, L. E., ALALWAN, H. K., KEAN, R., CALVERT, G., NILE, C. J., LAPPIN, D. J., ROBERTSON, D., WILLIAMS, C., RAMAGE, G. & SHERRY, L. 2017. Candida albicans biofilm heterogeneity does not influence denture stomatitis but strongly influences denture cleansing capacity. *Journal of Medical Microbiology,* 66**,** 54-60.

O'DONNELL, L. E., MILLHOUSE, E., SHERRY, L., KEAN, R., MALCOLM, J., NILE, C. J. & RAMAGE, G. 2015. Polymicrobial Candida biofilms: friends and foe in the oral cavity. *FEMS Yeast Research,* 15**,** fov077.

O PETERS, O. A., BARDSLEY, S., FONG, J., PANDHER, G. & DIVITO, E. 2011. Disinfection of root canals with photon-initiated photoacoustic streaming. *Journal of Endodontics,* 37**,** 1008-1012.

OCHOA-RODRÍGUEZ, V. M., TANOMARU-FILHO, M., RODRIGUES, E. M., GUERREIRO-TANOMARU, J. M., SPIN-NETO, R. & FARIA, G. 2019. Addition of zirconium oxide to Biodentine increases radiopacity and does not alter its physicochemical and biological properties. *Journal of Applied Oral Science,* 27.

OKINO, L., SIQUEIRA, E., SANTOS, M., BOMBANA, A. & FIGUEIREDO, J. 2004. Dissolution of pulp tissue by aqueous solution of chlorhexidine digluconate and chlorhexidine digluconate gel. *International Endodontic Journal,* 37**,** 38-41.

OMAR ZAKI, S. S., IBRAHIM, M. N. & KATAS, H. 2015. Particle size affects concentration-dependent cytotoxicity of chitosan nanoparticles towards mouse hematopoietic stem cells. *Journal of Nanotechnology,* 2015.

ORDINOLA-ZAPATA, R., PETERS, O. A., NAGENDRABABU, V., AZEVEDO, B., DUMMER, P. M. H. & NEELAKANTAN, P. 2020. What is of interest in Endodontology? A bibliometric review of research published in the International Endodontic Journal and the Journal of Endodontics from 1980 to 2019. *International Endodontic Journal*.

ØRSTAVIK, D. 2019. Apical periodontitis: microbial infection and host responses. In Essential endodontology: prevention and treatment of apical periodontitis. John Wiley & Sons, 1-10.

OSSENI, S., BONOU, S., SAGBO, E., AHOUANSOU, R., AGBAHOUNGBATA, M., NEUMEYER, D., VERELST, M. & MAURICOT, R. 2018. Synthesis of Calcium Phosphate Bioceramics Based on Snail Shells: Towards a Valorization of Snail Shells from Republic of Benin. *American Journal of Chemistry,* 8**,** 90-95.

OUYANG, X., KOLEVA, D., YE, G. & VAN BREUGEL, K. 2017. Understanding the adhesion mechanisms between CSH and fillers. *Cement and Concrete Research,* 100**,** 275-283.

P SILVA, P., GUEDES, D. F. C., NAKADI, F. V., PÉCORA, J. D. & CRUZ-FILHO, A. M. D. 2013. Chitosan: a new solution for removal of smear layer after root canal instrumentation. *International Endodontic Journal,* 46**,** 332-338.

PAFILIS, E., BĒRZIŅŠ, R., ARVANITIDIS, C. & JENSEN, L. 2017. EXTRACT 2.0: interactive identification of biological entities mentioned in text to assist database curation and knowledge extraction. *Biodiversity Information Science and Standards,* 1**,** e20152.

PAINE, R. T. 1969. A note on trophic complexity and community stability. *The American Naturalist,* 103**,** 91-93.

PALMA-GUERRERO, J., LOPEZ-JIMENEZ, J., PÉREZ-BERNÁ, A., HUANG, I. C., JANSSON, H. B., SALINAS, J., VILLALAÍN, J., READ, N. & LOPEZ-LLORCA, L.

2010. Membrane fluidity determines sensitivity of filamentous fungi to chitosan. *Molecular Microbiology,* 75**,** 1021-1032.

PAPA, J., CAIN, C. & MESSER, H. 1994. Moisture content of vital vs endodontically treated teeth. *Dental Traumatology,* 10**,** 91-93.

PARK, Y., KIM, M.-H., PARK, S.-C., CHEONG, H., JANG, M.-K., NAH, J.-W. & HAHM, K.-S. 2008. Investigation of the antifungal activity and mechanism of action of LMWS-chitosan. *Journal of Microbiology and Biotechnology,* 18**,** 1729-1734.

PARSEK, M. R. & SINGH, P. K. 2003. Bacterial biofilms: an emerging link to disease pathogenesis. *Annual Reviews in Microbiology,* 57**,** 677-701.

PARYANI, K. & KIM, S. G. 2013. Regenerative endodontic treatment of permanent teeth after completion of root development: a report of 2 cases. *Journal of Endodontics,* 39**,** 929-934.

PATIL, K. & PATIL, M. 2009. Principle of Radiographic. In Textbook of Oral Radiology. 213.

PATTANAIK, S., JENA, A. & SHASHIREKHA, G. 2019. In vitro comparative evaluation of antifungal efficacy of three endodontic sealers with and without incorporation of chitosan nanoparticles against Candida albicans. *Journal of Conservative Dentistry,* 22**,** 564–567.

PECIULIENE, V., REYNAUD, A., BALCIUNIENE, I. & HAAPASALO, M. 2001. Isolation of yeasts and enteric bacteria in root-filled teeth with chronic apical periodontitis. *International Endodontic Journal,* 34**,** 429-434.

PEETERS, E., NELIS, H. J. & COENYE, T. 2008. Comparison of multiple methods for quantification of microbial biofilms grown in microtiter plates. *Journal of Microbiological Methods,* 72**,** 157-165.

PEKKAN, G. 2016. Radiopacity of dental materials: An overview. *Avicenna Journal of Dental Research,* 8**,** 8-8.

PERSOON, I. F., BUIJS, M. J., ÖZOK, A. R., CRIELAARD, W., KROM, B. P., ZAURA, E. & BRANDT, B. W. 2017. The mycobiome of root canal infections is correlated to the bacteriome. *Clinical Oral Investigations,* 21**,** 1871-1881.

PIERCE, C. G., UPPULURI, P., TRISTAN, A. R., WORMLEY JR, F. L., MOWAT, E., RAMAGE, G. & LOPEZ-RIBOT, J. L. 2008. A simple and reproducible 96-well plate-based method for the formation of fungal biofilms and its application to antifungal susceptibility testing. *Nature Protocols,* 3**,** 1494-1500.

PINHEIRO, E., GOMES, B., FERRAZ, C., SOUSA, E., TEIXEIRA, F. & SOUZA-FILHO, F. 2003. Microorganisms from canals of root-filled teeth with periapical lesions. *International Endodontic Journal,* 36**,** 1-11.

PIRES, M. D., CORDEIRO, J., VASCONCELOS, I., ALVES, M., QUARESMA, S. A., GINJEIRA, A. & CAMILLERI, J. 2021. Effect of different manipulations on the physical, chemical and microstructural characteristics of Biodentine. *Dental Materials,* 37**,** e399-e406.

PODAR, R., KULKARNI, G. P., DADU, S. S., SINGH, S. & SINGH, S. H. 2015. In vivo antimicrobial efficacy of 6% Morinda citrifolia, Azadirachta indica, and 3% sodium hypochlorite as root canal irrigants. *European Journal of Dentistry,* 9**,** 529-534.

PORTENIER, I., HAAPASALO, H., RYE, A., WALTIMO, T., ØRSTAVIK, D. & HAAPASALO, M. 2001. Inactivation of root canal medicaments by dentine, hydroxylapatite and bovine serum albumin. *International Endodontic Journal,* 34**,** 184-188.

POTTEN, C. S. & WILSON, J. W. 2009. The development of epithelial stem cell concepts. In Essentials of stem cell biology. Elsevier, 17-27.

PRABHAKAR, J., SENTHILKUMAR, M., PRIYA, M. S., MAHALAKSHMI, K., SEHGAL, P. K. & SUKUMARAN, V. G. 2010. Evaluation of antimicrobial efficacy of herbal alternatives (Triphala and green tea polyphenols), MTAD, and 5% sodium hypochlorite against Enterococcus faecalis biofilm formed on tooth substrate: an in vitro study. *Journal of Endodontics,* 36**,** 83-86.

PRADEEP, P., RANDHYA, R., SHANAVAS PALLIYAL, M. K. & HIMA, S. 2018. An in vitro comparative evaluation of shear bond strength of biodentine and MTA. *International Journal of Applied Dental Sciences,* 4**,** 01-03.

PRITCHARD, A. 1969. Statistical bibliography or bibliometrics. *Journal of Documentation,* 25**,** 348-349.

PUJAR, M., PATIL, C. & KADAM, A. 2011. Comparison of antimicrobial efficacy of Triphala,(GTP) Green tea polyphenols and 3% of sodium hypochlorite on Enterococcus faecalis biofilms formed on tooth substrate: in vitro. *Journal of International Oral Health,* 3**,** 23-29.

PUNIA, S. K., NADIG, P. & PUNIA, V. 2011. An in vitro assessment of apical microleakage in root canals obturated with gutta-flow, resilon, thermafil and lateral condensation: A stereomicroscopic study. *Journal of Conservative Dentistry,* 14**,** 173-177.

QADIRI, S. Y. & MUSTAFA, S. 2019. Role of calcium hydroxide in root canal therapy: A comprehensive review. *Journal of Advanced Medical and Dental Sciences Research,* 7**,** 1-3.

QIAN, W., MA, T., YE, M., LI, Z., LIU, Y. & HAO, P. 2019. Microbiota in the apical root canal system of tooth with apical periodontitis. *BMC Genomics,* 20**,** 175-185.

R KIM, R. J.-Y., KIM, M.-O., LEE, K.-S., LEE, D.-Y. & SHIN, J.-H. 2015. An in vitro evaluation of the antibacterial properties of three mineral trioxide aggregate (MTA) against five oral bacteria. *Archives of Oral Biology,* 60**,** 1497-1502.

RAAFAT, D., VON BARGEN, K., HAAS, A. & SAHL, H.-G. 2008. Insights into the mode of action of chitosan as an antibacterial compound. *Applied and Environmental Microbiology,* 74**,** 3764-3773.

RABEA, E. I., BADAWY, M. E.-T., STEVENS, C. V., SMAGGHE, G. & STEURBAUT, W. 2003. Chitosan as antimicrobial agent: applications and mode of action. *Biomacromolecules,* 4**,** 1457-1465.

RAGHAVENDRA, S. S., JADHAV, G. R., GATHANI, K. M. & KOTADIA, P. 2017. Bioceramics in endodontics–a review. *Journal of Istanbul University Faculty of Dentistry,* 51**,** 128-137.

RAHIMI, S., SHAHI, S., TORABI, Z., REZAIE, Y., GHASEMI, N. & ABOLHASANI, S. 2018. The effect of a mineralized bone graft on the surface microhardness of mineral trioxide aggregate and biodentine. *Iranian Endodontic Journal,* 13**,** 83-87.

RAHMAN, B. & GOSWAMI, M. 2021. Comparative evaluation of indirect pulp therapy in young permanent teeth using biodentine and theracal: a randomized clinical trial. *Journal of Clinical Pediatric Dentistry,* 45**,** 158-164.

RAHMAN, M. A. & HALFAR, J. 2014. First evidence of chitin in calcified coralline algae: new insights into the calcification process of Clathromorphum compactum. *Scientific Reports,* 4**,** 6162.

RAMAGE, G., SAVILLE, S. P., THOMAS, D. P. & LOPEZ-RIBOT, J. L. 2005. Candida biofilms: an update. *Eukaryotic Cell,* 4**,** 633-638.

RAMAGE, G., WALLE, K. V., WICKES, B. L. & LÓPEZ-RIBOT, J. L. 2001. Standardized method for in vitro antifungal susceptibility testing of

Candida albicansbiofilms. *Antimicrobial Agents and Chemotherapy,* 45, 2475-2479.

RAMAGE, G., WICKES, B. L. & LÓPEZ-RIBOT, J. L. 2007. Inhibition on Candida albicans biofilm formation using divalent cation chelators (EDTA). *Mycopathologia,* 164, 301-306.

RAPACKA-ZDONCZYK, A., WOZNIAK, A., NAKONIECZNA, J. & GRINHOLC, M. 2021. Development of antimicrobial phototreatment tolerance: Why the methodology matters. *International Journal of Molecular Sciences,* 22, 2224.

REGAN, J., GUTMANN, J. & WITHERSPOON, D. 2002. Comparison of Diaket and MTA when used as root-end filling materials to support regeneration of the periradicular tissues. *International Endodontic Journal,* 35, 840-847.

REN, Y., WANG, C., CHEN, Z., ALLAN, E., VAN DER MEI, H. C. & BUSSCHER, H. J. 2018. Emergent heterogeneous microenvironments in biofilms: substratum surface heterogeneity and bacterial adhesion force-sensing. *FEMS Microbiology Reviews,* 42, 259-272.

REYES-CARMONA, J. F., FELIPPE, M. S. & FELIPPE, W. T. 2010. A phosphate-buffered saline intracanal dressing improves the biomineralization ability of mineral trioxide aggregate apical plugs. *Journal of Endodontics,* 36, 1648-1652.

RICUCCI, D. & SIQUEIRA 2010. Biofilms and apical periodontitis: study of prevalence and association with clinical and histopathologic findings. *Journal of Endodontics,* 36, 1277-1288.

RICUCCI, D., SIQUEIRA JR, J. F., BATE, A. L. & FORD, T. R. P. 2009. Histologic investigation of root canal–treated teeth with apical periodontitis: a retrospective study from twenty-four patients. *Journal of Endodontics,* 35, 493-502.

RICUCCI, D., SIQUEIRA JR, J. F., LOGHIN, S. & LIN, L. M. 2017. Pulp and apical tissue response to deep caries in immature teeth: A histologic and histobacteriologic study. *Journal of Dentistry,* 56, 19-32.

ROBERTS, A. E., KRAGH, K. N., BJARNSHOLT, T. & DIGGLE, S. P. 2015. The limitations of in vitro experimentation in understanding biofilms and chronic infection. *Journal of Molecular Biology,* 427, 3646-3661.

RÔÇAS, I. N., PROVENZANO, J. C., NEVES, M. A. & SIQUEIRA JR, J. F. 2016. Disinfecting effects of rotary instrumentation with either 2.5% sodium hypochlorite or 2% chlorhexidine as the main irrigant: a randomized clinical study. *Journal of endodontics,* 42, 943-947.

RÔÇAS, I. N., SIQUEIRA JR, J. F. & SANTOS, K. R. 2004. Association of Enterococcus faecalis with different forms of periradicular diseases. *Journal of Endodontics,* 30, 315-320.

ROLPH, H., LENNON, A., RIGGIO, M., SAUNDERS, W., MACKENZIE, D., COLDERO, L. & BAGG, J. 2001. Molecular identification of microorganisms from endodontic infections. *Journal of Clinical Microbiology,* 39, 3282-3289.

ROSSI-FEDELE, G., ESTRELA, C., PULIKKOTIL, S. J. & NAGENDRABABU, V. 2019. Machine-assisted Agitation Reduces Postoperative Pain during Root Canal Treatment: A Systematic Review and Meta-analysis from Randomized Clinical Trials. 45, 387-393.

ROUSSEAU, R. & LEUVEN, K. 2008. Reflections on recent developments of the h-index and h-type indices. *COLLNET Journal of Scientometrics and Information Management,* 2, 1-8.

RUIZ-LINARES, M., DE OLIVEIRA FAGUNDES, J., SOLANA, C., BACA, P. & FERRER-LUQUE, C. M. 2022. Current status on antimicrobial activity of a tricalcium silicate cement. *Journal of Oral Science,* 64**,** 113-117.

RUKSAKIET, K., HANÁK, L., FARKAS, N., HEGYI, P., SADAENG, W., CZUMBEL, L. M., SANG-NGOEN, T., GARAMI, A., MIKÓ, A. & VARGA, G. 2020. Antimicrobial efficacy of chlorhexidine and sodium hypochlorite in root canal disinfection: a systematic review and meta-analysis of randomized controlled trials. *Journal of Endodontics,* 46**,** 1032-1041.

S KIM, S., SONG, M., SHIN, S.-J. & KIM, E. 2016. A randomized controlled study of mineral trioxide aggregate and super ethoxybenzoic acid as root-end filling materials in endodontic microsurgery: long-term outcomes. *Journal of Endodontics,* 42**,** 997-1002.

SABIR, A., TABBU, C. R., AGUSTIONO, P. & SOSROSENO, W. 2005. Histological analysis of rat dental pulp tissue capped with propolis. *Journal of Oral Science,* 47**,** 135-138.

SAHAR-HELFT, S., EREZ, A., SHAY, B., ASSAD, R., FUNK, B. & POLAK, D. 2019. Enhancing Er: YAG bactericidal effect against Enterococcus faecalis biofilm in vitro. *Lasers in Medical Science,* 34**,** 1717-1721.

SAITO, D., COUTINHO, L. L., SAITO, C. P. B., TSAI, S. M., HÖFLING, J. F. & GONÇALVES, R. B. 2009. Real-time polymerase chain reaction quantification of Porphyromonas gingivalis and Tannerella forsythia in primary endodontic infections. *Journal of Endodontics,* 35**,** 1518-1524.

SAKAMOTO, M., RÔÇAS, I., SIQUEIRA JR, J. & BENNO, Y. 2006. Molecular analysis of bacteria in asymptomatic and symptomatic endodontic infections. *Oral Microbiology and Immunology,* 21**,** 112-122.

SÁNCHEZ-SANHUEZA, G., BELLO-TOLEDO, H., GONZÁLEZ-ROCHA, G., GONÇALVES, A., VALENZUELA, V. & GALLARDO-ESCÁRATE, C. 2018. Metagenomic study of bacterial microbiota in persistent endodontic infections using Next-generation sequencing. *International Endodontic Journal,* 51**,** 1336-1348.

SAOUD, T. M., MARTIN, G., CHEN, Y.-H. M., CHEN, K.-L., CHEN, C.-A., SONGTRAKUL, K., MALEK, M., SIGURDSSON, A. & LIN, L. M. 2016a. Treatment of mature permanent teeth with necrotic pulps and apical periodontitis using regenerative endodontic procedures: a case series. *Journal of Endodontics,* 42**,** 57-65.

SAOUD, T. M. A., HUANG, G. T.-J., GIBBS, J. L., SIGURDSSON, A. & LIN, L. M. 2015. Management of teeth with persistent apical periodontitis after root canal treatment using regenerative endodontic therapy. *Journal of Endodontics,* 41**,** 1743-1748.

SAOUD, T. M. A., MISTRY, S., KAHLER, B., SIGURDSSON, A. & LIN, L. M. 2016b. Regenerative endodontic procedures for traumatized teeth after horizontal root fracture, avulsion, and perforating root resorption. *Journal of Endodontics,* 42**,** 1476-1482.

SAQUIB, N., ZAGHLOUL, M. S., MAZROU, A. & SAQUIB, J. 2017. Cardiovascular disease research in Saudi Arabia: a bibliometric analysis. *Scientometrics,* 112**,** 111-140.

SARKAR, N., ANAND, P., MOISEYEVA, R. & RITWIK, R. 2003. A modified Portland Cement for dental use: Its interaction with simulated oral environment. *Transactions of the Indian Ceramic Society,* 62**,** 200-204.

SARKAR, N., CAICEDO, R., RITWIK, P., MOISEYEVA, R. & KAWASHIMA, I. 2005. Physicochemical basis of the biologic properties of mineral trioxide aggregate. *Journal of Endodontics,* 31**,** 97-100.

SASSONE, L. M., FIDEL, R., FIDEL, S., VIEIRA, M. & HIRATA, R., JR. 2003. The influence of organic load on the antimicrobial activity of different concentrations of NaOCl and chlorhexidine in vitro. *International Endodontic Journal,* 36**,** 848-852.

SATO, T., YAMAKI, K., ISHIDA, N., SHOJI, M., SATO, E., ABIKO, Y., HASHIMOTO, K., TAKEUCHI, Y., MATSUYAMA, J. & SHIMAUCHI, H. 2012. Rapid quantification of bacteria in infected root canals using fluorescence reagents and a membrane filter: a pilot study on its clinical application to the evaluation of the outcomes of endodontic treatment. *International Journal of Dentistry,* 2012**,** 172935.

SC 2011. SCIENTIFIC OPINION - Statistical significance and biological relevance. EFSA Scientific Committee. *EFSA Journal,* 9**,** 2372.

SCHÄFER, E. & OLTHOFF, G. 2002. Effect of three different sealers on the sealing ability of both thermafil obturators and cold laterally compacted Gutta-Percha. *Journal of Endodontics,* 28**,** 638-642.

SCHAUDINN, C., CARR, G., GORUR, A., JARAMILLO, D., COSTERTON, J. & WEBSTER, P. 2009. Imaging of endodontic biofilms by combined microscopy (FISH/cLSM–SEM). *Journal of Microscopy,* 235**,** 124-127.

SCHAUDINN, C., JARAMILLO, D., FREIRE, M., SEDGHIZADEH, P., NGUYEN, A., WEBSTER, P., COSTERTON, J. & JIANG, C. 2013. Evaluation of a nonthermal plasma needle to eliminate ex vivo biofilms in root canals of extracted human teeth. *International Endodontic Journal,* 46**,** 930-937.

SCHMALZ, G. & ARENHOLT-BINDSLEV, D. 2009. Basic Aspects. In Biocompatibility of dental materials. Springer, 1-12.

SCHOLAR, E. M., SCHOLAR, E. M. & PRATT, W. B. 2000. The antimicrobial drugs, Oxford University Press, USA.

SEGURA-EGEA, J., GOULD, K., ŞEN, B. H., JONASSON, P., COTTI, E., MAZZONI, A., SUNAY, H., TJÄDERHANE, L. & DUMMER, P. 2018. European Society of Endodontology position statement: the use of antibiotics in endodontics. *International Endodontic Journal,* 51**,** 20-25.

SEN, B., PISKIN, B. & DEMIRCI, T. 1995. Observation of bacteria and fungi in infected root canals and dentinal tubules by SEM. *Dental Traumatology,* 11**,** 6-9.

SENAN, E. M., ALHADAINY, H. A., GENAID, T. M. & MADFA, A. A. 2018. Root form and canal morphology of maxillary first premolars of a Yemeni population. *BMC Oral Health,* 18**,** 94.

SEPTODONT 2010. Biodentine active biosilicate technology: scientific file. Septodont Saint-Maur-des-Fossés.

SEYAM, S., NORDIN, N. A. & ALFATAMA, M. 2020. Recent progress of chitosan and chitosan derivatives-based nanoparticles: pharmaceutical perspectives of oral insulin delivery. *Pharmaceuticals,* 13**,** 307.

SHAALA, L. A., ASFOUR, H. Z., YOUSSEF, D. T., ŻÓŁTOWSKA-AKSAMITOWSKA, S., WYSOKOWSKI, M., TSURKAN, M., GALLI, R., MEISSNER, H., PETRENKO, I. & TABACHNICK, K. 2019. New source of 3D chitin scaffolds: the Red Sea demosponge Pseudoceratina arabica (Pseudoceratinidae, Verongiida). *Marine Drugs,* 17**,** 92.

SHAHI, S., VAHED, S. Z., FATHI, N. & SHARIFI, S. 2018. Polymerase chain reaction (PCR)-based methods: Promising molecular tools in dentistry. *International Journal of Biological Macromolecules,* 117**,** 983-992.

SHEN, Y., PENG, B., YANG, Y., MA, J. & HAAPASALO, M. 2015. What do different tests tell about the mechanical and biological properties of bioceramic materials? *Endodontic Topics,* 32**,** 47-85.

SHERRY, L., LAPPIN, G., O'DONNELL, L. E., MILLHOUSE, E., MILLINGTON, O. R., BRADSHAW, D. J., AXE, A. S., WILLIAMS, C., NILE, C. J. & RAMAGE, G. 2016. Viable compositional analysis of an eleven species oral polymicrobial biofilm. *Frontiers in Microbiology*, 7, 912.

SHERRY, L., RAJENDRAN, R., LAPPIN, D. F., BORGHI, E., PERDONI, F., FALLENI, M., TOSI, D., SMITH, K., WILLIAMS, C. & JONES, B. 2014. Biofilms formed by Candida albicans bloodstream isolates display phenotypic and transcriptional heterogeneity that are associated with resistance and pathogenicity. *BMC Microbiology,* 14, 182.

SHIN, J. M., LUO, T., LEE, K. H., GUERREIRO, D., BOTERO, T. M., MCDONALD, N. J. & RICKARD, A. H. 2018. Deciphering endodontic microbial communities by next-generation sequencing. *Journal of Endodontics,* 44, 1080-1087.

SHRESTHA, A. & KISHEN, A. 2012. The effect of tissue inhibitors on the antibacterial activity of chitosan nanoparticles and photodynamic therapy. *Journal of Endodontics,* 38, 1275-1278.

SHRESTHA, A. & KISHEN, A. 2016. Antibacterial nanoparticles in endodontics: a review. *Journal of Endodontics,* 42, 1417-1426.

SHRESTHA, A., ZHILONG, S., GEE, N. K. & KISHEN, A. 2010. Nanoparticulates for antibiofilm treatment and effect of aging on its antibacterial activity. *Journal of Endodontics,* 36, 1030-1035.

SHUPING 2000. Orstavik D, Sigurdsson A, Trope M. Reduction of intracanal bacteria using nickel-titanium rotary instrumentation and various medications. *Journal of Endodontics,* 26, 751-755.

SIDDIQUE, R., RANJAN, M., JOSE, J., SRIVASTAV, A., RAJAKEERTHI, R. & KAMATH, A. 2020. Clinical quantitative antibacterial potency of garlic-lemon against sodium hypochlorite in infected root canals: A double-blinded, randomized, controlled clinical trial. *Journal of International Society of Preventive & Community Dentistry,* 10, 771–778.

SIMON, S. & GOLDBERG, M. 2014. Regenerative endodontics: regeneration or repair? In The Dental Pulp. Springer, 267-276.

SINHA, N., PATIL, S., DODWAD, P. K., PATIL, A. C. & SINGH, B. 2013. Evaluation of antimicrobial efficacy of calcium hydroxide paste, chlorhexidine gel, and a combination of both as intracanal medicament: An in vivo comparative study. *Journal of Conservative Dentistry,* 16, 65-70.

SIQUEIRA 2003. Microbial causes of endodontic flare-ups. *International Endodontic Journal,* 36, 453-463.

SIQUEIRA, ANTUNES, H. S., RÔÇAS, I. N., RACHID, C. T. & ALVES, F. R. 2016. Microbiome in the Apical Root Canal System of Teeth with Post-Treatment Apical Periodontitis. *PLOS ONE,* 11, e0162887.

SIQUEIRA, RICUCCI, D. & ROÇAS, I. N. 2015. Bacterial Biofilms and Endodontic Disease: Histobacteriological and Molecular Exploration. In The Root Canal Biofilm. Springer, 103-125.

SIQUEIRA & RÔÇAS, I. N. 2009. Distinctive features of the microbiota associated with different forms of apical periodontitis. *Journal of Oral Microbiology,* 1,2009, doi: 10.3402/jom.v3401i3400.2009.

SIQUEIRA & RÔÇAS, I. N. 2014. Present status and future directions in endodontic microbiology. *Endodontic Topics,* 30, 3-22.

SIQUEIRA, RÔÇAS, I. N., FAVIERI, A. & LIMA, K. C. 2000. Chemomechanical reduction of the bacterial population in the root canal after instrumentation and irrigation with 1%, 2.5%, and 5.25% sodium hypochlorite. *Journal of Endodontics,* 26, 331-334.

SIQUEIRA, RÔÇAS, I. N. & RICUCCI, D. 2019. Internal tooth anatomy and root canal instrumentation. In The Root Canal Anatomy in Permanent Dentition. Springer, 277-302.

SIQUEIRA, J. & RÔÇAS, I. 2016. Microbiology of endodontic infections. In Cohen's Pathways of the Pulp. Elsevier, 599-625.

SIQUEIRA, J. F. & RÔÇAS, I. N. 2004. Polymerase chain reaction–based analysis of microorganisms associated with failed endodontic treatment. *Oral Surgery, Oral Medicine, Oral Pathology, Oral Radiology, and Endodontology,* 97**,** 85-94.

SIQUEIRA, J. F. & RÔÇAS, I. N. 2022. A critical analysis of research methods and experimental models to study the root canal microbiome. *International Endodontic Journal,* 55**,** 46-71.

SIREN, E., HAAPASALO, M., RANTA, K., SALMI, P. & KEROSUO, E. 1997. Microbiological findings and clinical treatment procedures in endodontic cases selected for microbiological investigation. *International Endodontic Journal,* 30**,** 91-95.

SJÖGREN, U., FIGDOR, D., PERSSON, S. & SUNDQVIST, G. 1997. Influence of infection at the time of root filling on the outcome of endodontic treatment of teeth with apical periodontitis. *International Endodontic Journal,* 30**,** 297-306.

SJÖGREN, U., FIGDOR, D., SPÅNGBERG, L. & SUNDQVIST, G. 1991. The antimicrobial effect of calcium hydroxide as a short-term intracanal dressing. *International Endodontic Journal,* 24**,** 119-125.

SOAMES, J. V. & SOUTHAM, J. C. 2005. Oral pathology, Oxford University Press.

SOLANKI, N. P., VENKAPPA, K. K. & SHAH, N. C. 2018. Biocompatibility and sealing ability of mineral trioxide aggregate and biodentine as root-end filling material: A systematic review. *Journal of Conservative Dentistry,* 21**,** 10-15.

SOLER, J. M. 2007. Separating the articles of authors with the same name. *Scientometrics,* 72**,** 281-290.

SPENCER, H., IKE, V. & BRENNAN, P. 2007. the use of sodium hypochlorite in endodontics—potential complications and their management. *British Dental Journal,* 202**,** 555-559.

SU, Y., WANG, C. & YE, L. 2011. Healing rate and post-obturation pain of single- versus multiple-visit endodontic treatment for infected root canals: a systematic review. *Journal of Endodontics,* 37**,** 125-132.

SUNDQVIST, G. 1992. Associations between microbial species in dental root canal infections. *Oral Microbiology and Immunology,* 7**,** 257-262.

SUNDQVIST, G., FIGDOR, D., PERSSON, S. & SJÖGREN, U. 1998. Microbiologic analysis of teeth with failed endodontic treatment and the outcome of conservative re-treatment. *Oral Surgery, Oral Medicine, Oral Pathology, Oral Radiology, and Endodontology,* 85**,** 86-93.

SWIMBERGHE, R., COENYE, T., DE MOOR, R. & MEIRE, M. 2019. Biofilm model systems for root canal disinfection: a literature review. *International Endodontic Journal,* 52**,** 604-628.

T WU, T., ZIVANOVIC, S., DRAUGHON, F. A. & SAMS, C. E. 2004. Chitin and chitosan value-added products from mushroom waste. *Journal of Agricultural and Food Chemistry,* 52**,** 7905-7910.

TAKAMIYA, A. S., MONTEIRO, D. R., BERNABÉ, D. G., GORUP, L. F., CAMARGO, E. R., GOMES-FILHO, J. E., OLIVEIRA, S. H. P. & BARBOSA, D. B. 2016. In vitro and in vivo toxicity evaluation of colloidal silver nanoparticles used in endodontic treatments. *Journal of Endodontics,* 42**,** 953-960.

TAMBAKAD, P. B. & NAIDU, J. 2016. Pulp and periodontal regeneration of an avulsed permanent mature incisor using platelet-rich plasma after delayed replantation: a 12-month clinical case study. *Journal of Endodontics,* 42, 66-71.

TANALP, J., KARAPıNAR-KAZANDAĞ, M., DÖLEKOĞLU, S. & KAYAHAN, M. B. 2013. Comparison of the radiopacities of different root-end filling and repair materials. *The Scientific World Journal,* 2013.

TARAZONA, B., VIDAL-INFER, A. & ALONSO-ARROYO, A. 2017. Bibliometric analysis of the scientific production in implantology (2009–2013). *Clinical oral Implants Research,* 28, 864-870.

TENNERT, C., SCHURIG, T., AL-AHMAD, A., STROBEL, S. L., KIELBASSA, A. M. & WRBAS, K.-T. 2017. Antimicrobial influence of different root canal filling techniques in experimentally infected human root canals. *Quintessence International,* 48, 273-280.

THEIN, Z. M., SAMARANAYAKE, Y. H. & SAMARANAYAKE, L. P. 2006. Effect of oral bacteria on growth and survival of Candida albicans biofilms. *Archives of Oral Biology,* 51, 672-680.

THOMPSON, D. F. & WALKER, C. K. 2015. A descriptive and historical review of bibliometrics with applications to medical sciences. *Pharmacotherapy: The Journal of Human Pharmacology and Drug Therapy,* 35, 551-559.

TIKHONOV, V. E., STEPNOVA, E. A., BABAK, V. G., YAMSKOV, I. A., PALMA-GUERRERO, J., JANSSON, H.-B., LOPEZ-LLORCA, L. V., SALINAS, J., GERASIMENKO, D. V. & AVDIENKO, I. D. 2006. Bactericidal and antifungal activities of a low molecular weight chitosan and its N-/2 (3)-(dodec-2-enyl) succinoyl/-derivatives. *Carbohydrate Polymers,* 64, 66-72.

TORABINEJAD, M., HANDYSIDES, R., KHADEMI, A. A. & BAKLAND, L. K. 2002. Clinical implications of the smear layer in endodontics: a review. *Oral Surgery, Oral Medicine, Oral Pathology, Oral Radiology, and Endodontology,* 94, 658-666.

TORABINEJAD, M., HONG, C., MCDONALD, F. & FORD, T. P. 1995. Physical and chemical properties of a new root-end filling material. *Journal of Endodontics,* 21, 349-353.

TORABINEJAD, M., KHADEMI, A. A., BABAGOLI, J., CHO, Y., JOHNSON, W. B., BOZHILOV, K., KIM, J. & SHABAHANG, S. 2003. A new solution for the removal of the smear layer. *Journal of Endodontics,* 29, 170-175.

TORABINEJAD, M., WATSON, T. & FORD, T. P. 1993. Sealing ability of a mineral trioxide aggregate when used as a root end filling material. *Journal of Endodontics,* 19, 591-595.

TORABINEJAD, M. & WHITE, D. J. 1995. Tooth filling material and method of use. Google Patents, US5415547A.

TRAN, K. T., TORABINEJAD, M., SHABAHANG, S., RETAMOZO, B., APRECIO, R. M. & CHEN, J.-W. 2013. Comparison of efficacy of pulverization and sterile paper point techniques for sampling root canals. *Journal of Endodontics,* 39, 1057-1059.

TROPE, M., BUNES, A. & DEBELIAN, G. 2015. Root filling materials and techniques: bioceramics a new hope? *Endodontic Topics,* 32, 86-96.

TSAI, G.-J. & SU, W.-H. 1999. Antibacterial activity of shrimp chitosan against Escherichia coli. *Journal of Food Protection,* 62, 239-243.

TSUKADA, G., TANAKA, T., TORII, M. & INOUE, K. 2004. Shear modulus and thermal properties of gutta percha for root canal filling. *Journal of Oral Rehabilitation,* 31, 1139-1144.

URURAHY, M. S., CURYLOFO-ZOTTI, F. A., GALO, R., NOGUEIRA, L. F. B., RAMOS, A. P. & CORONA, S. A. M. 2017. Wettability and surface morphology of eroded dentin treated with chitosan. *Archives of Oral Biology,* 75, 68-73.

VAN DER SLUIS, L. W., VERHAAGEN, B., MACEDO, R. & VERSLUIS, M. 2016. The role of irrigation in endodontics. In Lasers in Endodontics. Springer, 45-69.

VAN TONDER, A., JOUBERT, A. M. & CROMARTY, A. D. 2015. Limitations of the 3-(4, 5-dimethylthiazol-2-yl)-2, 5-diphenyl-2H-tetrazolium bromide (MTT) assay when compared to three commonly used cell enumeration assays. *BMC Research Notes,* 8, 1-10.

VANDEVORD, P. J., MATTHEW, H. W., DESILVA, S. P., MAYTON, L., WU, B. & WOOLEY, P. H. 2002. Evaluation of the biocompatibility of a chitosan scaffold in mice. *Journal of Biomedical Materials Research,* 59, 585-590.

VERA, J., SIQUEIRA, J. F., RICUCCI, D., LOGHIN, S., FERNÁNDEZ, N., FLORES, B. & CRUZ, A. G. 2012. One-versus two-visit endodontic treatment of teeth with apical periodontitis: a histobacteriologic study. *Journal of Endodontics,* 38, 1040-1052.

VERSIANI, M. A. & KELEŞ, A. 2020. Applications of Micro-CT Technology in Endodontics. In Micro-computed Tomography (micro-CT) in Medicine and Engineering. Springer, 183-211.

VERSIANI, M. A. & ORDINOLA-ZAPATA, R. 2015. Root canal anatomy: implications in biofilm disinfection. In The Root Canal Biofilm. Springer, 155-187.

VERT, M., DOI, Y., HELLWICH, K.-H., HESS, M., HODGE, P., KUBISA, P., RINAUDO, M. & SCHUÉ, F. 2012. Terminology for biorelated polymers and applications (IUPAC Recommendations 2012). *Pure and Applied Chemistry,* 84, 377-410.

VIEIRA, A. P. M., ARIAS, L. S., DE SOUZA NETO, F. N., KUBO, A. M., LIMA, B. H. R., DE CAMARGO, E. R., PESSAN, J. P., DELBEM, A. C. B. & MONTEIRO, D. R. 2019. Antibiofilm effect of chlorhexidine-carrier nanosystem based on iron oxide magnetic nanoparticles and chitosan. *Colloids and Surfaces B: Biointerfaces,* 174, 224-231.

VIGUERAS, S. H., ZÚNIGA, M. D., JANÉ-SALAS, E., NAVARRETE, L. S., SEGURA-EGEA, J. J., VELASCO-ORTEGA, E. & LÓPEZ-LÓPEZ, J. 2016. Viruses in pulp and periapical inflammation: a review. *Odontology,* 104, 184-191.

VINOTHKUMAR, T. S., RUBIN, M. I., BALAJI, L. & KANDASWAMY, D. 2013. In vitro evaluation of five different herbal extracts as an antimicrobial endodontic irrigant using real time quantitative polymerase chain reaction. *Journal of Conservative Dentistry,* 16, 167.

VIOLICH, D. & CHANDLER, N. 2010. The smear layer in endodontics–a review. *International Endodontic Journal,* 43, 2-15.

VISTICA, D. T., SKEHAN, P., SCUDIERO, D., MONKS, A., PITTMAN, A. & BOYD, M. R. 1991. Tetrazolium-based assays for cellular viability: a critical examination of selected parameters affecting formazan production. *Cancer Research,* 51, 2515-2520.

VOGT, L. 2009. The future role of bio-ontologies for developing a general data standard in biology: chance and challenge for zoo-morphology. *Zoomorphology,* 128, 201-217.

W YANG, W., ZHANG, J. & MA, R. 2020. The prediction of infectious diseases: A bibliometric analysis. *International Journal of Environmental Research and Public Health,* 17, 1-19.

W ZHANG, W., CHEN, Y., SHI, Q., HOU, B. & YANG, Q. 2020. Identification of bacteria associated with periapical abscesses of primary teeth by

sequence analysis of 16S rDNA clone libraries. *Microbial Pathogenesis,* 141, 103954.

W ZHOU, W., ZHENG, Q., TAN, X., SONG, D., ZHANG, L. & HUANG, D. 2017. Comparison of mineral trioxide aggregate and iRoot BP plus root repair material as root-end filling materials in endodontic microsurgery: a prospective randomized controlled study. *Journal of Endodontics,* 43, 1-6.

WALTIMO, T., SIREN, E., TORKKO, H., OLSEN, I. & HAAPASALO, M. 1997. Fungi in therapy-resistant apical periodontitis. *International Endodontic Journal,* 30, 96-101.

WANG, Z. 2015. Bioceramic materials in endodontics. *Endodontic Topics,* 32, 3-30.

WANG, Z., SHEN, Y. & HAAPASALO, M. 2013. Effect of smear layer against disinfection protocols on Enterococcus faecalis–infected dentin. *Journal of Endodontics,* 39, 1395-1400.

WANI, T. U., PANDITH, A. H. & SHEIKH, F. A. 2021. Polyelectrolytic nature of chitosan: Influence on physicochemical properties and synthesis of nanoparticles. *Journal of Drug Delivery Science and Technology,* 65, 102730.

WELLER, R. N., NIEMCZYK, S. P. & KIM, S. 1995. Incidence and position of the canal isthmus. Part 1. Mesiobuccal root of the maxillary first molar. *Journal of Endodontics,* 21, 380-383.

WIDBILLER, M., JEANNEAU, C., GALLER, K. M. & LAURENT, P. 2022. Biocompatibility and Bioactive Properties of Biodentine TM. In Biodentine™. Springer, 31-50.

WIDBILLER, M., LINDNER, S., BUCHALLA, W., EIDT, A., HILLER, K.-A., SCHMALZ, G. & GALLER, K. 2016. Three-dimensional culture of dental pulp stem cells in direct contact to tricalcium silicate cements. *Clinical Oral Investigations,* 20, 237-246.

WIDMER, C., SKUTAS, J., EASSON, C., LOPEZ, J. V., TORNECK, C., FLAX, M. & SAYIN, T. C. 2018. Culture-independent Characterization of the Microbiome of Healthy Pulp. *Journal of Endodontics,* 44, 1132-1139.

WIEME, A. D., SPITAELS, F., AERTS, M., DE BRUYNE, K., VAN LANDSCHOOT, A. & VANDAMME, P. 2014. Effects of growth medium on matrix-assisted laser desorption–ionization time of flight mass spectra: a case study of acetic acid bacteria. *Applied and Environmental Microbiology,* 80, 1528-1538.

WILLIAMS, J. & BILLINGTON, R. 1987. A new technique for measuring the radiopacity of natural tooth substance and restorative materials. *Journal of Oral Rehabilitation,* 14, 267-269.

WILSON, A. D. 1976. Specification test for the solubility and disintegration of dental cements: a critical evaluation of its meaning. *Journal of Dental Research,* 55, 721-729.

WINNENBURG, R., WÄCHTER, T., PLAKE, C., DOMS, A. & SCHROEDER, M. 2008. Facts from text: can text mining help to scale-up high-quality manual curation of gene products with ontologies? *Briefings in Bioinformatics,* 9, 466-478.

WONG, J., ZOU, T., LEE, A. H. C. & ZHANG, C. 2021. The Potential Translational Applications of Nanoparticles in Endodontics. *International Journal of Nanomedicine,* 16, 2087–2106.

XU, C., LEI, C., MENG, L., WANG, C. & SONG, Y. 2012. Chitosan as a barrier membrane material in periodontal tissue regeneration. *Journal of Biomedical Materials Research Part B: Applied Biomaterials,* 100, 1435-1443.

Y KIM, Y., FLYNN, T. R., DONOFF, R. B., WONG, D. T. & TODD, R. 2002. The gene: the polymerase chain reaction and its clinical application. *Journal of Oral and Maxillofacial Surgery,* 60**,** 808-815.

Y ZHOU, Y., MILLHOUSE, E., SHAW, T., LAPPIN, D. F., RAJENDRAN, R., BAGG, J., LIN, H. & RAMAGE, G. 2018. Evaluating Streptococcus mutans strain dependent characteristics in a polymicrobial biofilm community. *Frontiers in Microbiology,* 9**,** 1498.

YADAV, P., CHAUDHARY, S., SAXENA, R. K., TALWAR, S. & YADAV, S. 2017. Evaluation of Antimicrobial and Antifungal efficacy of Chitosan as endodontic irrigant against Enterococcus Faecalis and Candida Albicans Biofilm formed on tooth substrate. *Journal of Clinical and Experimental Dentistry,* 9**,** e361-e367.

YAMAUCHI, N., YAMAUCHI, S., NAGAOKA, H., DUGGAN, D., ZHONG, S., LEE, S. M., TEIXEIRA, F. B. & YAMAUCHI, M. 2011. Tissue engineering strategies for immature teeth with apical periodontitis. *Journal of Endodontics,* 37**,** 390-397.

YANCHESHMEH, S. S. 2020. Examining the Factors Affecting Endodontic Therapy Failure. *Journal of Molecular Biology Research,* 10**,** 1; 2020.

YE, M., NEETOO, H. & CHEN, H. 2008. Control of Listeria monocytogenes on ham steaks by antimicrobials incorporated into chitosan-coated plastic films. *Food Microbiology,* 25**,** 260-268.

YILMAZ, B., DINCOL, M. E. & YALCIN, T. Y. 2019. A bibliometric analysis of the 103 top-cited articles in endodontics. *Acta Odontologica Scandinavica,* 77**,** 574-583.

YOO, J. S., CHANG, S.-W., OH, S. R., PERINPANAYAGAM, H., LIM, S.-M., YOO, Y.-J., OH, Y.-R., WOO, S.-B., HAN, S.-H. & ZHU, Q. 2014. Bacterial entombment by intratubular mineralization following orthograde mineral trioxide aggregate obturation: a scanning electron microscopy study. *International Journal of Oral Science,* 6**,** 227-232.

YOSHINO, P., NISHIYAMA, C. K., MODENA, K. C. D. S., SANTOS, C. F. & SIPERT, C. R. 2013. In vitro cytotoxicity of white MTA, MTA Fillapex® and Portland cement on human periodontal ligament fibroblasts. *Brazilian Dental Journal,* 24**,** 111-116.

YOUNG, T., ALSHANTA, O.-A., KEAN, R., BRADSHAW, D., PRATTEN, J., WILLIAMS, C., WOODALL, C., RAMAGE, G. & BROWN, J. L. 2021. Candida albicans as an essential “keystone” component within polymicrobial oral biofilm models? *Microorganisms,* 9**,** 59.

ZANCAN, R. F., CALEFI, P. H. S., BORGES, M. M. B., LOPES, M. R. M., DE ANDRADE, F. B., VIVAN, R. R. & DUARTE, M. A. H. 2019. Antimicrobial activity of intracanal medications against both Enterococcus faecalis and Candida albicans biofilm. *Microscopy Research and Technique,* 82**,** 494-500.

ZANDI, H., PETRONIJEVIC, N., MDALA, I., KRISTOFFERSEN, A. K., ENERSEN, M., RÔÇAS, I. N., SIQUEIRA JR, J. F. & ØRSTAVIK, D. 2019. Outcome of endodontic retreatment using 2 root canal irrigants and influence of infection on healing as determined by a molecular method: a randomized clinical trial. *Journal of Endodontics,* 45**,** 1089-1098.

ZANZA, A., REDA, R., PAGNONI, F. & PATIL, S. 2022. Future Trends in Endodontics: How Could Materials Increase the Long-Term Outcome of Root Canal Therapies?. *Materials,* 15**,** 3473.

ZARGAR, N., ASHRAF, H., MARASHI, S., SABETI, M. & AZIZ, A. 2020. Identification of microorganisms in irreversible pulpitis and primary endodontic

infections with respect to clinical and radiographic findings. *Clinical Oral Investigations,* 24**,** 2099-2108.

ZEHNDER, M., WALTIMO, T., SENER, B. & SÖDERLING, E. 2006. Dentin enhances the effectiveness of bioactive glass S53P4 against a strain of Enterococcus faecalis. *Oral Surgery, Oral Medicine, Oral Pathology, Oral Radiology, and Endodontology,* 101**,** 530-535.

ZEID, S., ALOTHMANI, O. S. & YOUSEF, M. K. 2015. Biodentine and mineral trioxide aggregate: an analysis of solubility, pH changes and leaching elements. *Life Science Journal,* 12**,** 18-23.